MINISTÉRIO DA CIÊNCIA, TECNOLOGIA E INOVAÇÕES
INSTITUTO NACIONAL DE PESQUISAS ESPACIAIS

sid.inpe.br/mtc-m21d/2022/08.05.00.18-TDI

ASSESSMENT OF FIRE OCCURRENCE WITHIN PROTECTED AREAS IN THE AMAZON BASIN FROM 2003 TO 2020

Ana Carolina Moreira Pessôa

Doctorate Thesis of the Graduate Course in Remote Sensing, guided by Drs. Liana Oighenstein Anderson, and Thiago Fonseca Morello Ramalho da Silva, approved in July 29, 2022.

URL of the original document:
<http://urlib.net/8JMKD3MGP3W34T/47CUJ72>

INPE
São José dos Campos
2022

PUBLISHED BY:

Instituto Nacional de Pesquisas Espaciais - INPE
Coordenação de Ensino, Pesquisa e Extensão (COEPE)
Divisão de Biblioteca (DIBIB)
CEP 12.227-010
São José dos Campos - SP - Brasil
Tel.:(012) 3208-6923/7348
E-mail: pubtc@inpe.br

MINISTÉRIO DA CIÊNCIA, TECNOLOGIA E INOVAÇÕES
INSTITUTO NACIONAL DE PESQUISAS ESPACIAIS

sid.inpe.br/mtc-m21d/2022/08.05.00.18-TDI

ASSESSMENT OF FIRE OCCURRENCE WITHIN PROTECTED AREAS IN THE AMAZON BASIN FROM 2003 TO 2020

Ana Carolina Moreira Pessôa

Doctorate Thesis of the Graduate Course in Remote Sensing, guided by Drs. Liana Oighenstein Anderson, and Thiago Fonseca Morello Ramalho da Silva, approved in July 29, 2022.

URL of the original document:
<http://urlib.net/8JMKD3MGP3W34T/47CUJ72>

INPE
São José dos Campos
2022

Cataloging in Publication Data

Pessôa, Ana Carolina Moreira.

P439a Assessment of fire occurrence within protected areas in the Amazon basin from 2003 to 2020 / Ana Carolina Moreira Pessôa. – São José dos Campos : INPE, 2022.

xxviii + 242 p. ; (sid.inpe.br/mtc-m21d/2022/08.05.00.18-TDI)

Thesis (Doctorate in Remote Sensing) – Instituto Nacional de Pesquisas Espaciais, São José dos Campos, 2022.

Guiding : Drs. Liana Oighenstein Anderson, and Thiago Fonseca Morello Ramalho da Silva.

1. Indigenous lands. 2. Causal effect. 3. Econometrics. 4. Wildfire. 5. Geoprocessing. I.Title.

CDU 528.8:630*432

MINISTÉRIO DA CIÊNCIA, TECNOLOGIA E INOVAÇÕES

INSTITUTO NACIONAL DE PESQUISAS ESPACIAIS
Serviço de Pós-Graduação - SEPGR

DEFESA FINAL DE TESE DE ANA CAROLINA MOREIRA PESSÔA
BANCA Nº 195/2022, REG. 130117/2018

No dia 29 de julho de 2022, as 09h, por teleconferência, o(a) aluno(a) mencionado(a) acima defendeu seu trabalho final (apresentação oral seguida de arguição) perante uma Banca Examinadora, cujos membros estão listados abaixo. O(A) aluno(a) foi **APROVADO(A)** pela Banca Examinadora, por unanimidade, em cumprimento ao requisito exigido para obtenção do Título de Doutora em Sensoriamento Remoto. O trabalho precisa da incorporação das correções sugeridas pela Banca e revisão final pelo(s) orientador(es).

Título: "ASSESSMENT OF FIRE OCCURRENCE WITHIN PROTECTED AREAS IN THE AMAZON BASIN FROM 2003 TO 2020"

Membros da Banca:

Dr. Luiz Eduardo Oliveira e Cruz de Aragão - Presidente - INPE
Dra. Liana Oighenstein Anderson - Orientadora - CEMADEN
Dr. Thiago Fonseca Morello Ramalho da Silva - Orientador - UFABC
Dr. Yosio Edemir Shimabukuro - Membro Interno - INPE
Dra. Dolors Armenteras - Membro Externo - Universidad Nacional de Colombia
Dra. Paula Carvalho Pereda - Membro Externo - USP

Documento assinado eletronicamente por **Yosio Edemir Shimabukuro**, **Pesquisador**, em 11/08/2022, às 11:32 (horário oficial de Brasília), com fundamento no § 3º do art. 4º do Decreto nº 10.543, de 13 de novembro de 2020.

Documento assinado eletronicamente por **Liana Oighenstein Anderson**, **Pesquisador**, em 11/08/2022, às 16:25 (horário oficial de Brasília), com fundamento no § 3º do art. 4º do Decreto nº 10.543, de 13 de novembro de 2020.

Documento assinado eletronicamente por **PAULA Carvalho PEREDA (E)**, **Usuário Externo**, em 11/08/2022, às 16:34 (horário oficial de Brasília), com fundamento no § 3º do art. 4º do Decreto nº 10.543, de 13 de novembro de 2020.

Documento assinado eletronicamente por **Luiz Eduardo Oliveira E Cruz de Aragão**, **Chefe da Divisão de Observação da Terra e Geoinformática**, em 12/08/2022, às 11:08 (horário oficial de Brasília), com fundamento no § 3º do art. 4º do Decreto nº 10.543, de 13 de novembro de 2020.

Documento assinado eletronicamente por **Thiago fonseca morello ramalho da silva (E)**, **Usuário Externo**, em 12/08/2022, às 14:19 (horário oficial de Brasília), com fundamento no § 3º do art. 4º do Decreto nº 10.543, de 13 de novembro de 2020.

A autenticidade deste documento pode ser conferida no site https://sei.mcti.gov.br/verifica.html, informando o código verificador **10119409** e o código CRC **D0A61868**.

Referência: Processo nº 01340.005206/2022-51 SEI nº 10119409

"Em estudos de mudanças globais, os discípulos de cada disciplina normalmente consideram que sua disciplina é a chave. Todos estão parcialmente certos – todas as disciplinas são chaves, porém as mais importantes são as ausentes".

Foster Brown

Aos povos da Amazônia que resistem como heróis.

Ao Bruno Pereira e ao Dom Phillips para serem lembrados e homenageados.

ACKNOWLEDGEMENTS

The journey has not been simple. This thesis is the physical product of my intellectual growth during these four years of study. I am proud of what it has become, far from being the thesis I imagined at the beginning but far beyond what I thought I was capable of halfway through. It would be easy if those four years were just summarized in one thesis, but life was much more than that. I am happy and grateful for what I have become along the way, not the best version of me, but the best version of me I can be. I am enormously grateful to the people who somehow made this journey lighter.

To the National Institute for Space Research (INPE) for putting up with me a few more years and resisting its total wrecking, allowing students like me to still be able to get quality training in Remote Sensing.

To the National Council for Scientific and Technological Development (CNPq) for financial support.

To the Inter-American Institute for Global Change Research (IAI), for the financial support for the Multi-Actor Adaptation Plan to cope with Forests under Increasing Risk of Extensive fires (MAP-FIRE) project (grant number SGP-HW 016).

To my advisor, Liana, for buying my ideas and giving me space and freedom to develop myself by studying what I like. And for sharing unique moments and experiences around the world that made me grow professionally and as a person. Your horizontal conduct and conversation on equal terms make you my biggest inspiration in the art of mentoring.

To my co-supervisor, Thiago Morello, for having accepted the challenge of leading me between the lines of Economics and for having the patience to teach me everything repeatedly.

To my colleague Juan Doblas for his ready availability to help me remotely with the development of routines in Google Earth Engine.

To my colleague Celso Silva Jr., for providing several databases used in this thesis and for sharing this learning moment with me. You are an inspiration.

To my friends from Labuta who made the Doctorate a moment of sharing and collaboration. I will carry you along forever!

To my grandmother, Iracy, for having spared no effort in giving me the best education ever.

To all my family, who have always been examples and made the academic career a family tradition. Especially my mother, who gives me all the support I need to continue my career being the mother I always wanted to be.

To my friend and companion Wagner, for not giving up on me and dreaming this moment with me.

To my greatest masterpiece of these four years. Nuno, my son, I did not finish this thesis for you; I finished it myself. I know you were the person who paid the most for all this effort. I do not promise you a better world or a healthy Amazon. Unfortunately, that is beyond my reach. However, I promise you more presence. You and I and our family together already make our world better. I love you.

Finally, to that spiritual force that always accompanies me.

To all, my sincere gratitude!

A jornada até aqui não foi simples. Essa tese é o produto físico resultado do meu crescimento intelectual durante esses quatro anos de estudo. Estou orgulhosa do que ela se tornou, longe de ser a tese imaginada no início, mas muito além que pensei ser capaz no meio do caminho. Seria fácil se esses quatro anos se resumissem a somente uma tese, mas a vida foi muito mais que isso. Sou feliz e grata com o que me tornei no decorrer do caminho, não a melhor versão de mim, mas a possível de ser. Sou enormemente grata a pessoas que tornaram essa jornada mais leve de alguma forma.

Ao Instituto Nacional de Pesquisas Espaciais (INPE), por me aturar mais alguns anos e resistir ao seu sucateamento total, permitindo que alunos como eu ainda possam ter uma formação de qualidade em Sensoriamento Remoto.

Ao Conselho Nacional de Desenvolvimento Científico e Tecnológico (CNPq), pelo auxílio financeiro.

Ao *Inter-American Institute for Global Change Research* (IAI) pelo apoio financeiro ao projeto *Multi-Actor Adaptation Plan to cope with Forests under Increasing Risk of Extensive fires* (MAP-FIRE: projeto número SGP-HW 016).

A minha orientadora, Liana, por ter comprado minhas ideias e me dado espaço e liberdade para me desenvolver estudando o que eu gosto. E também por dividir momentos e experiências únicas ao redor do mundo que me fizeram crescer profissionalmente e como pessoa. Sua conduta horizontal e sua conversa de igual para igual fazem de você a minha maior inspiração na arte de orientar.

Ao meu co-orientador, Thiago Morello, por ter topado o desafio de me conduzir nas entrelinhas da Economia e ter tido paciência de me ensinar repetidas vezes tudo de novo.

Ao colega Juan Doblas, pela pronta disponibilidade em me ajudar remotamente com o desenvolvimento das rotinas no Google Earth Engine.

Ao colega Celso Silva Jr., pela disponibilização de diversos bancos de dados utilizados nesta tese, e por compartilhar comigo esse momento de formação. Você é inspiração.

Aos meus amigos de Labuta que fizeram do Doutorado um momento de partilha e colaboração. Carregarei vocês para sempre!

A minha avó, Iracy, por não ter medido esforços para me dar a melhor educação sempre.

A toda minha família, que sempre foram exemplos, e que tornaram a carreira acadêmica uma tradição familiar. Em especial a minha mãe, que mais do exemplo, me dá todo o suporte necessário para eu continuar a minha carreira sendo a mãe que sempre quis ser.

Ao meu amigo e companheiro Wagner, por não ter desistido de mim e ter sonhado esse momento junto comigo.

A minha maior obra prima desses 4 anos. Nuno, meu filho, não terminei essa tese por você, terminei por mim. E sei que você foi a pessoa que mais pagou por todo esse esforço. Não te prometo um mundo melhor, nem uma Amazônia saudável, infelizmente isso está além do meu alcance. Mas te prometo mais presença. Você e eu e nossa família junta, já fazem nosso mundo melhor. Te amo.

Por fim, a essa força espiritual que me acompanha sempre.

A todos, sinceramente, minha Gratidão!

ABSTRACT

The Amazon has been pushed into an amplified fire-prone system. The traditional fire dynamic has changed over the last decades due to agricultural intensification and demographic growth. Deforestation advance and forest degradation intensification result in a more fragmented landscape, favoring fire entry into the forest. Worsening this scenario, global climate models predict a drier Amazon in the 21st century. The climate is changing, and the intensity and frequency of extreme drought events generate ideal conditions for an increase in forest susceptibility to fires. In this context, political mechanisms to break this cycle and ensure the conservation of tropical ecosystems are needed, and protected areas are considered suitable strategies to tackle this challenge. Nevertheless, the last few years have been marked by setbacks in the environmental governance of these areas and by the rising of illegal activities that result in forest degradation. Thus, providing evidence for policy formulation and informing decision-makers about the role of protected areas in mitigating forest degradation caused by fires within protected areas is essential for prioritizing actions in their favor. This thesis, therefore, proposes to evaluate, through quantitative analysis and based on empirical data, the role of protected areas in curbing fire occurrence in the Amazon basin. In this sense, the thesis's main objective was achieved by answering three main questions: (1) is there a quantitative and spatial difference in the relative performance between burned area products, considering burned area over the forest and non-forest land covers? (2) Is fire an imminent and growing threat to protected areas in the Amazon basin? (3) Have protected areas affected fire occurrence in the Amazon basin from 2003 to 2020? As an input to data choice to be used to answer critical questions about the role of protected areas, we found that global burned area products used interchangeably on a regional scale could significantly underestimate the impacts of fire and, consequently, fire-related carbon emissions. Further, we estimated an annual average of 79,196 km² of the burned area from 2003 to 2020 in the Amazon basin, with the burned area peak registered in 2010. From the total area that burned throughout this period, only 28% was registered within protected areas, and among what annually burns inside protected areas, on average, 17% are registered within Indigenous lands. On average, 85% of what burns within protected areas yearly comes from fires ignited outside them. Differences-in-differences econometric estimates revealed a statistically negative effect of the protected area on fire. Estimates show that if, on average, one pixel-year became protected, there would be a decrease in the burned area of about 0.02 km² (2 $ha.pixel^{-1}.year^{-1}$). That is, for each piece of land of 2,800 ha protected, 2 ha are prevented from being burned yearly. Even though protected areas have recorded significantly smaller burned areas than their surroundings over the years, the proportion of inside burning in relation to the total burned per year has been increasing, signaling an increase in the threat to which these areas are exposed. The creation of new protected areas and management improvement of the existing ones, as well as law enforcement in their surroundings, should be a priority in national environmental agendas, given the relevance of these areas for the conservation of the largest tropical forest in the world.

Keywords: Indigenous lands. Causal effect. Econometrics. Wildfire. Geoprocessing.

AVALIAÇÃO DA OCORRÊNCIA DE FOGO EM ÁREAS PROTEGIDAS NA BACIA AMAZÔNICA DE 2003 A 2020

RESUMO

A Amazônia está se tornando um sistema bastante propenso ao fogo. A dinâmica tradicional do uso do fogo na região mudou nas últimas décadas, principalmente devido à intensificação da agricultura e ao crescimento demográfico. O avanço do desmatamento e a intensificação da degradação florestal resultam em uma paisagem mais fragmentada, que por sua vez favorece a entrada do fogo na floresta. Agravando esse cenário, modelos climáticos globais preveem uma Amazônia mais seca no século XXI. De fato, o clima está mudando, e a intensidade e frequência dos eventos de secas extremas geram condições ideais para o aumento da suscetibilidade das florestas aos incêndios. Nesse contexto, são necessários mecanismos políticos para quebrar esse ciclo e garantir a conservação dos ecossistemas tropicais. As áreas protegidas são consideradas estratégias adequadas para enfrentar esse desafio. No entanto, os últimos anos têm sido marcados por retrocessos na governança ambiental dessas áreas e pelo aumento de atividades ilegais que resultam em degradação florestal. Assim, fornecer evidências para a formulação de políticas e informar os tomadores de decisão sobre o papel das áreas protegidas na mitigação da degradação florestal causada por incêndios em áreas protegidas é essencial para priorizar ações em seu favor. Esta tese, portanto, se propõe a avaliar, por meio de análises quantitativas e com base em dados empíricos, o papel das áreas protegidas na mitigação da ocorrência de fogo na bacia Amazônica. Nesse sentido, o objetivo principal da tese foi alcançado ao responder a três questões principais: (1) existe uma diferença quantitativa e espacial no desempenho relativo entre os produtos da área queimada, considerando a área queimada sobre as coberturas florestais e não florestais? (2) O fogo é uma ameaça iminente e crescente às áreas protegidas na bacia amazônica? (3) As áreas protegidas afetaram a ocorrência de incêndios na bacia amazônica de 2003 a 2020? Como subsídio para a escolha de dados a serem usados para responder a questões-chave sobre o papel das áreas protegidas, mostramos que produtos globais de área queimadas usados de forma indistinta em escala regional podem subestimar significativamente os impactos do fogo e, consequentemente, as emissões de carbono relacionadas a ele. Além disso, estimamos uma média anual de 79.196 km² de área queimada de 2003 a 2020 na bacia Amazônica, com o pico de área queimada registrado em 2010. Do total de área queimada ao longo deste período, apenas 28% foi registrado em áreas protegidas e entre do que anualmente queima dentro, em média 17% são registrados em terras indígenas. Em média, 85% do que queima dentro de áreas protegidas por ano provem de incêndios iniciados fora delas. Além disso, a Bolívia é o país que queima relativamente a maior área em floresta, considerando a área total de floresta em cada país. As estimativas econométricas de diferenças-em-diferenças revelaram um efeito estatisticamente negativo da área protegida tanto na área queimada quanto nos incêndios ativos, mostrando assim que a proteção foi capaz de reduzir a ocorrência de fogo. As estimativas demonstram que se em média um pixel-ano se tornasse protegido, haveria uma diminuição da área queimada em cerca de 0,02 km² (2 $ha.pixel^{-1}.ano^{-1}$). Ou seja, para cada pedaço de terra de 2.800 ha protegidos, 2 ha são evitados de serem queimados por ano. Embora as áreas protegidas

tenham registrado áreas queimadas significativamente menores do que o seu entorno ao longo dos anos e tenham tido seu efeito inibitório contra a ocorrência de fogo confirmado com nossas estimativas, a proporção de área queimada dentro delas em relação ao total queimado por ano vem aumentando, sinalizando um aumento na ameaça a que essas áreas estão expostas. Dada a relevância dessas áreas para a conservação da maior floresta tropical do mundo, concomitante ao nível de ameaça a que estão expostas, a criação de novas áreas protegidas e o aprimoramento da gestão das existentes, bem como a aplicação da lei em seus entornos, deve ser prioridade nas agendas ambientais nacionais.

Palavras-chave: Terras indígenas. Efeito causal. Econometria. Incêndios florestais. Geoprocessamento.

LIST OF FIGURES

Page

LIST OF TABLE

Page

CONTENTS

Page

1 INTRODUCTION

Protected areas, including those with resident human populations, are necessary for an effective global strategy to minimize climate change and preserve tropical forests and ecosystem services (NEPSTAD et al., 2006). They account for more than half of the Amazon basin territory and guard strongholds of wild environments and cultural assets, essential for maintaining natural resources and ecosystem services for the planet's health and human well-being, regionally and globally. Furthermore, protected areas are effective shields against forest loss (AMIN et al., 2019; NEPSTAD et al., 2006; PFAFF et al., 2015a; SZE et al., 2022), prevent biodiversity loss (GELDMANN et al., 2013; PAIVA et al., 2020) and bring critical socioeconomic benefits to the regions where they are implemented (FERRARO; HANAUER, 2014; NAIDOO et al., 2019). In addition to being home to countless indigenous ethnicities and traditional communities, contributing to the protection of the cultural diversity of the Amazon, protected areas also help the planet, playing an essential role in climate patterns and constituting a valuable carbon sink (NOGUEIRA et al., 2018; SHI et al., 2020).

Although protected areas are effective in stopping the advance of deforestation while bringing several other benefits, these areas are not immune to deforestation, forest degradation, or climate change (DE OLIVEIRA et al., 2020; RORATO et al., 2021; VILLÉN-PÉREZ et al., 2020). The degree of deforestation has been increasing within these areas, leading to consequent forest fragmentation. The climate is also changing. Regions such as the southeast of the Brazilian Amazon have already registered an average increase of 2.5°C in temperature and a 24% decrease in precipitation (GATTI et al., 2021). This new climate configuration may transform the Amazon region into a carbon source instead of a sink, as it is traditionally described (GATTI et al., 2021). It further highlights the role of protected areas in offsetting the region's carbon emissions. Unfortunately, scientists already claim that the Amazon is close to reaching the tipping point, beyond which the changes resulting from its drying are irreversible (NOBRE et al., 2016). Nevertheless, if there is any hope of resilience and adaptation to these changes, it lives in the last portions of preserved forests in the region, which are largely within protected areas (SOARES-FILHO et al., 2010).

Deforestation rise within protected areas reflects the expansion of the agricultural frontier, mining activities, weak legislation on land titling, and the weakening of environmental policies (ARMENTERAS et al., 2019; ARMENTERAS; SCHNEIDER; DÁVALOS, 2019; DE OLIVEIRA et al., 2020; MATAVELI; DE OLIVEIRA, 2022). With particularities aside, this scenario seems to have occurred in the context of each country that is part of the Amazon basin in the last three years (EUFEMIA et al., 2022). Coupled with the deforestation process, fire occurrence also rose (SILVA JUNIOR et al., 2022). Fire is not only used to clear newly deforested lands but also to maintain pastures and agricultural areas later implanted. Thus, even with no deforestation, fire is still present in the system due to human activities (BARLOW et al., 2020). Moreover, once the environment becomes more flammable due to climate change, the fire traditionally used in a controlled way starts to reach adjacent forests more frequently, thus causing a relevant source of forest degradation and, consequently, carbon emission (BARLOW et al., 2020). Indeed, this process generates positive feedback, in which climate change makes the rainforest more vulnerable to fire, and the increasingly present fire boosts CO2 emissions, ultimately contributing to worsening climate change (COCHRANE, 2003). In another perspective, increasing fire frequency transforms forests into ecosystems increasingly vulnerable to degradation (ARMENTERAS et al., 2021). Therefore, reversing this trend is indispensable to mitigating and adapting to global climate change (ARMENTERAS et al., 2021).

This new climate and landscape configuration scenario threatens the integrity and ability of protected areas to play their role. Even avoiding deforestation, these areas may still be under increasing threat of degradation, becoming progressively vulnerable to fires. Although some research has been done on the role of such land use regulation policies in mitigating fire occurrence (NELSON; CHOMITZ, 2011; NEPSTAD et al., 2006; TASKER; ARIMA, 2016), they usually use fire as a proxy for deforestation. This way, they disregard specific mechanisms of fire occurrence in the Amazon, besides not quantifying avoided burned area extent, considering updated fire information. Thus, protected areas' effectiveness evaluation needs to include their role in avoiding fire occurrence and extent, considering this changing climate scenario. This thesis, therefore, proposes to evaluate, through quantitative analysis and based on empirical data, the role of protected areas in curbing fire occurrence in the Amazon basin. The project aims to

inform local and global policy, contributing to the production of scientific information to aid in decision-making regarding risk assessments and strategies to mitigate and adapt to the impacts of environmental changes.

1.1 Motivation and objectives

Considering the gap in the scientific literature of detailed and updated studies of the effect of protected areas on fire occurrence in the Amazon basin, the main objective of this thesis was to establish a methodology capable of formally quantifying such an effect. Therefore, the thesis answers two main questions:

i. Is fire a growing threat to Amazonian protected areas?
ii. What is the effect of protected areas on fire occurrence in the Amazon basin?

In this way, the quantification of the effect of the protected areas on fire occurrence implemented in this thesis was supported by three specific questions detailed below, divided by Chapters.

Chapter 3 brings an intercomparison in the Brazilian Amazon biome of three global burned area products and one regional, considering the total burned area detected and its influence on fire-related C emission. The motivation regarding this chapter relies on the necessity of having reliable measurements of burned area extent for the region, a prerequisite essential for a well-founded estimate of the effect of protected areas on fire. Therefore, the following question was proposed:

Q1: In the Amazon context, are there quantitative and spatial differences in the relative performance among burned area products, considering burned area over forest and non-forest land covers?

- H1.0: No: Even being developed independently and for different purposes and scales, the quantitative and spatial differences between the burned area products are negligible for the Amazon region, regardless of land cover. This result is probably due to the similarities in the algorithms for burned area detection shared among the products.
- H1.1: Yes: There are quantitative and spatial differences in burned area detection provided by the different products, both in forest and non-forest areas, and this

confers a significant difference in the fire-related carbon emission estimates in the Amazon region.

The second specific research objective, Chapter 4, is the formal measurement of the fire threat level that protected areas have been exposed to over the last 20 years. For this chapter, the motivation is based on the recognition that fire is widely used in the Amazon, constituting a persistent land cover change and agricultural practice used by all types of landowners and populations. Regardless of its purpose, fire can cause several impacts. Different factors are linked to a more significant threat to fire, and these factors are not always present similarly inside and outside protected areas. With that in mind, the following question was proposed:

Q.2: Is fire an imminent and growing threat to protected areas in the Amazon basin?

- H2.0: No: Fire occurrence within protected areas is negligible compared to outside, and its annual rate has remained constant in recent years. This result is probably because the factors that result in an increased fire threat have not changed significantly in recent years within protected areas.
- H2.1: Yes: The share of fire registered inside protected areas compared to the outside has been growing over the years.

Finally, the third specific objective of this research, explored in Chapter 5, considers that protected areas' inhibitory effect on fire can be confounded with other policies or factors' effects. This lack of identification may turn the estimates of the effect of the protected areas on fire biased or even non-detectable. Such effect has been estimated before in other studies, but never specifically for the Amazon basin and with a long and updated time series. Filling this gap is crucial to support policy to subsidize better management of protected areas, providing them with conditions to maximize their effectiveness against forest degradation. Therefore, the following question was proposed:

Q.3: Have protected areas affected fire occurrence in the Amazon basin from 2003 to 2020?

- H3.0: No: The protected areas had no significant effect on fire occurrence in the Amazon basin, considering an unbiased estimate.

- H3.1: Yes: The protected areas significantly and negatively affected fire occurrence in the Amazon basin, considering an unbiased estimate.

1.2 Thesis outline

This document is organized in a paper format, aggregating one paper that has already been published and two others in the analysis maturation and finalization process. Five chapters are provided, in addition to the introduction chapter, which is divided into a literature review, three chapters bringing the three different research papers, and the last chapter bringing the final remarks. The chapters are better described below.

Chapter 2 presents the main concepts of fire types that occur in the Amazon and how they are inserted in this tropical environment. It also summarizes the several impacts caused by fire, whether they are caused directly or indirectly by fire, such as the impact on human health due to smoke inhalation. In addition, it detailed aspects of fire-related carbon emissions and how future climate scenarios can worsen fire occurrence. Finally, a brief overview of land use regulation by protected areas in the countries of the Amazon basin is made, considering particularities in the different national contexts. With all this discretized, a fire occurrence chain was produced, showing the factors that directly and indirectly interfere in the occurrence of fire, inside and outside protected areas, and factors related to protected areas placement.

The burned area products intercomparison study aimed to base justifications for adopting the database used in the other chapters and understand the limitations that might be implicit in the estimates of protected areas' effect on fire. Chapter 3 brings an intercomparison of three global burned area products and one regional, developed independently and for different purposes and scales. It assessed the differences between products regarding total burned area detected, and their influence on fire-related C emission, in the Brazilian Amazon biome for 2015.

Chapter 4 provides a detailed diagnosis of the burned area by land cover inside and outside protected areas from 2003 to 2020 in the Amazon basin. From the chain of factors related to fire occurrence established in Chapter 2, analyzes are carried out to assess the increase in the threat to fire within protected areas. In this chapter, the protection

categories are discretized to evaluate the dynamics of fire occurrence according to each category.

Finally, Chapter 5, building on Chapters 2, 3, and 4 in terms of process understanding and database performance, provides a simplified attempt to quantity the protected area effect on fire occurrence based on an Econometric hybrid approach, combining Matching with Differences-in-Differences techniques. This combined approach allows for measuring the causal effect of protection on fires by considering several sources of bias. Moreover, using it obtains more reliable estimates given the many tests of methodological consistency and robustness required by the technique.

2 LITERATURE REVIEW

2.1 Fire occurrence in the Amazon: an environmental context

Before approaching the threat imposed by fires to Amazonian ecosystems, it is necessary to understand how fire is inserted into this system. Firstly, naturally occurring fires are a rare event in the Amazon with return intervals of hundreds if not thousands of years (BUSH et al., 2008). However, fires are often used as a tool to clear the land and maintain existing farmland and pasture, which makes their occurrence primarily associated with human activity (COCHRANE, 2003; PAUSAS; KEELEY, 2009). Furthermore, the slash-and-burn agriculture practice has been used in Amazon for many centuries (PEDROSO JUNIOR; MURRIETA; ADAMS, 2008), and it consists of cutting, drying, and burning the natural vegetation in a patch, which is cultivated for years and then left to regrow (PIVELLO, 2011). At first, the traditional burning activities were highly controlled to ensure the continued regeneration of forest resources (PIVELLO, 2011). Nonetheless, this dynamic changed over the last decades, mainly due to agricultural intensification and rural demographic growth (PEDROSO JUNIOR; MURRIETA; ADAMS, 2008), and the modern slash-and-burn practices have been shown to result in net deforestation, compromising the sustainability of these systems.

Increasing demand for agricultural land and forest-related products has exacerbated the link between fire and tropical deforestation by creating conditions conducive to expanded forest access (BARBER et al., 2014) and indirectly changing climatic patterns (ARAGÃO et al., 2008; MALHI et al., 2008). In addition, forests are facing extensive degradation in the Amazon. Consequently, the environment has become more conducive to fire ignition sources leaking into adjacent forests, mainly due to boosting the fuel concentration and altering the conducive to combustion and propagation (PARISIEN; MORITZ, 2009). Indeed, such degradation happens mostly on already fragmented and degraded forests that are more likely to burn (ARAGÃO et al., 2007; ARMENTERAS et al., 2017; CANO-CRESPO et al., 2015; COCHRANE, 2003; SILVA JUNIOR et al., 2018). This greater fire probability occurrence in places already previously burned can be used to fire prediction, a piece of useful information for fire risk alert systems (ANDERSON et al., 2021). Furthermore, this scenario sets up positive feedback, where fragmented forests are more likely to be affected by uncontrolled fires, which degrade the

vegetation even more, resulting in increased carbon emissions. This synergism between forest fragmentation and fire is becoming increasingly important, with an annual increment of up to 11,770 $\pm$ 3,546 km² of new forest edge in the Amazon (SILVA JUNIOR et al., 2020a).

Compounding this fire-conducive loop is climate change. Global climate models predict a drier Amazon in the 21st century (LI et al., 2008), and extreme drought events' intensity and frequency increase may push Amazonia toward an amplified fire-prone system (MALHI et al., 2009). The reason why droughts influence the occurrence of fires includes several factors, which ultimately culminate in increasing vegetation fire susceptibility (COCHRANE, 2003). Silva Junior et al. (2019) showed that in 2010 and 2015/2016, there were significant rainfall and temperature anomalies in the Brazilian Amazon biome. Especially during the extreme drought in 2015/2016, positive active fire anomalies resulted from increased burned forests. As dry seasons get longer and drier, low humidity generates ideal conditions for intentional fires, an agricultural management practice with undesired and often uncontrollable effects due to anomalous weather conditions (BUSH et al., 2008; NEPSTAD et al., 1999). In this way, considering this new climatic scenario in the region, even the traditional fire use embedded in the culture of several traditional communities and indigenous peoples can be harmful to the maintenance of forests.

Among the Amazonian countries, only Brazil had a significant negative temporal trend in deforestation from 2001 to 2015 (- 773 km² year^{-1}) (SILVA JUNIOR et al., 2020a). This considerable decrease in deforestation in Brazil, accompanied by climate change consequences, caused a relative decoupling of fire occurrence and deforestation, opposing to what would be expected for controlled fires (ARAGÃO et al., 2018). Between 2004 and 2017, there was a 75% reduction in deforestation rates (INPE, 2022). However, in 2017 there was an increase of approximately 18% in the number of active fires per square kilometer deforested, compared to the average of the last 13 years. It suggests an intensification of environmental degradation due to increased fire occurrence. Notwithstanding the growing deforestation dynamics in recent years, these processes are highly related. In 2019, the Brazilian Amazon registered abnormal increases in monthly active fire occurrence in the states of Roraima, Amazonas, and Acre, which also reached extreme levels of annual deforestation (SILVEIRA et al., 2020).

With all that understood, it is relevant to discretize the fire types in the Amazon. Fires in the region can be broadly classified as deforestation, maintenance, and forest fires with different temporal patterns related to climate conditions. However, in some cases, they are related to the ignition cause (ARMENTERAS et al., 2017). Deforestation fires are related to the process of forest clearing. Firstly, the vegetation is felled and left to dry, and then fire is used to prepare the area for agriculture or pasture (BARLOW et al., 2020). Maintenance fire is used on previously cleared lands as a soil management tool. These two fire types are supposed to be controlled and are still widely used in the Amazon (COCHRANE, 2003; MALHI et al., 2008; MORTON et al., 2008). However, fire has its most significant impact when it escapes from its intended purpose (COCHRANE, 2003). When these uncontrolled fires strike forest formations, they are called forest fires, a synergistic consequence of drought and human activity (BUSH et al., 2008). Hereafter, the term 'fire' will generally refer to all fire types. Current literature addresses the difference between controlled and uncontrolled fires considering forest fires alone or the total effect of fire. The impacts caused only by controlled fires still need to be better studied, especially as regards their contribution to greenhouse gas (GHG) emissions.

2.2 Fire occurrence in the Amazon: a political context

The Amazon basin countries do not have the same land use policies and climate action plans nor the same economic or infrastructure development (ARMENTERAS et al., 2017). Thus, the fire occurrence dynamic is expected to obey different patterns in each country. Nevertheless, all tropical forest edges in all countries are becoming increasingly more exposed to further disturbances (ARMENTERAS et al., 2017). As a result of the increased desiccation, forest structure and composition are being affected, causing forest degradation, a decline in living biomass, and finally, a reduction in their capacity to act as a carbon sink (BALCH et al., 2015). The following paragraphs will, however, bring particularities of the Amazonian territory occupation and consequently of fire occurrence in some of the different countries of the Amazon basin.

Deforestation in the Amazon is driven by the competitive use of land and the weak land titling regulation, which facilitates the illegal appropriation of public lands. Historically, Brazil's livestock contribution to deforestation has already hit 80% of the total deforested area (BRASIL, 2004). However, in the early 2000s, the expansion of mechanized soybean

agriculture in the Brazilian Amazon significantly changed the nature of deforestation activities, requiring a larger cleared area than pastures and ultimately converting the land in less than one year (MORTON et al., 2006). This recent land dynamic also includes the use of fire and intensifies the dependence on it since the same land patch needs to be cleared more often (MORTON et al., 2008). Furthermore, unlike the traditional slash-and-burn practice, this newly deforested land is not later left to regrow, which may compromise soil quality over the years (BALCH et al., 2011).

Land grabbing is also a relevant process of land occupation in the Brazilian Amazon. The weak land titling legislation (BRITO et al., 2019) and the history of recurring amnesties for environmental liabilities make it common to appropriate public lands. Land grabbers clear the forest to signal land occupation and claim land rights (BRITO et al., 2019), which culminates in an increase in deforestation and fire occurrence. A Law revision in 2017 (BRASIL, 2017) extended to 2017 the cutoff date when landholders that occupied federal public areas could request a land title from the federal government upon compliance with some requirements. This extension can cost between 1.1 and 1.6 million hectares of the deforested area until 2027 (BRITO et al., 2019). It is just another sign of a government that prioritizes the privatization of public lands at a price well below the market (BRITO et al., 2019) at the cost of using these lands for the benefit of Brazilian society. This dynamic is especially alarming, knowing that 360,000 km² of public land overlaps with private property. Almost half of this area is represented by undesignated lands, with low governance power and a high risk of illegal appropriation (CARVALHO et al., Submitted).

In Bolivia, the expansion of land cultivation and cattle during the 90's also triggered high deforestation rates in the Amazon region of the country (PERZ; ARAMBURÚ; BREMNER, 2005). However, as in Brazil, most deforestation appears not to ensue due to the activities of smallholders, who most often focus on labor-intensive and land-efficient coca production rather than land-extensive soybeans, cattle, or timber (PERZ; ARAMBURÚ; BREMNER, 2005). In addition, agricultural and livestock expansion in Bolivia is boosting forest fragmentation, which, combined with the droughts experienced in the region in the last decades, are causing greater fire permeability in tropical forests of that country (MAILLARD et al., 2020).

As in most Amazonian countries, the Colombian Amazon went through economic cycles of occupation, which included agricultural and livestock production. However, deforestation in Colombia has relevant particularities regarding that country's insurgency, coca production, and oil exploration. Peasant resistance to rural violence partly underlies insurgency movements such as the FARC, which have curbed, in some sense, the transformation of vast forests in many parts of Colombia (ARMENTERAS; SCHNEIDER; DÁVALOS, 2019). Since the signing of Colombia's peace accords late in 2016, deforestation probability within Colombian protected areas increased by 52%, and fire occurrence in that country is strongly correlated with forest loss (ARMENTERAS; SCHNEIDER; DÁVALOS, 2019). This correlation is not a defense of armed conflicts within these areas but, instead, evidence that urgent actions should have accompanied guerrilla demobilization in Colombia. Such actions include real-time forest monitoring, expanding programs to pay for ecosystem services at the frontier, and integrating demobilized armed groups as staff of protected areas (ARMENTERAS; SCHNEIDER; DÁVALOS, 2019). Unlike the other Amazonian countries, Colombia's deforestation roots are deep, institutional, and societal (ARMENTERAS et al., 2019). Land grabbing also constitutes a significant threat to the forests of this country since institutional incentives for land speculation coupled with extreme inequality in tenure are the main engine of deforestation (ARMENTERAS et al., 2019).

Land settlement in Ecuador's Amazon also has proceeded slowly and over a long time but accelerated in the 1970s following oil discoveries during the 1960s. Consequently, the Ecuadorian Amazon has experienced profound land use and cover changes during the last decades. In this country, the Amazonian region occupation is mostly related to oil exploration-led frontier expansion, various social responses, and spillovers from Plan Colombia[1], which led coca producers to migrate to Ecuador (PERZ; ARAMBURÚ; BREMNER, 2005). These well-documented changes are slowly modifying the physical environment of the region from one dominated by the classic humid tropics to one more reminiscent of the eastern Amazon basin with cyclical moisture and temperature gradients, consequent emergent fire regimes, and persistent deforestation (MESSINA; COCHRANE, 2007). In contrast to the Amazon in Bolivia and parts of Brazil, land use

[1] Plan Colombia was a military operation to protect oil infrastructure and eradicate coca plantations (PETRAS, 2001).

in the Ecuadorian Amazon is not generally geared for exports (PERZ; ARAMBURÚ; BREMNER, 2005), other than the coca plantations that were brought into the country in response to Plan Colombia.

Peruvian Amazon became more occupied during the 80s and 90s when the insurgent group Sendero Luminoso encouraged smallholder coca production to finance land settlement. At the same time, cattle ranching has emerged as an important activity in the region, largely a response to national economic growth during the 90s and plans for a transoceanic highway through Brazil and Peru (PERZ; ARAMBURÚ; BREMNER, 2005). Moreover, as in Ecuador, the oil industry also set an important economic activity in the region and is highly related to road opening (FINER et al., 2015). Unlike other Amazonian regions, in Peru, fire frequency increases with drought and proximity to roads. However, particularly in this region of the Amazon was found that decreases in rural population also increase fires, probably due to increased flammability of emptying rural landscapes and reduced capacity to control fire (URIARTE et al., 2012).

In Venezuela, the main deforestation processes were historically concentrated in the northern region of the Orinoco River (PACHECO; AGUADO; MOLLICONE, 2014). Compared to other Amazonian countries, the Venezuelan Amazon historically registered low deforestation rates (PERZ; ARAMBURÚ; BREMNER, 2005), possibly associated with its remoteness from most development planning and population change (PERZ; ARAMBURÚ; BREMNER, 2005). Although in the mid-80s, the agricultural census indicates a low percentage of cropland and cattle production in the Venezuelan Amazon, recent forest loss and fires are most likely resulted from the expansion of the agricultural frontier (PACHECO; AGUADO; MOLLICONE, 2014). Venezuela was already the third Amazonian country most affected by wildfires from 2001 to 2018 (DA PONTE et al., 2021). Along with Ecuador, it had its Indigenous lands most affected by fires in numbers relative to each country's total Amazon Basin area (SILVA JUNIOR et al., 2022).

2.3 Fire impacts

Both controlled and uncontrolled fires have many direct and indirect impacts on the environment, economy, and population (ANDERSON et al., 2015; BARLOW et al., 2020; CAMPANHARO et al., 2019, 2021) (Table 2.1). Environmental impacts are those related to the atmosphere, biodiversity, soil, and water. Besides, forest fires can

destabilize the carbon stocks of tropical ecosystems, promote direct economic losses to the forestry, agriculture, and transportation sectors, and impact the population's health (CAMPANHARO et al., 2021).

Table 2.1 - Fire impacts and their respective effect and scale information.

	Effect	Scale
Social impacts		
Death	D and/or I	L
Injured	D and/or I	L
Respiratory diseases	I	R
Psychological traumas	D and/or I	R
Accidents	D and/or I	R
Economic impacts		
Tourism drop	I	R
Cultural resources losses	D	L
Production loss	D and/or I	L
Infrastructure damage	D	R
Environmental impacts		
Atmosphere		
Aerosols and CO_2 emissions	D and/or I	G
Changes in weather patterns	I	G
Atmosphere heating	I	G
Biodiversity		
Biodiversity reduction	D	L
Changing habitats	D	L
Biota death	D and/or I	L
Soil		
Change in physical soil properties	D	L
Soil organic matter burn	D	L
Increase erosive processes	I	L
Water		
Change water quality	I	L
Hydrological cycle change	I	R

Note: D = direct; I = Indirect. G = Global; R = Regional; L = Local.

When evaluating fire impacts, it is also important to consider the effect and scale. First, fire impacts can be classified as direct or indirect. Direct effects are those caused by fire and its sub-products, such as smoke and ash. The indirect ones, in turn, are those caused due to the consequences of fire occurrence (RYAN et al., 2012). The extent of impacts can be evaluated from a local to a global scale, affecting several agents differently. In general, fire impacts interconnect, forming a complex chain so that the few direct effects trigger others at different scales and affect different actors (Table 2.1).

Wood burning, such as forest and agricultural fires, emits significant quantities of known health-damaging pollutants, including several carcinogenic compounds (CAMPANHARO et al., 2021; NAEHER et al., 2007). The increased accidental forest fires and long-burning events resulted in a growing concern about woodsmoke's potential health impacts. Carmo et al. (CARMO et al., 2010) suggested that the particulate matter levels of burnings in the Amazon are associated with adverse effects on children's respiratory health. Corroborating, Campanharo et al. (CAMPANHARO et al., 2021) found a positive effect of fire on hospitalizations due to respiratory illnesses. 5% of respiratory hospitalizations were estimated to be attributable to fire-induced pollution, corresponding to 822 cases per month. In addition to respiratory diseases and other social impacts, the overload of aerosols released into the atmosphere during fires can affect the water cycle, the pollution burden of the atmosphere, and the dynamics of atmospheric circulation (ANDREAE et al., 2004).

When it reaches forest formations, fire affects local diversity. Besides the immediate direct effect, the impact caused by fire on the forest ecosystem can last for years, reducing forest biomass by enhancing tree mortality rates (SILVA et al., 2018a). In the Amazon, fire-induced tree mortality increases by up to 462% in a drought year, causing a sharp decline in canopy cover and aboveground live biomass, favoring widespread invasion by flammable grasses across the forest edge area where fires are more intense (BRANDO et al., 2014). Silva et al. (2018a) found that fire-affected forests in Amazon have biomass levels 24.8 $\pm$ 6.9% below unburned forests after 31 years, showing that biomass loss through mortality is not sufficiently compensated by incremental growth and recruitment. These two studies prove that fire-affected ecosystems do not fully recover even after many years of regeneration.

Translating fire impacts into economic costs, Campanharo et al. (2019) estimated a total economic loss for Brazilian Acre state in 2010 of US$ 243.36 $\pm$ 85.05 million, and from 2008 to 2012, US$ 307.46 $\pm$ 85.41 million. This cost estimation included direct impact on land use and land cover, carbon stocks, CO_2 emissions, and indirect impact on human illness. Investing this amount in environmental initiatives could favor positive feedback by potentially reducing the fire incidence, and the economic cost of the impact caused. Therefore, increasing human presence in fire-prone ecosystems requires increased efforts

to actively manage fires for ecosystem conservation and human well-being (ANDELA et al., 2019; MORITZ et al., 2014).

Despite many impacts, using fire as a tool also confers some benefits. It consists of an inexpensive and accessible soil management tool for agricultural producers, allowing low-cost land preparation, low-cost elimination of slashed vegetation during deforestation, low-cost pasture management, and low-effort subsistence production. These benefits are considerable, even with repeated burnings reducing soil quality in the long term, considering a shorter fallow. Because of this, it is important to contextualize its use in impact assessments.

2.3.1 Fires and carbon emissions

Despite so many negative impacts, perhaps the biggest concern worldwide is the contribution of fires to increasing CO_2 in the atmosphere, making them play an essential role in climate change (ANDERSON et al., 2015; SILVA JUNIOR et al., 2021c; SILVEIRA et al., 2020). One of the international scenario's most prominent fire-related environmental impacts is its contribution to CO_2 emissions (ARAGÃO; SHIMABUKURO, 2010; GATTI et al., 2014; SILVA et al., 2018a; SILVA JUNIOR et al., 2021c). Forest fires contribute significantly to climate change, removing plant biomass and transferring the associated carbon (C) to the atmosphere (GATTI et al., 2014). Consequently, the atmospheric C concentrations increase, influencing the greenhouse effect. Fire-related C emissions are accounted for by national-level inventories indirectly by accounting for deforestation. However, the emissions not associated with deforestation are not properly accounted for yet, which could underestimate a gross release of 989 ± 504 Tg CO_2 in the Amazon, an amount more than half as great as from old-growth forest deforestation during drought years (ARAGÃO et al., 2018; SILVA JUNIOR et al., 2021c). Therefore, the increasing fire susceptibility imposed by droughts (SILVA JUNIOR et al., 2019) and the projection of future drier conditions turn the C emission in the Amazon more dominated by forest fires, rather than the prevalence of emissions from fires directly associated with deforestation processes (ARAGÃO et al., 2018).

During extreme drought, gross C emissions can be up to 1.7 times higher than in a normal climatic year (GATTI et al., 2014). Moreover, fire-related C emissions can destabilize

Amazon's C balance once drought tends to increase the variance of the photosynthetic capacity of Amazon forests (ANDERSON et al., 2018). For example, considering C losses from fire under extreme drought conditions, Gatti et al. (2014) found that vegetation turned from a net C sink to being C neutral.

In 2010, the fire-related C emissions were 0.51 $\pm$ 0.12 Pg C $year^{-1}$ (GATTI et al., 2014) for the entire Amazon basin, corresponding to 57% of global emissions resulting from land use change (0.9 $\pm$ 0.7 Pg C $year^{-1}$). In the same year, forest fires in Legal Amazon alone contributed 86% (68% to 103%) of the annual C emissions target set by the National Climate Change Plan, Decree nº 7,390/2010 (ANDERSON et al., 2015). Silva Junior et al. (2019) estimated that, during the droughts registered in 2010 and 2015/2016, fire-related CO_2 emissions were 0.47 Pg CO_2. When considering Brazil's national target for reducing carbon emissions (approximately 0.11 Pg CO_2 per year from 2006 to 2017), fire-related CO_2 emissions only in 2010 represented 209% of it. Besides, Silva et al. (2018a) found that the carbon stock depletion caused by drought-induced forest fires can last for more than 30 years, significantly reducing forest biomass and high wood density trees. The increased frequency and extent of these drought-induced forest fires can slow down or stall the post-fire recovery of Amazonian forests (SILVA et al., 2018a).

Finally, it is evident the considerable participation of fires in C emissions and the growing tendency of this contribution if considering the projections of future climate change. Therefore, in order to comply with national C emission reduction targets established under international agreements, it is essential that this contribution is duly accounted for (SILVA JUNIOR et al., 2021c). Policymakers, then, must review current fire-related legal instruments and the already adopted anti-deforestation policies and focus on adapting them or designing new instruments capable of properly incorporating the effects of climate change on C emissions. This revision must include a coherent plan for regularizing and protecting the public and indigenous lands and actions committed to Amazonia's local social, environmental, and economic development (SILVA JUNIOR et al., 2021a).

2.4 Land use regulation policies

Land use regulation is a political mechanism ensuring that strategic public or private lands are safeguarded to guarantee common goods for society. Then, protected areas can be

defined as all public or private areas under land-use restrictions that contribute to protecting native ecosystems, even if they were created for purposes other than environmental conservation (SOARES-FILHO et al., 2010). Studies have shown that protected areas, including those with resident human populations, are necessary for an effective global strategy to minimize climate change and preserve tropical forests and ecosystem services (MELILLO et al., 2016; NEPSTAD et al., 2006, 2009; NOGUEIRA et al., 2018; RICKETTS et al., 2010; SOARES-FILHO et al., 2010). For example, it is estimated that protected areas in the Brazilian Amazon biome accounted for 54% of the forest remnant and contained 56% of its carbon up to 2010 (SOARES-FILHO et al., 2010). If properly implemented, protected areas have the potential to avoid 8.0 $\pm$ 2.8 Pg of C emissions by 2050 (SOARES-FILHO et al., 2010), albeit the benefits associated with their implementation go far beyond avoided carbon emissions. Protected areas are also recognized as effective instruments for reducing biodiversity loss (GELDMANN et al., 2013) and improving socioeconomic conditions (FERRARO; HANAUER, 2014; NAIDOO et al., 2019).

An important mechanism of protected areas is their categorization. The categories are fundamental to ensure the strict protection of critical ecosystems because they are highly threatened or contain endangered species. However, they also guarantee the legality of occupation and traditional activities by communities that depend on the natural resources of these areas. Another important case is the possibility of coupling the protection of ecosystems and ecologically based tourism, which is done in all Amazonian countries through national parks and natural monuments (SALVIO; GOMES, 2018). Creating a protected area intrinsically imposes restrictions on land use, and, therefore, the correct categorization is essential to achieving its specific objectives. It is common to encompass protected natural areas and indigenous lands for more comprehensive studies on protected areas. Other areas are often not included in national inventories, making it difficult to obtain spatial data on them, and/or their size makes the analysis scale incompatible with the spatial data most used today[2].

[2] This is the case of Brazilian quilombolas territories and private areas protected under the Brazilian Forest Code.

Indigenous lands are generally a portion of the national territory inhabited by one or more indigenous tribes. They are intended to guarantee their productive activities, indispensable for preserving the environmental resources necessary for their well-being and physical and cultural reproduction, according to their customs and traditions (BRASIL, 1988). Although there is a consensus that indigenous peoples have the original right to their lands of traditional occupation, the legislation of each Amazonian country for the recognition of these lands differs. Therefore, the administrative process of demarcation goes through different spheres according to each country. Likewise, there are differences in the management and land use rules within these areas, but all Amazonian countries reaffirmed their objective to guarantee the way of life of indigenous populations.

Protected natural areas, broadly referred to in this thesis as protected areas, are those provided for in the National Systems of Protected Areas. Each Amazonian country designates and describes specific protected categories provided by law that are possible to be created (Table 2.2). These systems are also unique by country; despite many nomenclature overlaps, they also have many national particularities. The same name often describes quite different categories between countries, and the opposite is true; two different names may refer to the same type of land use regulation in two countries (SALVIO; GOMES, 2018). Table A.1 presents the specific national description of each category found in each country.

In an international context, to understand the role of different protection categories for environmental conservation and human well-being, national-specific categories must be homogenized in a common spectrum among all countries. Only this way, a minimum of coherence in intra-category analyses is guaranteed. In this sense, the International Union for Conservation of Nature (IUCN) proposes seven broad categories into which national categories can be classified. IUCN protected area management categories classify protected areas according to their management objectives. The categories are recognized as the global standard for defining and recording protected areas and, as such, are increasingly being incorporated into government legislation. However, like all generalizations, the suggested IUCN categories do not accommodate the particularities of

each country, and often the original national description does not fully fit IUCN definitions (SALVIO; GOMES, 2018).

Table 2.2 - National systems of Protected Areas of the Amazonian countries.

Country	Original system name	Creation year
Bolivia	Sistema Nacional de Áreas Protegidas (SNAP)	1992
Brazil	Sistema Nacional de Unidades de Conservação da Natureza (SNUC)	2000
Colombia	Sistema Nacional de Áreas Protegidas (SINAP)	1994
Ecuador	Sistema Nacional de Áreas Protegidas del Ecuador (SNAP)	1976
French Guiana	Espaces protégés de Guyane	2013
Guyana	National Protected Areas System (NPAS)	2011
Peru	Sistema Nacional de Áreas Naturales Protegidas por el Estado (SINANPE)	1997
Suriname	-	-
Venezuela	Áreas Bajo Regime de Administración Especial (ABRAE)	1989

Based on the original national descriptions, a simpler categorization was suggested in this thesis. It considers whether the protected area is indigenous land or the restriction level on the use of natural resources (Table A.1). This type of category generalization has been used before in other studies (e.g., NOLTE et al., 2013; PFAFF et al., 2015b; SOARES-FILHO et al., 2010). Each protected area was categorized in one of the three categories based on its original definition and with subsequent confirmation by specialist collaborators in each country[3].

In addition, protected areas can still be classified according to the jurisdiction of their creation. Jurisdiction for managing protected areas can be federal, departmental, or municipal. The national categories are often followed in other jurisdictions, such as Brazil and Peru. However, it is also the case that each jurisdiction adopts different categories, nomenclatures, and descriptions according to the jurisdiction, as in Bolivia. Although jurisdiction has already been proven as a relevant factor in the effectiveness of these areas

[3] We thank Dr. Galia Selaya (Bolivia), Dr. Dolors Armenteras (Colombia), MSc. Lorena Benitez (Ecuador), Ms. Géraldine Derroire (French Guiana), Ms. Odacy Davis (Guyana), MSc. Eddy Mendoza (Peru), Ms. Kaminie Tajib (Suriname), Dr. Roberto Rivera-Lombardi (Venezuela) for their valuable contribution in reviewing the final categorization used in this chapter.

(HERRERA; PFAFF; ROBALINO, 2019), this aspect will not be addressed in this thesis, considering all protected areas, regardless of their jurisdiction.

The role of protected areas in curbing deforestation has already been the subject of many studies (ANDAM et al., 2008; NEPSTAD et al., 2006; PFAFF et al., 2015a; SOARES-FILHO et al., 2010). Despite being often portrayed scientifically, there is still a gap in the literature on the role of these areas in mitigating fire occurrence in the Amazon. Nepstad et al. (2006) found that protected areas, including those that allow human residency, have reduced fire in the Brazilian Amazon. However, their analysis only included data from 1998, which does not give us a long-term and up-to-date idea about the process. Nelson and Chomitz (2011) found that from 2000 to 2008, indigenous lands reduced forest fire incidence by 16 percentage points in Latin America. This study provides important evidence of the protected areas' role in fire occurrence. However, it does not detail the results at the national level, which makes it difficult to incorporate relevant information into policy decisions, in addition to not including important political and economic dynamics in the post-2008 Amazon region.

2.5 Fire within land use regulation policies: when and where is it legal to use fire?

Fire ecology, or simply the study of the interaction of fire with the environment, is still a topic that has not been properly addressed in the legislature of the Amazon countries. Indeed, there is a gap in the Amazonian country's legal frameworks to address fire use and management (MISTRY et al., 2019). In contrast with the substantial progress in environmental legislation and establishment of national and regional forest programs over the last 20 years, the current Brazilian government has also highlighted national governments' virtual inability to control or limit increasing deforestation and forest degradation (EUFEMIA et al., 2022). Rather than preventative and (sustainable) management, regulations are frequently focused on fire suppression and risk adaptation approaches, such as capacity building for fire brigades. (EUFEMIA et al., 2022). Then, the following paragraphs will present a brief review of relevant points of each Amazonian country's fire regulations.

In Brazil, the fire was mentioned in the second Forest Code in 1998. Despite prohibiting fire use, by any means, in forests and other vegetation formations, it included an exception to the use of fires in farming and forestry practices if regional or local particularities could

justify it. This exception activity was later regulated by Decree nº 2661/1998. Considering the precautionary rules, this decree authorized fire use under a controlled burning regime, defined as the fire used as a production and management tool, and for scientific and technological research purposes, in areas with previously defined physical limits and subject to prior license. The Decree nº 2661/1998 has regulated the National System for Prevention and Combating Forest Fires (PREVFOGO) under the Brazilian Institute of Environment and Renewable Natural Resources (IBAMA) coordination. PREVFOGO is responsible for developing programs to order, monitor, prevent and combat forest fires, including raising the population's awareness of inadequate fire use risks (BRASIL, 1998). The new Forest Code, which came into force in 2012, also brings the same regulation for fire use. However, it brings the authorization for controlled burning in protected areas, considering fire as a tool for the management of the native vegetation, whose ecological characteristics are associated evolutionarily to fire occurrence (BRASIL, 2012). These regulations, however, do not define the permitted burning area or specific seasons at which burnings are allowed. Furthermore, an aggravating factor in fire fighting, control, and prevention actions is the stratification and distribution of roles across administrative levels. The lack of more concrete role definitions contributes to uncoordinated and inefficient practices in combatting fires in the Brazilian Amazon (EUFEMIA et al., 2022).

Unlike other Amazonian countries, Brazil stood out in deforestation reduction during the last 20 years (INPE, 2022). Political efforts highlight the importance of combating deforestation and forest degradation. Brazil has already accomplished an 84% reduction in deforestation rate in 2012 compared to 2004 (INPE, 2022). The reduction in deforestation followed the adoption of a set of policies. The most notable one is the Action Plan for Prevention and Control of Deforestation in Amazonia (PPCDAm). However, even with the reduction in deforestation, the proportion of fire per kilometer deforested increased (INPE, 2017), showing that fire can be a process uncoupled from deforestation (ARAGÃO et al., 2018). In addition, since 2019, deforestation rates have sharply increased (SILVA JUNIOR et al., 2021a), going back to rates found two decades ago (INPE, 2022). No different, fire occurrence has broken records year after year since 2019, forcing the government to adopt urgent and often ineffective and costly measures (EUFEMIA et al., 2022; SILVEIRA et al., 2020; VALE et al., 2021). This dynamics of coupling-decoupling between deforestation and fire is evidence that anti-deforestation

policies alone may not be enough to contain and prevent fires, especially considering the social aspect of fire use in the Amazon region. Besides, climate change, coupled with a lack of governance, is boosting fire occurrence and stifling any positive effect policies might have on fire.

In Bolivia, the environmental agenda has been dampened by adopting incentives for predatory development in terms of exploiting or even destroying natural resources. Since 2013, the government has passed several regulations allowing for agricultural expansion, unsustainable infrastructure development (such as regional road networks), violations of land rights and land tenure in forested areas, and the promotion of deforestation (FUNDACIÓN SOLÓN, 2020). Two regulations mark this recent setback in the Bolivian environmental agenda; firstly, Law 1171, from 2019, established the guidelines for the National Policy of Integrated Fire Management. Although this law regulates all administrative sanctions for unauthorized burning, its enforcement was soon put on hold due to pressure from the agroindustry sectors (FUNDACIÓN SOLÓN, 2020). Again in 2019, Supreme Decree 3973 authorized land clearing for agricultural activities in two large departments of eastern Bolivia adjacent to the Amazon rainforest, clearing the way for the pressure over natural resources to get even closer to the forest. This political approach reflects the high rates of deforestation in the region and, consequently, the rising occurrence of fires.

In the Colombian Amazon, fires are associated with advances in agricultural and livestock activities, tenure inequality, the weakness of property rights, and poor fire-management practices (ARMENTERAS et al., 2019). In Colombia, the political context is particularly relevant in deforestation and forest degradation dynamics. Armed guerrillas occupied regions with the highest concentration of protected areas for decades (EUFEMIA et al., 2022). Although these regions have been impacted by coca production, deforestation and forest degradation intensified after a peace agreement between the largest guerrilla group, FARC-EP, and the Colombian government was signed in 2016 (ARMENTERAS; SCHNEIDER; DÁVALOS, 2019). The increase in forest degradation in the Colombian Amazon reflects, in part, the weak governance of fire use in the region. Indeed, there are regulatory gaps in farmers' and local communities' fire use and management (EUFEMIA et al., 2022). Like Bolivia, the few pro-environmental initiatives that emerge in Colombia,

such as Fire Management Law 221, soon prove largely ineffective and unimplemented. This scenario is strongly linked to an extractive (often centralized) political and economic agenda (EUFEMIA et al., 2022). Indeed, this contradicts Colombia's leading role in legally recognizing the Colombian Amazon as a “subject of rights.”

The Ecuadorian Amazon is also highly impacted by deforestation and forest fires, reflecting the historical disconnection of environmental policies regulating fire use and protected areas (EUFEMIA et al., 2022). However, the importance of ecotourism to the regional economy has led to the adoption of preventive measures and alternative practices for using and managing fire in agricultural activities. These measures became the core of the national program “Amazon without Fire” (PASF) and the creation of the National Committee for Integrated Fire Management (Conamif), both public policy instruments established in the Regulations of the National Environmental Code (EUFEMIA et al., 2022). Among the Amazonian countries, Ecuador is taking the leading role in recognizing the importance of fire-regulated and controlled use by implementing alternative practices that contribute to protecting the environment and improving community living conditions (EUFEMIA et al., 2022).

As a French overseas department, French Guiana responds to French and EU legislative frameworks on environmental policies (EUFEMIA et al., 2022). Disregarding site-specific fire use, culturally or economically, the French Environmental Code, the national forest law, and several decrees on national parks make fires in protected areas illegal. In Guiana, incorporating REDD+ into the National Forest Plan and Policy and the Code of Practice for Timber Harvesting includes regulations supporting fire suppression and prevention (EUFEMIA et al., 2022). These regulations are mostly based on the implementation of forest carbon financing mechanisms and capacity-building schemes of national forest fire management (RODRÍGUEZ et al., 2011). The mismatch between such regulations and the extensive burning in the region evidences the governance lack and weak institutions to properly implement them (EUFEMIA et al., 2022). Suriname has comparatively few environmental policy instruments at the national level, which reflects the lack of fire management capacity (EUFEMIA et al., 2022). Going against the recognition of the fundamental role of indigenous lands in environmental conservation, the Surinamese government accumulates conflicts with indigenous peoples with its

inadequate approach to protected areas implementation, including violation of human and land rights (HAALBOOM; CAMPBELL, 2012).

Likewise, the Brazilian approach, the Peruvian fire legal framework, is more reactive, focusing primarily on effective fire suppression rather than on preventive measures to control and regulate fires or on the development of forestry (MOURAO; MARTINHO, 2019). For instance, regulations in the National Service of Natural Protected Areas and National Plan for Risk Management and Adaptation to Climate Change in the Agricultural Sector include mechanisms to deal with existing fires in a timely and planned manner, aiming to minimize their impacts, especially on rainforests (EUFEMIA et al., 2022). However, as in Brazil, the lack of concrete roles in fire management, and in the Peruvian case, the shared responsibility among different ministries (environmental and agriculture) may lead to a lack of coordinated approach, limiting the implementation of current legislation (EUFEMIA et al., 2022).

Venezuela, on the other hand, is moving in the opposite direction. Its fire-management programs and policies prioritize proactive and preventive measures rather than being simply reactive (EUFEMIA et al., 2022). The new Forest Law, from 2013, provides a new set of activities related to human–forest relations that promotes popular consultation at both regional and local levels. This approach has been called "intercultural and participatory fire management." It is a space for dialogue and collaborative research that supports a new paradigm based on the knowledge exchange between indigenous people, farmers, scientists, and authorities (ELOY et al., 2019). However, Venezuela historically faces several challenges regarding the socio-economic and political aspects. These challenges undermine its capacity to fight illegal activities in the Amazon region, mainly related to mining. Even though its protagonist role in participative fire management shows an important advance in recognition of traditional knowledge as part of the solution to environmental degradation, and as such, it should be seen as a model by other countries in the Amazonian region.

3 INTERCOMPARISON OF BURNED AREA PRODUCTS AND ITS IMPLICATION FOR CARBON EMISSION ESTIMATIONS IN THE AMAZON[4]

3.1 Introduction

Naturally occurring fires are a rare event in the Amazon, with return intervals of hundreds if not thousands of years (BUSH et al., 2008). However, fires are often used as a tool to clear the land after deforestation or maintain existing farmland and pasture, which means their occurrence in the Amazon is primarily associated with human activity (COCHRANE, 2003; PAUSAS; KEELEY, 2009). These two fire types, deforestation fires and management fires, impose risks on adjacent forests, and when these are impacted, the third main type of fire occurs, the forest fires. Forest fires contribute significantly to global climate change, consuming plant biomass and transferring part of the carbon (C) stock to the atmosphere (GATTI et al., 2014). For example, the gross C emissions from forest fires across the Brazilian Amazon (270 ± 137 Tg C $year^{-1}$) (ARAGÃO et al., 2018) corresponded to 80% of the Brazilian emissions resulting from land use change (338 ± 142 Tg C) (DE AZEVEDO et al., 2018) during drought years. Additionally, forest fires in the Brazilian Legal Amazon contributed 86% (68% to 103%) to the annual C emission reduction target (ANDERSON et al., 2015) set by the Brazilian National Climate Change Plan (BRASIL, 2018).

Despite this remarkable contribution, forest fire-related C emissions are not yet accounted for in national-level inventories. The quantification of deforestation-related fire emissions in these inventories takes into account the strong relationship between these two processes (r^2 = 84%, $p < 0.004$) (ARAGÃO et al., 2008). However, in the last decade, a relative decoupling between deforestation and fire incidence has been observed, disaggregating these two processes in terms of emissions (ARAGÃO et al., 2018). This pattern has been associated with an amplification of forest fragmentation (SILVA JUNIOR et al., 2018) and an increase in extreme drought frequency (ARAGÃO et al., 2018), favoring the leakage of deforestation and management of fires into surrounding forests. These anomalous climate events have happened more often during the last few decades

[4] This chapter is an adapted version of the paper: PESSÔA, A. C. M. et al. Intercomparison of Burned Area Products and Its Implication for Carbon Emission Estimations in the Amazon. Remote Sensing, v. 12, n. 23, p. 3864, 25 nov. 2020.

(JIMÉNEZ-MUÑOZ et al., 2016; MARENGO et al., 2011), and global climate models predict a drier Amazon in the 21st century (COX et al., 2008; LI; FU; DICKINSON, 2006). Recently, the area of burned forests relative to the total burned area has increased during extreme droughts. For example, an increase of 51–99% in the forest burned area was observed in the 2015/2016 extreme drought years in relation to the average from 2006 to 2016 (SILVA JUNIOR et al., 2019). In addition, fires reduce forest carbon storage by approximately 25% compared to pristine forests (SILVA et al., 2018a), highlighting the impact of forest fires on the carbon balance. Therefore, the prevalence of forest fires during extreme droughts makes it urgent to account for non-deforestation fire-related carbon emissions (SILVA JUNIOR et al., 2019).

In order to have fire-related C emissions adequately accounted for, it is essential to accurately estimate the extent, location, and land cover affected. In this sense, several methodological approaches have been developed using remote sensing applications to detect and monitor fires (ANDERSON et al., 2015; GIGLIO et al., 2018; PENHA et al., 2020; PETTINARI; CHUVIECO, 2018; SHIMABUKURO et al., 2015). The burned area can be detected by remote sensing in various ways. The diversity of methodologies, the availability of multiple sensors, and the fast development of new technologies reflect the high number of burned area products. They can be developed for different purposes, reach different scales, and present different spatial resolutions, varying considerably in distribution, size, and frequency of mapped fires (MOUILLOT et al., 2014). Therefore, there is a need for reliable burned area extent estimation to improve fire-related C emission estimates in this region. In this sense, intercomparison is an important and practical tool for characterizing burned area products according to their performance (HUMBER et al., 2019; PADILLA et al., 2015) when field validation points are not available.

Nonetheless, intercomparison implicitly assumes that, as a whole, the products being compared provide a reasonable approximation of the conditions on the ground (HUMBER et al., 2019). It should be recognized as a complementary evaluation to product validation. Since no product is a ground portrait, and all have limitations, choosing which product to use should consider the advantages and disadvantages of the data use objective, considering the regional performance. It must be recognized that the

main challenge is trying to precisely balance the pros and cons and identifying the implications of choice.

Only a few studies have been conducted to compare different burned area products (FORNACCA; REN; XIAO, 2017; HUMBER et al., 2019; PADILLA et al., 2014; RUIZ et al., 2014; TSELA et al., 2014). Currently, there is a dearth in the literature providing a regional intercomparison of burned area products for the Amazon (HUMBER et al., 2019). Therefore, it is critical to evaluate the relative performances of the most-used global burned area products in forest and non-forest areas to provide clear information regarding their limitations and implications. This work performed an intercomparison of three global burned area products and one regional; all developed independently and for different purposes and scales. The study considered the total burned area detected and its influence on fire-related C emission in the Brazilian Amazon biome for 2015. The specific objectives were as follows: (i) evaluate the differences and similarities among the products regarding the total burned area detected, considering burned areas detected over forest and non-forest land covers; (ii) evaluate the differences and similarities in fire-related carbon emission estimates, and (iii) evaluate the spatial differences and similarities among the products. We hypothesize that the product variation increases in forest areas due to the difficult distinction of the burned areas in this land cover type (ANDERSON et al., 2017; PEREIRA et al., 2004; ROY; BOSCHETTI, 2009).

The next sections are organized to provide a brief review of burned area detection techniques with remote sensing data, followed by the description of the study area and the burned area products considered in this study. We finally describe our intercomparison approaches and present their results regarding the burned area and committed C emissions.

3.2 Burned area detection by remote sensing

The detection and mapping of burned areas aim to produce spatially-explicit data on the extent of fire-affected areas, usually using data from optical sensors on the solar spectrum (CHUVIECO et al., 2019). This data ranges from the visible light (0.4–0.7 μm) to the short wave infrared (SWIR) bands (1.4–2.2 μm). The radiation reflected by the Earth's surface in these spectral regions (reflectance) is influenced by the target chemical and physical characteristics and the sun–target–sensor geometry (CHUVIECO et al., 2019).

Data from the thermal infrared spectrum (0.7–2.2 μm) can also be used to map burned areas, but they are commonly integrated with other optical bands (PEREIRA et al., 1999). The near-infrared (NIR, 0.7-1.0 μm) and SWIR (1.4–2.2 μm) spectral regions are especially sensitive to forest structure changes (PLENIOU; KOUTSIAS, 2013b). Therefore, they are widely used to generate spectral indices or ratios for burned area detection (BOSCHETTI; STROPPIANA; BRIVIO, 2010; CHUVIECO; MARTÍN; PALACIOS, 2002; LONG et al., 2019; MITHAL et al., 2018; PLENIOU; KOUTSIAS, 2013a; SILVA et al., 2004). However, due to a strong variability in the spectral characteristics of both pre- and post-fire conditions and the fire intensity and severity, using such indices may lead to the misclassification of burned areas, especially in forest environments (BOSCHETTI; STROPPIANA; BRIVIO, 2010). Furthermore, as all of them are based on reflectance changes related to the immediate charcoal/ash deposition and lingering changes in the vegetation structure, they are also highly dependent on the temporal behavior of such conditions (CHUVIECO; MARTÍN; PALACIOS, 2002; MELCHIORRE; BOSCHETTI, 2018).

A burned area mapping algorithm based on spectral indices derived from moderate resolution imaging spectroradiometer (MODIS) imagery and daily active fire data is described by Giglio et al. (GIGLIO et al., 2018). Their final product, MODIS Direct Broadcast Monthly Burned Area Product Collection 6 (MCD64A1), presented a global omission error of 0.73 (BOSCHETTI et al., 2019), showing the conservative aspect of their methodology, and the underestimation that unsupervised algorithms can generate. When considering tropical forest ecosystems, the omission and commission errors are still higher (0.9060 and 0.6350, respectively) (BOSCHETTI et al., 2019). Bastarrika et al. (2014) developed a supervised burned area mapping software (BAMS), which analyzes the temporal behavior of a multispectral index derived from Landsat images. However, their algorithm has only been tested in temperate forests, and its application for burned area mapping in tropical regions is more complex. Some of the challenges regarding burned area mapping in tropical forests are the high and persistent cloud cover and canopy closure, which can preclude the detectability of understory fires.

Another way to highlight features of interest, such as burned areas, is through a linear spectral mixing model (LSMM) (ANDERSON et al., 2005). LSMM is based on a linear

relation representing the spectral mixture of different targets within a pixel. The data dimensionality (the number of reflectance bands) is reduced by generating fraction images to represent the proportion of each target of interest within the resolution cell. Usually, the LSMM is processed to represent three targets (e.g., vegetation, soil, and shade). Shade fraction images are more efficient than spectral indices in mapping burned areas in the Amazon (ANDERSON et al., 2005). Many studies have used LSMM to detect burned areas in the Brazilian Amazon (ANDERSON et al., 2005; CARDOZO et al., 2014; LIMA et al., 2012; SHIMABUKURO et al., 2009, 2014). They use moderate and/or coarse-resolution images (e.g., MODIS and/or Landsat, respectively) to perform LSMM, followed by shade fraction image segmentation and unsupervised classification. This approach proved to be an efficient method for mapping burned areas. However, all these studies require a final manual image interpretation procedure to minimize misclassifications.

A fundamental parameter that influences the detection of burned areas by satellites is the sensor resolution, both spatial and temporal. Most fire occurrence products are developed with satellite data with a coarse spatial resolution (> 250 m). Coarse spatial resolution images make the development of automatic mapping very challenging due to the variability in the spectral characteristics of the burned area. On the other hand, a medium spatial resolution (~30 m) gives more reliability to evaluating the burned area (SHIMABUKURO et al., 2015). However, these sensors often have worse temporal resolutions, and their longer revisit time decreases the chances of obtaining cloud-free images. This can be critical for burned area mapping over tropical regions, where the recovery of the spectral signal of vegetation can be quick, and cloud cover is persistent (LONG et al., 2019). The spatial resolution can also induce the underestimation of small fires, leading to a considerable underestimation of the global burned area (GIGLIO et al., 2018; RANDERSON et al., 2012). For example, this limitation can underestimate fires in croplands by as much as ten times (GIGLIO et al., 2018).

3.3 Study area

The study area corresponds to the Brazilian Amazon biome below the equator line. The area comprises about 74% of the Legal Amazon, and 73% of its 3,583,565 km² was covered by forest in 2016 (Figure 3.1). The study area includes the states of Acre (AC),

Rondônia (RO), and portions of the states of Amazonas (AM), Pará (PA), Amapá (AP), Maranhão (MA), Mato Grosso (MT), Tocantins (TO) and Roraima (RR) (Figure 3.1).

Figure 3.1 - Study area located in the Legal Amazon. Forest proportion in a 10x10 km grid cell, extracted by the PRODES forest mask of 2016 used to select burned areas over forest. It is presented the total area of each Brazilian state that intersects the study area and their respective percentage area and forest area within the considered boundaries.

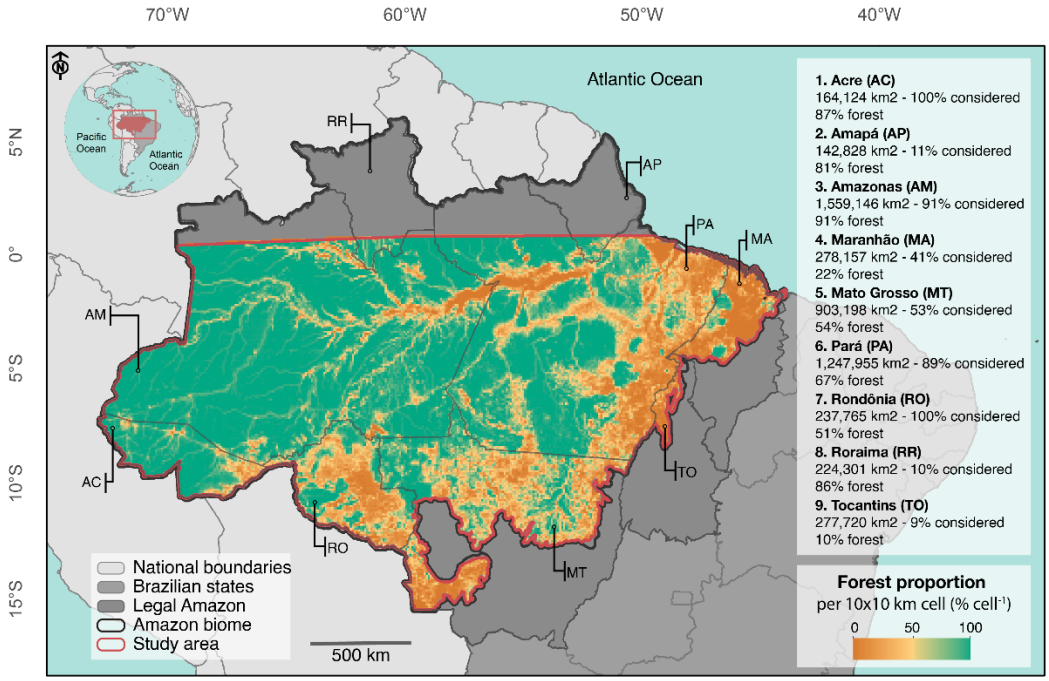

Table 3.1 - List of Brazilian states included in the study area, their respective total area, and forest area within the study area boundaries.

State		State area (km^2)	State area within the study area (km^2)	Proportion of the state area within the study area (%)	Forest area within the study area (km^2)	Forest proportion within the study area (%)
Rondônia	**RO**	237,765	237,765	100	121,777	51
Acre	**AC**	164,124	164,124	100	142,368	87
Amazonas	**AM**	1,559,147	1,413,520	91	1,288,699	91
Roraima	**RR**	224,301	21,393	10	18,475	86
Pará	**PA**	1,247,955	1,110,326	89	742,538	67
Amapá	**AP**	142,829	15,304	11	12,415	81
Tocantins	**TO**	277,721	23,973	9	2,288	10
Maranhão	**MA**	278,157	114,860	41	25,583	22
Mato Grosso	**MT**	903,198	480,699	53	260,016	54
	Total	**5,035,197**	**3,581,964**	**71**	**2,614,158**	**73**

For the regional analysis, we considered only the percentage of area that falls within the study region of states with more than 40% of their area considered and under similar rainfall regimes (dry season from July to October) (Figure 3.1, Table 3.1). In addition, since the TREES product does not consider the northern hemisphere region in its mapping

due to the difficulty in obtaining cloud-free images, we excluded this region from our analyses to consider the common mapping area among all four products.

3.4 Materials and methods

3.4.1 Burned area products

Currently, more than 13 open-access burned area products are available worldwide (Table B.1), which are widely used. We considered three global burned area products and one regional product for the intercomparison evaluation (TREES, MCD64A1, GABAM, and Fire_cci) (Table 3.2). The products were chosen to consider the spatial scale since we would like to compare the global products with a regional one and the spatial resolution. In addition, we would like to analyze the effect of higher-resolution inputs in burned area detection. Therefore, we chose two global products that are widely used in the literature (MCD64A1 and Fire_cci), a recently published global product that has a spatial resolution of 30 m (GABAM), and a regional product developed particularly for the Amazon region (TREES).

Table 3.2 - Specifications of the burned area products to be compared.

Name	Developer	Scale	Time Span	Sensors/Inputs	Spatial Resolution	Reference
TREES	TREES—INPE	Regional (Brazilian Amazon)	2006–2016	MODIS	250 m	(1)
MCD64A1 c6	NASA	Global	2000–present	MODIS (surface reflectance and active fires)	500 m	(2)
GABAM	Institute of Remote Sensing and Digital Earth—Chinese Academy of Sciences	Global	2000, 2005, 2010, 2015 and 2018	Landsat 8 OLI	30 m	(3)
Fire_cci v.5.0	ESA	Global	2001–2016	MOD09GQ (surface reflectance) MOD09GA (quality flags) MCD14ML (active fires)	250 m	(4)

Note: (1) (ANDERSON et al., 2005, 2015; SHIMABUKURO et al., 2009); (2) (GIGLIO et al., 2018); (3) (LONG et al., 2019); (4) (CHUVIECO et al., 2018).

The Tropical Ecosystems and Environmental Sciences lab (TREES), based on the National Institute of Space Research (INPE), developed their burned area product on a regional basis that covers 86% of the Amazon biome, developed as part of multiple projects[5] (ANDERSON et al., 2005, 2015; SHIMABUKURO et al., 2009). Their product,

[5]Project Amazonica—NERC/grant: NE/F005806/1; Project *Estimativa de emissões de CO2 por desmatamento e degradação florestal utilizada como subsidio para definição de municípios prioritários para monitoramento e controle*—CAPES/grant; Project Mapping and monitoring forest degradation using remote sensing data with medium and moderate spatial resolution—FAPESP/grant: 16/19806-3.

called here TREES, is available upon request for 2006 to 2016 in an annual composite dataset. The product was developed using a hybrid classification method to delineate burned areas. First, the images of bands 1, 2, and 6 (red, near-infrared, and medium infrared) of the product MOD09A1Q1 were used as input to the LSM model. Then, a water mask is applied to avoid the detection of water pixels, and unsupervised classification of the shade fraction image is carried out. In this fraction image, the burned areas are highlighted, facilitating the distinction of these targets on the terrestrial surface (SHIMABUKURO et al., 2009). Subsequently, an expert inspection is carried out to improve the accuracy of the final map, especially in forested areas, where burned areas can be easily confused or undetected (ANDERSON et al., 2005, 2015). Finally, the map accuracy resulting from the methodology adopted by TREES was quantified using a point-based method, considering a study case in Mato Grosso state for 2010 (ANDERSON et al., 2017). This product presents an overall accuracy for forested (0.9920) burned areas slightly higher than for non-forested (0.9630) burned areas (Table 3.3).

Table 3.3 - Accuracy information of four burned area products.

Burned Area Product	Overall Accuracy	Omission Error	Commission Error	Validation Method Summary	Reference
TREES					
Forest areas	0.9920	0	0.1600	Point-based validation. A stratified random sample of 300 points was distributed over the burned and unburned forest on Landsat images for Mato Grosso state, 2010. The points are verified by experienced interpreters.	(ANDERSON et al., 2017)
Non-forest areas	0.9630	0.4852	0.1067		
MCD64A1 c6					
Global	0.9970	0.7260	0.4020	Globally distributed reference dataset from March 1st, 2014, to March 19th, 2015, consisting of high-resolution reference maps derived from 1116 Landsat images visually interpreted. These independent reference data were selected using a stratified random sampling approach that allows for the probability sampling of Landsat data in both time and space.	(BOSCHETTI et al., 2019)
Tropical forests	0.9940	0.9060	0.6350		
GABAM	0.9392	0.3013	0.1317	It considered 80 validation sites globally, from where it acquired data from Landsat 8, CBERS-4 MUX, and Gaofen-1 WFV. The reference burned areas were mapped with a semi-automatic classification method and refined with the manual edition.	(LONG et al., 2019)
Fire_cci v5.0	0.9972	0.7090	0.5123	A stratified random sample of 1200 pairs of Landsat images, covering the whole globe from 2003 to 2014.	(CHUVIECO et al., 2018)

MCD64A1 is a global dataset on burned areas developed by the National Aeronautics and Space Administration (NASA). The product has been freely available from 2000 to the present. Incorporating MODIS surface reflectance data coupled with 1 km MODIS active

fire observations, its algorithm uses a burn-sensitive vegetation index (VI) to create dynamic thresholds applied to produce the monthly composite data (GIGLIO et al., 2018). The current collection (c6) algorithm has already improved from older ones. In addition, there is a continuous effort to minimize its limitations (more details in Table A.1). The product has been applied as input for the development of other burned area products (ARTÉS et al., 2019; GIGLIO; RANDERSON; VAN DER WERF, 2013), as well as for the development of the Global Fire Atlas. The Global Fire Atlas includes information on ignition locality, fire line, speed, and direction of spread, which is essential to understanding the dynamics of individual fires and, therefore, better characterizing the changing role of fire in the Earth system (ANDELA et al., 2019). It has also been used as input for biomass burning emissions models (RANDERSON et al., 2012; SHI; MATSUNAGA; YAMAGUCHI, 2015) to study the relation between fire and land cover change (FANIN; VAN DER WERF, 2015), and to track the response of fire occurrence to climate change (CHEN et al., 2017).

The Global Annual Burned Area Mapping (GABAM) is a recently released burned area product developed by Long et al. (2019). It is built from an automated algorithm implemented on Google Earth Engine (GEE). It uses reflectance data from the Landsat 8 Operational Land Imager (OLI) and spectral indexes information as input for a Random Forest model. A final step consists of burned area shaping through a region growth approach (LONG et al., 2019). GABAM is currently the global dataset with the highest spatial resolution (30 m). However, it is only available for 2000, 2005, 2010, 2015, and 2018 and in a yearly composite, which does not allow seasonal analysis within a year. Nevertheless, its validation process showed lower omission (0.3013) and commission (0.1317) errors compared to Fire_cci and MCD64A1 (Table 3.3). Implementing the algorithm in GEE constitutes a great advance in mapping approaches since the tool is open source, provides an extensive catalog of medium-resolution images, and allows for cloud processing, which considerably increases the data incorporated in the process.

The product Fire Disturbance (Fire_cci) is part of the Climate Change Initiative (CCI) program developed by the European Space Agency (ESA). A MODIS dataset is used to map the burned areas, including reflectance images (MOD09GQ), quality masks (MOD09GA), and active fires (MOD14ML) (CHUVIECO et al., 2018) (Table 3.2). The

images are aggregated into monthly composites, and the classification algorithm is based on region growth after selecting seed pixels. Spatial and temporal parameters are then used to reduce commission and omission errors (CHUVIECO et al., 2018). The final product is made available on a global scale. Version 5.0 was used in this work since it was the most updated version when this work was developed. Among the products developed using coarse spatial resolution data, Fire_cci was the first to provide a global dataset with a 250 m resolution. Its validation process indicated an overall accuracy of 0.9972, with 0.7090 global omission errors and 0.5123 commission errors (Table 3.3). A new version of Fire_cci (version 5.1) was recently released (LIZUNDIA-LOIOLA et al., 2020). The new version brings improvements to the burned area detection algorithm, which has allowed the detection of more burned areas globally compared to version 5.0, and expands the time from 2001 to 2019 (LIZUNDIA-LOIOLA et al., 2020). However, even with the improvements, the product has omission and commission errors similar to the previous version. Evaluating the southern hemisphere of South America, the product detects less burned area than the product MCD64A1 for the period 2005–2011. Its performance improvement seems much smaller than the results obtained for the African continent (LIZUNDIA-LOIOLA et al., 2020).

In the following sections, these products will be called TREES, MCD64A1, GABAM, and Fire_cci. We considered only burned area polygons detected between June and November 2015 to guarantee temporal compatibility among the products analyzed. For GABAM, burned areas throughout the year were considered, as this is the only temporal resolution available. In order to extract the burned area over the forest, we applied the old-growth forest mask of 2016, produced by the Amazon Forest Deforestation Calculation Program (PRODES) (INPE, 2022) (Figure 3.1). It covers the period of August 2015 to July 2016 and is thus a conservative mask for forest cover. The non-forest class corresponds to other land covers. It is important to highlight that, despite the TREES product presenting the best results regarding errors of omission and commission. Because it is a product designed specifically for the study region involving a visual interpretation correction phase, we did not consider it as reference data. Our objective here was to compare the products with each other and to analyze the relative performance of each one in mapping burned areas in the Amazon, not to validate them based on a reference. We emphasize that each product has its development methodology, which incorporates

advantages and limitations and even assumes that, as a whole, the product provides a reasonable approximation of the conditions on the ground, none of which is the truth to be used as a reference.

3.4.2 Committed gross carbon emission estimation

To estimate the committed gross carbon emission, we used the above-ground biomass (AGB) map developed by Environmental Monitoring via Satellite in The Amazon Biome - MSA/Amazon Fund - Subproject 7 - Estimating Biomass in the Amazon (EBA). The above-ground biomass (AGB) was estimated at three different levels based on 836 LiDAR transects randomly distributed across 3.5 million km² of the Amazon forest. The methodology was based on LiDAR AGB estimates (LONGO et al., 2016) and validated using field inventory AGB data (CHAVE et al., 2014). Then, the LiDAR AGB was extrapolated for the Amazon biome by using a nonparametric regression method (Random Forest) to model the AGB by using remote sensing data of MODIS vegetation index, Shuttle Radar Topography Mission data (SRTM), precipitation data from the Tropical Rainfall Measuring Mission, Synthetic Aperture Radar data of the Phased Array type L-band Synthetic Aperture Radar and geographic coordinates. The coefficient of determination and the root mean squared error obtained with the final model of the third level of AGB estimation were $R^2 = 0.7485$ and RMSE = 54.36 Mg ha^{-1}, respectively.

The estimated AGB uncertainty map was calculated by propagating the uncertainties through the different levels of biomass estimation, field plots (first level), LiDAR transect (second level), and satellite (third level). The first and second levels were calculated according to Longo et al. (2016), considering calibration uncertainty, representativeness uncertainty, and prediction uncertainty. Next, the wall-to-a-wall uncertainty map was developed, propagating the total LiDAR AGB uncertainty to all cells covered by the AGB map of the Amazon biome. This was calculated using the mean and standard deviation of the AGB by the total uncertainty and AGB value of each cell of the LiDAR transect. Then, a hundred AGB wall-to-wall maps were generated using the normal distribution values for AGB, remote sensing variable, and random forest regression model. The final uncertainty map was generated by calculating each cell's standard deviation of AGB.

The EBA map covers the Amazon biome, providing AGB density information for 2016 at a 250 m spatial resolution and an associated uncertainty map. Even though our analysis

was done for 2015, we used the map for 2016 because just a minimum fraction (2%) of the burned area of 2015 overlapped the deforested area of PRODES 2016 (Table 3.4). Therefore, the emissions associated with these areas were considered negligible compared to the total amount estimated for each burned area product.

Table 3.4 - Total burned area and its intersection area with PRODES 2016.

	Burned area Non-forest + Forest (km²)	**Burned area over PRODES 2016 (km²)**	**%**
TREES	35558.6	658.8	1.85
MCD64A1	34514.1	513.1	1.49
GABAM	28193.3	750.8	2.66
Fire_cci	14924.3	243.2	1.63

The committed carbon gross emission was estimated based on the relationship between the biomass before and after the fire, measured within a maximum one-year gap (Equation 3.1).

$$B_f = 0.05 \cdot B_i^{1.47} \quad (3.1)$$

Bf is the above-ground living biomass (Mg ha^{-1}) after the fire, and *Bi* is the initial above-ground living biomass given by the AGB map. The difference between *Bi* and *Bf* gives us the committed biomass density. After we applied this model to obtain the committed biomass density per cell, we transformed this density map into an absolute biomass value by calculating the correct biomass proportion given the cell area. Then, following the Intergovernmental Panel on Climate Change's (IPCC) approach (IPCC, 2013), we obtained the committed carbon map by multiplying the biomass per 0.5, that is, the amount of committed carbon per pixel. The committed carbon emission is the sum of all cells that fall within the burning polygons, considering the different products. The same approach was used for the biomass uncertainty map since it provides a biomass density value to be used as an uncertainty interval of the value presented in the AGB map, thus resulting in a committed carbon uncertainty map. In the same way, the uncertainty of the committed carbon emission is the sum of all cells that fall within the burning polygons, considering the different products.

Table 3.5 - Summary of the data used for developing.

Reference	Location	Vegetation type	Control (Mg.ha^{-1})	Mean AGB after fire (Mg.ha^{-1})
(1)	Brasília (15º 51'S, 47º63'W)	Cerrado	7.128	2
			7.321	0.237
			8.625	2.226
			10.031	1.604
(2)	Tailândia (Central-eastern Pará)	Tropical moist evergreen forest	295	270
(3)	Rio Maró, westernmost Pará (02°44′S; 55°41′W)	Riverbanks forests	424.3	341.7
(4)	Rio Maró, westernmost Pará (02°44′S; 55°41′W)	*Terra firme* forests	95.4	46.8
			91	54
(5)	Paragominas (NE of Pará)	Dense forest with vines	485	339.5
	Santana do Araguaia (South of Pará)	Transitional forest	390	273
	Alta Floresta (North of Mato Grosso)	Open forest	370	259
(6)	Alta Floresta (North of Mato Grosso)	Open forest	199	88
(7)	Roraima	Dense forest	237	202.3
(8)	Acre (southwest region)	Open forest	203	212
	Amazonas (central region)	Dense forest	230	286

Note: (1) (KAUFFMAN; CUMMINGS; WARD, 1994); (2) (COCHRANE; SCHULZE, 1999); (3) (HAUGAASEN; BARLOW; PERES, 2003); (4) (BARLOW et al., 2002); (5) (ALENCAR; NEPSTAD; DIAZ, 2006); (6) (ALENCAR; NEPSTAD; MOUTINHO, 2005); (7) (BARBOSA; FEARNSIDE, 1999); (8) (SILVA et al., 2018a).

This model shows a strong correlation between the incidence of fire and the initial biomass existing before burning. The hypothesis assumes that with increased biomass, microclimate conditions are more conducive to maintaining humidity within the canopy, reducing the intensity and susceptibility to fire spreading (BRANDO et al., 2012). This method is an improvement of Anderson et al. (2015) since it incorporates new data from Silva et al. (2018a). We adopted the committed gross carbon emission model adjusting the relationship between biomass before and after fire through a power function. All values compiled for establishing the equation were derived from measurements of AGB within one year after fire occurrence (Table 3.5). This method only accounts for the short-term (1 year) carbon loss, although it is reported in the literature that long-term biomass losses may happen for as much as 30 years after a fire event (SILVA et al., 2018a). The update function is shown in Figure 3.2, where we found a highly significant relationship between biomass before (control) and after the fire ($R^2 = 0.95$).

Figure 3.2 - Relationship between initial biomass and remaining biomass after fire events. Plots compiled from the literature have burned only once, with measurements taken within one year of the fire event.

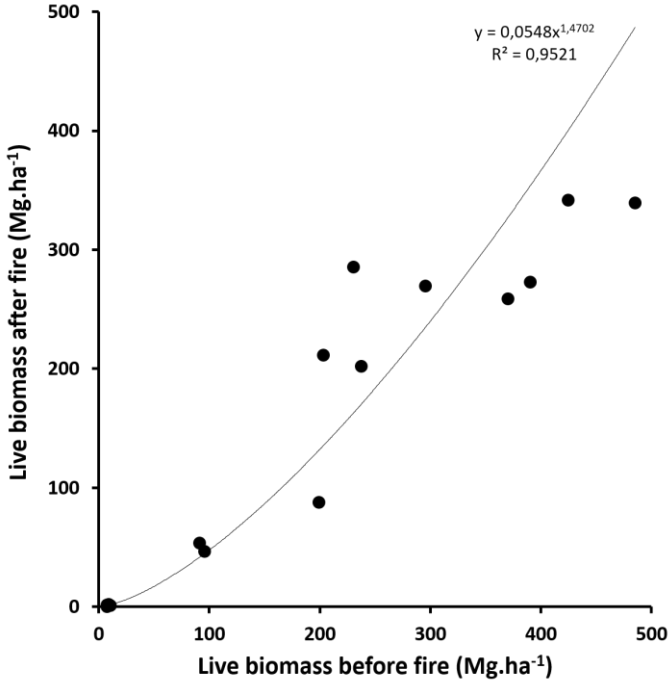

3.4.3 Total and regional analysis

We adopted two approaches for the analyses: the vector approach, which was applied to evaluate the agreement between the total burned area detected by each product and to estimate its impact on carbon emission, and the matrix approach, which was applied to investigate the spatial variations in these results.

The total burned area was computed for each of the four products on the vector approach, considering the forest and non-forest classes. This processing was carried out using the 'rgeos' package (BIVAND; RUNDEL, 2018) in R statistical software (R CORE TEAM, 2020). Subsequently, the C emission maps (EBA and EBA uncertainty) were used separately to extract the sum of committed gross C emissions within each burned area polygon, considering the different land cover classes. This process was carried out on R, using the 'raster' package (HIJMANS, 2017). Of the total 113,190 km² burned area detected, considering all four products, 0.3% was not considered due to polygon size incompatibility with the resolution of the carbon data. The most affected product was GABAM, whose deleted polygons summed 133.3 km2. This area, however, represents

only 0.5% of the total burned area of this product and, therefore, can be considered insignificant. The estimates were also made separately for each Brazilian state included in the study area to generate information for decision-making since the states have autonomy in seeking investments under Reducing Emissions from Deforestation and Forest Degradation (REDD+) initiatives.

We compared the absolute value of the difference in C emission estimate between every burned area product pair with the maximum uncertainty value between them to assess whether the error embedded in the burned area data is greater than the estimated emission uncertainty. Therefore, this strategy can be considered conservative since the maximum uncertainty value was used for the comparison. The following conditions were tested (Equation 3.2):

$$IF \begin{cases} |C_{p1} - C_{p2}| - \max\left(UC_{p1}, UC_{p2}\right) > 0; \textit{the burned area product choice significantly alters the carbon emission estimation} \\ |C_{p1} - C_{p2}| - \max\left(UC_{p1}, UC_{p2}\right) < 0; \textit{the burned area product choice does not significantly alter the carbon emission estimation} \end{cases} \quad (3.2)$$

C_{p1} is the committed gross C emission estimation using burned area product 1n, and C_{p2} is the same, using a second burned area product. UC_{p1} is the committed gross C emission uncertainty associated with the estimation using burned area product 1 and UC_{p2}, the same as using a second burned area product. Therefore, if the absolute value of the difference between the committed gross C emission estimation among the two products is smaller than the committed gross C emission estimation uncertainty, we can conclude that the difference among the products is within what is expected for the uncertainty of the AGB data. Therefore, the choice of one product or another does not cause significant over- or underestimation of committed gross C emission in the considered area.

For the matrix approach, the burned area products, considering the different land covers, were incorporated into a regular grid with an approximately 10 km spatial resolution. The incorporation accounted for the proportion of the polygon falling inside each grid cell. This process was run on R using the 'raster' package (HIJMANS, 2017). The statistical comparison between the six possible combinations of product pairs was carried out using the non-parametric Kolmogorov–Smirnov two-sample test (SMIRNOV, 1939). We used a bootstrap approach, implemented in R statistical software v.4.0.2 (R CORE TEAM, 2020), with 10,000 iterations. For each iteration, the algorithm randomly raffled a sample

of 10% of the total cells in each case with replacement. Finally, based on the bootstrap results, we calculated the mean and standard deviation of the 10,000 p-values. The comparison considered only cells that presented burning detection by at least one product.

Subsequently, the regular grid was converted into raster files carrying the burned area information for each combination of burned area product and land cover for the spatial comparison. Like the statistical comparison, we considered only cells that presented burning detection by at least one product. The burned area maps were then compared two by two, within each land cover class, using the fuzzy numerical method implemented in the Map Comparison Kit 3 (MCK) application (VISSER; DE NIJS, 2006). The fuzzy numerical method considers grades of similarity between pairs of cells in two numerical maps. Although it is a cell-by-cell comparison method, it considers the neighborhood to express the similarity of each cell in a value between 0 (fully distinct) and 1 (fully identical) (RIKS BV, 2013). The fuzzy technique allows one to distinguish real differences from minor mapping artifacts, besides giving a spatial assessment and clarifying the location of disagreement and the severity (RIKS BV, 2011).

Considering that the burned area registered in a cell is partly defined by the cells found in its proximity, the fuzziness of location influence level is accounted for via a function. In this study, we adopted an exponential decay function with a Halving distance equal to 2 and considered the neighborhood radius equal to 4. This is the default setting for the algorithm implemented in MCK. In the fuzzy numerical model, the similarity of two values (a and b) is calculated following Equation 3.3. The resulting statistic for overall similarity is then the average similarity over the whole area considered.

$$S(a,b) = 1 - \frac{|a-b|}{\max(|a|,|b|)} \tag{3.3}$$

3.5 Results

3.5.1 Vector approach: intercomparison of total burned area

The four burned area products differ according to the total area mapped and, consequently, the total C that is emission-related (Figure 3.3). The most similar products in the total mapped area and C emissions are TREES and MCD64A1. MCD64A1 presents only 2.9% less total burned area than TREES, 0.9% in non-forest and 10% in forest areas (Figure 3.4). The most significant difference occurs between TREES and Fire_cci, with

the second mapping 58% less burned areas; 52% and 78% for non-forest and forest, respectively.

Figure 3.3 - (a) Total burned area mapped by TREES, MCD64A1, GABAM, and Fire_cci over forested and non-forested areas, considering the whole study area. (b) Committed gross carbon emission related to fires according to the four burned area products.

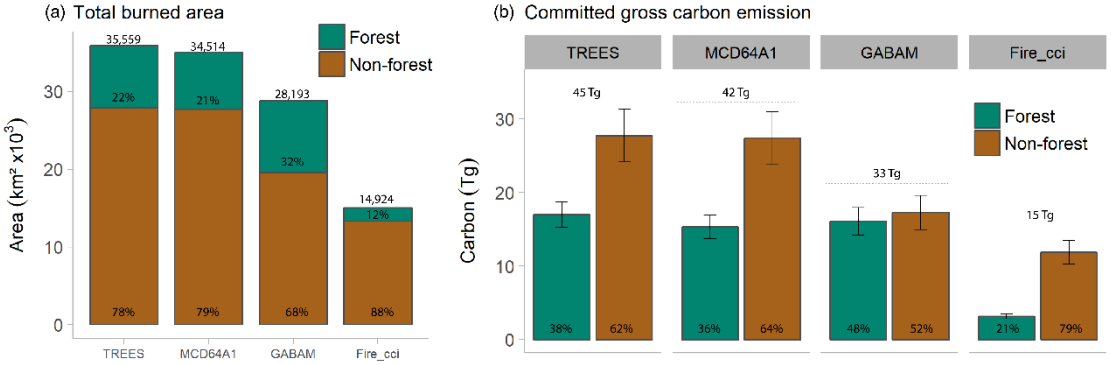

Regionally, TREES, MCD64A1, and GABAM present the same pattern of the burned area both over non-forest and forest, whereby eastern Amazonian forests (Pará state) were the most affected area (Figure 3.4, Figure 3.5). Despite this, GABAM presents 41% more forest area mapped in this region than TREES and 22% more than MCD64A1. GABAM also presents more burned area over forest in central Amazonia (Amazonas state), mapping 120% more burned area than TREES and 85% more than MCD64A1. On the other hand, in the far east Amazonia (Maranhão state), GABAM has a poorer performance, mapping up to 53% less burned area than the TREES product.

In southwestern Amazonia, in Acre state, we also observed great divergence between the products. TREES presents more burned areas in non-forest than the other products, and the difference can be up to 40 times compared with Fire_cci. Interestingly, GABAM presents the highest forest burned area mapped, close to the TREES product and 160 times larger than the Fire_cci product. Fire_cci, in general, registered less burned area in all cases and sites.

Figure 3.4 - Burned area and committed gross carbon emission registered by TREES, MCD64A1, GABAM, and Fire_cci products.

	Non-forest		*Forest*	
	Burned Area (km²)	**Committed gross carbon emission (Tg)**	**Burned Area (km²)**	**Committed gross carbon emission (Tg)**
TREES				
AC	599.87	0.90 ± 0.11	325.75	0.90 ± 0.09
AM	1,851.42	2.80 ± 0.35	799.00	2.29 ± 0.23
MA	3,627.20	2.28 ± 0.32	1,588.15	2.05 ± 0.23
MT	6,926.70	6.35 ± 0.84	2,054.39	4.20 ± 0.42
PA	11,758.06	11.28 ± 1.48	2,366.94	5.43 ± 0.55
RO	2,809.91	3.93 ± 0.48	851.24	2.09 ± 0.22
Study Area	**27,573.16**	**27.54 ± 3.58**	**7,985.46**	**16.96 ± 1.73**
MCD64A1				
AC	82.83	0.09 ± 0.01	30.91	0.08 ± 0.01
AM	1,960.86	2.84 ± 0.35	953.27	2.40 ± 0.24
MA	4,603.61	3.16 ± 0.44	1,044.92	1.45 ± 0.17
MT	7,223.08	6.06 ± 0.83	1,744.56	3.39 ± 0.35
PA	11,464.73	12.13 ± 1.58	2,724.44	6.14 ± 0.64
RO	1,998.08	2.78 ± 0.34	682.85	1.65 ± 0.17
Study Area	**27,333.20**	**27.06 ± 3.56**	**7,180.95**	**15.12 ± 1.58**
GABAM				
AC	119.85	0.14 ± 0.02	346.97	0.85 ± 0.10
AM	744.66	1.15 ± 0.14	1,762.93	3.42 ± 0.39
MA	3,438.36	2.27 ± 0.32	741.10	0.88 ± 0.10
MT	3,964.23	2.89 ± 0.42	2,038.23	3.19 ± 0.35
PA	8,942.08	7.77 ± 1.06	3,328.48	6.00 ± 0.71
RO	1,990.32	2.82 ± 0.36	776.11	1.49 ± 0.17
Study Area	**19,199.50**	**17.04 ± 2.31**	**8,993.81**	**15.82 ± 1.82**
Fire_cci				
AC	14.73	0.02 ± 0.00	2.16	0.01 ± 0.00
AM	1,109.61	1.54 ± 0.20	185.02	0.46 ± 0.05
MA	556.72	0.30 ± 0.05	149.41	0.17 ± 0.02
MT	5,170.08	3.95 ± 0.57	789.22	1.32 ± 0.14
PA	5,267.84	4.68 ± 0.64	467.33	0.88 ± 0.10
RO	1,059.98	1.34 ± 0.17	152.21	0.31 ± 0.03
Study Area	**13,178.97**	**11.82 ± 1.62**	**1,745.36**	**3.14 ± 0.34**

AC = Acre; AM = Amazonas; MA = Maranhão; MT = Mato Grosso; PA = Pará; RO = Rondônia.

Figure 3.5 - Total burned area mapped by TREES, MCD64A1, GABAM, and Fire_cci over forested and non-forested areas, per Brazilian state within the study area.

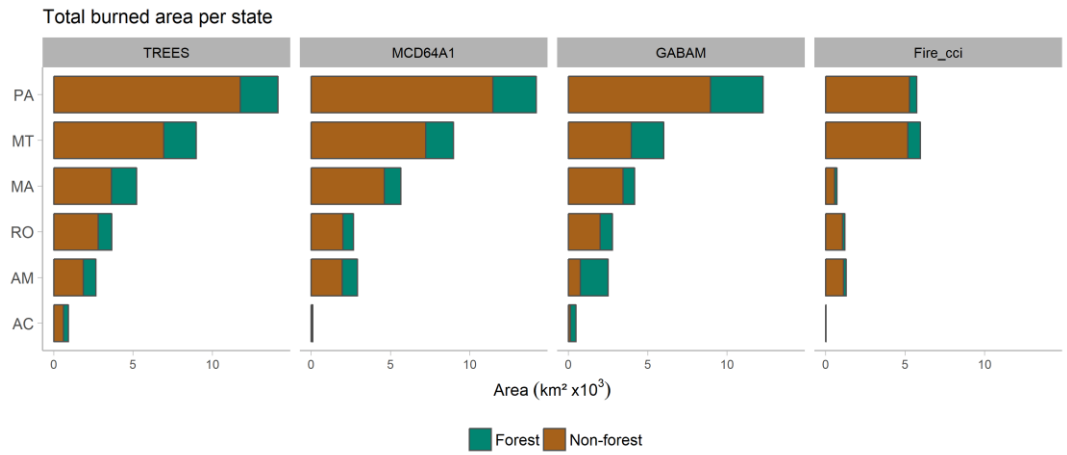

3.5.2 Vector approach: impact on committed gross carbon emissions estimates

Such differences in the burned area among the products are reflected in the variance observed in the committed gross C emission estimates (Figure 3.4). Using the Fire_cci product resulted in 29.54 ± 3.36 Tg C less estimated carbon emitted, a difference of 66% compared to the regional map developed by TREES. In contrast, the use of MCD64A1 results in only 5% (2.32 ± 0.17 Tg C) less than the carbon emission estimated by TREES. If only the forest areas are analyzed, TREES is also the product that generates the highest carbon emission, at 16.96 ± 1.73 Tg C for 2015. The product closest to this estimate is GABAM, with a difference of 11% (Figure 3.4). Even though GABAM presented a greater area of burned forest than TREES, it had a lower carbon emission estimate. This is due to the distinct spatial dispersion of the burned areas detected by each product. Since the emission is estimated as a function of initial biomass, it will depend on the spatial location of each burned area (Figure 3.6).

Figure 3.6 - Above ground biomass map from EBA and polygons of burned forest both from TREES and GABAM products.

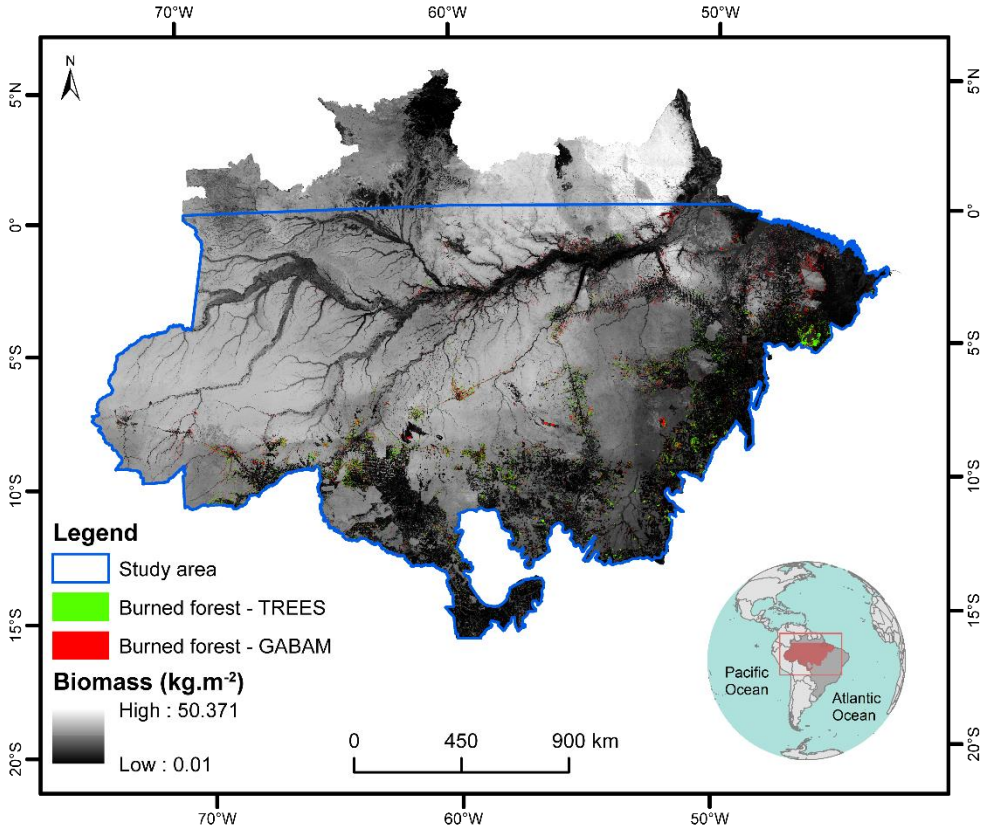

For comparing works that use Baccini as AGB input to estimate carbon emission, we compare our results using EBA with results using Baccini. Although its relative course

resolution compared to Baccini data (30 m), the EBA biomass data includes an uncertainty map, which is essential for our analysis. Baccini map is a global dataset that provides AGB for 2000 at approximately 30 m spatial resolution. It was used as a reference widely considered in the literature (ANDERSON et al., 2015; BRINCK et al., 2017; CAMPANHARO et al., 2019; LONGO et al., 2016). The biomass density (in Mg ha^{-1}) was generated by the statistical relationship between data collected in situ and LiDAR Geoscience Laser Altimeter System (GLAS) data, acquired over 40,000 points. In addition to the field data and GLAS, reflectance data derived from Landsat 7 ETM+, elevation data, and biophysical variables are used to estimate carbon stock. Random Forest modeling was used to build the statistical relationship (BACCINI et al., 2012). Since the map is from 2000, all deforestations detected by PRODES between 2001 and 2016 were incorporated into the map. Assuming the characteristics of changes in land use and land cover in the Amazon biome (COUTINHO et al., 2013), AGB was adjusted considering the pattern observed for pasture areas. Therefore, according to values proposed by (ROSAN, 2017) for the Amazon, AGB in deforested areas was adjusted to 16.6 Mg ha^{-1}. For the comparison, both AGB and AGB uncertainty maps were resampled to match Baccini spatial resolution, using the 'nearest' approach. Then, all the methodological steps adopted to estimate carbon emission were repeated using the Baccini dataset, and the results are presented in Figure 3.7. The same pattern can be observed with the Baccini dataset, considering the total emission in the study area. Nonetheless, the Baccini dataset seems to overestimate the committed gross C emission compared to the EBA dataset, which makes the EBA estimates conservative.

Figure 3.7 - Difference between the committed gross carbon emission estimates calculated by EBA and Baccini AGB maps.

	Non-forest			*Forest*		
	CGCE EBA (Tg)	**CGCE Baccini (Tg)**	**Difference (EBA - Baccini)**	**CGCE EBA (Tg)**	**CGCE Baccini (Tg)**	**Difference (EBA - Baccini)**
TREES						
AC	0.8988	0.7479	0.1508	0.9008	0.9426	-0.0417
AM	2.8020	2.0821	0.7200	2.2939	2.2647	0.0292
MA	2.2761	6.1801	-3.9040	2.0455	4.8657	-2.8202
MT	6.3525	7.2748	-0.9223	4.1955	5.9858	-1.7903
PA	11.2849	13.5485	-2.2636	5.4341	6.5947	-1.1607
RO	3.9279	3.1502	0.7777	2.0924	2.4000	-0.3076
Study Area	**27.5422**	**32.9835**	**-5.4413**	**16.9621**	**23.0534**	**-6.0913**
MCD64A1						
AC	0.0887	0.0752	0.0135	0.0794	0.0858	-0.0064
AM	2.8355	2.3406	0.4949	2.4044	2.7733	-0.3688
MA	3.1612	7.9061	-4.7450	1.4546	3.0348	-1.5802
MT	6.0644	7.1677	-1.1033	3.3894	4.9422	-1.5528
PA	12.1309	13.9630	-1.8321	6.1418	7.5858	-1.4441
RO	2.7821	2.2084	0.5737	1.6531	1.9518	-0.2987
Study Area	**27.0627**	**33.6611**	**-6.5984**	**15.1227**	**20.3737**	**-5.2510**
GABAM						
AC	0.1441	0.1164	0.0278	0.8514	0.7108	0.1406
AM	1.1535	1.0441	0.1094	3.4177	2.7560	0.6617
MA	2.2655	5.5940	-3.3286	0.8822	1.8524	-0.9702
MT	2.8893	3.8515	-0.9622	3.1854	3.7728	-0.5875
PA	7.7673	10.2850	-2.5178	6.0015	5.6356	0.3660
RO	2.8248	2.1836	0.6413	1.4865	1.4629	0.0236
Study Area	**17.0446**	**23.0747**	**-6.0301**	**15.8246**	**16.1905**	**-0.3659**
Fire_cci						
AC	0.0155	0.0132	0.0023	0.0053	0.0052	0.0001
AM	1.5374	0.9746	0.5627	0.4561	0.4650	-0.0089
MA	0.3023	0.8800	-0.5777	0.1727	0.4412	-0.2686
MT	3.9499	4.8130	-0.8631	1.3196	2.1343	-0.8147
PA	4.6816	4.9836	-0.3019	0.8804	1.1635	-0.2831
RO	1.3372	1.0657	0.2715	0.3085	0.3851	-0.0766
Study Area	**11.8239**	**12.7301**	**-0.9062**	**3.1425**	**4.5944**	**-1.4519**

CGCE = Committed Gross Carbon Emission

For the southern and western Amazonian states (Acre, Mato Grosso, and Rondônia), the TREES product presented emission estimates superior to all other products for forest and non-forest. For example, in the Acre state, the emissions estimated using TREES were 57 (0.90 ± 0.11 Tg C) and 171 (0.90 ± 0.09 Tg C) times larger than those derived by using Fire_cci for non-forest and forest, respectively. On the other hand, in eastern Amazonia, Pará state, although the emission estimates using TREES and MCD64A1 were similar (16.72 ± 2.02 and 18.27 ± 2.23 Tg C, respectively), the differences between them still resulted in up to 9% more carbon emission than was estimated using the MCD64A1 product, mainly due to the larger forest area mapped by this product.

So far, we have observed differences between the burned area products that can generate under- or overestimates of carbon emissions. Using the reasoning presented in Equation 3.2, we show that for non-forest land cover, TREES and MCD64A1 are the only products

that can be used with no significant difference (Figure 3.8). Therefore, choosing these two products may bring over- or underestimates for forest areas. In this case, the comparison of GABAM with these two products showed results within the range of uncertainty. Analyzing each state separately, we observed the spatial difference in this pattern. For non-forest areas in Acre, for example, no product can be used similarly to another. Likewise, in the forest areas in Maranhão, all products showed differences in their estimates of carbon emissions that were greater than their uncertainty (Figure 3.8). In general, the choice of the Fire_cci product always results in underestimating carbon emissions compared to the others (Figure 3.4).

Figure 3.8 - Carbon emissions difference analysis. The lower diagonal contains the absolute value of the difference in carbon emissions (Tg) between the products. The upper diagonal indicates if the difference is greater (green upside triangle) or lower (red downside triangle) than the maximum uncertainty value between them.

	Non-forest				*Forest*			
Study area	**TREES**	**MCD64A1**	**GABAM**	**Fire_cci**	**TREES**	**MCD64A1**	**GABAM**	**Fire_cci**
TREES	**0**	▼	▲	▲	**0**	▲	▼	▲
MCD64A1	0.4795	**0**	▲	▲	1.8394	**0**	▼	▲
GABAM	10.4977	10.0181	**0**	▲	1.1375	0.7019	**0**	▲
Fire_cci	15.7183	15.2388	5.2206	**0**	13.8196	11.9802	12.6821	**0**
Acre	**TREES**	**MCD64A1**	**GABAM**	**Fire_cci**	**TREES**	**MCD64A1**	**GABAM**	**Fire_cci**
TREES	**0**	▲	▲	▲	**0**	▲	▼	▲
MCD64A1	0.8101	**0**	▲	▲	0.8214	**0**	▲	▲
GABAM	0.7547	0.0554	**0**	▲	0.0495	0.7720	**0**	▲
Fire_cci	0.8833	0.0732	0.1286	**0**	0.8956	0.0742	0.8461	**0**
Amazonas	**TREES**	**MCD64A1**	**GABAM**	**Fire_cci**	**TREES**	**MCD64A1**	**GABAM**	**Fire_cci**
TREES	**0**	▼	▲	▲	**0**	▼	▲	▲
MCD64A1	0.0335	**0**	▲	▲	0.1106	**0**	▲	▲
GABAM	1.6485	1.6820	**0**	▲	1.1238	1.0132	**0**	▲
Fire_cci	1.2647	1.2981	0.3838	**0**	1.8378	1.9484	2.9616	**0**
Maranhão	**TREES**	**MCD64A1**	**GABAM**	**Fire_cci**	**TREES**	**MCD64A1**	**GABAM**	**Fire_cci**
TREES	**0**	▲	▼	▲	**0**	▲	▲	▲
MCD64A1	0.8850	**0**	▲	▲	0.5909	**0**	▲	▲
GABAM	0.0107	0.8957	**0**	▲	1.1634	0.5724	**0**	▲
Fire_cci	1.9738	2.8588	1.9631	**0**	1.8728	1.2819	0.7095	**0**
Mato Grosso	**TREES**	**MCD64A1**	**GABAM**	**Fire_cci**	**TREES**	**MCD64A1**	**GABAM**	**Fire_cci**
TREES	**0**	▼	▲	▲	**0**	▲	▲	▲
MCD64A1	0.2881	**0**	▲	▲	0.8061	**0**	▼	▲
GABAM	3.4632	3.1751	**0**	▲	1.0101	0.2040	**0**	▲
Fire_cci	2.4026	2.1145	1.0606	**0**	2.8759	2.0698	1.8658	**0**
Pará	**TREES**	**MCD64A1**	**GABAM**	**Fire_cci**	**TREES**	**MCD64A1**	**GABAM**	**Fire_cci**
TREES	**0**	▼	▲	▲	**0**	▲	▼	▲
MCD64A1	0.8460	**0**	▲	▲	0.7077	**0**	▼	▲
GABAM	3.5176	4.3636	**0**	▲	0.5675	0.1403	**0**	▲
Fire_cci	6.6033	7.4492	3.0856	**0**	4.5536	5.2614	5.1211	**0**
Rondônia	**TREES**	**MCD64A1**	**GABAM**	**Fire_cci**	**TREES**	**MCD64A1**	**GABAM**	**Fire_cci**
TREES	**0**	▲	▲	▲	**0**	▲	▲	▲
MCD64A1	1.1458	**0**	▼	▲	0.4393	**0**	▼	▲
GABAM	1.1030	0.0427	**0**	▲	0.6059	0.1666	**0**	▲
Fire_cci	2.5907	1.4449	1.4877	**0**	1.7838	1.3446	1.1780	**0**

▲ Difference is greater than the maximun uncertainty value.

▼ Difference is lower than the maximun uncertainty value.

3.5.3 Matrix approach: statistical and spatial intercomparison

Corroborating the differences in magnitude found in the vector analysis, the TREES and MCD64A1 products were the only ones that did not present significant differences at a 95% confidence level ($p > 0.05$). The same pattern can be observed when forest and non-

forest are analyzed separately (Table 3.6). Considering this comparison, the bootstrap approach resulted in 81% of the 10,000 iterations (84% for forest and 82% for non-forest) of non-significant p-values ($p > 0.05$). All the other combinations resulted in 100% significant p-values at a 95% confidence level.

Table 3.6 - Mean and standard deviation of p-values resulted from 10,000 iterations of the Kolmogorov-Smirnov two-sample test, raffling different samples of 10% of the total grid cells of 10x10km. It was considered only cells that presented burned area percentage by at least one product.

	TREES x MCD64A1	TREES x GABAM	TREES x Fire_cci	MCD64A1 x GABAM	MCD64A1 x Fire_cci	GABAM x Fire_cci
Total (Sample size = 1,434 cells)						
Mean	2.33E-01	0	2.55E-15	0	1.52E-13	0
SD	2.01E-01	0	6.16E-14	0	5.82E-12	0
Forest (Sample size = 1,215 cells)						
Mean	3.12E-01	0	9.56E-18	0	1.14E-13	0
SD	2.74E-01	0	5.35E-16	0	6.74E-12	0
Non-forest (Sample size = 1,229 cells)						
Mean	2.70E-01	5.55E-19	2.31E-14	2.22E-20	3.31E-13	0
SD	2.43E-01	5.44E-17	7.85E-13	1.57E-18	1.44E-11	0

The four products also present spatial divergence. Despite the small difference in total mapped area, TREES and MCD64A1 also presented spatial divergence, mainly in the extreme north of the study area and in the Acre state (Figure 3.9). The GABAM product presents a lot of small patches of burned areas, which reflects the higher number of cells with a low burn proportion (Figure 3.10). Although this product does not present the highest burned area, it includes the most spatially broad mapping among those considered. Analyzing the correlation, given by scatter plots of the percentage of burned area per cell among the different pairs of products, we observed that all relations are statistically significant at a 95% confidence level ($p < 0.05$). The relation between TREES and MCD64A1 is the closest to 1. The determination coefficients are, however, intermediate for all comparisons, ranging from 0.47 (TREES vs. Fire_cci) to 0.66 (MCD64A1 vs. GABAM) (Figure 3.11).

Figure 3.9 - Burned area spatialization in a 10 km × 10 km regular grid. Each grid cell contains the burned proportion indicated by the color gradient.

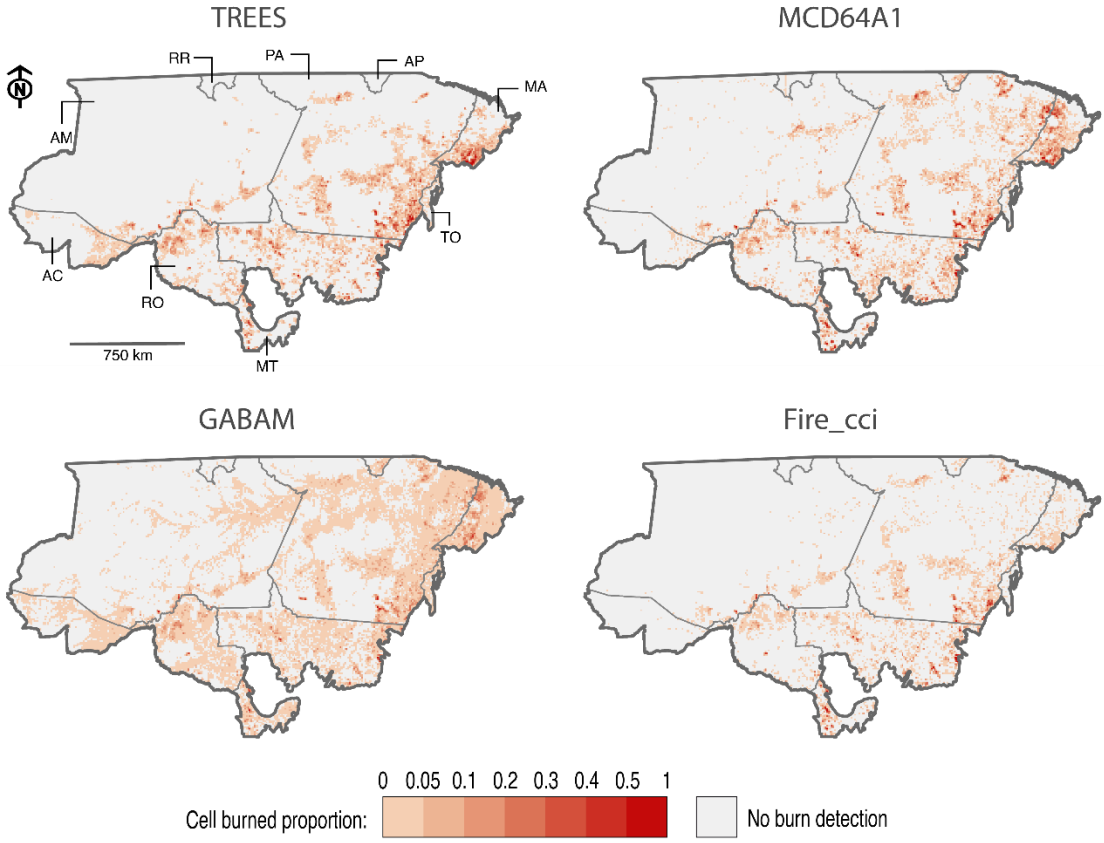

Figure 3.10 - Number of cells in different burned proportion classes.

	0	0 - 0.05	0.05 - 0.1	0.1 - 0.2	0.2 - 0.3	0.3 - 0.4	0.4 - 0.5	> 0.5
TREES	28,986	4,371	1,030	667	192	78	37	38
MCD64A1	28,843	4,627	902	608	229	99	45	46
GABAM	22,084	11,784	944	443	98	25	13	8
Fire_cci	31,195	3,438	389	244	58	37	16	22
Total	**111,108**	**24,220**	**3,265**	**1,962**	**577**	**239**	**111**	**114**

The similarity analysis allows the identification of the pairs of products that are the most spatially coherent. The similarity indexes are generally medium to low between all products (Table 3.7). Considering the study area, the similarity indexes are always between 0.4 and 0.5, regardless of the land cover. When we distinguish between forest and non-forest areas, we can see two patterns: relative higher indexes when Fire_cci is considered for comparisons in non-forest areas and relative lower indexes when GABAM is considered for comparisons in forest areas. The first pattern can be explained by the reduced extent mapped by the Fire_cci product; the more conservative the mapping, the greater the chance of being more similar to other products, and this is the case for Fire_cci.

The second pattern, on the other hand, can be explained by the opposite reasoning. GABAM has the largest extent mapped in forest areas and, therefore, has a greater chance of mapping areas the other products did not.

Figure 3.11 - Scatter plots of the percentage of burned area per cell among the different pairs of products. It was considered only cells that presented burned area percentage by at least one product. All relations are statistically significant at a 95% confidence level.

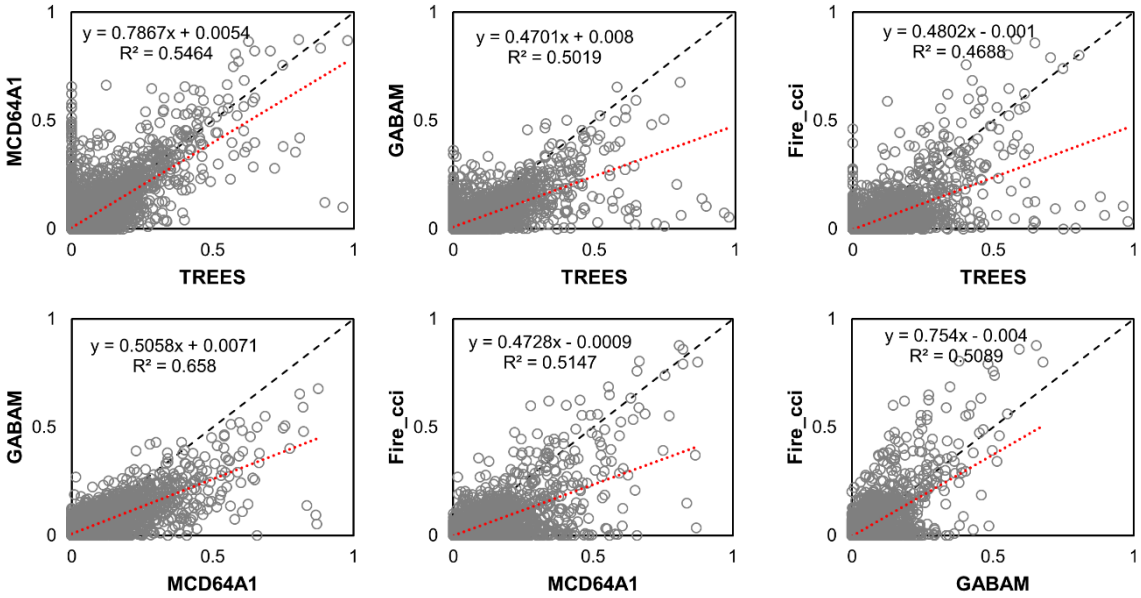

Regionally, the extreme west and extreme east (Acre and Maranhão, respectively) are the regions where most differences in mapping occur, denoted by the broad range of similarities among the products. In Acre, the relatively high similarity index found for MCD64A1 and Fire_cci (0.784) shows that both products presented less burned area detected in this state. These products did not present as much burned area as was captured by the TREES product (less 88% and 98%, respectively) in both land covers. When analyzing GABAM compared to MCD64A1 and Fire_cci, we observed that the lower similarity indexes are mainly due to forest-affected areas for the study area and the Acre and Amazonas states. GABAM is the product with the highest detection of forest fires in Acre and Amazonas; its mapping areas were approximately 161 and 10 times greater than those of Fire_cci in the forest areas of these states, respectively. However, GABAM presents relatively poor performance for the eastern forests in Maranhão state. Although the overall similarity for the Maranhão state is already relatively low compared to the other states, we see that the indexes for the non-forest areas are lower than the ones for the forest, indicating a greater divergence between the products for non-forest areas in this state (Table 3.7).

Table 3.7 - Overall similarity for each burned area product comparison pair, considering the whole area and separating it into non-forest and forest areas. The result is provided for the entire study area and for each Brazilian state considered separately. The similarity index ranged from 0 (fully distinct) to 1 (fully identical) and was calculated using the fuzzy numerical algorithm for map comparison.

	Study area	AC[1]	AM[2]	MA[3]	MT[4]	PA[5]	RO[6]
Total							
TREES x MCD64A1	0.408	0.194	0.316	0.458	0.459	0.406	0.451
TREES x Fire_cci	0.483	0.114	0.610	0.437	0.529	0.491	0.395
TREES x GABAM	0.467	0.470	0.495	0.395	0.529	0.416	0.544
MCD64A1 x Fire_cci	0.507	0.784	0.389	0.369	0.544	0.493	0.583
MCD64A1 x GABAM	0.450	0.164	0.376	0.489	0.468	0.474	0.465
Fire_cci x GABAM	0.414	0.073	0.463	0.254	0.555	0.387	0.408
Non-forest							
TREES x MCD64A1	0.428	0.242	0.390	0.474	0.464	0.421	0.456
TREES x Fire_cci	0.505	0.153	0.653	0.459	0.543	0.510	0.413
TREES x GABAM	0.449	0.276	0.420	0.436	0.484	0.424	0.513
MCD64A1 x Fire_cci	0.533	0.798	0.454	0.396	0.553	0.520	0.607
MCD64A1 x GABAM	0.472	0.651	0.406	0.489	0.445	0.484	0.480
Fire_cci x GABAM	0.480	0.670	0.513	0.312	0.563	0.445	0.443
Forest							
TREES x MCD64A1	0.515	0.291	0.433	0.674	0.551	0.507	0.507
TREES x Fire_cci	0.542	0.151	0.580	0.699	0.572	0.543	0.425
TREES x GABAM	0.513	0.519	0.504	0.608	0.583	0.451	0.514
MCD64A1 x Fire_cci	0.573	0.790	0.464	0.614	0.600	0.548	0.578
MCD64A1 x GABAM	0.493	0.202	0.382	0.673	0.527	0.498	0.463
Fire_cci x GABAM	0.446	0.090	0.408	0.546	0.553	0.418	0.386

[1]AC = Acre; [2]AM = Amazonas; [3]MA = Maranhão; [4]MT = Mato Grosso; [5]PA = Pará; [6]RO = Rondônia.

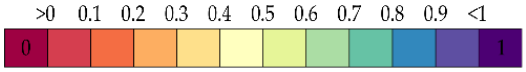

Even though most values of similarity indexes are intermediate, as they are averages for each region, similarity scale extremities can be observed spatially in Figure 3.12 (and Figure 3.13 and Figure 3.14, for the burned area over forest and non-forest, respectively).

Figure 3.12 - Similarity maps for each burned area product comparison pair. The similarity index was calculated considering only cells that presented burned area detection by at least one product. The similarity index goes from 0 (lowest similarity) highlighted by dark red to 1 (highest similarity) highlighted by dark purple.

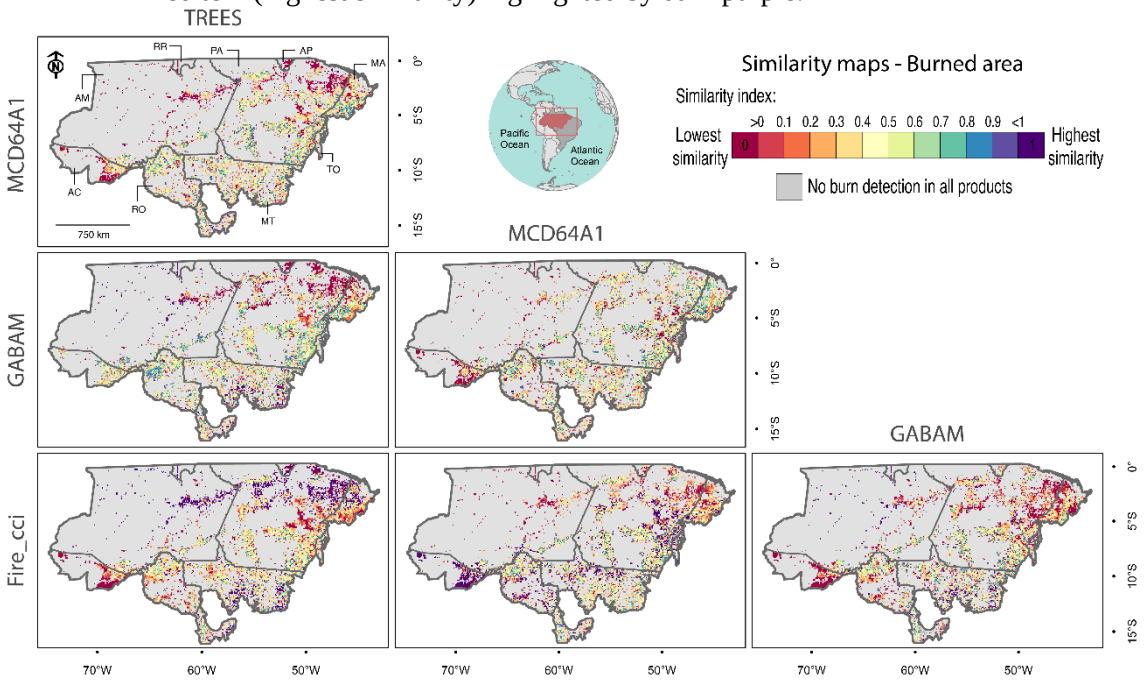

Figure 3.13 - Similarity maps for each burned area product comparison pair, considering burned area over forest. The similarity index was calculated considering only cells over forest that presented burned area detection by at least one product. The similarity index goes from 0 (lowest similarity) highlighted by dark red to 1 (highest similarity) highlighted by dark purple.

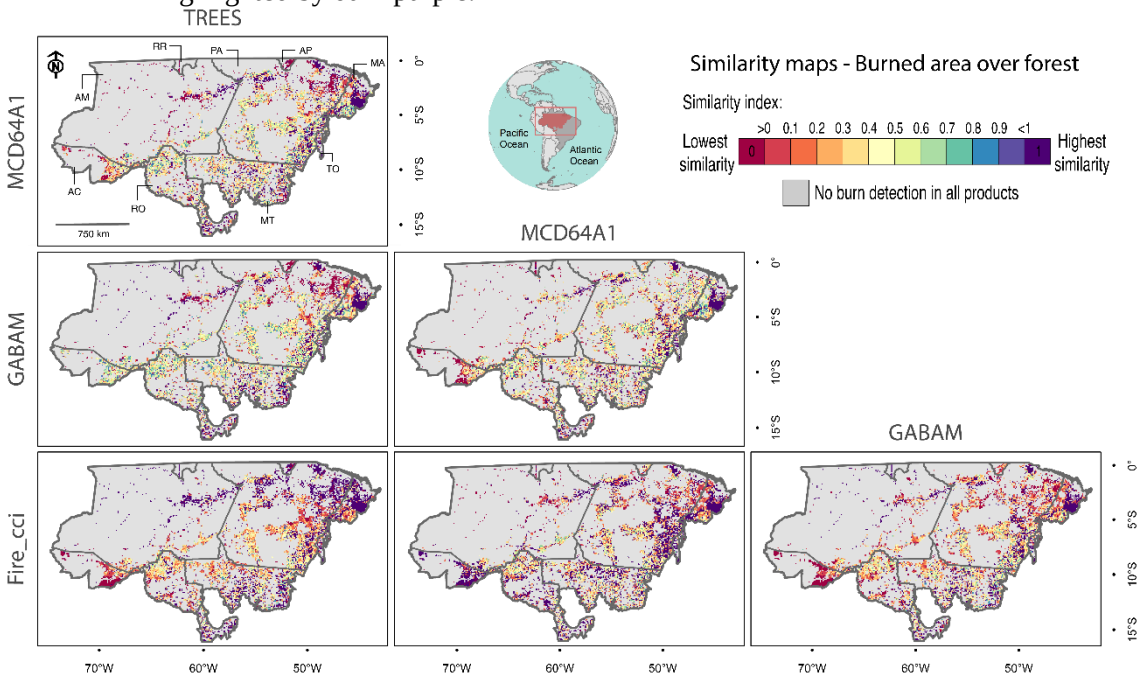

This visual-spatial analysis allows the identification of regions that are the more cohesive, or not, among the burned area products. Between TREES and MCD64A1, most of the low similarity registries occur in the northern region, where MCD64A1 presents better performance, and in southwestern Amazonia, where TREES registers more burned area (Figure 3.15a). Between TREES and GABAM, little similarity occurs in the north, mainly in the northeast of the Pará and Amazonas states, where GABAM presented more fire-affected areas. Even in Acre, where these products present approximately equal estimates in forest-affected areas, there is divergence, mainly in the western part of the state (Figure 3.15b). The same occurs between MCD64A1 and GABAM, with the addition of minor similarities in the Rondônia state. The low performance of Fire_cci in mapping as much burned area as the other products are highlighted in Figure 3.15, which shows that most cells contain information exclusively from TREES or MCD64A1 or a combination of them.

Figure 3.14 - Similarity maps for each burned area product comparison pair, considering burned area over non-forest. The similarity index was calculated considering only cells over non-forest that presented burned area detection by at least one product. The similarity index goes from 0 (lowest similarity) highlighted by dark red to 1 (highest similarity) highlighted by dark purple.

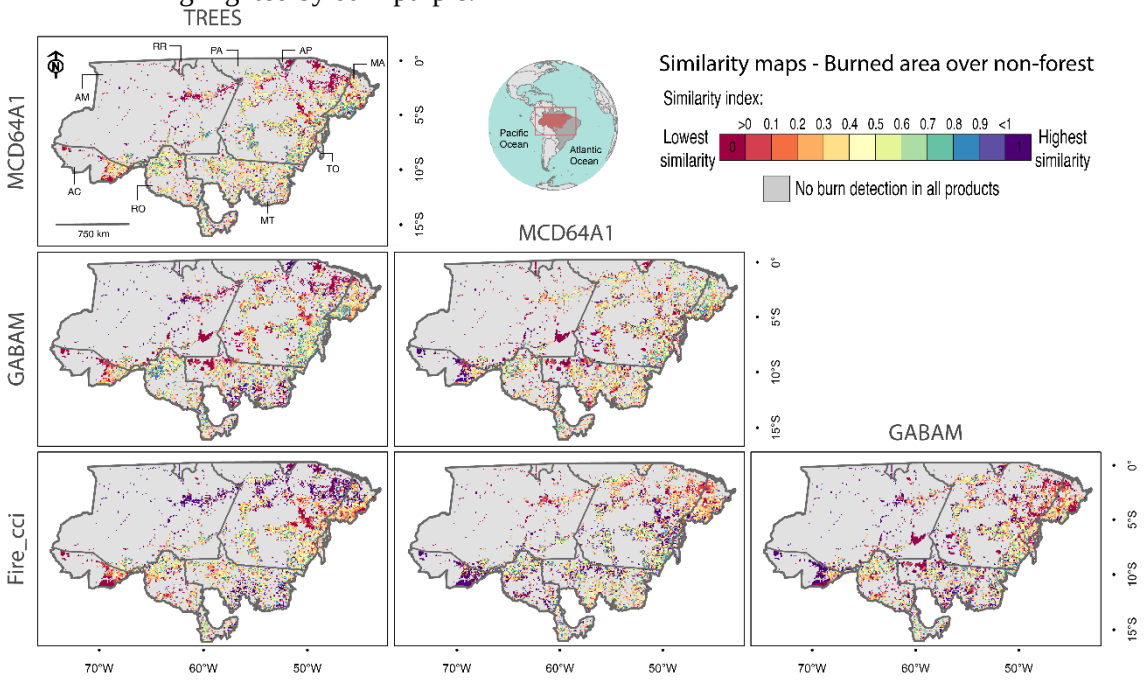

Figure 3.15 - Confusion maps considering (a) TREES, MCD64A1 and Fire_cci burned area products, and (b) TREES, MCD64A1, and GABAM burned area products. The 10km cells are colored according to the occurrence of information from each product or combination, disregarding the burned area proportion in each cell.

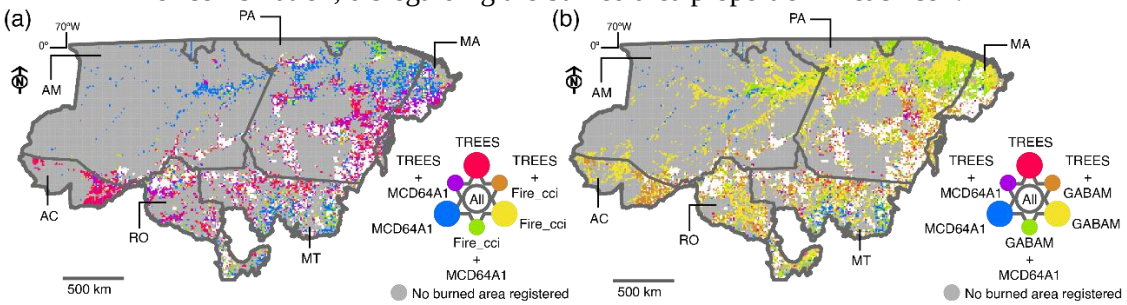

3.6 Discussion

Every sensor considered to generate a burned area product has characteristics and specifications that incorporate limitations in the final product, affecting their performances regionally. The daily temporal resolution of MODIS data ensures a higher frequency of data acquisition and minimizes cloud cover, important factors for monitoring tropical areas. Depending on the time elapsed after the fire, the signs of burned areas can be removed quickly due to climatic conditions and the speed of vegetation regeneration (ALONSO-CANAS; CHUVIECO, 2015). Currently, with daily global products available, MODIS data have been widely used in burned area detection with 500m spatial resolution (GIGLIO; SCHROEDER; JUSTICE, 2016; JUSTICE et al., 2002). Landsat data have a 16-day temporal resolution but with the advantage of a 30m spatial resolution in the optical spectrum. The spatial resolution allows a better definition of the boundaries of the burned area, avoiding a greater mixture of pixels from burned and unburned patches (LONG et al., 2019). In addition, its long time series allows one to trace historical trends in fire dynamics (MEDDENS et al., 2018). Therefore, the final user needs to understand such characteristics to consider which product is most appropriate for their application. In addition to the limitations of each data set, the spatial evaluations of the burned areas revealed that the similarities between the products varied regionally. Depending on the scale of the study to be developed, the choice of which product to use can significantly impact the final result.

Regarding the total burned area mapped, we can separate the products into two groups: two very similar products (MCD64A1 and TREES) and two others (GABAM and Fire_cci). Although the GABAM product presents 21% less total burned area compared

to the TREES product, GABAM was the product that registered the most burned forest, reaching 11% more than the TREES product. This shows that the spatial resolution of GABAM (30 m) gives an advantage to mapping this land cover. In addition, GABAM presents the smallest commission error, considering the error related to forest areas for the TREES product. Although some studies indicate that the use of MODIS data at a 250 m spatial resolution can underestimate burned area by approximately 25% in relation to manually digitized burn scars based on Landsat images at a 30 m resolution (MORTON et al., 2011; ROY; BOSCHETTI, 2009), in a global comparison between the GABAM and Fire_cci products using the proportion of burned area in 0.25° × 0.25° grids, GABAM generally underestimated burned scars. The inconsistency was attributed to the difference in spatial resolution of data sources (LONG et al., 2019). GABAM's higher resolution can allow better delineation of fire pixels, resulting in fewer pixels classified as burned globally. However, our study shows that this statement can change in the regional analysis since the GABAM product registered almost twice as much (1.9 times) total burned area as the product Fire_cci for the study area considered.

Nevertheless, GABAM's developers warn that using Landsat images as the data source decreases the number of valid observations, considering Landsat's temporal resolution and cloud contamination, which may explain its performance compared to TREES and MCD64A1 products. This limitation is especially critical in tropical regions, where vegetation recovery is quick and cloud cover is persistent (LONG et al., 2019). Using coarse-resolution images to detect fire can be justified since they generally offer higher temporal frequency (GIGLIO et al., 2018; PETTINARI; CHUVIECO, 2018).

Among the products developed using coarse spatial resolution data, Fire_cci was the first to provide a global dataset with a 250 m resolution. Its validation process for version 5.0 indicated an overall accuracy of 0.9972, with 0.7090 global omission errors and 0.5123 commission errors (Table 3.3) (CHUVIECO et al., 2018). Similarly, version 5.1 presented a 0.6710 global omission error and 0.5440 commission error (LIZUNDIA-LOIOLA et al., 2020). The errors reflect the conservative nature of this dataset, which may explain the great difference compared to other products. Its developer argues that, although globally higher than MCD64A1 c6, its errors for version 5.0 are better compensated, with a tendency towards underestimation, than most existing global products (CHUVIECO et al., 2018). Fire_cci's developers highlight its better detection

accuracy for small patches (<100 ha) compared to MCD64A1 in a sample over Africa (CHUVIECO et al., 2018), although both had high errors for these small fires. Version 5.1 brings improvements in this direction. Despite the significant contribution of this product to fire modeling based on burned area global analysis, we show that regionally, the use of this product can be critical in underestimating the overall burned area and, thus, the fire-related impacts on carbon emissions.

In general, coarse-resolution products are unable to adequately detect small fires (<100 ha) (RODRIGUES et al., 2019). This limitation can lead to a considerable underestimation of global burned area (GIGLIO et al., 2018; RANDERSON et al., 2012), underestimating fires in croplands by as much as ten times (GIGLIO et al., 2018). The newest collection (c6) in the MCD64A1 offers significantly better detection of small burns (<100 ha) compared to older versions, but in general, it remains unable to map them adequately. It underestimated fire perimeter length in all vegetation classes, and care should be taken when using it for cropland regions (ANDELA et al., 2019). Given its higher spatial resolution, GABAM detects small burned areas better. Although it was the product that presented the greatest range of mapping, it was not the one that detected the most extensive total area. Furthermore, when analyzing the regular grid of 10 km spatial resolution, most cells that had burned areas in GABAM recorded small burn proportions, suggesting small burnt patches.

The product MCD64A1 was the one presenting the biggest difference in omission and commission errors related to TREES, reaching commission errors 75% higher than the TREES product for forest areas and 83% higher for non-forest areas. The high omission error presented by this product, especially for tropical forests, also indicates the conservatism adopted in its methodology. Surprisingly, MCD64A1 was the product that came closest to the regional product TREES in the total burned area detected. Shimabukuro et al. (2015) estimated a difference of 21% between the MCD64A1 and a product built with Landsat TM images using the same methodology as TREES for the Mato Grosso state. Here, we found a difference of only 0.15% between MCD64A1 and TREES for the Mato Grosso state, considering the total burned area. However, this difference can reach 15%, considering burned areas over the forest. When analyzing the whole study area, these products registered significant spatial divergences. The product MCD64A1 recorded more fires in the north and northwest of the study area, mainly in

the state of Amazonas, compared to TREES. The TREES product concentrates on more exclusive mapped areas in the southwest, mainly in the Acre state. The burned areas in the north of the study area, presented by the MCD64A1 and the product GABAM, seem to follow the hydrography (Figure 3.16). One hypothesis would be that these burned areas would partially correspond to flooded regions. Many detected areas occur along the margins of the Amazonas river, and water presents low reflectance in all wavelengths, similar to burned areas. As a brief analysis, we assessed the burned areas of the four products in relation to the hydrography to calculate the proportion of intersections (Table 3.8). Even the percentages of the burned area over the hydrography mask are small for all four products (maximum of 1.5%), and MCD64A1 and GABAM are the products with the largest overlap (1.5% and 0.9%, respectively). If we compare regionally, Amazonas is the state with the largest overlap presented by these two products (10.3% and 4%, respectively).

Figure 3.16 - Study area and the hydrography of the region.

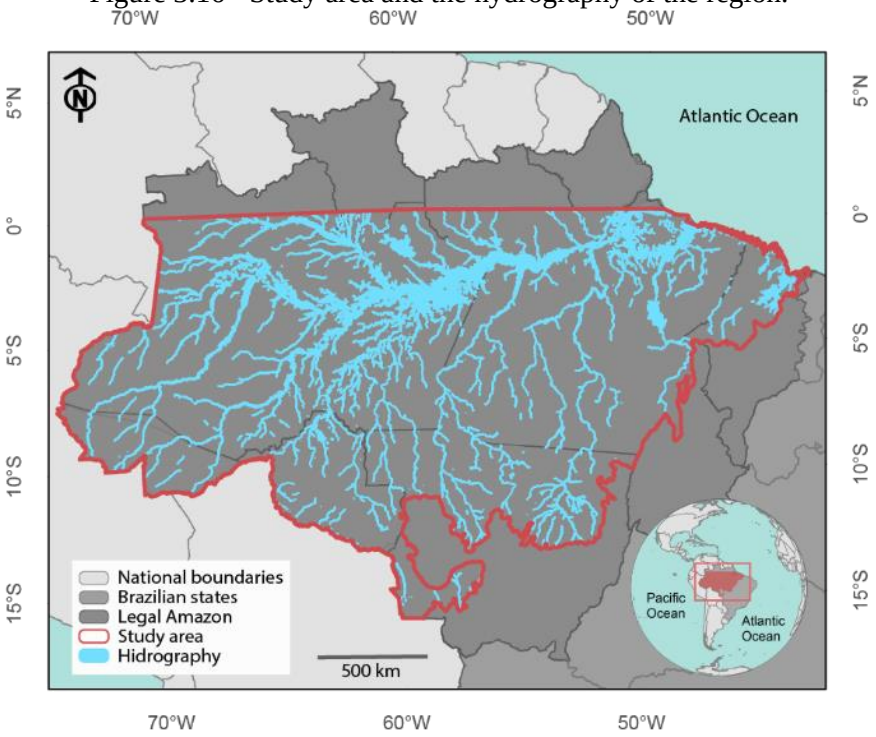

Source: INPE (2022).

Table 3.8 - Total burned area and its intersection area with the hydrography.

Product	State	Burned area [Non-forest + Forest (km²)]	Burned area over hydrography (km²)	%
TREES	AC	925.6	0.3	0.03
	AM	2650.4	11.9	0.45
	MA	5215.3	13.3	0.25
	MT	8981.1	4.6	0.05
	PA	14125.0	11.7	0.08
	RO	3661.1	0.7	0.02
	Study Area	35558.6	42.6	0.12
MCD64A1	AC	113.7	0.0	0.00
	AM	2914.1	299.2	10.27
	MA	5648.5	22.1	0.39
	MT	8967.6	14.9	0.17
	PA	14189.2	160.8	1.13
	RO	2680.9	22.1	0.82
	Study Area	34514.1	519.0	1.50
GABAM	AC	466.8	2.2	0.46
	AM	2507.6	101.3	4.04
	MA	4179.5	16.1	0.38
	MT	6002.5	13.5	0.22
	PA	12270.6	72.0	0.59
	RO	2766.4	38.0	1.38
	Study Area	28193.3	243.0	0.86
Fire_cci	AC	16.9	0.7	4.25
	AM	1294.6	15.5	1.19
	MA	706.1	1.0	0.14
	MT	5959.3	11.1	0.19
	PA	5735.2	4.7	0.08
	RO	1212.2	1.0	0.08
	Study Area	14924.3	34.0	0.23

The detection of burned forests worldwide is made difficult when the fire does not reach the forest canopy since the spectral signal does not change sufficiently to be detectable by remote sensors. It has been shown that in areas with high leaf area index (LAI) and percent tree cover, there is a misdetection of burned areas (PEREIRA et al., 2004; ROY; BOSCHETTI, 2009). Therefore, our initial hypothesis was that the variation between the products would increase in forest-affected areas. We expected that the regional product TREES, in which there is manual image interpretation, would present greater sensitivity for mapping burned forests (ANDERSON et al., 2017). However, this hypothesis was not sustained in most cases. Firstly, GABAM, which has a 30 m spatial resolution, was the product that most detected burned forests, leading us to consider that spatial resolution can be very important for burned forests detection. In an intercomparison analysis between FireCCISFD11 (20 m), a Sentinel-2 burned area product derived for 2016 in Sub-Saharan Africa, MCD64A1 c6 and Fire_cci v.5.0, the Sentinel product was found to be more accurate than any global product for detecting small fires, detecting 4.9 Mkm², 80% more than MCD64A1 c6 (2.7 Mkm²) and 97% more than Fire_cci v.5.0 (2.5 Mkm²) (LIZUNDIA-LOIOLA et al., 2020). Since all these three products used MODIS active

fires to train their algorithms, the improved performance of FireCCISFD11 should be mostly attributed to the spatial resolution of the input reflectance (LIZUNDIA-LOIOLA et al., 2020). However, the study did not distinguish land cover classes in its analyses. Additionally, in our analysis, even though the burned area difference was greater in burned forests between MCD64A1 and TREES and between Fire_cci and GABAM, the difference in the burned area was greater in non-forest areas in most cases. There is no rule to support this hypothesis, and it is possible to observe variations between products spatially.

For a study that aims to quantify fire-related C emission, the choice of the burned area product must consider the scale of the process to be observed. For the study area, the difference between products can reach 29.54 ± 3.36 Tg C yr^{-1} when comparing the global product Fire_cci and the regional TREES. The average value corresponds to 21% of the total gross CO_2 emissions from forest fires in 2015 in the Brazilian Amazon biome (ARAGÃO et al., 2018). In the Acre state, even the most similar products, TREES, and GABAM, differed by 0.8 ± 0.33 Tg C, equivalent to 23% of the average biomass loss during an extreme drought year in this state (CAMPANHARO et al., 2019). The same comparison with Fire_cci can result in a difference of more than 50% of the average biomass loss in a drought year in Acre state. The differences in estimates can be significant, but it is necessary to consider that biomass data bring uncertainty into these estimates, an intrinsic factor in the development of the data. Thus, when calculating the carbon emission related to fire, the choice between burned area products can reflect significant differences in the estimates, or irrelevant differences, considering the biomass data's uncertainty level. For non-forest areas, in most cases, MCD64A1 and TREES presented irrelevant differences in fire-related carbon emissions, which means that the difference in emission estimates using these products is smaller than the biomass data uncertainty. For forest areas, there is more variability among the states. All comparisons with Fire_cci resulted in significant differences. Therefore, it is recommended to undertake

The map scale can also influence the differences in the burned area products. It is more feasible to adapt the mapping method regionally over the wide range of pre- and post-burn conditions, considering specific dynamics for different ecosystems. Work on a regional scale also allows for a manual post edition of the automatic burn classification,

minimizing the omission and commission errors (ANDERSON et al., 2017; SHIMABUKURO et al., 2009; SILVA et al., 2018b). The adoption of global burned area products in regional analyses, in general, can result in a significant underestimation of the fire-affected area, which varies spatially. For example, the underestimation shown here between TREES and MCD64A1 for Acre state (88% less burned area registered by MCD64A1 compared to TREES) was again found for 2019 by Silva et al. (2020), with the same percentage of less burned area registered by MCD64A1 compared to their product, which also includes a manual edition in its mapping methodology. Although the final manual edition procedure has a high time and human resource cost, it can avoid as much as 20% of the underestimation of the burned area compared to methods that do not consider this step (SHIMABUKURO et al., 2015). Additionally, studies considering a time series can assess whether the spatial variation is systematic. In this case, this variation can be used as a guideline for improvements in mapping.

Finally, we also highlight that the most probable result of comparing different data is obtaining different patterns, which was indeed the case. However, it may also be relevant to point out that some patterns are similar, which means that the four burned area products can cross-validate each other to some extent. The more the sources point to a given pattern, the more reliable the pattern is. Moreover, we consider the continuous process of improving global burned area products as fundamental to strengthening environmental conservation in the Amazon, as they are often used as inputs for technical reports and public policy formulation. Furthermore, in the absence of an official national product for the long-term monitoring of fire-degraded forests, global products provide the only reliable and operational option to expose the magnitude of the fire-related socioeconomic and environmental losses we are currently experiencing in the region (BARLOW et al., 2020).

3.7 Conclusions

This work performed an intercomparison of four burned area products, one being a regional burned area map developed by TREES–INPE, and the other being global products. We analyzed the difference in the total area mapped over forest and non-forest areas and their influence on fire-related C emission estimates in the Amazon for the year 2015.

The four burned area products differ according to the total area mapped and, consequently, total related C emission. Only accounting for the magnitude of the difference, the most similar products are TREES and MCD64A1, both for non-forest and forest areas. The products that stand out the most are TREES and Fire_cci, and the difference between the two can reach 78% less burned area detected by Fire_cci in forest areas considering the Amazon and 99% in Acre. The difference between products was not higher in forest areas in all comparisons, and regionally analyzing the initial hypothesis of more significant variation in these areas cannot be sustained in most cases.

Despite the broader coverage of the GABAM product, it does not have the magnitude of the total burned area recorded by TREES and MCD64A1, and this is linked to the use of Landsat 30 m data. Furthermore, Landsat images' more extended temporal resolution makes it difficult to obtain data without cloud interference. Besides, better spatial resolution can either decrease the mapped area due to a better scar delineation or increase the contribution of small polygons. Therefore, the better spatial resolution of the Fire_cci product (250 m) compared to MCD64A1 (500 m) does not appear to have conferred an advantage for mapping fire-affected areas in the Amazon.

Besides, when these products are used to estimate fire-related carbon emissions, the choice between them can lead to significant changes in estimates. For example, using Fire_cci may result in 29.54 ± 3.36 Tg C less estimated carbon emitted, a difference of 66% less compared to the regional product TREES. Considering non-forest areas in the Amazon, and for the analysis of carbon emission estimates specifically, the difference between adopting TREES and MCD64A1 is within the expected error for the biomass dataset. For forest areas, the comparisons within the expected error are GABAM, TREES, GABAM and MCD64A1. This analysis varied across the Brazilian Amazon states, and no single rule existed.

Overall, for Amazon, the global product MCD64A1 was the closest to the regional product TREES, but regionally there are still significant differences between them, especially in forest areas. It was shown here that global products used interchangeably on a regional scale could significantly underestimate the impacts of fire and, consequently, fire-related carbon emissions. As such, the end-user must choose the product based on the phenomenon and scale to be studied, considering the parameters of the data used in

the mapping and the limitations conferred by such in the final result. The choice process can involve merging more than one product to optimize its advantages and produce more consistent data for the user's needs, getting closer to the true total burned area and its regional distribution. Additionally, the information herein still serves as evidence for improving burned area detection algorithms in the Amazon, subsidizing the development of new and more accurate products for the region.

4 OUR HOME ON FIRE: A DESCRIPTIVE ANALYSIS OF FIRE OCCURRENCE WITHIN PROTECTED AREAS IN THE AMAZON BASIN

4.1 Introduction

Natural fire ignitions rarely occur in humid tropical forests like the Amazon (BUSH et al., 2008). Fire presence in this environment is intertwined with human activities (HANTSON; PUEYO; CHUVIECO, 2015; PAUSAS; KEELEY, 2009). Indeed, global fire size distribution is strongly influenced by human activity, which explains great part of its global variance (HANTSON; PUEYO; CHUVIECO, 2015). Despite the impact of increasing population density being mainly to reduce fire frequency, it increases by 10 to 20% relative to its value at no population in areas with up to 0.1 people per km² (KNORR et al., 2014). In the Amazon, a region that only intensified its occupation from the 60s onwards, and, in general, population expansion creates a greater threat of fire in this environment. At first, the traditional burning activities in the Amazon were generally highly controlled to ensure the continued regeneration of forest resources (PIVELLO, 2011). Nonetheless, this dynamic changed over the last decades, mainly due to agricultural intensification and rural demographic growth (PEDROSO JUNIOR; MURRIETA; ADAMS, 2008).

The greater impact that fire has had on these socio-natural ecosystems reflects climate change side effects already in place (GATTI et al., 2021). For example, in the Amazon, climate change is making drought periods longer (MARENGO et al., 2018), more intense, and extreme drought events more frequent (RIBEIRO NETO et al., 2022; SILVA JUNIOR et al., 2019). These three factors, the increase in dry season length, the decrease in rainfall during the dry season, and more intense and extreme droughts, turn Amazonian landscapes more susceptible to wildfires (MARENGO et al., 2018).

In turn, the current rate of climate change is a direct consequence of human contribution to the increase of greenhouse gas concentration in the atmosphere. During 2010, an anomalous drought year, gross carbon emissions due to fire in the Amazon were 1.7 times higher (0.51 $\pm$ 0.12 Pg C) than during the subsequent non-drought year (GATTI et al., 2014). This value corresponded to 57% of 2010 global emissions from land-use change (0.9 $\pm$ 0.7 Pg C) (FRIEDLINGSTEIN et al., 2010). The impact of fire on the carbon budget amplifies the effects of climate change, which will ultimately affect its occurrence,

thus setting up a positive feedback loop (JOLLY et al., 2015). Therefore, political strategies and mechanisms are needed, aiming at the integrity of ecological functions and the provision of ecosystem services.

In this sense, protected areas can be defined as all public or private areas under land-use restrictions that contribute to protecting native ecosystems, even if they were created for purposes other than environmental conservation (SOARES-FILHO et al., 2010). Studies have shown that protected areas, including those with resident human populations, are necessary for an effective global strategy to minimize climate change and preserve tropical forests and ecosystem services (MELILLO et al., 2016; NEPSTAD et al., 2006, 2009; NOGUEIRA et al., 2018; RICKETTS et al., 2010; SOARES-FILHO et al., 2010). For example, it is estimated that protected areas in the Brazilian Amazon biome accounted for 54% of the forest remnant and contained 56% of its carbon up to 2010 (SOARES-FILHO et al., 2010). If properly implemented, protected areas have the potential to avoid 8.0 ± 2.8 Pg of C emissions by 2050 (SOARES-FILHO et al., 2010), albeit the benefits associated with their implementation go far beyond avoided carbon emissions. Protected areas are also recognized as effective instruments for reducing biodiversity loss (GELDMANN et al., 2013) and improving socioeconomic conditions (FERRARO; HANAUER, 2014; NAIDOO et al., 2019).

Although protected areas are a flagship for tropical forest conservation, several factors in the Amazon region affect their effectiveness in curbing fire occurrence. For instance, agricultural and urban expansion push deforestation closer to the edges of these areas, often entering their borders (DE OLIVEIRA et al., 2020; MATAVELI et al., 2021; MATAVELI; DE OLIVEIRA, 2022). In addition, the weak land titling regulation (ARMENTERAS et al., 2019), recurrent among Amazonian countries, and significant setbacks in environmental legislation in recent years (VILLÉN-PÉREZ et al., 2020), drive deforestation and forest degradation into public lands, including protected areas. In Brazil, land grabbing within protected areas (MATAVELI; DE OLIVEIRA, 2022; RORATO et al., 2021) has resulted from the wrecking of public monitoring and command and control agencies, weakening governance over these areas (DE OLIVEIRA et al., 2020; MATAVELI; DE OLIVEIRA, 2022). The current president's constant anti-environmental speech brings a sense of impunity to environmental offenders

(FERRANTE; FEARNSIDE, 2022), making the situation even worse. Along with deforestation comes forest fragmentation and all the degradation that comes from it (SILVA JUNIOR et al., 2018, 2020a). Additionally, selective logging is still a relevant factor that aggravates forest degradation (BRANCALION et al., 2018). Degraded forests, which occur mainly on the borders of these protected areas, are more vulnerable to fires (BERENGUER et al., 2021; SILVA JUNIOR et al., 2018).

Protected areas' role in mitigating climate change through deforestation avoidance has attracted more attention from researchers, being better portrayed scientifically (ANDAM et al., 2008; NEPSTAD et al., 2006; PFAFF et al., 2015a; SOARES-FILHO et al., 2010). Thus, there are still gaps in the scientific literature on the role of these areas in mitigating fire occurrence in the Amazon, considering the current dynamic of anthropogenic activities and climate change. Nevertheless, Nepstad et al. (2006) found that protected areas, including those that allow human residency, have reduced fire in the Brazilian Amazon. However, their analysis only included data from 1998, which does not give us a long-term and up-to-date idea about the process. Further, Nelson and Chomitz (2011) found that from 2000 to 2008, indigenous lands reduced forest fire incidence by 16 percentage points in Latin America. This study provides important evidence of the protected areas' role in fire. However, it does not detail the results at the national level, which makes it challenging to incorporate relevant information into policy decisions, in addition to not including important political and economic dynamics in the post-2008 Amazon region. Nolte and Agrawal (2013) also evaluated protected areas' effectiveness in curbing forest fires and found a significant negative effect compared to similar unprotected areas, independently of the management effectiveness level of particular areas. In this case, the authors analyzed fire occurrence from 2000 to 2010.

Furthermore, studies have already evaluated the impacts of climate change on protected areas' biodiversity (HANNAH, 2008) or the role of these areas in mitigating climate change, mainly as a potential carbon sink (MELILLO et al., 2016; RICKETTS et al., 2010; SHI et al., 2020; SOARES-FILHO et al., 2010). However, there is still a gap in understanding how the climate changes, specifically within protected areas. Although there is already strong evidence of climate change in the Amazon (ALMEIDA et al., 2017; GATTI et al., 2021; MARENGO et al., 2018), it has not yet been evaluated whether

this variability occurs within protected areas, and if so, whether it occurs at the same rate as outside.

Considering the existing literature and the increasing threats to which these Amazonian protected areas are exposed, a detailed and updated formal study of fire occurrence within protected areas becomes relevant. Such a diagnosis can be used as concrete evidence of what is happening within these areas. More specifically, how fire occurrence and drivers patterns have changed over the last few decades and how we can ensure that these areas continue to be a bulwark in conserving the environment and maintaining the ways of life of indigenous and traditional peoples. Therefore, the main objective of this chapter was to carry out a recent and in-depth diagnosis of fire occurrence and its main drivers in protected areas of the Amazon basin. Broadly, we want to answer if fire occurrence is an increasing threat to Amazonian protected areas. Contrasting to what was observed outside these areas, we aimed to assess the threat level that protected areas have been exposed to between 2003 and 2020. Specifically, the following research questions were formulated:

Q1. What is the pattern of fire occurrence inside and outside protected areas in the Amazon basin? Has this pattern changed in the period from 2003 to 2020? Is the pattern occurring within the categories of protected areas different from what happens outside them? We want to measure if burned area extent differs inside from outside protected areas and if the pattern changes over time. Among the protected areas categories, we want to measure if there is a difference in the burned area extent registered within them. This will be the initial comparison of what happens inside and outside these areas and the first evidence of their performance regarding fire occurrence.

Q2. What is burning? The pattern of the burned area by land use and land cover class might change according to protection status, and we want to answer if, inside protected areas, more natural land cover is burned compared to outside. This would highlight a greater threat to natural ecosystems when a fire occurs within protected areas. In addition, the fire that occurs in natural vegetation can be associated with illegal activities within protected areas, which reflects a greater threat.

Q3. Where is fire ignition occurring? Here, we want to assess where the fire occurring inside protected areas comes from, measuring the proportion of fire ignition that occurs inside protected areas and the share of burnt scars ignited outside that enter these areas.

Answering this question will give us evidence of the imminent fire occurrence threat level posed to these areas and where that threat mostly comes from, inside or outside them.

Q4. Is population density correlated to fire occurrence in the Amazon basin? Given the fire occurrence dynamic described in the previous questions, we want to evaluate the pattern of the relation between fire occurrence and population in the Amazon basin from 2003 to 2020. Population dynamics and its relationship with fire in the Amazon will show us the drivers behind the observed patterns of fire occurrence within protected areas. In addition, we want to test the prediction capacity of fire occurrence probability given the population density. The rationale here considers that increasing population density in the region would pose a greater threat to fire occurrence if there is a significant relationship between population and fire.

Q5. Does the pattern of climate change observed outside protected areas also occur inside? Finally, we want to assess whether the environment within protected areas is becoming more fire-prone, as is already observed in the Amazon. For that, climatic conditions of temperature and precipitation during the dry season from 2003 to 2020 will be evaluated inside and outside protected areas. This last question will give us evidence on one more factor of the fire occurrence triangle, reinforcing if protected areas are exposed to a more fire-susceptible environment.

4.2 Materials and methods

4.2.1 Study area

The study area comprises the whole extension of the Amazon Basin (EVA; HUBER, 2005), excluding the subregions of ‘Planalto’ and ‘Andes.’ Even not including the whole region classified as Amazonia *sensu latissimo* by Eva and Huber (2005), we refer to the region considered as the Amazon basin for this study. This area spans nine South American countries: Bolivia, Brazil, Colombia, Ecuador, French Guiana, Guyana, Peru, Suriname, and Venezuela, and it adds up to more than 6 million square kilometers (Table 4.1 and Figure 4.1). All nine countries host 95% of the remaining Amazonian old-growth forests (EVA; HUBER, 2005).

The largest portion of the study area is located in the Brazilian territory (62%). Although Peru presents the largest number of protected areas (1,598), Brazil has the largest

extension of it (2,250,716 km²). In terms of proportion to the country area within the Amazon basin, only Guyana and Suriname have less than half of their territory protected, even though this proportion, in all countries, can be potentially overestimated due to overlapping[6] between protected area categories. Considering the study area as a whole, the overlapping corresponds to approximately 8% of the protected area, which takes the total proportion of the protected area from 54% to 49%, thus keeping almost half of the study area under some type of protection. Venezuela has the largest average size of protected areas, contributing to the 42 thousand km² overlapping between protected areas seen in that country. The largest protected area is the Indigenous Land Yanomami, created in 1992 in northern Brazil.

Table 4.1 - Study area descriptive numbers.

Country	Area within Amazon basin (km²)	% country area	Protected areas (N)	Protected area (km²)	% protected area within Amazon basin	Average protected area (km²)	Maximum protected area (km²)	Minimum protected area (km²)
Bolivia	436,809	40%	103	274,327	63%	2,663	15,985	0.3
Brazil	4,192,787	49%	627	2,250,716	54%	3,590	94,818	0.1
Colombia	480,891	42%	209	371,856	77%	1,779	58,448	0.4
Ecuador	74,484	29%	241	72,700	98%	302	10,231	0.5
French Guiana	83,617	100%	19	53,031	63%	2,791	20,515	1.2
Guyana	210,614	100%	5	9,992	5%	1,998	3,717	617.4
Peru	639,518	50%	1,598	345,987	54%	217	24,918	0.0
Suriname	145,018	100%	14	21,695	15%	1,550	15,971	67.6
Venezuela	446,713	49%	32	221,194	50%	6,912	75,603	5.2
Total	*6,710,451*	*49%*	*2,848*	*3,621,497*	*54%*			

We defined protected areas as all public or private areas under land-use restrictions that contribute to protecting native ecosystems, even if they were created for purposes other than environmental conservation (SOARES-FILHO et al., 2010). In the Amazon basin, we considered protected areas the indigenous lands and areas of public or private domain intended for some level of protection and provided in the national systems of protected areas[7]. An important mechanism of protected areas is their categorization. In this chapter, we homogenize the protected areas present in each Amazonian country into three broader categories: Indigenous Lands, Direct Use Protected Areas, and Indirect Use Protected Areas (Table 4.2). Table A.1 presents the specific national description of each category

[6] Overlaps occur when more than one protected area occupies the same location, often because they are areas upon different protection categories. For example, it is not uncommon for indigenous lands to be located within other categories of protection, such as national parks, biological reserves, etc.

[7] There are still a range of protected areas on private land that are not necessarily regulated by protected area systems. This is the case of Permanent Protection Areas and Legal Reserves, provided for in the Brazilian Forest Code. These areas will not be analyzed in this chapter.

found in each country and its correspondence to the category used in this work. In this chapter, we considered all protected areas, regardless of jurisdiction.

Figure 4.1 - Study area.

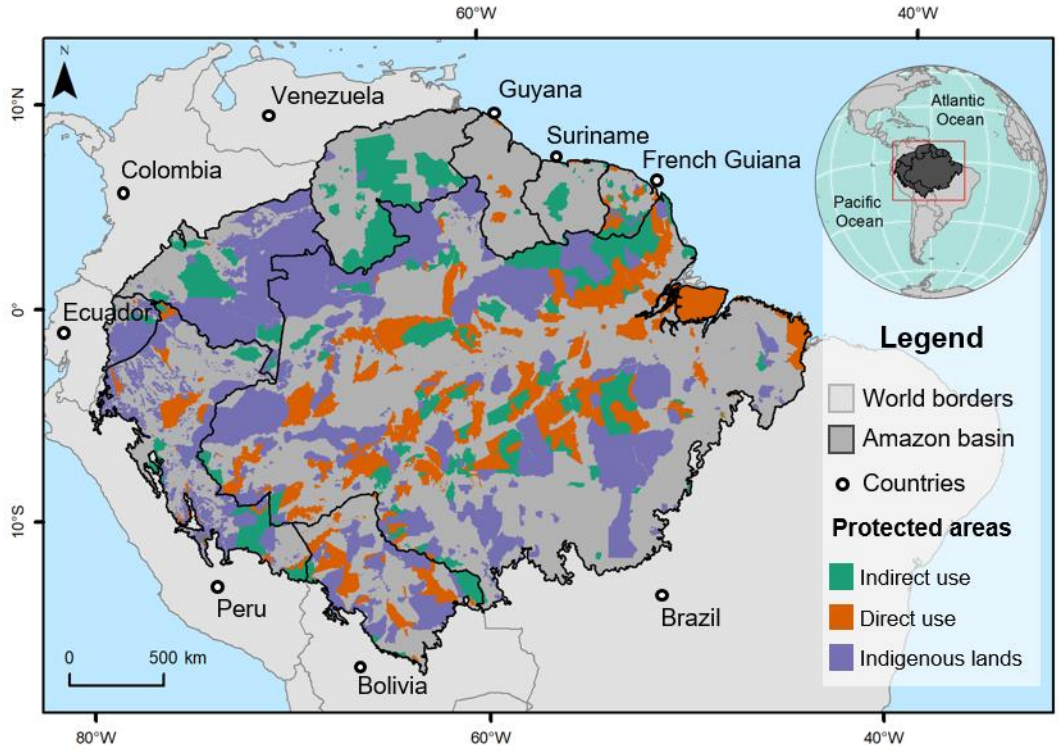

Source: RAISG (2022).

Table 4.2 - Description of each protected area category defined in the scope of this chapter.

Category		Description
Indirect use protected areas	IU	Protected areas whose main objective is the conservation of ecosystems, not allowing human populations to reside in their interior, and have a high level of activity restriction. They allow only the indirect use of natural resources.
Direct use protected areas	DU	Protected areas that aim to balance environmental conservation with the management of sustainable activities, allowing human populations to reside in the interior and the direct use of natural resources. They have moderate to low levels of activity restriction.
Indigenous lands	IL	Territories that were demarcated for indigenous peoples to guarantee their traditional way of life and subsistence.

4.2.2 Spatial dataset and data analysis

Protected areas data was obtained from the Amazon Network of Georeferenced Socio-Environmental Information (RAISG, from the Portuguese acronym; Figure 4.1 and Table

4.3). The data was downloaded in July 2021, which included updates till 2020[8]. It used data from National and Departmental Natural Protected Areas and Indigenous Territories, which are jointly called protected areas here.

Protected areas without a creation date were excluded from the dataset. We first consulted local experts with knowledge of the current situation, then we defined the creation date where it was possible to find the information. In the rest of the entries without a creation date, we confirmed the impossibility of specifying an exact date. This represented 12% of the PA dataset (356 PAs). Also, these cases were spatially concentrated, mainly belonging to Ecuador (137), Guyana (108), and Peru (108). Moreover, the overlap between protection categories was handled following the order of prioritization, IU protected areas, DU protected areas, and IL. In other words, if a pixel fell within more than one protection category, it was assigned the category following our prioritization criteria.

The protected area information was incorporated into a regular 5 km grid, considering the centroid of each pixel. A binary variable was created to receive one of the pixel centroid fell within a protected area and 0 otherwise. The Euclidian distance from the pixel centroid to the edge of the nearest protected area was also calculated. This distance took negative values if the centroid was inside a protected area. All information regarding the respective protected area, such as creation year, size, and category, was then incorporated into that specific pixel. Finally, another binary variable was created to designate whether the pixel was within an active protected area in the current year or not. If the protected area creation date was before the current analyzed year, this binary variable received 1, and 0 otherwise. This way, we only considered being within a protected area if the protection was active during the current year of analysis.

In this chapter, we present five independent analyses, each to answer the explicit questions in the objectives (Figure 4.2). Each analysis was performed with specific datasets and analytical methods and will be described separately in the following sections. Table 4.3 brings the specifications of the main datasets included in this chapter's analysis.

[8] Downloaded from https://www.amazoniasocioambiental.org/pt-br/mapas in November 2020.

Figure 4.2 - General flowchart of the data analysis in Chapter 4.

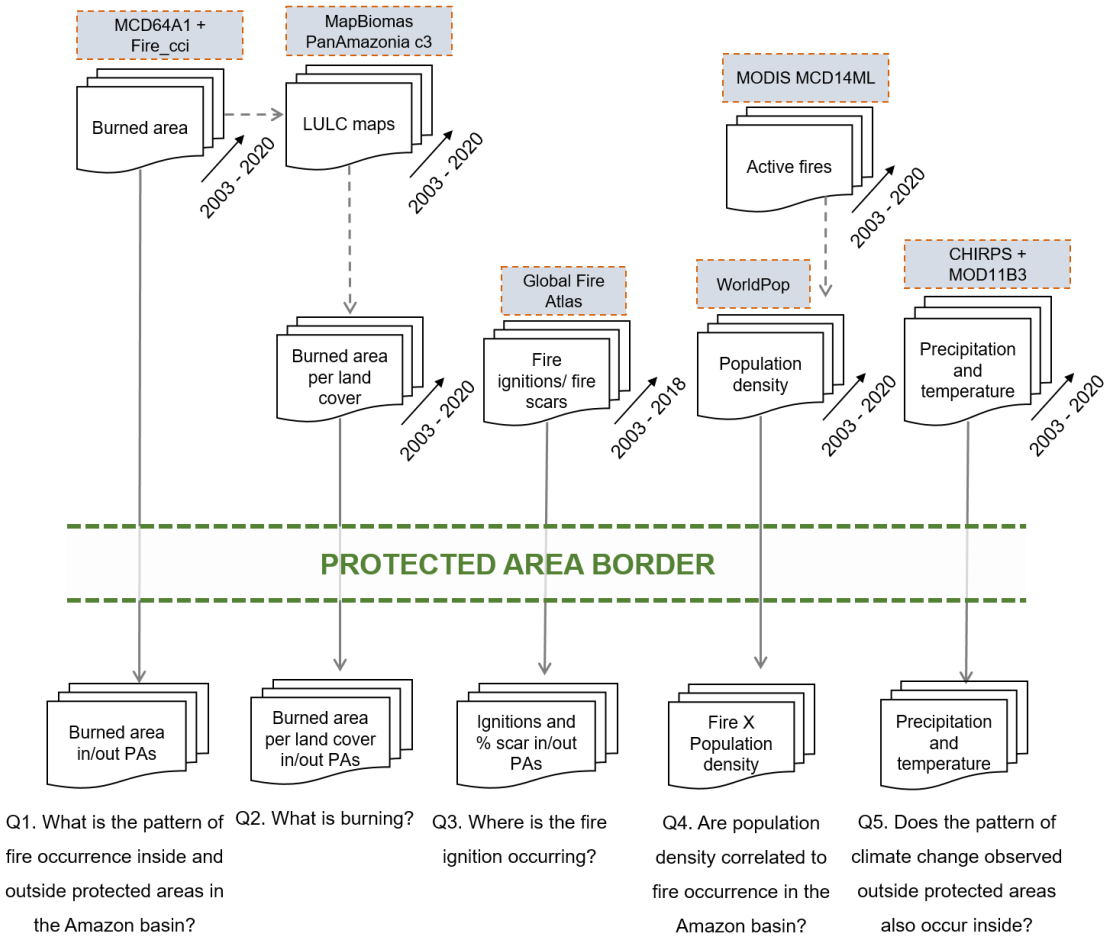

Table 4.3 - Dataset description and specifications.

Product	Description	Original resolution	Time span	Source
MCD64A1 c6	Annual burned area	500m	2003-2020	(GIGLIO, LOUIS et al., 2015)
Fire_cci v5.0	Annual burned area	250m	2003-2020	(CHUVIECO et al., 2018)
MCD14ML	Annual active fire	Point data	2003-2020	(GIGLIO, LOUIS, 2000)
Global Fire Atlas	Annual fire ignition and individual fire scar	Point and polygon data	2003-2020	(ANDELA et al., 2019)
CHIRPS	Monthly precipitation	0.05° (~ 5 km)	2003-2020	(FUNK et al., 2015)
MOD11B3	Monthly land surface temperature	1km	2003-2020	(WAN, ZHENGMING; HOOK, SIMON; HULLEY, GLYNN, 2015a)
Silva Junior et al.	Annual old-growth forest deforestation	30m	2003-2020	(SILVA JUNIOR et al., 2020b)
Silva Junior et al.	Annual secondary forest deforestation	30m	2003-2020	(SILVA JUNIOR et al., 2020b)
Silva Junior et al.	Annual secondary forest	30m	2003-2020	(SILVA JUNIOR et al., 2020b)
MapBiomas	Annual land use and land cover classes	30m	2003-2020	MapBiomas PanAmazonia collection 3
WorldPop	Annual population count	1km	2003-2020	(LLOYD et al., 2019)

4.2.3 Data analysis

4.2.3.1 Fire occurrence pattern within Amazonian protected areas

We calculated the total burned area inside and outside protected areas, considering their respective categories from 2003 to 2020. We used two different fire data sources (Table 4.3); the Moderate Resolution Imaging Spectroradiometer (MODIS) burned area product MCD64A1 version 6 (GIGLIO, LOUIS et al., 2015) and the Fire Disturbance (Fire_cci) product, which is part of the Climate Change Initiative (CCI) program developed by the European Space Agency's (ESA) (CHUVIECO et al., 2018). As suggested in Pessôa et al. (2020), the two burned area data were added together to minimize regionally burned area underestimations and maximize the intrinsic benefits of each of the products. The product choice was based on their availability at Google Earth Engine (GEE) Platform by mid-2022, at the Amazon basin level, and for the time series from 2003 to 2020. First, the products were transformed into annual binary products (burned/non-burned) and then merged into a single product of 250 m spatial resolution (Fire_cci product resolution). Finally, this joint product was resampled into the regular 5 km grid considering each pixel's annual proportion of the burned area. This processing was entirely done in Google Earth Engine (GEE). Burned area proportions in each pixel were transformed into the area by multiplying it by the pixel area (approximately 30.98 km²). The final analyzes were performed by tabularly aggregating the grid data by protection status (inside and outside protected areas), year, country, and protection category.

4.2.3.2 Burned area per land use and land cover classes

The burned area analysis by land use and land cover (LULC) class was performed using the merged burned area data (MCD64A1 + Fire_cci). This hybrid data was overlayed with data from the Annual Land-Use and Land-Cover Mapping Project (MapBiomas PanAmazonia collection 3) or secondary LULC data developed from it by Silva Junior (2020b) (Table 4.3). MapBiomas PanAmazonia dataset provides 36 years of LULC classification using images of 30-m spatial resolution) and details about the processing of the dataset and class definition can be found in MapBiomas (2021). We extracted annual information on forest extension, farming, other natural formations, and others. Other natural formations include savannas, mangroves, flooded forests, and non-forest natural formations. The ‘other’ class includes mostly non-vegetated classes. In addition to these

classes, it was also considered secondary forest and deforestation of old growth and secondary forest obtained from Silva Junior (2020b). From the forest formation map from 1985 (the first year classified by MapBiomas), every pixel that turned into any non-natural class in the following year was classified as old-growth forest deforestation. Deforestation of old-growth forests only occurs once, and it is not possible to reclassify a given pixel as an old-growth forest at any time. This pixel, which is no longer an old-growth forest, can become several classes, and if at some point it reverts to a forest, it is classified as a secondary forest. Secondary forests' deforestation occurs when secondary forests are converted to any non-natural class in the following year. This type of deforestation can happen several times since secondary forests are reversible.

The overlaying process of burned area and LULC data, and its subsequent resample into the regular 5 km grid considering the annual proportion of burned area per LULC in each pixel, was entirely done in Google Earth Engine (GEE). Similarly to the burned area per LULC, the raw LULC data was also incorporated into the regular grid. All this information was transformed into the area by multiplying it by the pixel area (approximately 30.98 km²). The final analyzes were performed by tabularly aggregating the grid data by protection status (inside and outside protected areas), year, country, and protection category.

4.2.3.3 Fire ignition analysis

For the fire ignition analysis, we used data from the Global Fire Atlas (ANDELA et al., 2019) for the period from 2003 to 2018, as this is the available time for this dataset (Table 4.3). However, the data for 2018 is only available up to November, and estimates for this specific year could be slightly underestimated. This dataset provides information on individual burn scars for each year and their respective ignition point. Firstly, we incorporated the ignition point information into the 5 km grid used in the previous analysis, considering the sum of ignition in each pixel per year. With the fire ignition and protected areas information in the grid, we analyzed their occurrence by protection category. First, the fire ignition within the study area was identified and classified according to their location, outside or inside protected areas. 483,213 fire ignition points were within the study area during the 15 years analyzed. We then calculated the distance from each ignition point to the border of the nearest protected area. Finally, we identified

the respective burn scar for each ignition point and calculated the proportion of the area inside and outside protected areas for each burn scar.

4.2.3.4 The relation between fire and population density

Unlike the other analyzes in this chapter, the relationship between population and fire occurrence was evaluated by aggregating data on a grid of approximately 10 km spatial resolution. We used data from the MODIS active fire product MCD14ML version 6 (GIGLIO, LOUIS, 2000), filtered for data acquired from the Aqua platform with a confidence level higher than 30%. The active fires were annually grouped and incorporated into the grid, considering the count in each pixel. In addition, the population count was obtained from the WorldPop data (Table 4.3). The WorldPop project combines a range of geospatial datasets into a flexible regression tree framework to reallocate contemporary aggregated spatial population count data (LLOYD et al., 2019). Its original resolution is 1 km, so summing was used as an aggregation method to incorporate it into an approximately 10 km grid annually.

Once the WorldPop population count data was modeled, we compared it with two other datasets to assess whether there was too much discrepancy between datasets. We compared it with the Gridded Population of the World (GPW) v4 (CENTER FOR INTERNATIONAL EARTH SCIENCE INFORMATION NETWORK-CIESIN-COLUMBIA UNIVERSITY, 2018) data and the statistical grid of the national census developed by the Brazilian Institute of Geography and Statistics - IBGE (IBGE, 2011). This comparison analysis aggregated all datasets in the approximately 10 km grid, considering only the Brazilian Amazon limits for 2010 since the Brazilian census grid is only available for this space-time scale. GPW population input was collected at the most detailed spatial resolution available from the 2010 Population and Housing Censuses results, which occurred between 2005 and 2014. The input data, in this case, was extrapolated to produce population estimates for the years 2000, 2005, 2010, 2015, and 2020. The Brazilian Census Statistical Grid divides the territory into pixels of 200 x 200 m in urban areas and 1 x 1 km in rural areas, allowing data to be aggregated regardless of political-administrative divisions. We observed that the determination coefficient (R^2) between the three possible comparison pairs is always greater than 75% (Figure 4.3), reaching 97% when WorldPop is compared with GPW. This underpins the choice to use

the WorldPop product in this chapter since it is the only one that provides annual data for the study period of this work (2003-2020), and it is not significantly different from other products.

Figure 4.3 - Comparisons between population count data for the Brazilian Legal Amazon in 2010. Comparisons were made between: WorldPop x Census Grid (a), GPW x Census Grid (b) and GPW x WorldPop (c).

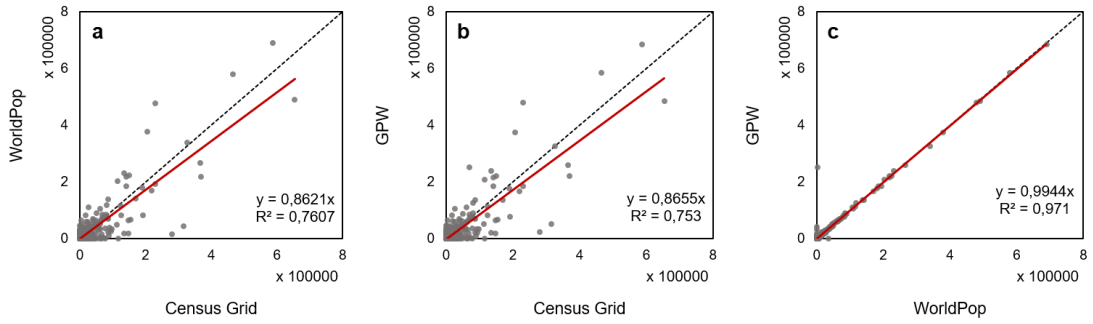

Data from WorldPop, GPW, and the Brazilian Census Grid.

As our objective was to understand the population density pattern of where fire occurs, we only considered pixels that registered active fire in at least one year from 2003 to 2020. Therefore, we used the quantile method to separate the mean population count (2003-2020) into ten classes with approximately similar observation numbers. Further, we divided the lower and upper classes into three classes using the first quartile and median, and the third quartile, respectively. This subdivision was carried out to highlight the upward and downward aspects of the relation curve. This way, summing the observations of these three smaller classes will approximately result in the observation number of the other classes (Table 4.7).

The distribution of fire occurrence in each population class described above was evaluated with boxplot plots. The relationship between population and fire occurrence was visually evaluated with scatterplots. We observed that there is a range from low to high fire occurrence in each population class, reaching different fire occurrence peaks according to the population classes. For the scope of this analysis, the high fire occurrence cells were selected, which is what differs on a spectrum of population density. To better visualize this pattern, we separated each population class's ten highest fire occurrence points. Then, we fitted a local regression model using the LOESS (locally estimated scatterplot smoothing) method to these points. The LOESS method fits simple models to

localized subsets of the data to build up a function that describes the deterministic part of the variation in the data, point by point, generating a smooth curve through a set of data points. The inflection point of the LOESS curve, which is the point where the relationship between fire occurrence and population ceases to be increasing and becomes decreasing, was determined by the point of the lowest slope. We used logarithmic transformation in the population variable for the scatterplots to circumvent the concentrated distribution in values close to zero. This transformation required us to add 0.001 for all values of population count once this variable allows for zeros. Thus, points falling in the smallest logarithmic value in the scatterplots represent fire occurrence in pixels with no population.

We performed a sensitivity test of fire occurrence prediction according to population density. For this, we used a logistic regression model that uses the independent variable population to predict the probability of fire occurrence. The logistic model requires that the dependent variable be binary, so we created a variable that received the value one if the pixel registered fire in at least one year of the time series and 0 otherwise. The logistic regression coefficients estimation is carried out using maximum likelihood, which seeks to find the most likely coefficients estimates and maximize the probability that an event will occur. The model's performance was assessed by the "pseudo" R^2 suggested by Nagelkerke (1991) and by examining the predictive accuracy (confusion matrix). As the logistic regression model brings the estimators results in logarithmic form, we performed the exponentiation of the regression variables, thus obtaining the odds ratio for the independent variables, in this case, the population log. The odds ratio tells us the variation proportion in fire occurrence given one unit variation of the population variable.

We also built the ROC curve (Receiver Operating Characteristic Curve), which, associated with the logistic model, measures the prediction capacity of the proposed model through the predictions of sensitivity and specificity. Thus, the lower left point (0,0) means that a positive classification is not predicted; the opposite corner of the graph (1,1) classifies the unconditionally positive results, and; the point (0.1) represents an excellent rating. The further northwest of the graph the point is, the better. The cutoff point would then be the point on the ROC curve where the prediction has the highest sensitivity with the highest specificity. In our case, the cutoff point is the population value

that best predicts the threshold for fire occurrence. In addition, we calculated the Area under the ROC Curve (AUC), which aims to measure the performance of the curve in a single scalar value. The AUC indicator ranges from 0 to 1, and the closer to 1, the better the model performance, and it should never be below 0.5.

Studies have already used logistic regression models for fire prediction (ZAPATA-RÍOS et al., 2021). These models can be used to test the significance of explanatory variables of fire occurrence. Indeed, the more significant explanatory variables are considered, the more reliable the model's prediction is. The analysis presented here is only a first assessment of the relationship between fire and population. However, we recognize that the values obtained may not reflect reality since only one explanatory variable was considered. Our purpose here was to assess the significance and pattern of the relationship, not its magnitude.

Furthermore, to avoid spatial correlation, we randomly sampled 8000 pixels (half with fire occurrence in at least one year and another half without fire). This sample size represents approximately 10% of the entire dataset for this analysis. Although we recognize that this sample must be subjected to robustness checks, we did not perform these tests.

All the analyses were repeated, separating the period from 2003 to 2020 into dry and normal years. For instance, 2005, 2010, 2015, and 2016 were considered dry years, and the rest were considered normal years (MARENGO et al., 2008, 2011; SILVA JUNIOR et al., 2019). Finally, we aggregated the WorldPop annual data into the 5 km grid used in the previous analysis in this chapter to compare population metrics inside and outside protected areas.

4.2.3.5 Climate change within protected areas

Climatic conditions during the dry season are a critical factor in environmental vulnerability to fire (CARVALHO et al., 2021). Knowing this, we evaluated how climatic conditions of temperature and precipitation during the dry season have changed on an 18-year time scale and whether this variability follows the same pattern inside and outside protected areas. We used temperature data from MODIS MOD11B3 Monthly Land Surface temperature product (WAN, ZHENGMING; HOOK, SIMON; HULLEY,

GLYNN, 2015a) and monthly precipitation measures obtained from Rainfall Estimates from Rain Gauge and Satellite Observations - CHIRPS (FUNK et al., 2015) (Table 4.3). Both products were incorporated into the 5 km grid, considering each pixel's dry season average yearly. The temperature data originally had a lower spatial resolution. It was resampled to the grid resolution using the average metric to assign the value to the coarser pixel.

The average precipitation and temperature during the dry season definition considered the onset and duration of spatially explicit dry season periods defined by Carvalho et al. (2021). The authors defined dry season length as the number of consecutive months with rainfall lower than 100 mm (average from 1981 to 2019). This threshold is used because of tropical forests' mean monthly evapotranspiration value (VON RANDOW et al., 2004). With the persistence of rainfall below it, evapotranspiration exceeds rainfall, which can be used as an indicator of water deficit in these ecosystems (ARAGÃO et al., 2007; MALHI et al., 2002). This way, dry season timing is delimited by grouping pixels that share the same month for the onset and end of the dry season, resulting in 74 homogeneous regions across the Amazon basin. The average of the variables was calculated differently considering the specific dry season timing in each of these regions.

We first calculated temperature and precipitation anomalies during the dry season from 2003 to 2020. For this, we aggregated our dataset to obtain the average temperature and precipitation during the dry season per year and protection status (inside or outside protected areas). The idea was to compare the average value found in each protection category to the general average, which includes all the cases (inside + outside). For this, we defined anomaly as (Equation 4.1):

$$\boldsymbol{Anomaly} = \frac{(\boldsymbol{a} - \boldsymbol{mean})}{\boldsymbol{sd}} \tag{4.1}$$

Where *a* is the average temperature or precipitation per year per protection status, *mean* is the general average, and *sd* is the general standard deviation. Following, we calculated the mean temperature and precipitation during the dry season per year for the entire study area, as well as separately for inside and outside protected areas, to evaluate the general trend of climate variation. Finally, we evaluated the temporal trend of each climate variable per pixel using linear regression. We also evaluated the statistical significance of

the linear regression per pixel and only displayed significant trends on the final maps ($p < 0.05$).

4.3 Results and discussion

4.3.1 Fire occurrence pattern within protected areas

Among the protection categories, indigenous lands are the ones that accumulate the largest area, totaling more than 1.7 million km² in 2019 (Figure 4.4a). The expansion of protected areas advanced in the late 80s and has continued to rise to the present day. In the 1950s, IU protected areas prevailed, which began to change in the late 1980s when indigenous lands and DU protected areas gained prominence (Figure 4.4b). The categories are distributed differently among the Amazonian countries, with indigenous lands in Bolivia and Brazil corresponding to 48% of the total protected area in each country in 2019. In Colombia, Ecuador, and Peru, this figure exceeds 60% (Figure 4.4c). Most protected areas were created by 2002 in most countries (Figure4.4d), with a few exceptions.

Figure 4.4 - Protected area extent and creation until 2019 in each Amazon basin country. (a) The total accumulated area from 1959 to 2019 per protection category in the Amazon basin. (b) The relative percentage of each protection category from 1959 to 2019. (c) The relative percentage of each protection category in 2019 in each Amazonian country. (d) The proportion of protected area created over the years in relation to the total in 2019, per Amazonian country and protection category.

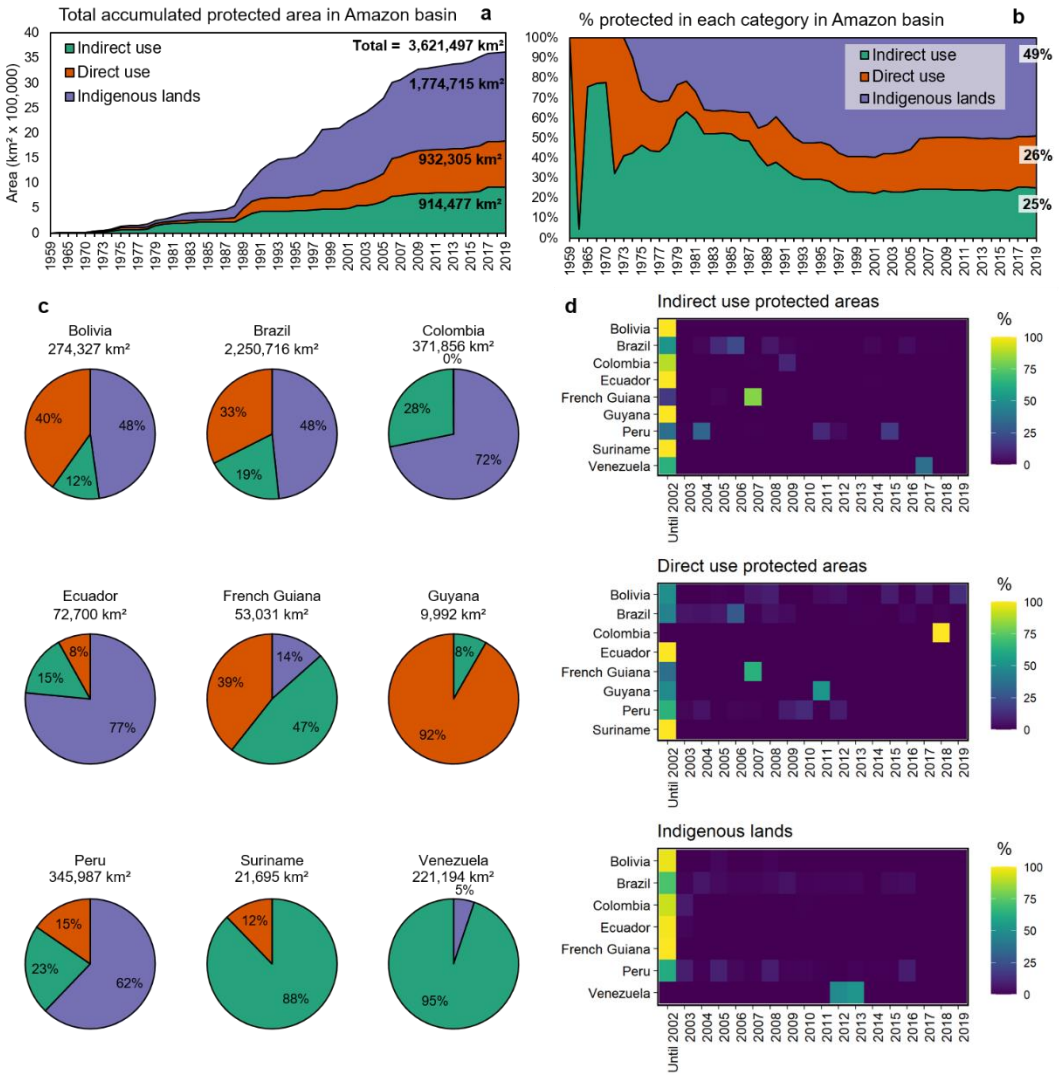

From 2003 to 2020, the maximum area that has already been affected by fire in the Amazon basin reaches 1.4 million km², corresponding to 21% of the basin area. This area is not the total burned extent since fires can affect the same area multiple times. Of the total accumulated burned area, 28% was within protected areas. We estimated that fires have affected, an average, 79,196 km² per year. In general, only 0.1% of the area under any type of protection is affected by fires, half of the rate registered outside protected areas. Thus, most of the burned area, on average, occurred outside protected areas (72%), and from the burned area registered inside, 61% (13,572 km² per year) occurred within

Indigenous lands (IL). In comparison, 28% (6,125 km² per year) occurred within Direct use (DU) protected areas and 11% (2,526 km² per year) within Indirect use (IU) protected areas.

Annually, we observed that the largest areas affected by fire occurred in years that registered extreme droughts in the Amazon region, mainly 2005 (130,340 km²), 2007 (135,999 km²), and 2010 (163,293 km²) (Figure 4.5). As El Niño, the phenomenon responsible for the drought in 2015/2016, affects the end of the year, it is likely that fire occurrence recorded in these two years was affected by the drought. Together (139,830 km²), they exceeded the affected area in 2005. In addition, in 2015, the water recharge in the forest during the rainy season was also hampered by the lack of rain, which made the forest more susceptible to fire 2016 (SILVA JUNIOR et al., 2019). Despite the period after 2010 being marked by the adoption of several anti-deforestation policies in the Amazon, studies have shown that while deforestation decreased under policy treatment, forest fires were less responsive to policies. Instead, fire events and burned areas were strongly influenced by precipitation (TASKER; ARIMA, 2016). Moreover, 2017 registered a larger burned area than 2015/2016 registries, probably due to the high availability of fuel material affected by previous years' drought.

The highest burned extent within protected areas was registered in 2010 (47,218 km²). However, 2011 registered 40% of the total burned area within protected areas, the highest proportion between 2003 and 2020 (Figure 4.5). In general, the area burned inside protected areas follows the same pattern as the area burned outside; when fire affects a greater area outside, a greater area inside protected areas is also affected. This shows that, although the extent affected by fire within protected areas is smaller, it is sensitive to factors that transcend the legal instrument of protection, such as climate and socio-economic aspects. In addition, it also attests to the ability to deal with firefighting and fire prevention in these areas since fire vulnerability is shared either inside or outside protected areas. Burned area proportion per year that occurs within protected areas, however, has grown more than twice from 2003 (18%) to 2020 (38%), showing an increasing threat to the protection of these areas (Figure 4.5).

Figure 4.5 - Burned area within protected areas. Burned area proportion inside and outside protected areas from 2003 to 2020 (left panel) and total burned area inside and outside protected areas (right panel). The dependent variable is displayed on the x-axis for visualization purposes.

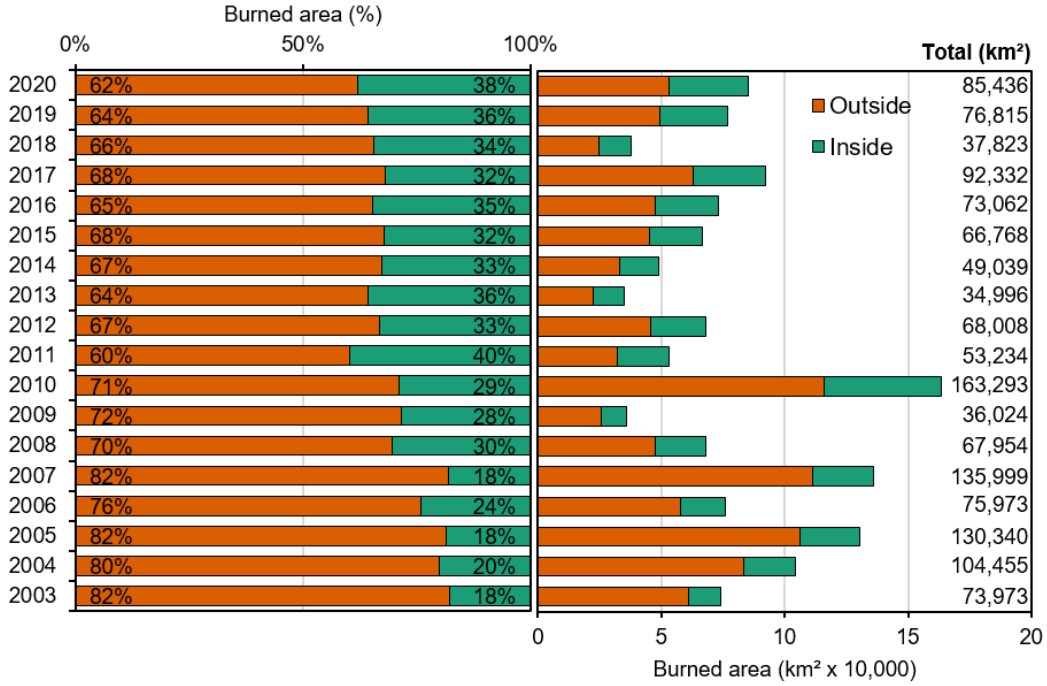

Brazil is the country that recorded the highest average area affected by fire between 2003 and 2020 (51,304 km² per year), which is expected given the territorial dimension belonging to the Amazon basin of this country, followed by Bolivia (24,275 km² per year) and Colombia (2,991 km² per year) (Table 4.4.). Although Brazil also registered the highest burned rate per year inside protected areas (11,286 km² per year), Suriname presented the highest burned area proportion inside protected areas (74%). The 119 km² burned on average per year within Suriname's protected areas represents 0.5% of the country's total protected area. Unfortunately, Bolivia wins in this regard, burning an average of 3.7% of its protected territory yearly. If we do not consider the recurrence of fire in the same area, with the observed rate, Bolivia could have its protected extension completely burned in just 28 years.

Table 4.4 - Burned area (mean from 2003 to 2020) in each Amazonian country.

Country		Inside ($km^2.year^{-1}$)	% total (inside + outside)	Outside ($km^2.year^{-1}$)	% total (inside + outside)	Total ($km^2.year^{-1}$)
Bolivia	BO	10,150.10 (5,421.89)	{42%}	14,125.31 (8,233.87)	{58%}	24,275.41
Brazil	BR	11,286.48 (4,519.34)	{22%}	40,017.62 (22,327.21)	{78%}	51,304.10
Colombia	CO	556.90 (388.28)	{19%}	2,434.56 (1,773.41)	{81%}	2,991.45
Ecuador	EC	0.01 (0.02)	{6%}	0.09 (0.39)	{94%}	0.10
French Guiana	GF	26.00 (18.93)	{39%}	40.79 (23.36)	{61%}	66.79
Guyana	GY	6.04 (6.62)	{9%}	60.09 (43.53)	{91%}	66.13
Peru	PE	24.57 (24.11)	{16%}	131.44 (128.71)	{84%}	156.01
Suriname	SR	118.92 (102.42)	{74%}	42.37 (36.25)	{26%}	161.29
Venezuela	VE	54.18 (46.37)	{31%}	120.38 (64.99)	{69%}	174.57

Absolute values are the mean burned area from 2003 to 2020. Values in parenthesis are standard deviations from the mean. Values in braces are percentages from the total burned area in each country.

Depicting the annual rates of the burned area within protected areas by protection categories, we observe that Indigenous lands (IL – 17%) are more affected than protected areas of direct (DU – 8%) or indirect use (IU – 3%) (Table 4.5). In 2010, all three categories registered the largest affected area. In general, the burned area in the Amazon basin grew in the last three years of the time series (2018-2020), both outside and inside protected areas. Particularly, direct use protected areas registered the highest proportion of burned area in relation to the total in 2020 (14%), reaching values close to the affected area in 2010 (12,263 km²).

Indirect use protected areas recorded an average of 11% of the total area extension affected by fire within protected areas per year. Over half of the area burned within protected areas occurred in IL in all years (Figure 4.6a). However, this proportion shrunk from 74% in 2003 to 51% in 2020, while the proportion registered in DU-protected areas increased from 13% in 2003 to 38% in 2020. Although, in absolute values, ILs register a greater area affected by fire, the share of DU in the total burned area registered within protected areas has increased (Figure 4.6b). This becomes even clearer when we

normalize the burned area in each category by the total area of each category each year. In general, DU-protected areas have a lower proportion of burned area in relation to IL, and eventually higher, but with closer values. In the last two years (2019-2020), however, the affected area proportion within DU-protected areas has exceeded that recorded in IL, reaching close to the value found outside protected areas in 2020.

Table 4.5 - Annual burned area inside protected areas in each protection category and outside protected areas, as well as their respective percentages in parenthesis. The last row brings burned area rate and standard deviation in parenthesis.

	Indirect use (km²)	Direct use (km²)	Indigenous lands (km²)	Outside (km²)	Total (km²)
2003	1,704 (2.3%)	1,742 (2.4%)	9,687 (13.1%)	60,840 (82.2%)	73,973
2004	2,769 (2.7%)	3,476 (3.3%)	14,594 (14.0%)	83,616 (80.0%)	104,455
2005	2,736 (2.1%)	5,222 (4.0%)	15,996 (12.3%)	106,386 (81.6%)	130,340
2006	1,396 (1.8%)	5,507 (7.2%)	11,357 (14.9%)	57,713 (76.0%)	75,973
2007	3,101 (2.3%)	5,498 (4.0%)	16,002 (11.8%)	111,398 (81.9%)	135,999
2008	1,949 (2.9%)	7,456 (11.0%)	11,174 (16.4%)	47,375 (69.7%)	67,954
2009	1,072 (3.0%)	2,470 (6.9%)	6,697 (18.6%)	25,784 (71.6%)	36,024
2010	5,326 (3.3%)	15,647 (9.6%)	26,245 (16.1%)	116,075 (71.1%)	163,293
2011	3,158 (5.9%)	5,423 (10.2%)	12,547 (23.6%)	32,105 (60.3%)	53,234
2012	2,907 (4.3%)	5,652 (8.3%)	13,929 (20.5%)	45,520 (66.9%)	68,008
2013	1,190 (3.4%)	2,301 (6.6%)	8,975 (25.6%)	22,530 (64.4%)	34,996
2014	2,336 (4.8%)	3,356 (6.8%)	10,342 (21.1%)	33,006 (67.3%)	49,039
2015	2,389 (3.6%)	6,196 (9.3%)	12,812 (19.2%)	45,371 (68.0%)	66,768
2016	3,383 (4.6%)	5,953 (8.1%)	16,042 (22.0%)	47,684 (65.3%)	73,062
2017	2,505 (2.7%)	8,492 (9.2%)	18,320 (19.8%)	63,015 (68.2%)	92,332
2018	1,547 (4.1%)	3,571 (9.4%)	7,923 (20.9%)	24,783 (65.5%)	37,823
2019	2,243 (2.9%)	10,027 (13.1%)	15,180 (19.8%)	49,365 (64.3%)	76,815
2020	3,757 (4.4%)	12,263 (14.4%)	16,474 (19.3%)	52,942 (62.0%)	85,436
Mean	2,526	6,125	13,572	56,973	79,196
(sd)	(1,039)	(3,611)	(4,546)	(29,271)	(35,450)

The analysis presented here consists of an initial diagnosis of fire occurrence inside and outside protected areas in the Amazon basin between 2003 and 2020. Protected areas continue to register lower absolute rates of burned area compared to their surroundings, which corroborates the results found in the literature, which attest to the fire-inhibitory effect of protected areas (NELSON; CHOMITZ, 2011; NEPSTAD et al., 2006). However, the burned proportion within these areas has increased over the years. We observed that IU-protected areas are the least affected by fire in absolute terms and in proportion to their area. On the other hand, IL maintained the highest absolute values of the burned area throughout the time series. However, DU-protected areas have the

steepest increasing share of their total area affected over the years. Therefore, protected areas, in general, are exposed to an increasing threat, which boosts their risk of environmental degradation and, consequently, their ecosystem integrity. The next question would be what is burning inside and whether the pattern changes when we look outside protected areas.

Figure 4.6 - Burned area within protected areas, considering their categories. Burned area proportion inside each protected areas category from 2003 to 2020 (a), and total burned area inside each protected areas category (b). The dependent variable is displayed on the x-axis for visualization purposes.

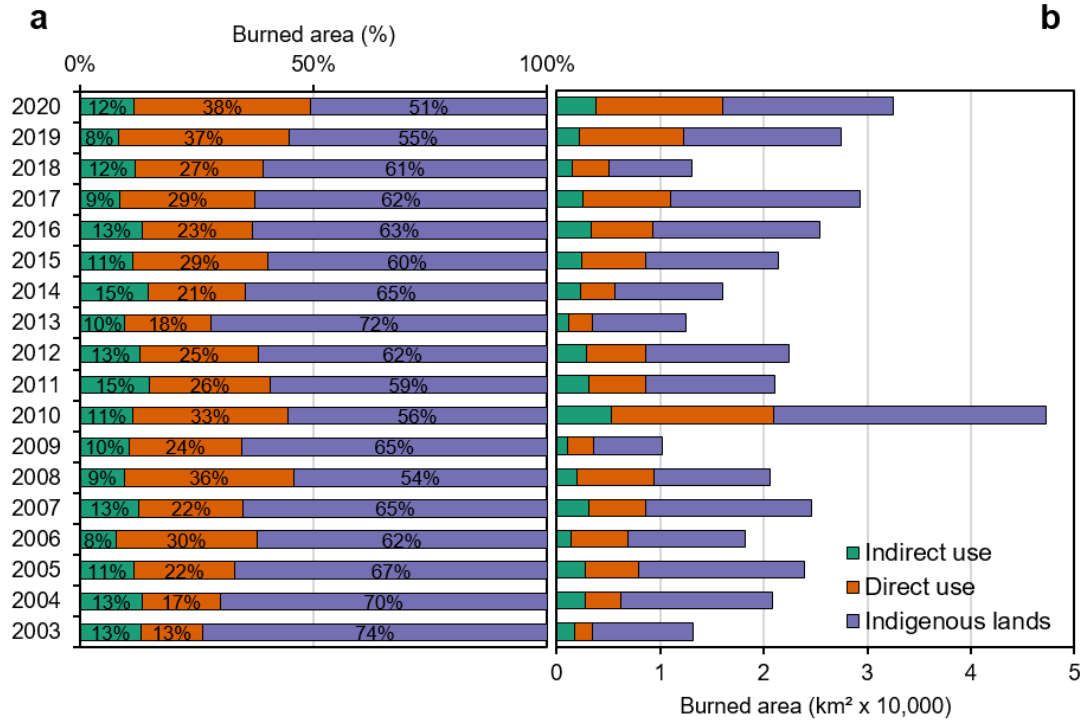

4.3.2 What is burning?

Of the 1.4 million km² burned area accumulated from 2003 to 2020 in the Amazon basin, 45% were registered in the class of other natural formations, which include savannas, grasslands, flooded forests, and mangroves (Figure 4.7). A total of 435,996 (31%) km² were registered in farming lands and 259,881 km² in old-growth forests (18%), an area larger than entire countries such as the Guianas and Suriname.

Figure 4.7 - Burned area rate (mean from 2003 to 2020) per land use and land cover class in the Amazon basin (for = forest; sec = secondary forest; nat = other natural formations; dfs = deforestation of secondary forest; dfp = deforestation of old growth forest; far = farming; oth = other).

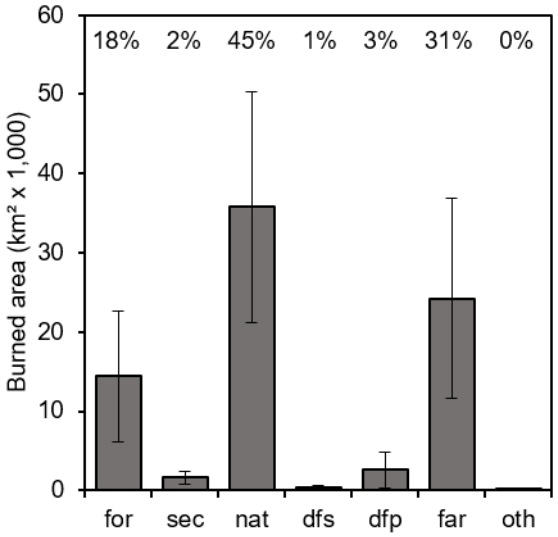

Forests burn on average 14,438 km² per year, representing 18% of the total burned per year (ranging from 3,940 km² in 2013 to 34,431 km² in 2010). There is no clear trend of increase or decrease in the burned area in old-growth forests between 2003 and 2020 (Figure 4.8), although, in 2020, the area recorded was greater than in years of extreme droughts, such as 2015/2016. The same happens with burned areas in secondary forests. After 2004, the year that marks the beginning of the PPCDAm, the burned area related to old-growth forest deforestation began to fall, reaching 92% from 2004 to 2009 (Figure 4.8). As of 2014, the burned area in this class remains stable at around 1,400 km² per year. In the last two years, though, there has been an increase, reaching a 112% increase in 2020, compared to the average from 2014 to 2018.

Figure 4.8 - Burned area per land use and land cover class. Burned area proportion per land use and land cover class from 2003 to 2020 (left panel) and total burned area per land use and land cover class (right panel). for = forest; sec = secondary forest; nat = other natural formations; dfs = deforestation of secondary forest; dfp = deforestation of old growth forest; far = farming; oth = other. The dependent variable is displayed on the x-axis for visualization purposes.

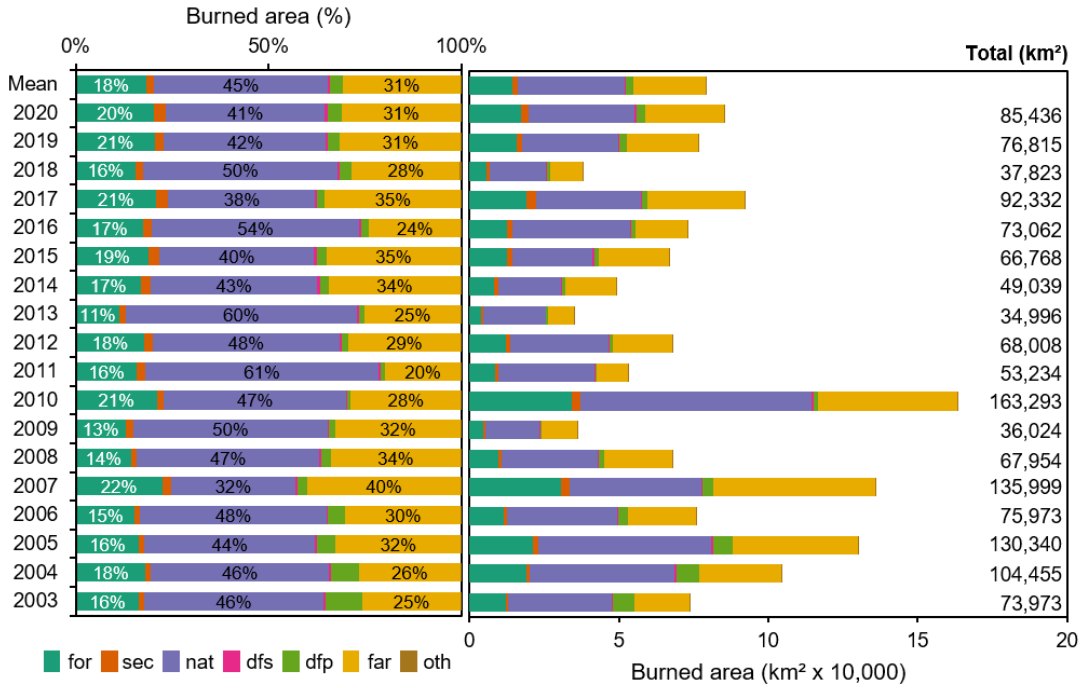

Old growth forest deforestation is the class that recorded the highest proportion of burned area compared to its total area (16% on average per year), considering the Amazon basin (Figure 4.9a, Table C.1 and Table C.2). Old growth forest is the class that burned the smallest area compared to its total in all years. Bolivia is the country that burns the largest forest proportion per year (0.79%), followed by Brazil (0.38%) and Colombia (0.11%) (Figure 4.9b). In 2010, Bolivia burned 3.5% of its old-growth forests, representing more than six thousand km² (Figure 4.9c). In the same year, Brazil burned 0.8% of its old-growth forest.

Figure 4.9 - Burned area in each land use and land cover class normalized by the total area of each land cover and land use class (a). Burned forest normalized by total forest area in each Amazonian country (b) from 2003 to 2020 (c). In panel (b), the dependent variable is displayed on the x-axis for visualization purposes. BO = Bolivia; BR = Brazil; CO = Colombia; EC = Ecuador; GF = French Guiana; GY = Guyana; PE = Peru; SR = Suriname; VE = Venezuela.

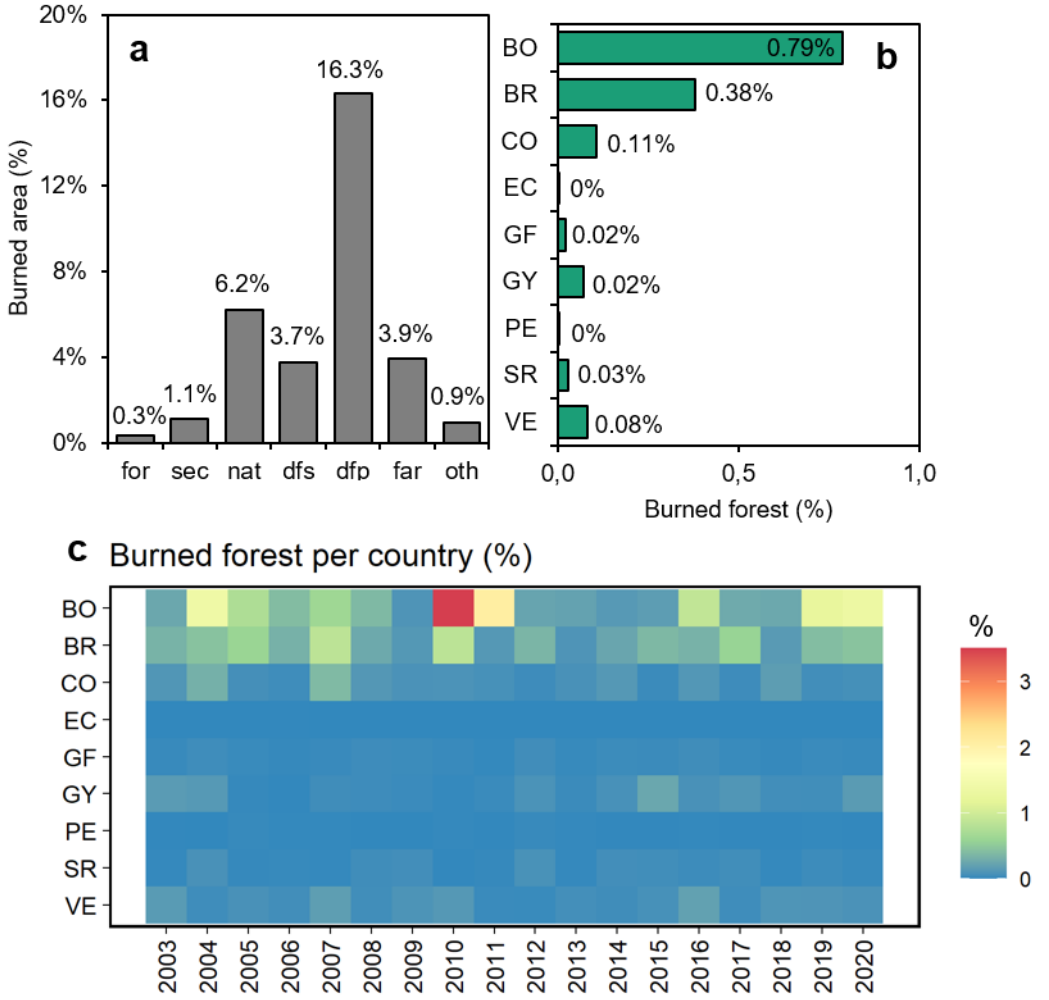

Considering that these numbers come from remote sensing data using automatic classifiers, errors are expected to be embedded in the estimates. On average, 2,279 km² of burned area in water were mapped per year, representing 3% of the total burned per year. Burned areas are commonly confused with water in automatic mappings due to the confounding spectral behaviors of these two targets. This may also partially explain the high value found for the burned areas in the class 'other natural formations' since flooded forests are included in this class. Even though studies have shown that flooded forests are fire-prone and could act as a potential conduit for spreading fires to upland forests (ALMEIDA et al., 2016), part of the burned area detected over them could potentially

represent a mapping error. However, it is impossible to ascertain the magnitude of this error with the available data.

Indirect use protected areas and IL burn mostly ‘other natural formations’ (72% and 75% respectively per year). Direct use protected areas presented a higher rate of burning in farming lands compared to the other protection categories; 22% of the burned area registered within this category per year is in farming lands (Figure 4.10). Besides, 3.5% of the burned area registered within DU-protected areas is related to old-growth forest deforestation, the highest proportion of burned area compared to other protected categories. Proportionally, the burned area registered outside protected areas mostly affects farming lands (38%). In general, fire occurrence within protected areas affects mostly natural land covers, i.e., old-growth forests, secondary forests, and other natural formations. The share of burning in natural land covers in IL reaches 92% of the total burned area within this category per year. Contrastingly, this share outside protected areas is, on average, 52% of the total burned area registered per year, and the rest is mostly concentrated in farming lands.

Figure 4.10 - Burned area rate per land use and land cover class inside each of the protected area categories and outside them. for = forest; sec = secondary forest; nat = other natural formations; dfs = deforestation of secondary forest; dfp = deforestation of old growth forest; far = farming; oth = other.

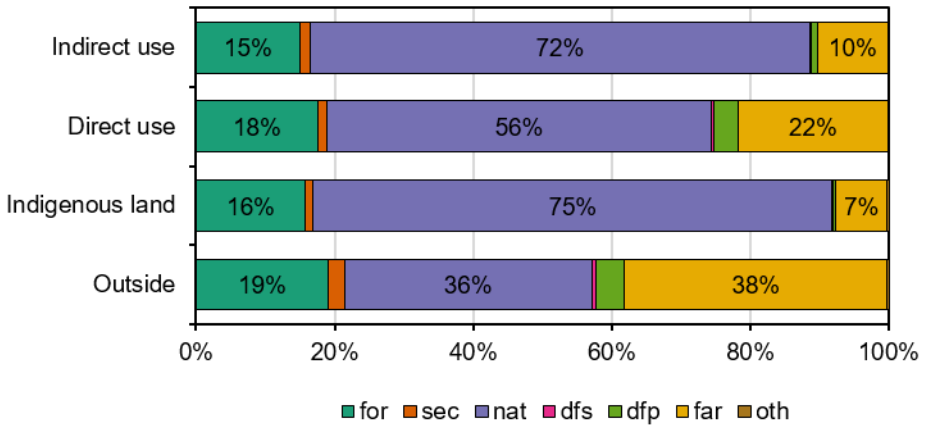

In absolute values, all land use and land cover classes have a greater area affected by fire outside protected areas per year (Table 4.6) and annually (Table C.3). Among the burned area within protected areas, IL concentrates the largest forest area affected by fire, registering an average of 2,137 km² per year, an area almost six times larger than what was registered within IU protected areas. For example, in 2010, the burned forest

registered within IL and IU protected areas increased respectively 128% and 127% compared to the average between 2003 and 2020. This increase reached 209% within DU-protected areas, representing 3,334 km² of burned forest in one year.

Table 4.6 - Burned area rate (mean from 2003 to 2020) and summary statistics per land use and land cover class inside each of the protected area categories and outside them. SD = Standard deviation; VC = Variation coefficient.

	Mean	% class total area	SD	Max.	Min.	VC(%)
Forest	**14,438**		**8,025**	**34,431**	**3,940**	**56**
Indirect use	377	(3%)	203	889	120	54
Direct use	1,076	(7%)	822	3,334	225	76
Indigenous land	2,137	(15%)	1,290	4,882	379	60
Outside	10,848	(75%)	6,620	25,507	2,792	61
Secondary forest	**1,599**		**770**	**3,067**	**609**	**48**
Indirect use	38	(2%)	22	83	8	58
Direct use	75	(5%)	49	180	13	66
Indigenous land	153	(10%)	100	331	35	65
Outside	1,333	(83%)	653	2,785	492	49
Other natural formations	**35,747**		**14,143**	**77,194**	**18,128**	**40**
Indirect use	1,823	(5%)	756	3,921	762	41
Direct use	3,408	(10%)	1,911	9,449	1,244	56
Indigenous land	10,172	(28%)	3,108	19,613	5,928	31
Outside	20,344	(57%)	9,492	44,211	10,053	47
Deforestation of secondary forest	**435**		**160**	**740**	**170**	**37**
Indirect use	6	(1%)	3	14	1	60
Direct use	20	(5%)	17	68	3	85
Indigenous land	23	(5%)	19	88	5	84
Outside	387	(89%)	139	570	151	36
Deforestation of primary forest	**2,585**		**2,152**	**7,504**	**516**	**83**
Indirect use	23	(1%)	19	69	3	81
Direct use	216	(8%)	163	686	47	76
Indigenous land	48	(2%)	27	116	12	56
Outside	2,298	(89%)	2,131	7,308	451	93
Farming	**24,222**		**12,314**	**54,175**	**8,740**	**51**
Indirect use	255	(1%)	116	448	51	45
Direct use	1,320	(5%)	892	2,878	132	68
Indigenous land	999	(4%)	433	1,587	309	43
Outside	21,648	(89%)	11,764	51,053	7,567	54
Other	**170**		**60**	**281**	**66**	**35**
Indirect use	4	(3%)	3	11	0	68
Direct use	11	(6%)	7	29	4	62
Indigenous land	41	(24%)	16	71	21	39
Outside	114	(67%)	42	181	39	36

Figure 4.11 brings heat graphs for each land cover class and the proportion of burned area per protection category from 2003 to 2020. It is clear from the graphs that larger burned areas have always been registered outside protected areas, regardless of the protection category. However, the most interesting aspect of this visualization form is the temporal tendency evidence of fire occurrence in each class and category. We observed, for

example, that burned forest is increasing within IL over the years ($p < 0.001$) and decreasing outside protected areas ($p < 0.001$). This same pattern is observed more subtly for the burned secondary forest area ($p < 0.001$). For burned areas related to old-growth forest deforestation, we observed a decreasing trend outside protected areas, at the cost of an increase inside DU-protected areas, similar to what happens with burned areas in farming lands.

Figure 4.11 - Burned area per land use and land cover class inside each of the protected area categories and outside them, normalized by total burned area in each land use and land cover class per year.

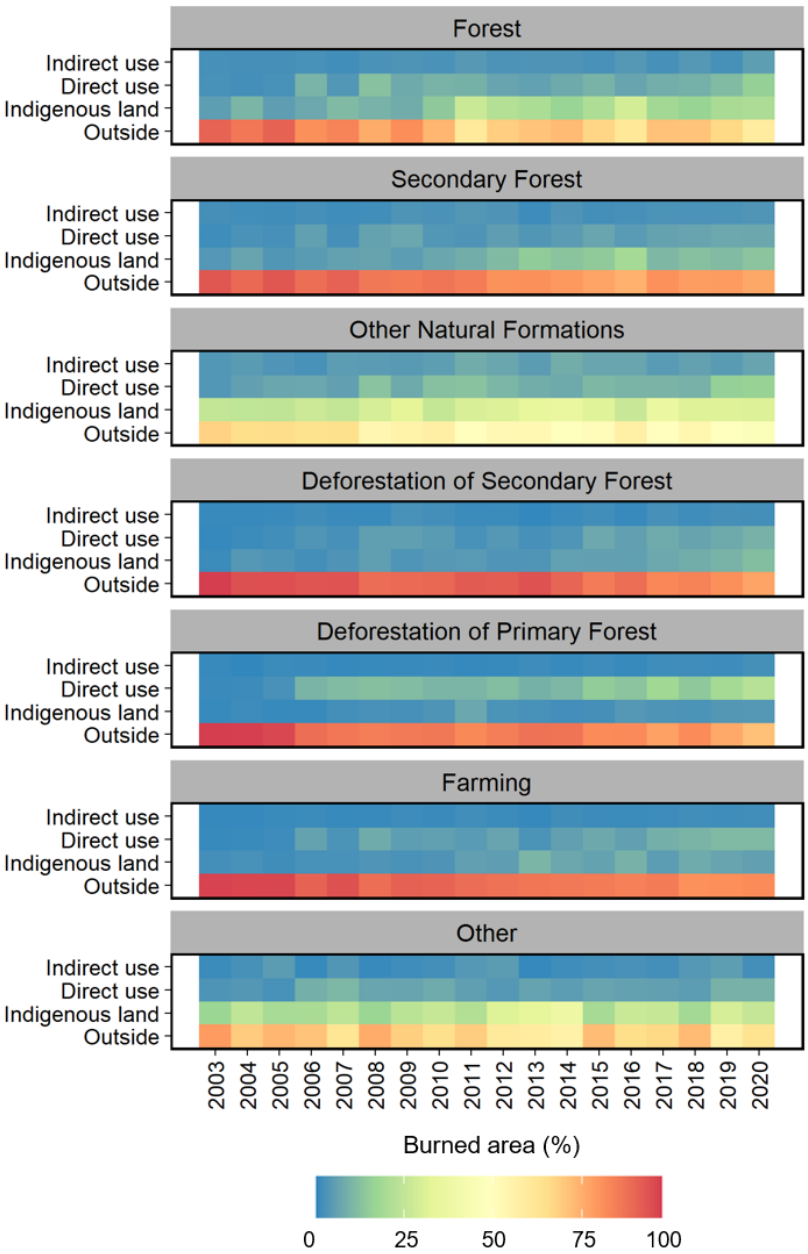

The decrease in the burned area related to deforestation outside protected areas, concomitant with the increase inside them, highlights the greater pressure these areas face and tells us about the drivers behind fire occurrence within these areas. With the expansion of the agricultural frontier and very outdated and flexible land tenure laws (ARMENTERAS et al., 2019), protected areas in the Amazon are at increased risk of illegal land grabbing, which inevitably increases pressure on the forest. This narrative corroborates with studies that have shown that native vegetation was the land cover most affected by fire from 1985 to 2020 in Brazil, representing 65% of the burned area, while the remaining 35% burned in areas dominated by anthropogenic land uses, mainly pasture (ALENCAR et al., 2022). Therefore, to better elucidate the type and drivers of fire within protected areas, we need to understand where this fire is coming from.

4.3.3 Where is fire ignition occurring?

From 2003 to 2018, 17% of the total fire ignitions occurred inside protected areas, compared to 83% outside protected areas. Despite this difference, from 2003 to 2018, the proportion of fires inside more than doubled, indicating an increasing trend over the period (Figure 4.12a). The year that recorded the highest number of ignitions within protected areas was 2017 (6,685), followed by the extreme drought registered during 2015/2016 in the Amazon. Therefore, when comparing the ignitions that occurred inside in relation to the total, the highest proportion was also recorded in 2017 (22%) (Figure 4.12a). As might be expected, fires that start outside protected areas can escape and enter the area under protection.

In the same way, the fire that starts within these areas can also reach its surroundings. From 2003 to 2018, 1,297,694 km² were burned throughout the basin, of which 25% occurred within protected areas[9]. Of the total area that burned inside protected areas, 85% came from fires ignited outside, albeit this only represents 21% of the total burned area from 2003 to 2020 (278,189 km²). On the other hand, 17% of the total burned area recorded outside protected areas came from fires ignited inside them, corresponding to 163,916 km² (Figure 4.12b). So, most of the burned area observed in the Amazon basin from 2003 to 2020, both inside (85%) and outside (83%) protected areas, comes from fires ignited outside these areas. Although these proportions are approximately equal,

[9] These numbers are based solely on the Global Fire Atlas dataset.

they represent very different absolute values, adding up to a burned area outside protected areas (970,601 km²) almost three times greater than inside (327,093 km²).

Figure 4.12 - Ignition occurrence and protected areas. Fire ignition occurrence inside and outside protected areas from 2003 to 2018 (a). Proportion and total burned area registered inside and outside protected areas caused by ignition occurred inside or outside protected areas (b). The dependent variable is displayed on the x-axis for visualization purposes.

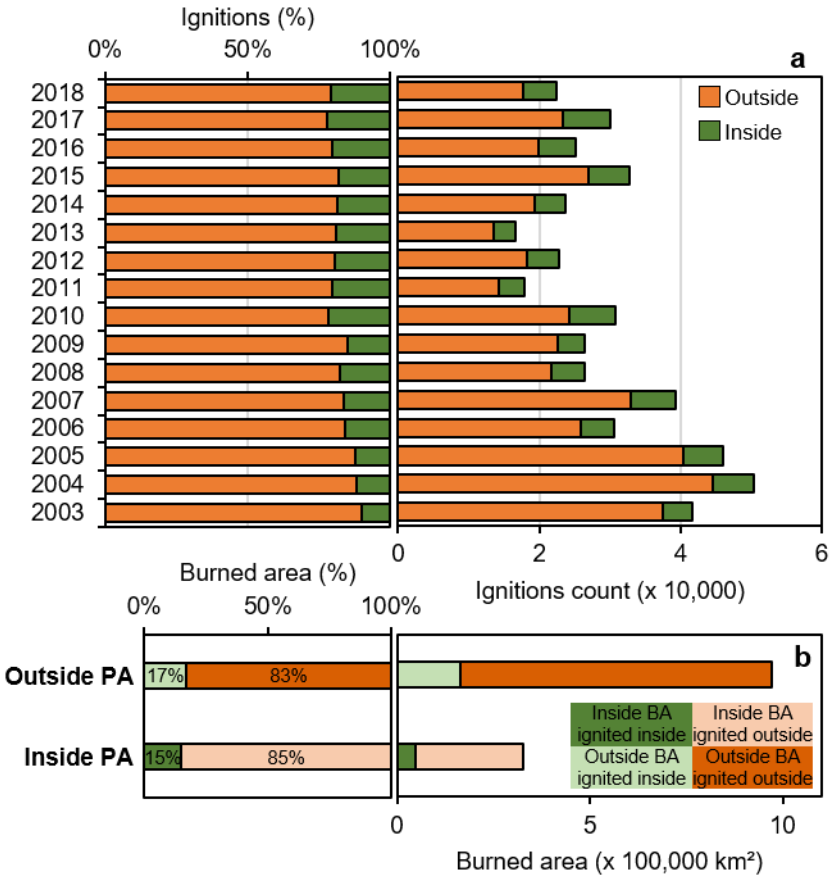

We have already shown that ignitions occur in greater numbers outside protected areas. However, the share of ignitions that occur outside compared to inside tells us about the threat these areas are exposed to. The lower the proportion of ignitions outside in relation to what occurs inside protected areas, the greater the occurrence of ignitions inside in relation to the total and, thus, the greater the threat to which these areas will be exposed. During the period studied, we observed a significant decrease in the proportion of ignitions that occur outside in relation to what occurs inside protected areas and, therefore, an increase in fire ignition threat to these areas (Figure 4.13a). Moreover, considering the fire ignition that occurs outside protected areas, the distance at which they occur from the

border influences the risk of fire entering the protection perimeter. This way, the burned area inside protected areas, which came from fires ignited outside, divided by the distance to the protection border, gives us an indication of imminent threat. We observed that, over the years, ignitions are occurring closer to protected areas' borders, which consequently influences a greater burned area within them (Figure 4.13b). Indeed, from 2003 to 2018, an average of 17,387 km² year^{-1} of fires ignited outside protected areas entered their borders. The proportion of burned area leaking to the inside perimeter, compared to the total burned, showed possible stability over the years, with an average of 25%. Surprisingly, in the last year, 2018, this proportion reached the same or greater value than years of extreme drought, when fire within protected areas is more expected. This proportion translates to the threat that fire started outside imposes on protected areas (Figure 4.13c).

Figure 4.13 - Fire threat over protected areas (PA) from 2003 to 2018. The ratio of fire ignition outside and inside protected areas (PA) from 2003 to 2020 (a). The ratio of burned area inside protected areas and distance from ignition point to the protected area border. We only consider ignitions that occurred outside PA (b). The proportion of burned area occurred inside protected areas compared to the total burned area per year from fires started outside over time (c).

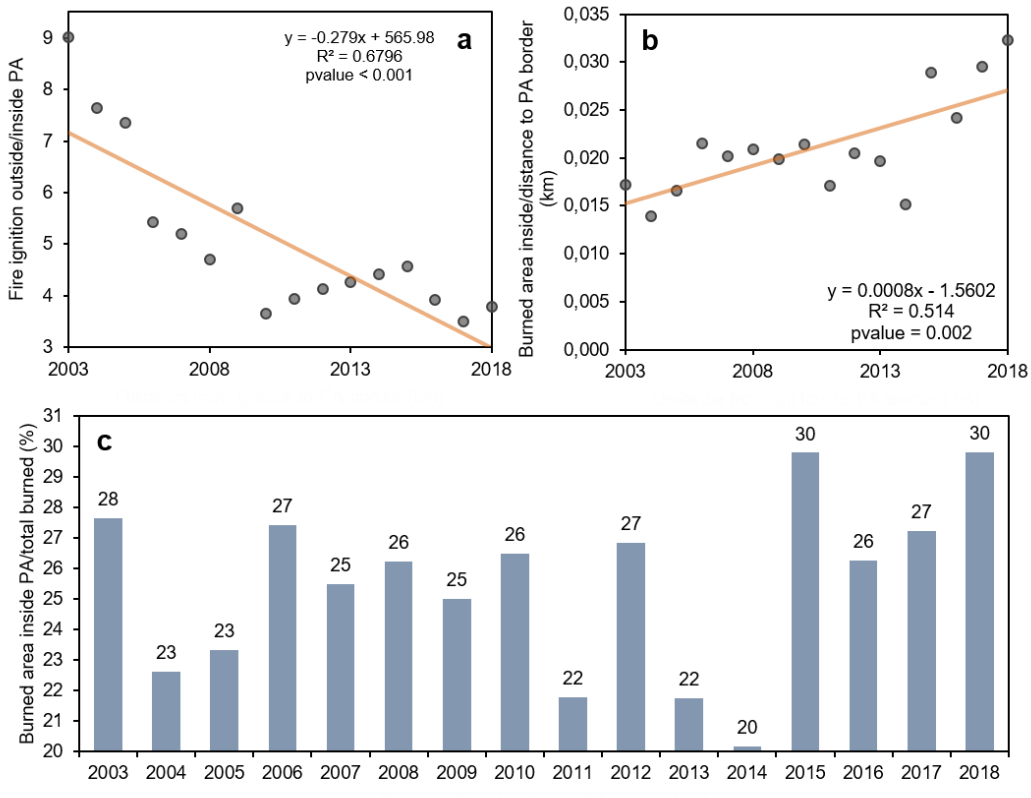

When we distinguished the categories of protected areas, we observed that the IL registered the highest percentage (Figure 4.14a) and absolute number (Figure 4.14b) of fire ignitions in relation to DU and IU-protected areas. Despite this, DU-protected areas presented the highest ignition density per square kilometer throughout the period (Figure 4.14c). From 2003 to 2018, the proportion of fire ignitions within IL decreased by 23%, to the detriment of a 39% increase in DU-protected areas and a 29% increase in IU-protected areas. In absolute numbers, IU and DU protected areas registered 50% and 62%, respectively, more fire ignitions in 2018 compared to 2003. In the same period, IL registered a reduction of only 10% in fire ignitions. Extreme droughts do not seem to be a determining factor in explaining fire ignition occurrence since peaks of ignition occurrence were observed in years that are not traditionally classified as dry, such as 2004 or 2017. However, among the known extreme dry years, 2010 was the extreme event that most affected fire ignition within protected areas, increasing its number by 70% in relation to the previous year. All categories were affected by an increase in ignitions, reaching a 93% increase in IL. However, there is a significant trend ($p < 0.05$) of decrease in fire ignition density per square kilometer, the only category that showed a significant trend ($p < 0.05$) and also decreased was IL. However, in the latter, the decrease was found at a lower rate. The IU and DU categories presented relative stability in fire ignitions per square kilometer, with no significant trend over time. DU-protected areas presented the highest ignition density in all years, averaging 31% and 72% greater than IL and IU-protected areas, respectively.

Figure 4.14 - Fire ignitions per protected area category from 2003 to 2018. Percentage in relation to total (a) and absolute number (b) of fire ignitions per protected area category. Fire ignitions density per protected area category from 2003 to 2018 (c). It was only considered ignitions occurred within protected areas. The dependent variable is displayed on the x-axis for visualization purposes.

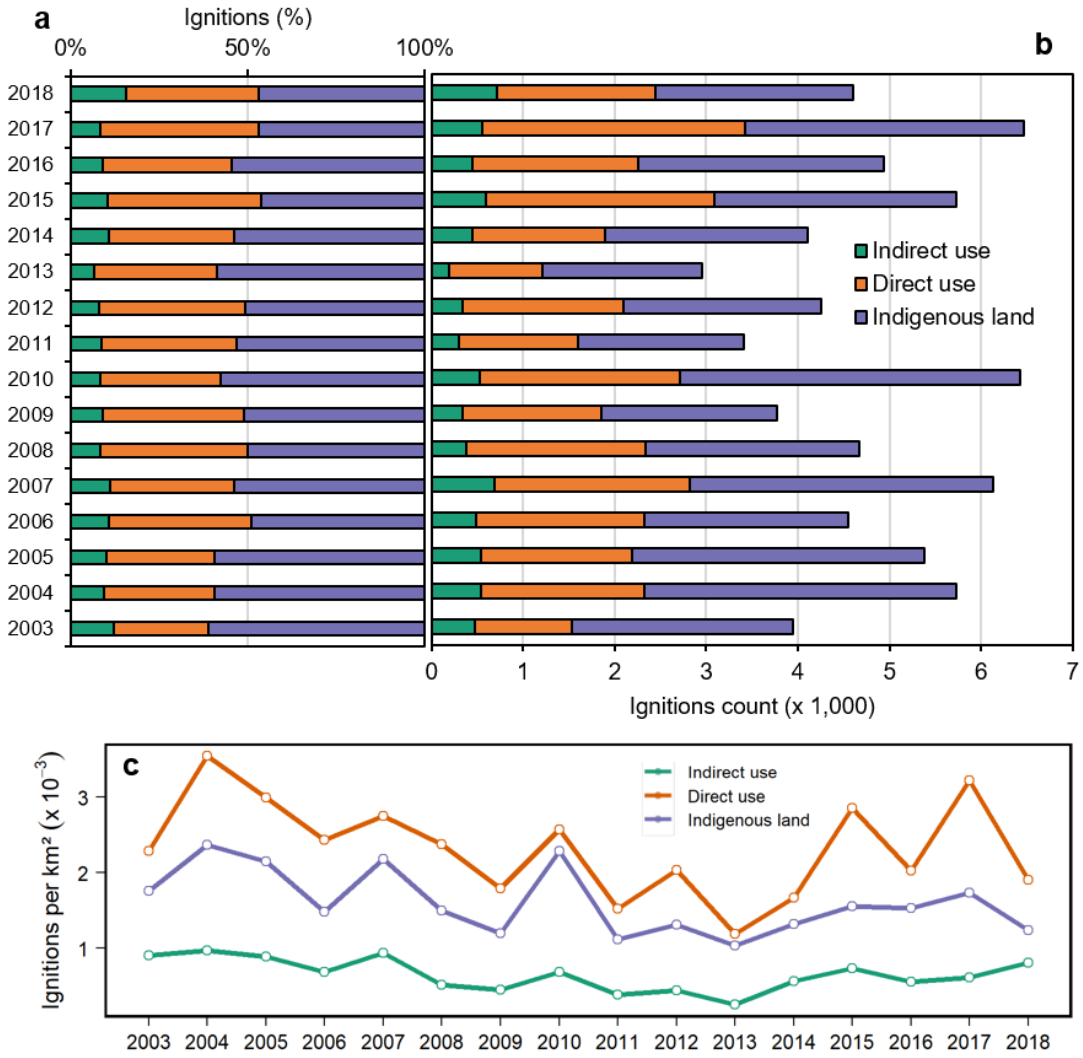

Finally, we calculated anomaly per year to indicate positive or negative anomalous years for fire ignition occurrence (Figure 4.15). To calculate the anomaly, we used each category's mean and standard deviation separately to analyze the intra-category anomalies. For example, as fire ignitions are lower inside protected areas than outside, if we use the general average, inside would always result in negative anomalies, regardless of the protection category.

Figure 4.15 - Fire ignition count (a, c, e, and g) and density (b, d, f, and h) anomalies from 2003 to 2020 inside each of the protected area categories and outside them.

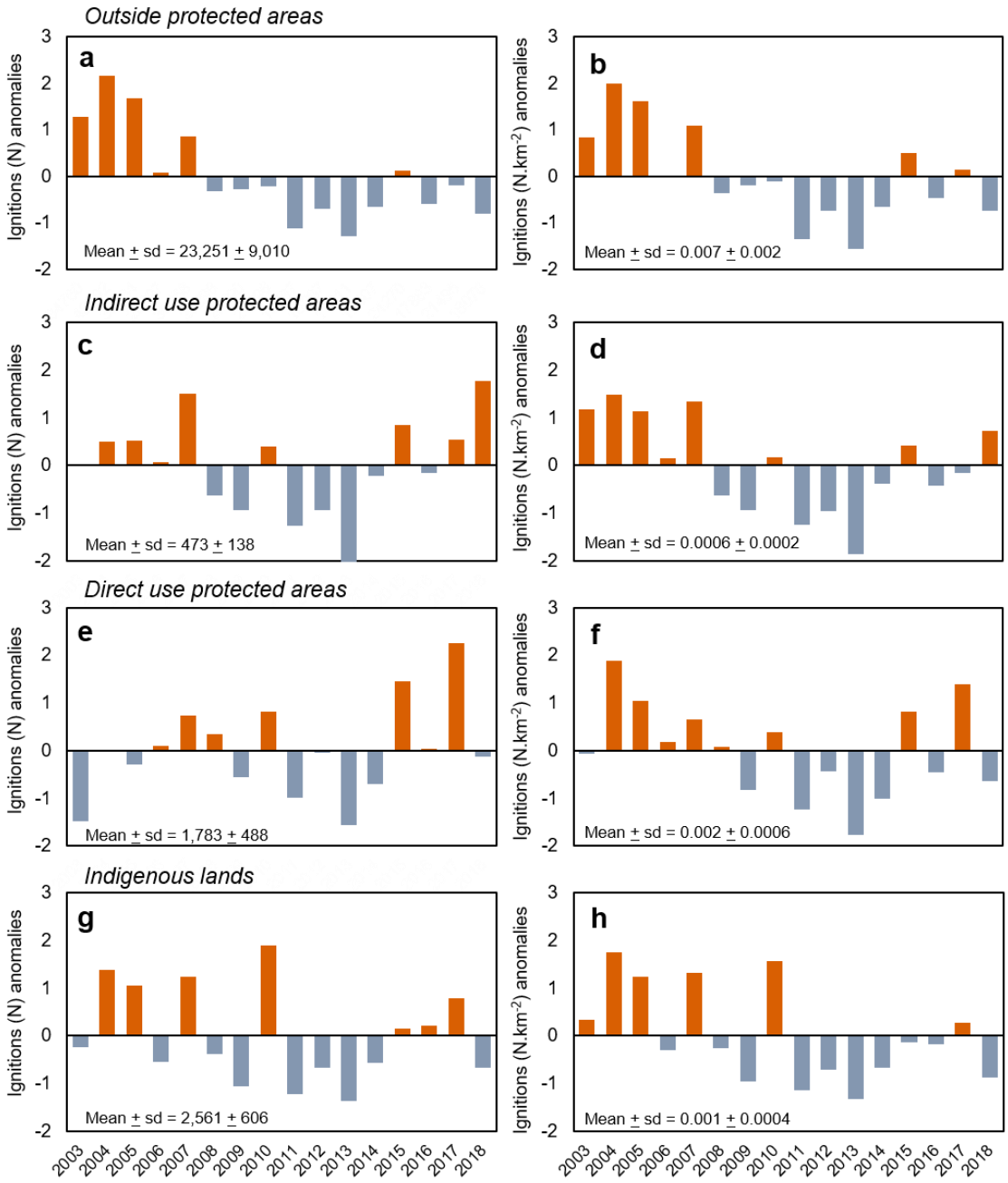

Outside protected areas, positive fire ignition occurrence anomalies are concentrated mostly at the beginning of the time series, between 2003 and 2007 (Figure 4.15 a and b). After that, positive anomalies are only found in 2015 for ignition number and 2015 and 2017 for ignition density. In addition to 2015 being an extremely dry year in the Amazon, there was also an increase in ignitions, both outside and inside protected areas. This did not occur in 2010, which despite the extreme drought, was a year that only registered

positive anomalies within IL and DU-protected areas. The highest positive anomaly for fire ignition count and density outside protected areas was observed in 2004. The lowest negative anomaly occurred in 2013 in all categories. In IL and DU protected areas, the highest anomaly of fire ignition count occurred in 2010 and 2017, respectively (Figure 4.15 e and g). For fire ignition density, the highest anomaly value for both categories occurred in 2004 (Figure 4.15 f and h). Interestingly, in IU-protected areas, the highest fire ignition positive anomaly value occurred in 2018, the year that all other categories showed negative anomalies (Figure 4.15c).

4.3.4 Is population density correlated to fire occurrence?

Population density can drive fire occurrence in the Amazon (HANTSON; PUEYO; CHUVIECO, 2015; KNORR et al., 2014). Fire is inserted into the Amazon system in different contexts. For example, land management, clearing of deforested lands, or criminal land grabbing (ALENCAR; RODRIGUES; CASTRO, 2020; BARLOW et al., 2020; SORRENSEN, 2009). With this, fire occurrence is expected to respond to a gradient of population density. Specifically, it is expected that the relationship between fire and population varies non-linearly in a population gradient (HANTSON; PUEYO; CHUVIECO, 2015). The relation would present an increasing curve in the first stage and a decrease in the second, in which the population density reaches a value such that it characterizes an environment less conducive to fire, configuring an inverted U-shaped curve.

The deflection point at which fire occurrence decreases with increasing population density can be explained in two ways. At first, the population density gradient is related to a gradient of flammability of the environment, in which higher densities would reflect environments more managed and with less flammable biomass and, therefore, less conducive to fires. Second, the population density gradient would be related to a greater ability to control fire simply because of the amplification of human resources. Thus, fire occurrence would increase with increasing population density until reaching a point at which the environment becomes less flammable due to soil management and fire become better controlled due to more human resources. On the other hand, increased fire occurrence might result in increased flammability of emptying rural landscapes and reduced capacity to control fire (URIARTE et al., 2012).

In our study area, the average population density between 2003 and 2020 is 3.6 habitants per km² and approximately 24.8 million people. Indeed, despite still being sparsely populated, the Amazon is not an inhospitable environment, and human presence reflects forest degradation due to its activities. The general pattern between 2003 and 2020 is an increase in population density, with an increase of 1.65 habitants, on average, per km² from 2003 to 2020 (Figure 4.16), or 0.1 habitants per year. Most of the Amazonian territory experienced an increase of 0 and 100 habitants per km² from 2003 to 2020. Taking the protection status comparison, the increase in population density from 2003 to 2020 inside protected areas was 0.47 habitants per km², contrasting with the 2.95 registered outside them.

Figure 4.16 - Difference in population density from 2003 to 2020. Gray voids on the map represent pixels with missing values.

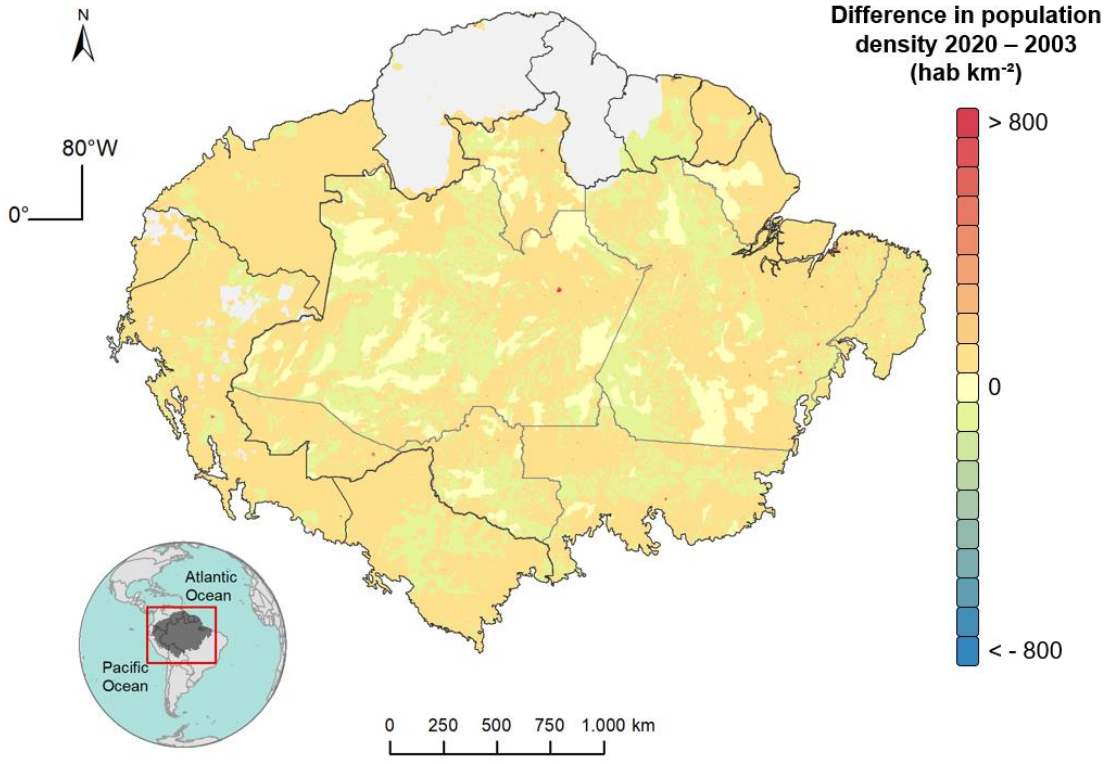

Table 4.7 - Summary statistics of fire occurrence and population information for each class of population count.

Population count classes	*Active fires* Mean ± sd	Median	Max.	*Population* Mean ± sd	Median	Max.	Min.	N
0 - 0.2	1.52 ± 2.84	0.33	23.94	0.03 ± 0.06	0.00	0.20	0.00	875
0.2 - 1	2.14 ± 3.53	0.56	25.72	0.57 ± 0.24	0.56	1.00	0.20	978
1 - 4	3.27 ± 4.62	1.11	29.56	2.36 ± 0.87	2.29	4.00	1.00	2,203
4 - 12	3.51 ± 4.79	1.50	36.56	7.89 ± 2.37	7.84	12.00	4.00	3,813
12 - 22	3.65 ± 4.83	1.67	35.06	16.55 ± 2.88	16.33	21.99	12.01	3,772
22 - 37	4.12 ± 5.18	2.06	38.17	29.15 ± 4.30	29.00	37.00	22.00	3,800
37 - 61	4.23 ± 5.10	2.28	38.06	48.13 ± 6.91	47.76	60.98	37.01	3,931
61 - 100	4.41 ± 5.24	2.44	40.00	78.97 ± 11.31	78.24	100.00	61.03	3,871
100 - 162	4.67 ± 5.42	2.78	39.17	128.67 ± 17.94	127.55	161.99	100.00	3,911
162 - 290	5.17 ± 5.34	3.39	35.11	217.75 ± 36.86	212.42	289.93	162.00	3,863
290 - 675	5.97 ± 5.94	4.17	57.50	435.27 ± 105.45	414.92	674.84	290.12	3,869
675 - 1524	6.22 ± 5.76	4.39	43.06	995.20 ± 231.09	952.89	1,522.98	675.18	1,938
1524 - 3450	5.94 ± 5.40	4.50	39.83	2,243.00 ± 532.56	2,125.88	3,449.89	1,524.72	969
> 3450	4.88 ± 4.60	3.61	34.50	17,467.00 ± 41,026.44	7,327.28	684,052.28	3,451.99	969

Note: Values refer to the period between 2003 and 2020.

The inverted U-shaped relationship is observed subtly in the mean and median values along the population gradient (Figure 4.17a and Figure 4.17b). However, it is more pronounced in the maximum values of fire occurrence (Figure 4.17c and Figure 4.17d). This is possibly due to many pixels with low fire occurrence (Table 4.7). Thus, the population gradient is linked to a fire occurrence gradient, reaching higher values until the population turning point, where the fire occurrence gradient deflects (Figure 4.17c and Figure 4.17d). Fire occurrence increases concurrently with population count, up to a fire peak close to 2.2[10] habitants per km². Pixels with a population density above this turning point seem to register a decrease in fire occurrence. In addition, this pattern is not homogenous among the Amazonian countries (Figure 4.18).

[10] This value is resulted from the point with lowest slope in a LOESS model runned between average fire count and log of population density, with the ten highest points in each mean population count class.

Figure 4.17 - Active fires per population count class. The classes refer to the mean population count from 2003 to 2020 per 10 x 10 km pixel. The mean population count in panels (c) and (d) is given using a logarithmic transformation. Active fires represent the mean (a, c and d) and median (b) value per 10 x 10 km pixel between 2003 and 2020. The boxes in panels (a) and (b) are drawn with widths proportional to the square roots of the number of observations in the groups. Outliers have been removed from the graphics to improve visualization. Panel (d) shows active fires per population count of the ten highest points in each mean population count class, so it was used the 10 pixels that registered the highest mean of active fires in each population count class.

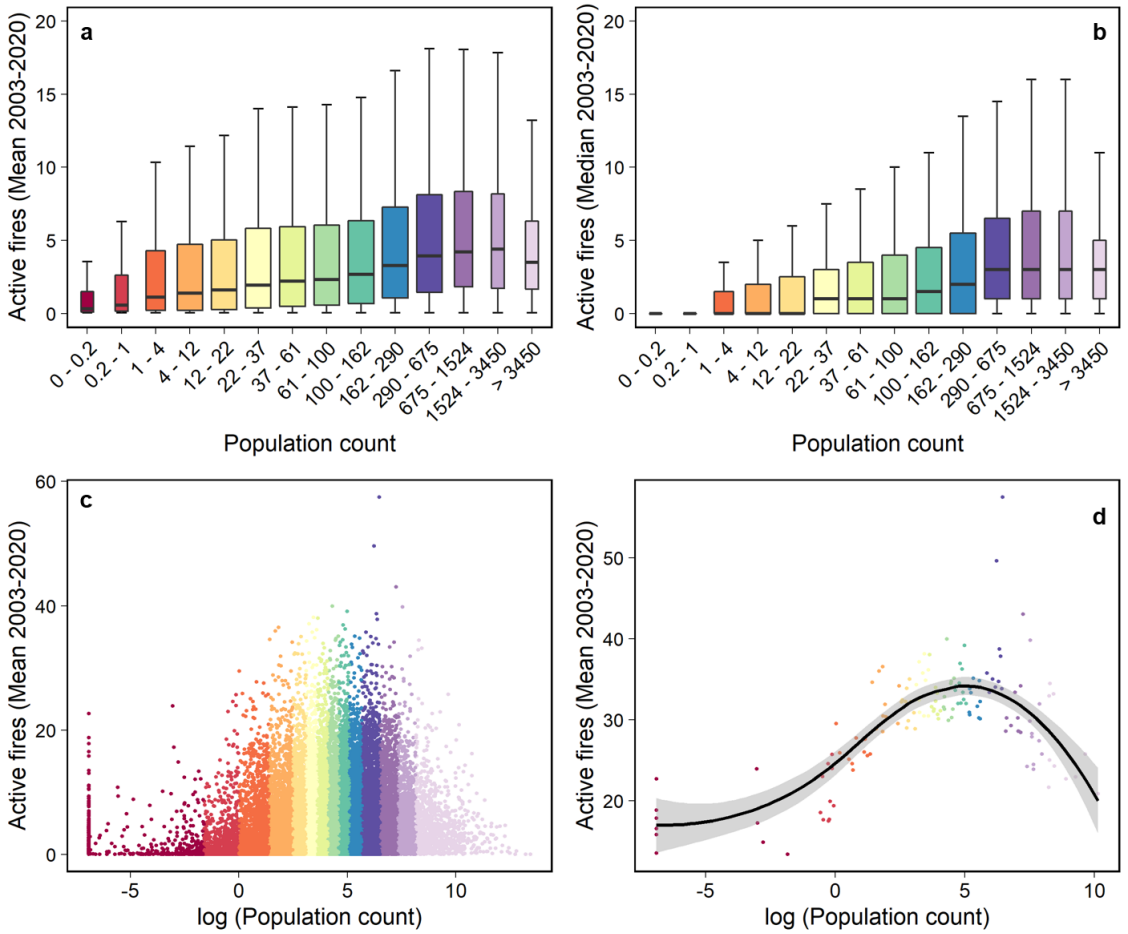

Figure 4.18 - Mean active fires per population count in each country of the Amazon Basin. The mean population count is given using a logarithmic transformation. Smaller panels show active fires per population count of the fifty highest points in each mean population count class, so it was used the 50 pixels that registered the highest mean of active fires in each population count class.

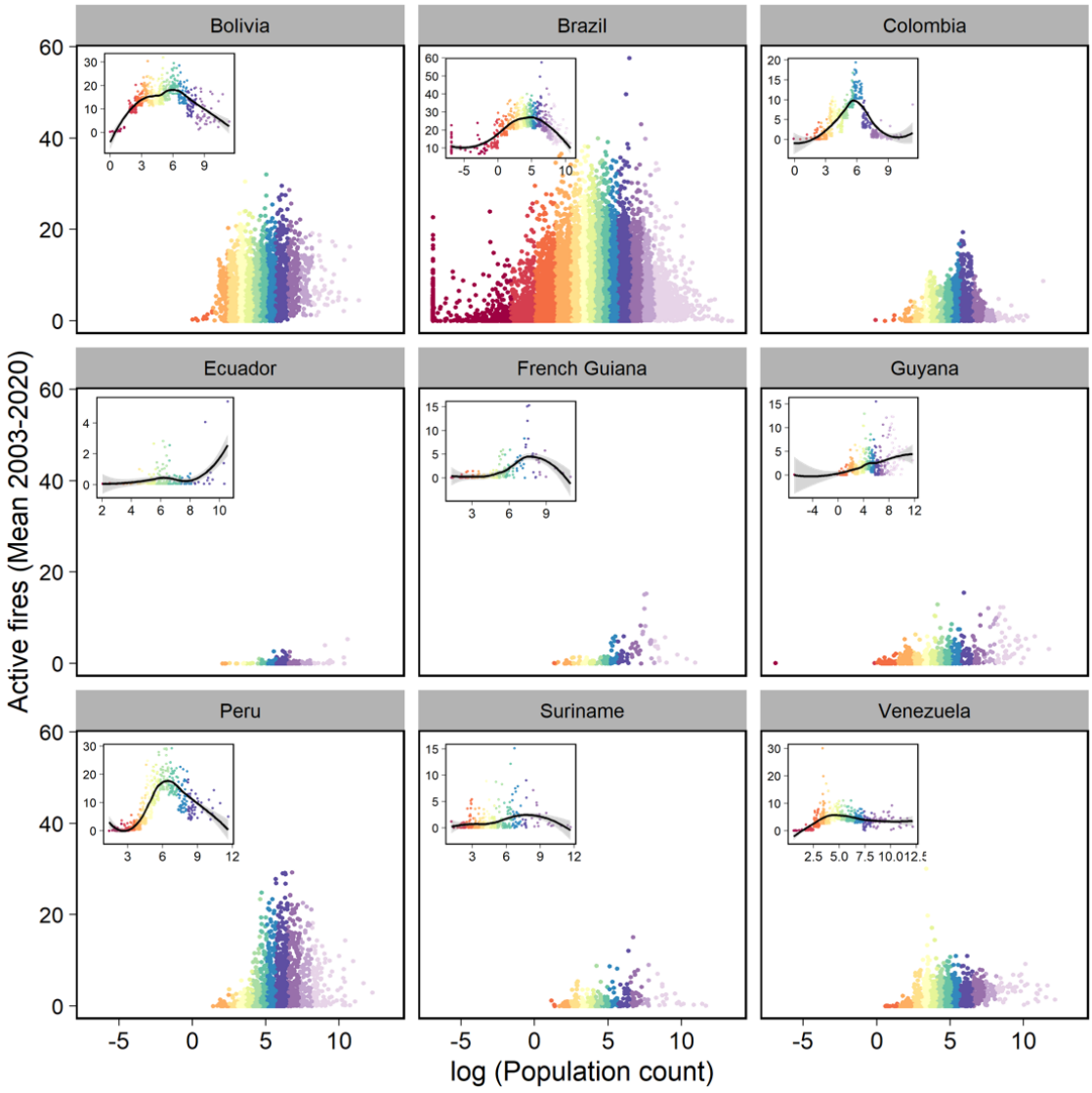

Extreme drought years preserve the same general pattern between fire and population. However, the deflection turning point of the inverted U-shaped curve seems to occur with lower population density during dry years; the fire peak happens in less populated pixels (Figure 4.19). Splitting the dataset into dry and non-dry years, we found that the fire peak

happens close to 0.14[11] and 3.1 habitants per km², respectively. Besides, as expected, the average of active fires reaches higher values during dry years.

Figure 4.19 - Active fires per population count class. The classes refer to the mean population count in normal years (a and c) and dry years (b and d) per 10 x 10 km pixel. We considered 2005, 2010, 2015, and 2016 as dry years and the other years from 2003 to 2020 as normal years. The mean population count is given using a logarithmic transformation. Active fires represent the mean value per 10 x 10 km pixel in normal years and dry years. Panels (c and d) show active fires per population count of the ten highest points in each mean population count class, so it was used the 10 pixels that registered the highest mean of active fires in each population count class.

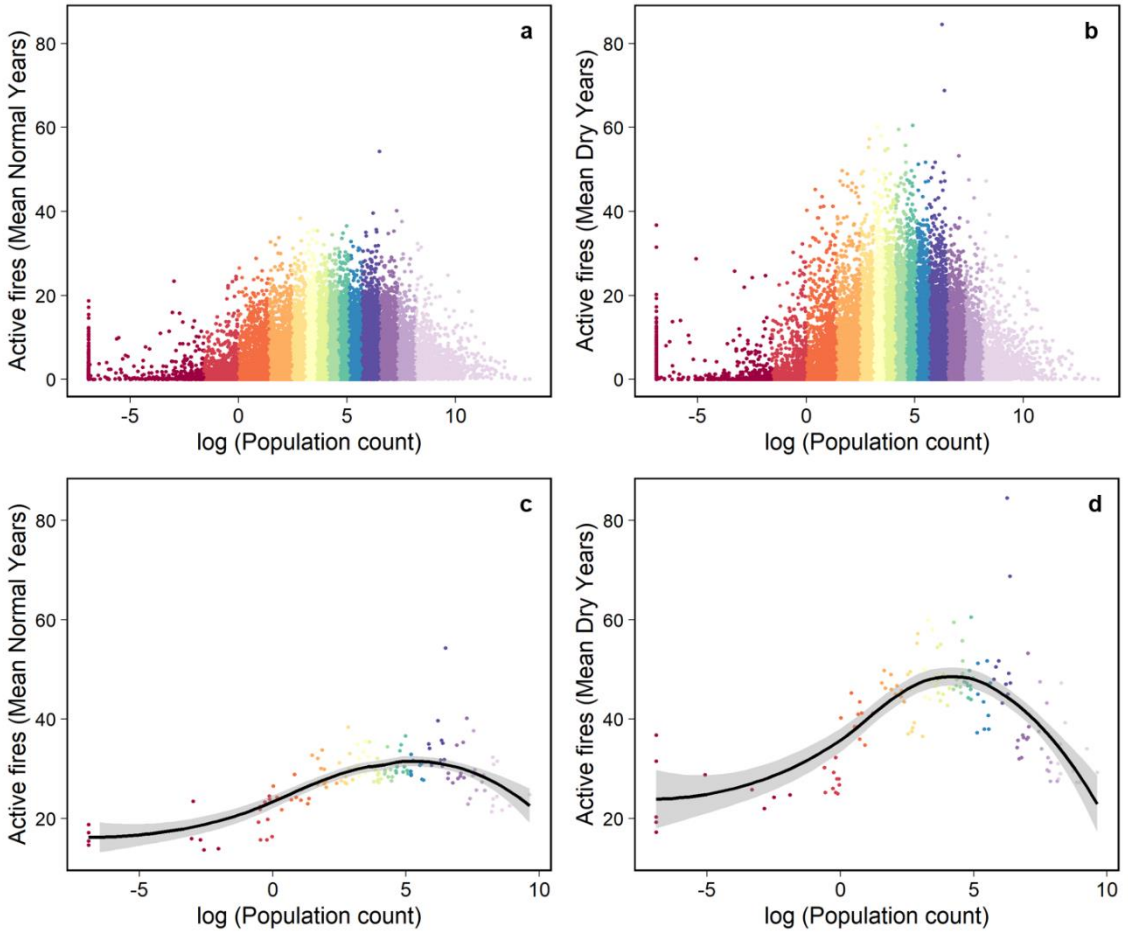

Globally, fire size distribution is strongly influenced by human activity (HANTSON; PUEYO; CHUVIECO, 2015). Knorr et al. (2014) have already shown in a global analysis that in areas with up to 0.1 habitants per km², fire frequency increases by 10 to 20% compared to areas with no habitants. This corroborates with the turning point we found for dry years in the Amazon basin. In tropical forests, population density and cropland

[11] These values are resulted from the point with lowest slope in a LOESS model runned between average fire count and log of population density, with the ten highest points in each mean population count class.

were positively correlated with the spatial pattern of burned area (ANDELA et al., 2017). In this environment, frequent fires for deforestation and agricultural management yielded a sharp rise in fire activity with the expansion of settled land uses (ANDELA et al., 2017; RUDEL et al., 2009). Although in the Brazilian Legal Amazon, the population ramped from 8 million in the ’70s to 28 million in 2020, population density in the region is still considered low, 5,6 habitants per km² (SANTOS; SALOMÃO; VERÍSSIMO, 2021). In the Amazon basin, the population in 2020 is estimated at 38 million. Considering that the whole region has 7.8 million km², the population density is even lower than in the Brazilian Amazon, with 4.9 habitants per km² (SANTOS; SALOMÃO; VERÍSSIMO, 2021).

We also tested the ability to predict the probability of fire occurrence given the population count of each pixel, considering the whole time series. We present the test summary statistics in Table 4.8. With a logistic regression model, we could observe that, in all cases, the coefficient of the population variable obtained positive values ($p < 0.001$). Thus, when the population increases, the chances of fire occurrence increase. In addition, the coefficient found for years of extreme drought is higher; that is, the increase in fire occurrence chance, given the increase in population, occurs at a higher rate. The Odds Ratio value brings a more direct interpretation of the *logit* model. We observed that for each unitary variation in the log of the population variable, the chances of fire occurrence increase by 58% (61% and 59% in dry and non-dry years, respectively).

All three cases obtained AUC values higher than 0.8 and, thus, higher than the critical threshold of 0.5. The cutoff is the value with the highest model performance, the point at which the model minimizes false positives and negatives. In our case, the cutoff value represents the population density that would best predict fire occurrence. The cutoff value found for years of extreme drought was lower than for the other years, once again showing that pixels with lower population density better predict fire occurrence during extreme droughts. In all cases, the accuracy of the model was 0.73 and with pseudo R^2 values around 0.3, which does not show a good general fit of the proposed model.

Table 4.8 - Statistical test results for predicting the probability of fire occurrence given the population count. We considered the 2005, 2010, 2015, and 2016 dry years and the other years from 2003 to 2020 as non-dry years.

	2003 - 2020	Dry years	Non-dry years
Coefficient	0.46***	0.47***	0.46***
Odds Ratio (Confidence interval at 95% confidence level)	1.58 (1.54 - 1.62)	1.61 (1.57 - 1.65)	1.59 (1.55 - 1.63)
AUC	0.82	0.81	0.81
Cutoff	0.59	0.52	0.56
Fire predicted with cutoff value (SD)	3.31 (0.06)	2.88 (0.05)	3.15 (0.06)
Accuracy	0.73	0.73	0.73
Pseudo R^2	0.35	0.36	0.35

Note: *** $p < 0.001$. Pseudo R^2 is calculated based on Nagelkerke (1991).

Finally, the average population density in our study area from 2003 to 2020 inside protected areas (1 habitant per km²) is more than seven times smaller than outside (7.2 habitants per km²). The population density distribution within protected areas presented higher frequencies of small densities, including a higher frequency of pixels without habitants (Figure 4.20a). During the studied period, population density tended to increase inside and outside protected areas, albeit outside presented a steeper increase rate per year (Figure 4.20b). Besides, population density outside protected areas was, in all years, higher than the overall average. The opposite is true for density within protected areas. Furthermore, the average distance to the nearest protected area border progressively increases with the augmentation of population density (Figure 4.20c).

Figure 4.20 - Population density inside and outside protected areas. Frequency (a), population density from 2003 to 2020 (b), and average distance to protected area (PA) border per population density (c) are given. Equations and statistics in panels b and c refer to linear regressions. The Red dashed line in panel b represents the overall mean population density from 2003 to 2020. In panel c, the protected area border, i.e., negative distance values, are related to pixels within protected areas.

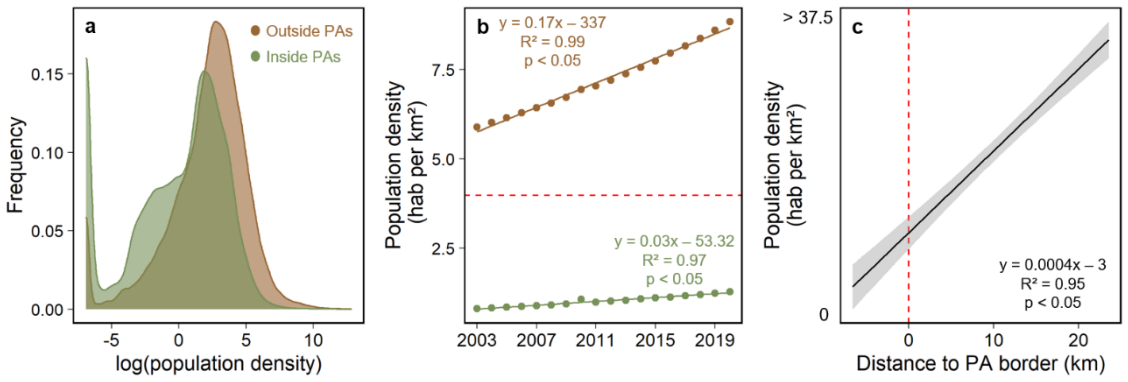

It is important to emphasize that the population data used here is a modeled count with limitations and built-in errors, like all spatial data. These models use, among other parameters, nightlight data, and in less developed regions, this can lead to an underestimation of the population. This is the case mainly in indigenous and traditional communities that do not have electricity supply. This partially explains the number of pixels that registered fires without inhabitants. As we analyzed mean values and on a broader spatial scale, we do not believe the general relationship pattern between fire occurrence and population would change with data refinement. In addition, the statistical test presented in this section consists of a preliminary analysis, which still needs to be subjected to further robustness checks of the model to be better evaluated.

4.3.5 Climate change within Amazonian protected areas [12]

Positive temperature anomalies, calculated as a departure from 2003 to 2020, were observed in all years, except for 2004, outside protected areas, with the highest value registered in 2015 (Figure 4.21). On the other hand, only negative temperature anomalies were registered inside protected areas, with the lowest value recorded in 2004. This is because the pattern of precipitation anomalies varies more than that of temperature. Outside protected areas, negative precipitation anomalies were recorded for 11 years, with the lowest value recorded in 2005. Inside protected areas, negative precipitation anomalies were only recorded for six years, with the lowest value recorded in 2015. The highest positive precipitation anomaly value was recorded inside and outside protected areas in 2013.

[12] Part of this section was presented at the 58th Annual Meeting of the Association for Tropical Biology and Conservation – ATBC 2022.

Figure 4.21 - Temperature and precipitation anomalies from 2003 to 2020, outside and inside protected areas in the Amazon basin.

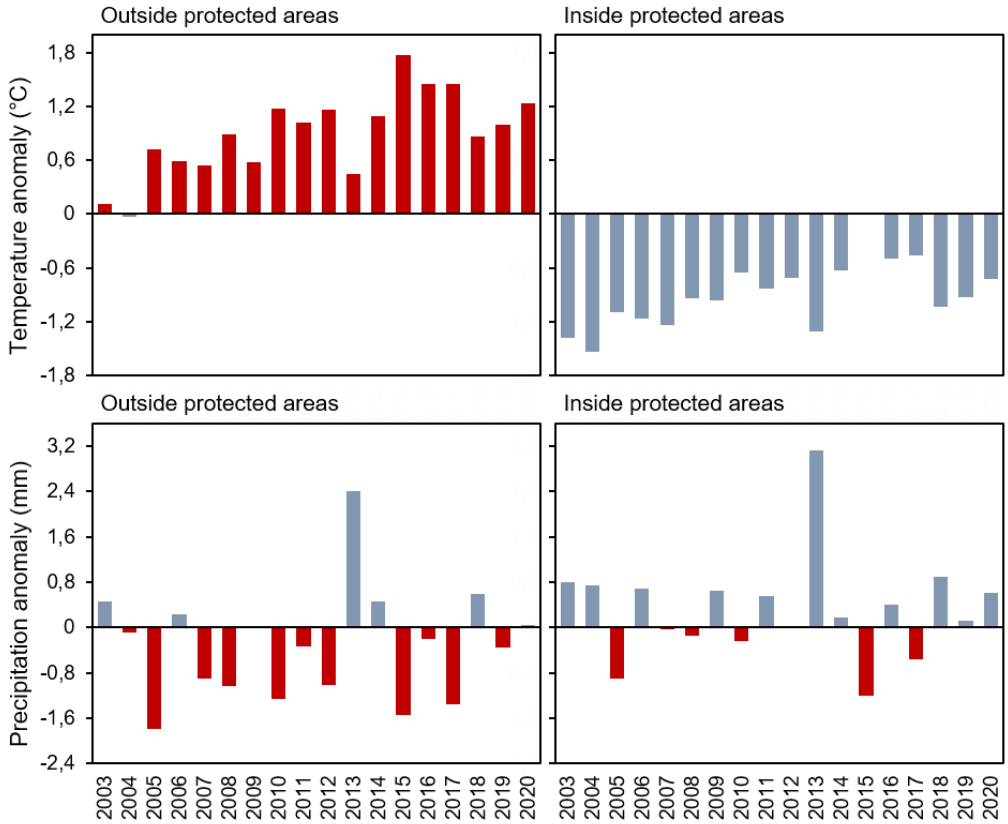

From 2003 to 2020, a positive trend in average temperature during the dry season in the Amazon basin is observed ($p < 0.05$). This trend gave an absolute increase of 0.8°C in 2020 compared to 2003, with an increased rate of 0.05°C per year. An increase of 1.42°C in 2030 compared to 2003 would imply that by 2050 the increase would reach more than 2°C if the temperature continues to increase at the current rate. The average temperature during the dry season increase trend is observed inside and outside protected areas ($p < 0.05$; Figure 4.22a). However, the increase rate outside protected areas is higher than inside.

Although precipitation during the dry season did not show a trend throughout our time series, higher absolute values are found inside protected areas compared to outside, except in 2014 (Figure 4.22b). From 2003 to 2020, above-average precipitation values during the dry season were registered for eleven years inside protected areas, while outside, they were registered only for six years.

Figure 4.22 - Temperature (a) and precipitation (b) trend during the dry season between 2002 to 2020 inside and outside protected areas in the Amazon basin.

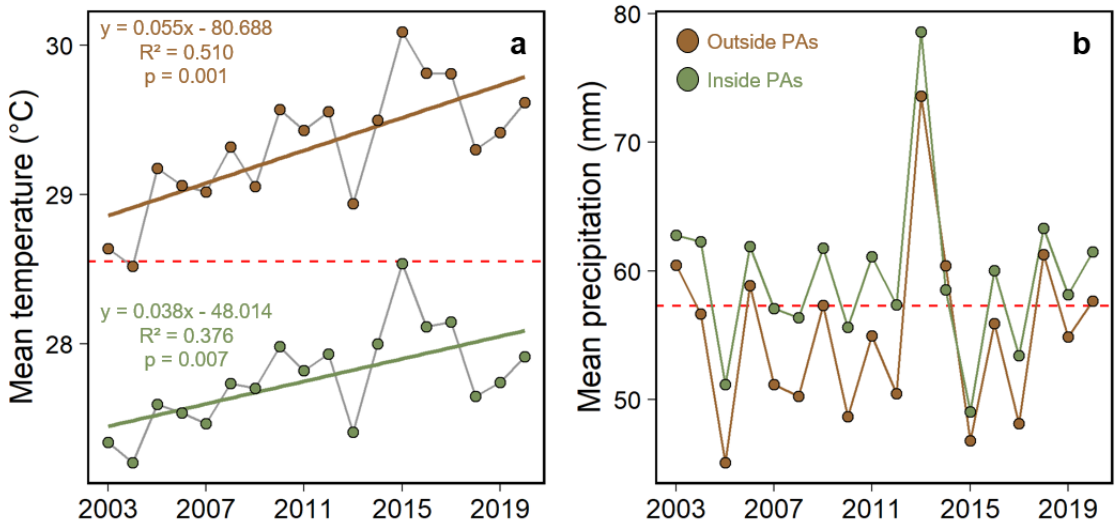

Most of the southern Amazon is subjected to increased temperatures during the dry season (Figure 4.23). Increased temperatures highly impact most of the region known as the Brazilian arc of deforestation. And even the central Brazilian Amazon, which houses the most pristine forests, is also impacted. Northwest and southeastern Bolivian Amazon are also highly impacted, as well as most of the Peruvian territory within the Amazon basin. Most of the pixels that presented significant negative temperature trends are either in central Colombia, at the edge of the Amazon basin border, or scattered in the north and northeastern Brazil.

Nonetheless, they represent only 2% of all significant pixels (Table 4.9). Of all pixels, 32% showed statistically significant trends, and 98% of them presented positive temperature trends during the dry season from 2003 to 2020. If we consider all pixels, regardless of their significance, 67% presented a positive trend (Table 4.9).

Figure 4.23 - Spatial distribution of pixels with positive (red) and negative (blue) trends in temperature during the dry season from 2003 to 2020 in the Amazon basin. Only pixels with a statistically significant trend are represented on the map.

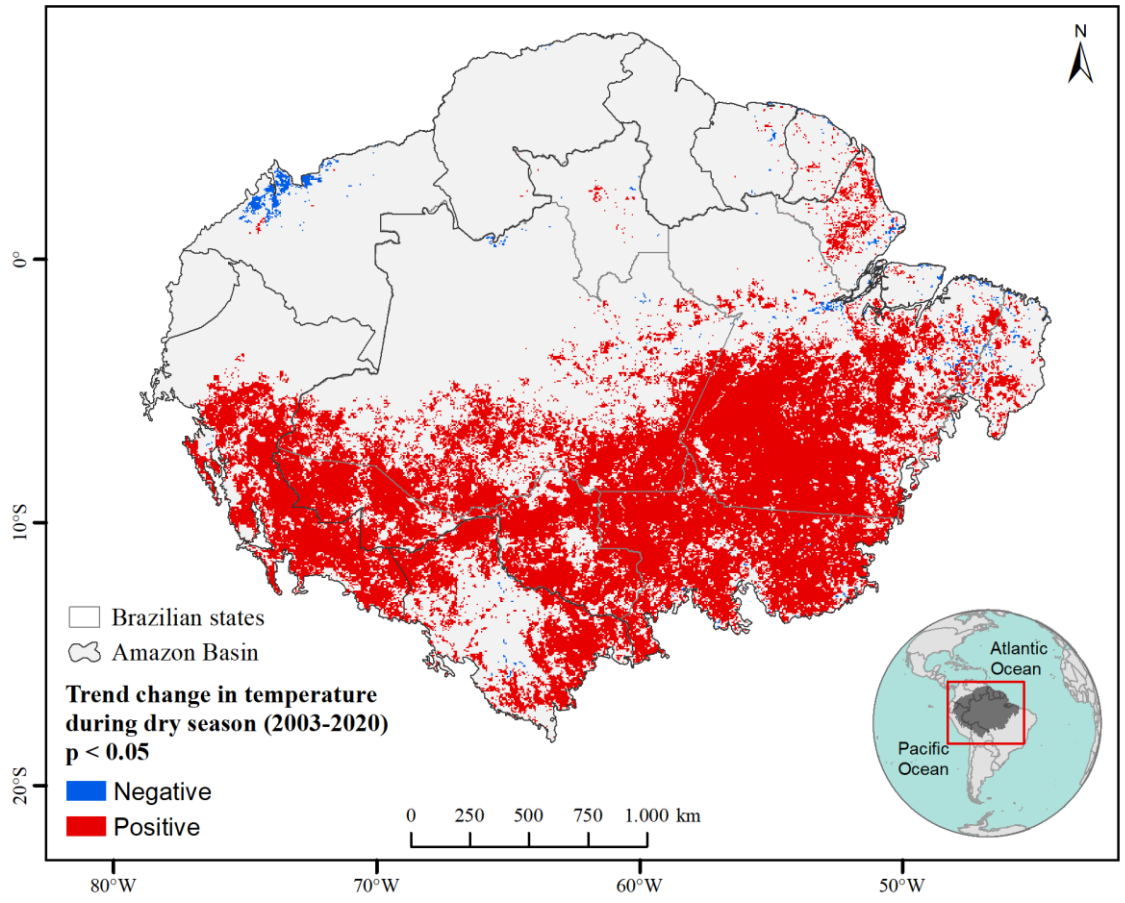

Table 4.9 - Number of pixels with positive, negative, or no temperature trends during the dry season from 2003 to 2020 in the Amazon basin.

	Positive	Negative	No trend	Total
p > 0.05	59,225	17,483	41,077	117,785
Outside PAs	30,295	8,606	14,929	53,830
Inside PAs	28,930	8,877	26,148	63,955
p < 0.05	71,764	1,257		73,021
Outside PAs	35,818	888		36,706
Inside PAs	35,946	369		36,315
Total	130,989	18,740	41,077	190,806

Note:PAs = protected areas

We observed a significant decrease in precipitation during the dry season, mostly in the central Brazilian Amazon, the southeastern Brazilian state of Pará, and the western state of Roraima (Figure 4.24). Conversely, a significant positive precipitation trend was found mostly in the southwestern part of the Amazon basin and northeastern Pará state. They represent 69% of the total significant pixels (Table 4.10). However, only 6% showed statistically significant trends. If we consider all pixels, regardless of their significance,

35% presented a negative precipitation trend during the dry season from 2003 to 2020 (Table 4.10).

Figure 4.24 - Spatial distribution of pixels with a positive (blue) and negative (red) trend in precipitation during the dry season from 2003 to 2020 in the Amazon basin. Only pixels with a statistically significant trend are represented on the map.

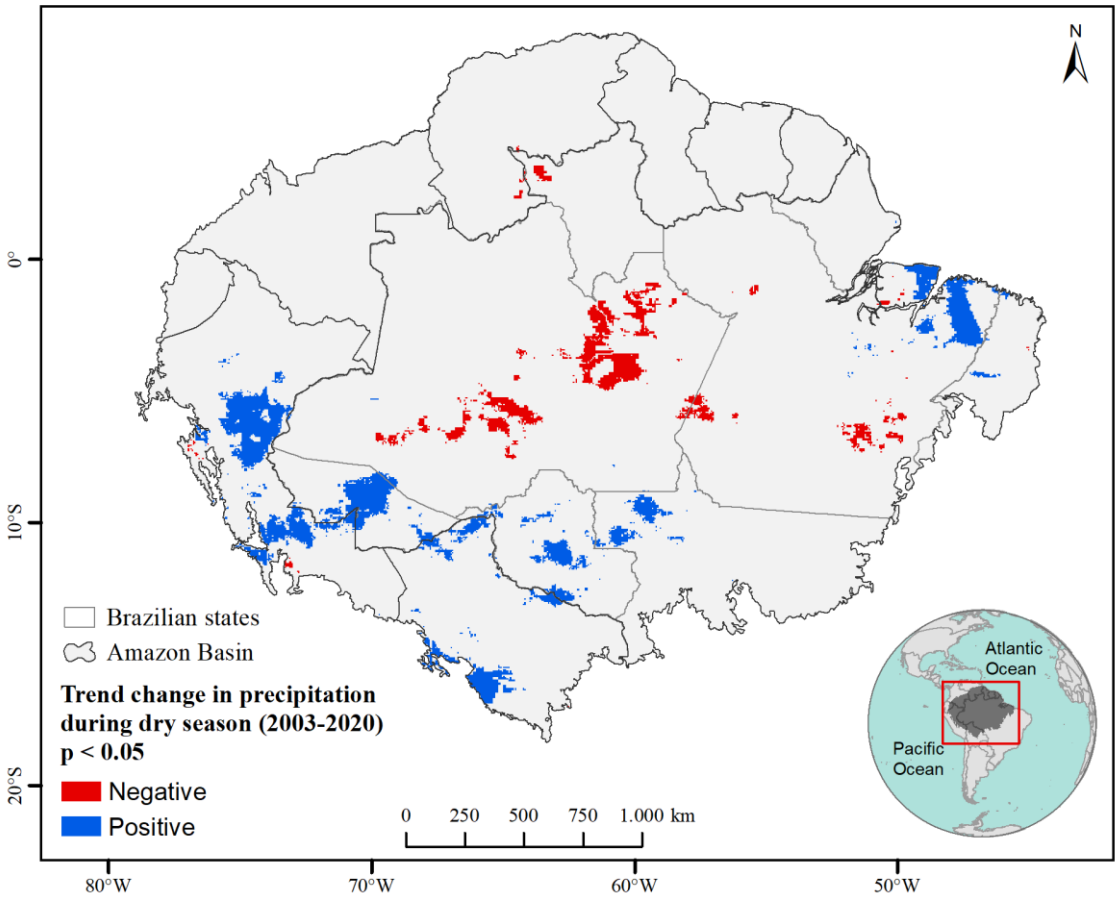

Table 4.10 - Number of pixels with positive, negative, or no precipitation trends during the dry season from 2003 to 2020 in the Amazon basin.

	Positive	Negative	No trend	Total
p > 0.05	75,474	62,758	41,077	179,309
Outside PAs	39,921	29,403	14,929	84,253
Inside PAs	35,553	33,355	26,148	95,056
p < 0.05	8,220	3,645		11,865
Outside PAs	4,099	2,171		6,270
Inside PAs	4,121	1,474		5,595
Total	83,694	66,403	41,077	191,174

Note:PAs = protected areas

As a global effort, a UN report has already shown that the national targets set in the context of COP26 may not be enough to limit global warming to the 1.5°C level (MATTHEWS; WYNES, 2022). Regionally, it is already possible to observe temperature increases exceeding the mid-century global goal (GATTI et al., 2021). Here, we showed

a positive temperature trend towards an increase in the average annual temperature during the dry season in more than half of the Amazon basin from 2003 to 2020. Although this increase happens inside and outside protected areas, the temperature baseline inside these areas is lower, and the increasing trend happens at a lower rate per year. Our results corroborate those of Almeida et al. (2017), which showed an annual increase rate in the average temperature of 0.03°C in the Brazilian Amazon from 1973 – 2013. Gatti et al. (2021) showed an average temperature increase reaching 2.5°C in the southeastern Brazilian Amazon, analyzing the period from 2010 to 2018. During the dry season, a reduction of rainfall accompanied by temperature increase could lead the ecosystems to a fire-prone, continually changing environment. If we consider the population dynamics in this region along with the changes that recurrent fire and deforestation are causing to the local climate, natural ecosystems within protected areas are seriously threatened by fires. Therefore, our results highlight the importance of short-term actions and policies to adapt and mitigate the impacts that climate change is already imposing on Amazonian ecosystems. We emphasize the critical role of protected areas as buffers for these changes and perhaps the last strongholds that bear climatic conditions favorable to the functionalities of Amazonian natural ecosystems.

4.4 Conclusions

In this chapter, we diagnosed fire occurrence in protected areas of the Amazon basin. We evaluated the threat level that protected areas have been exposed to between 2003 and 2020. Specifically, we found empirical evidence that:

i. The proportion of fire occurring within protected areas has increased. Moreover, years of extreme drought show greater burned areas inside and outside protected areas. Among the protection categories, IL registered the largest burned areas, albeit the share of the burned areas within DU and IU protected areas has increased. Therefore, the extent of the burned area within protected areas follows the general pattern of what occurs outside these areas, and extreme drought affects their interior and surroundings. In addition, more restrictive protection categories have a smaller area impacted by fire;

ii. the fire that occurs inside protected areas primarily affects natural areas. It was also shown that deforestation-related fire within protected areas has increased

over the years. Among the categories, IL is the one that registers the largest area of burned forest, despite more than half of what burns in the old-growth forest on average occurring outside protected areas;

iii. fire ignitions also mostly occur outside protected areas, although the proportion of what occurs inside them has increased over the years. Most of the burned area recorded within protected areas is from fires that started outside them. Among the protection categories, the IL are the ones that registered the highest number of ignitions, but DU protected areas registered a higher density of ignitions per square kilometer throughout the period studied;

iv. population density is correlated to fire occurrence in the Amazon basin. This relation is shaped by two moments, an increasing one in which population density would impose greater peaks of fire occurrence and a second decreasing one in which population density reaches a point that makes the environment less flammable. As expected, population density inside protected areas is lower than outside. However, it is increasing over the years, not only inside but around it, which puts greater pressure on its natural resources; finally,

v. climatic conditions of temperature and precipitation during the dry season varied from 2003 to 2020, and their variability changes inside and outside protected areas. Inside protected areas, the average temperature during the dry season is milder than outside, and the precipitation is, on average higher. These conditions give these areas a less fire-prone environment, although these conditions are changing.

Studies have already confirmed the inhibitory role of protected areas on fire (NELSON; CHOMITZ, 2011; NEPSTAD et al., 2006). These areas record less area impacted by fire and fewer ignitions. However, the environment within these areas and their surroundings are changing. Considering the fire occurrence triangle (ALENCAR; RODRIGUES; CASTRO, 2020), which conditions fire occurrence upon three factors in the Amazon (combustible material, weather conditions, and existence of ignition sources), we observe that the changes undergone by these areas in recent years have made them more vulnerable to fire. Here, we confirmed our hypothesis that fire occurrence in the Amazon basin is related to human presence. The expected inverted U-shaped curve between fire occurrence and population density was observed. Population density is increasing within

protected areas. In general, the average population density found within these areas shows that the population-fire relationship is still in the ascending phase; the greater the population density, the greater the fire occurrence. This pattern is progressively worsening throughout the years, boosting the threat of forest degradation within protected areas. Indeed, the environment becomes more fragmented with more people and deforestation. In turn, the climate is also inevitably being altered by large-scale climate change in the Amazon (GATTI et al., 2021).

Notwithstanding, we confirmed the general changing pattern, showing that, even inside protected areas, the climatic conditions are becoming more fire-prone. Furthermore, we showed that most of the burned area recorded within protected areas results from ignitions outside them. Therefore, the increase in population density and the enactment of environmental laws to combat and control illegal activities, not only within these areas but also in their surroundings, are key factors influencing the increase of fire occurrence in these areas. With all that, we conclude that fire is a growing threat to Amazonian protected areas.

The diagnosis presented in this chapter shows not only the potential of these areas as strongholds of a healthy environment capable of resisting climate change and forest degradation but also the level of threat to these areas are increasingly exposed to. Therefore, their inhibitory role, which was once confirmed, may not be sustained in the future scenario of increasing threat, climate change, and loss of governance in controlling illegal activities. Based on the evidence presented here, we can say that fires that occur within protected areas and that affect a large area of a natural land cover mostly result from human activities outside their boundaries. Therefore, the creation of new protected areas and management improvement of the existing ones should be a priority in national environmental agendas, given the relevance of these areas for the conservation of the largest tropical forest in the world. Furthermore, Tasker and Arima (2016) argue that fire occurrence in the Amazon is more related to climatic conditions than to land use regulation policies, such as protected areas. Indeed, we found that climatic conditions within protected areas are less fire-prone, but they are also changing. In a future scenario of increased forest fragmentation and climate change, the environment within these areas may become more flammable, ceasing its ability to contain fire.

Lastly, it is important to emphasize that protected areas are home to several traditional and indigenous communities, which, by directly depending on the natural resources of these areas, are committed to sustainable practices that they have been practicing for hundreds of years. Fire is often part of these practices, and making it strictly illegal without contextualizing its practice can push all these people into illegality. Hence, in the new scenario where we all have to adapt to environmental changes, alternatives must be provided, and environmental education must be intensified so that everyone has equal opportunities to replace fire with other land management techniques. Despite this, land cover change dynamics observed in recent years within protected areas show that forest degradation results from illegal activities in response to predatory development defended and driven by national governments. Such development model is leading to the downfall of the Amazon biome, and as such, traditional and indigenous communities are the most affected by this scenario. Further, protected areas have an important social role, improving life quality for those who live there and for everyone who enjoys their resources, whether they are water to drink or simply a wild environment to be. Indirectly, everyone benefits from these areas, and as such, everyone should feel equally responsible for them and scandalized by their destruction for the benefit of a few.

Nevertheless, even though we have presented a detailed diagnosis not present in any previous study of the effect of protected areas on fire in the Amazon basin, we have not measured, in this chapter, whether this specific land use regulation policy has a statistically significant inhibitory effect on fire. For this, robust statistical tests must be employed to isolate the policy effect from other diverse effects that may be co-acting in the fire inhibitory process. In the following chapter, we then present a formal statistical analysis in this sense.

5 THE ROLE OF PROTECTED AREAS IN REDUCING FIRE OCCURRENCE IN THE AMAZON BASIN FROM 2003 TO 2020

5.1 Introduction

Fire is an intrinsic element of many ecosystems in the world (BEHLING et al., 2004; OLIVEIRA et al., 2014; OVERBECK et al., 2018). In humid tropical forests, it hardly occurs naturally (BUSH et al., 2008) and is strongly associated with human activities (ALENCAR et al., 2022). Broadly, three fire types occur in the Amazon. The fire used in the deforestation process to clean the land, the fire used to manage already established agricultural areas, and finally, the fire that escapes from these first two and reaches adjacent forests, the so-called forest fires (BARLOW et al., 2020). In addition to the presence of the ignition source, two other factors condition fire occurrence in the Amazon: the flammable material availability and favorable weather conditions (ALENCAR; RODRIGUES; CASTRO, 2020). Deforestation advance (SILVA JUNIOR et al., 2021a) and the worsening of environmental degradation, which is largely underestimated (SILVA JUNIOR et al., 2021c), intensifies forest fragmentation. The more fragmented the largest forest edges proportion. Forest edges are subject to greater climatic variations (SILVA JUNIOR et al., 2018). These conditions favor the entry of fire into the forest (SILVA JUNIOR et al., 2018), and tree mortality increases once burned (SILVA et al., 2018a). All these together boost the combustible material within the forest, making it even more vulnerable to further fires. Worsening this scenario, global climate models predict a drier Amazon in the 21st century (LI et al., 2008). The climate is changing (GATTI et al., 2021), and the intensity and frequency of extreme droughts may push Amazonia toward an amplified fire-prone system (ARAGÃO et al., 2018; MALHI et al., 2009; SILVA JUNIOR et al., 2019).

Among the conservation policies, protected areas, including those with resident human populations, are considered an essential global strategy to preserve natural ecosystems (NEPSTAD et al., 2006, 2009; PAIVA et al., 2020; SOARES-FILHO et al., 2010). They have already been pointed out as efficient shields against deforestation (ANDAM et al., 2008; ASSUNÇÃO; GANDOUR; ROCHA, 2015; NEPSTAD et al., 2006; NOLTE et al., 2013). For example, during the first semester of 2020, only 14% of the fire registered in the Brazilian Amazon occurred within protected areas (ALENCAR; RODRIGUES;

CASTRO, 2020). However, the last few years have been marked by setbacks in the environmental governance of these areas (ARMENTERAS et al., 2019; MATAVELI; DE OLIVEIRA, 2022; RORATO et al., 2021; VILLÉN-PÉREZ et al., 2020) and the rising of illegal activities that result in forest degradation. Therefore, even historically registering lower forest degradation rates, the increasing exposure of protected areas to anthropic and climatic threats has become evident. Thus, providing evidence for policy formulation and informing decision-makers about the role of protected areas in mitigating forest degradation caused by fire is essential for prioritizing actions in favor of these areas.

This chapter uses spatial data on fires and protected areas of the Amazon basin to explore the role of protected areas in curbing fire occurrence from 2003 to 2020. Most existing studies on protected areas evaluation have focused on deforestation avoidance (e.g., ANDAM et al., 2008; HERRERA; PFAFF; ROBALINO, 2019; PFAFF et al., 2014, 2015a) and/or climate change mitigation (e.g., RICKETTS et al., 2010; SOARES-FILHO et al., 2010). To date, little research has robustly analyzed the role of protected areas in curbing fire occurrence. In the Amazon context, Nepstad et al. (2006) found that inhabited reserves in the Legal Amazon significantly reduced deforestation and fire by using an inside versus outside protected area comparison. Fire occurrence was four (indigenous lands) to nine (national forests) times higher along the outside *versus* the inside of the reserve perimeters in 1998. Although this study is relevant as a first assessment of the Amazon protected areas' performance, it relied on a naïve comparison, which does not consider confounders of the causal effect. In other words, it might have other factors influencing deforestation and fire occurrence within protected areas other than the regulation itself. Not accounting for this may pose a bias on effect estimation.

Hence, econometric approaches are often used to identify the causal effects of a particular policy on an outcome (PEIXOTO et al., 2017), giving their ability to deal with different sources of bias. Thus, establishing causal inferences between land regulation and fire occurrence is difficult for several reasons. First, there is the possibility of other factors that simultaneously affect protected areas' placement and fire occurrence. For instance, land profitability factors, such as distance to roads and rivers, have direct effects on the suitability of the creation of a protected area and the probability of fire occurrence (NEPSTAD et al., 2006; PFAFF et al., 2015b; SILVEIRA et al., 2020). One can control

for observable factors in the estimations to alleviate this concern. Duly addressing the non-randomization of policy placement and concurrent changes caused by observed and non-observed factors provides greater accuracy and precision in causal effect estimation. Since fire occurrence within protected areas is not solely influenced by land use regulation, Nelson and Chomitz (2011) found that, in Latin America, from 2000 to 2008, indigenous lands reduced forest fire incidence by 16 percentage points. Their econometric approach considered that fire occurrence within protected areas is influenced by several factors, such as economic and climatic. Tasker and Arima (2016), also considering confounding variables when analyzing the effect of protection on fire, found that fires in the Brazilian Amazon are more responsive to precipitation than policies. While one standard deviation decrease in precipitation from its normal could increase the burned area by 18 to 27%, they found that the increment in protected areas did not impact fires.

Although some research has been done on the role of protected areas in mitigating fire occurrence (NELSON; CHOMITZ, 2011; NEPSTAD et al., 2006; NOLTE; AGRAWAL, 2013; TASKER; ARIMA, 2016), they bring into light three main limitations. First, the use of fire as a proxy for deforestation (NELSON; CHOMITZ, 2011), disregarding the temporal dynamic of coupling-decoupling of both processes (ANDERSON et al., 2019; ARAGÃO; SHIMABUKURO, 2010) and the particularities of the fire phenomenon in the Amazon. Second, the lack of fire impacted extension quantification instead of only fire frequency (NELSON; CHOMITZ, 2011; NEPSTAD et al., 2006; NOLTE; AGRAWAL, 2013). Lastly, the disregard of a robust strategy to identify the protected areas' causal effect, causing thus probably bias by land patches being selected to be protected not at random and by the influence on fire level of other (policy, social, environmental) changes occurring simultaneously with the creation of protected areas (NEPSTAD et al., 2006). This chapter seeks to simultaneously fill these three gaps, making, thus, an innovative contribution to the extant literature. Another important novelty is embracing the whole Amazon basin in the analysis, thus going beyond the national-specific assessments of previous studies (NEPSTAD et al., 2006; TASKER; ARIMA, 2016). In addition to adopting a longer time series (2003 – 2020), updating the discussion on the topic and providing a more comprehensive and precise analysis than in previous studies.

Therefore, this study aims to evaluate, with an econometric approach and based on observational data, the effect of protected areas on curbing fire occurrence in the Amazon basin from 2003 to 2020, answering whether the creation of protected areas reduced the fire occurrence in the Amazon basin. The following sections were organized to describe in detail the econometric methods used as identification strategy and then provide a literature review on econometric empirical approaches applied to measure protected area effectiveness. Subsequently, we describe the study area and the dataset developed in this chapter. Finally, we present the results and discussion, closing the chapter with the conclusions.

5.2 Literature review

5.2.1 Theory of causal inference econometrics: a summary

5.2.1.1 Self-selection bias and matching

Causal inference econometrics provides statistical techniques for identifying the effect of a particular policy on an outcome variable of prime interest, what is commonly called the treatment effect (ANGRIST; PISCHKE, 2008). The basic idea is to use the techniques to mitigate the bias with which policy's effect can be measured with observational data. Two crucial characteristics of such data are that it refers to a policy to which observational units were not selected to be exposed at random, and the outcome variable may be affected by other factors besides the policy (ANGRIST; PISCHKE, 2008; YWATA; ALBUQUERQUE, 2011). The policy causal effect estimation begins with the challenge of establishing the counterfactual value of the outcome variable for the group under the influence of the policy. That is, the value observed in the potential state in which the group is not exposed to policy. In other words, for the effect of the policy to be measured accurately, it is necessary that the group exposed to the policy be compared with a group of individuals that adequately represents the situation of non-treatment (PEIXOTO et al., 2017). Naive comparisons of treatment and control groups, or even of the same group before and after treatment, cannot provide an accurate estimate of the policy's effect. In these cases, the situation of non-treatment after the implementation of the policy is unlikely to represent the situation of treatment in the potential stated without policy treatment. This is because many factors may have affected the treated group in addition to the policy itself, and treated and control groups differ in unobservable characteristics

that could be correlated with the process that determined whether they would be treated or not (PEIXOTO et al., 2017).

When we want to estimate the causal effect of a policy on an outcome variable of interest (*Y*), the value of such variable to the *i*-th individual may be referred to as *Yi(1)* in the treatment state and as *Yi(0)* if the individual is in the untreated (control) state. Each state is associated with a potentially different outcome for the same individual (PEIXOTO et al., 2017). Thus, if we could observe this individual in both situations, the difference $\Delta i = Yi(1)-Yi(0)$ would give the policy effect for this individual. However, it is naturally impossible to know the value of Δi for each individual since only one of the two potential results is concretely realized (PEIXOTO et al., 2017). Aggregate statistics, which can be identified under certain assumptions, are then used to circumvent this infeasibility of estimating the individual effect. Two such aggregations are the average treatment effect (ATE), which represents the mean policy effect for all individuals in the population, regardless of who was treated or not[13], and the average treatment effect on treated (ATT), which focuses only on the treated group[14].

Assuming that the policy effect is the same for all individuals, that is, that the treatment effect is homogeneous, the result observed for any individual *i* in the population is given by a linear regression model[15] (PEIXOTO et al., 2017). In this case, the biggest problem in identifying the causal effect of policies on a variable of interest is that the process that assigns individuals to specific treatment states is potentially correlated with unobservable factors that also determine the effect of treatment, what is called self-selection problem (PEIXOTO et al., 2017). This occurs mainly because policies are seldom implemented randomly. Several econometric methods address the problem of self-selection bias based on strategies that seek to adequately establish the counterfactual situation of each individual. For that, these approaches consider a wide range of socioeconomic and environmental predictors, besides the policy, to make treatment assignments as random as possible conditional on such predictors.

[13] The ATE can be defined by $ATE = E[Yi(1)-Yi(0)] = E[\Delta i]$ (PEIXOTO et al., 2017).
[14] The ATT can be defined by $ATT = E[Yi(1)-Yi(0)|Ti = 1] = E[\Delta i|Ti = 1]$, where *Ti* is a binary variable that takes value 1 if the individual *i* is treated (PEIXOTO et al., 2017).
[15] Defined by $Yi = \alpha + \beta Ti + \varepsilon i$, where εi is the unobservable component that affects the potential outcomes of individual *I* (PEIXOTO et al., 2017).

Matching is a commonly adopted method to address self-selection and isolate the policy effect from the effects caused by unobservable factors that affect the outcome variable (GALIANI; GERTLER; SCHARGRODSKY, 2005). More precisely, when assessing the effectiveness of protected areas on fire occurrence, it is true that land patches were not randomly selected to be protected. Instead, that was a function of observable characteristics such as agricultural profitability and other factors that the government may have considered drivers of the net benefit of protecting the particular patch.

Matching methods mitigate this bias by pairing treated and control observations with similar observable attributes that capture the net benefit of protecting a land patch. Such mitigation and the gain in accuracy of treatment effect estimation depend on two crucial assumptions. The first one is the ignorability of treatment assignment, in the sense that, after all, observable relevant covariates have been included in the analysis, treatment becomes random, and treatment effect becomes accurately measurable. This assumption requires that all relevant confounding variables have been included as controls (NELSON; CHOMITZ, 2011), which is not verifiable, but the omission of covariates nevertheless causes bias (ANDAM et al., 2008). The second assumption is that of common support between treated and controls; that is, all treated observations are assumed to have a comparable control unit, with comparability meaning equivalence in all covariates except the treatment status (MORELLO; ANJOLIM, 2021; PEIXOTO et al., 2017; WOOLDRIDGE, 2010).

For each individual in the treatment group, the matching estimator searches for the most similar individuals in the control group (regarding their vector of observable variables). Then, it summarizes the outcome variable of those individuals to obtain the individual's outcome in the treatment group would be, if it were not treated (counterfactual) (PEIXOTO et al., 2017). The main differences between the various matching estimators concern the metric used to define the difference between treated and control individuals in terms of the vector of observable variables (PEIXOTO et al., 2017). Furthermore, the methods also differ in how many individuals in the untreated (or treated) group will be matched to each individual in the treatment (or control) group to obtain their counterfactual (PEIXOTO et al., 2017).

Two widely used matching metrics are propensity scores (PS) and covariate matching (CV). First, the probability of the control being exposed to treatment is calculated using a multiple logistic regression model. This score (or probability) is used to match treated and untreated observations. The smaller the difference between the scores, the more similar they are (BALTAR; SOUSA; WESTPHAL, 2014). In the second, the similarities between pairs are defined using the Mahalanobis distance (MD) metric, in which the weights on factors are based on the inverse of the covariate variance-covariance matrix (ABADIE; IMBENS, 2011). The MD is a scale-free distance metric. If two observational units have identical covariates values, the MD is zero. Thus, the more similar the covariate values, the shorter the distance. When using it to match treated and control observations, we ensure that each pair will have similar covariate values and that the distribution of the covariates in the treatment groups in the matched sample will be similar. The main difference between the two metrics is that by using CV, the matching is performed on the covariate space and not based on a one-dimension unique score (KING; NIELSEN, 2019).

5.2.1.2 Concurrent changes in bias and differences-in-differences

Matching estimators assume that only time-fixed observable characteristics are sufficient to circumvent selection bias, and this hypothesis cannot be tested directly on the data (PEIXOTO et al., 2017). Thus, when important confounders of the outcome variable are time-varying observables or even time-invariant unobservables, not controlling for them can bias the causal effect estimated with matching. This may be called “concurrent changes bias” since it is caused by changes affecting the outcome variable that occur simultaneously as exposure to policy and could be captured in the variation of the outcome variable. To address such bias, the Differences-in-Differences (DiD) estimator is a well-suited option, as it is based both on variation across treatment status and time and may be coarsely described as based on a mix of before-and-after and treated-and-control differences of the outcome variable. They also allow further address heterogeneity of observational units by including a wide range of predictors.

Differences-in-Differences (DiD) estimators are based on a double subtraction. For simplicity, let it be considered that the outcome is observed for two groups during two periods. One of the groups is exposed to a treatment (policy) in the second period but not

in the first one. In turn, the second group, composed of the control group, was not exposed to the treatment in the two periods. The first DiD subtraction refers to the post- and pre-treatment time difference of the outcome variable for the treatment group. Then, the second subtraction calculates the difference of the first subtraction between treated and control groups (BERTRAND; DUFLO; MULLAINATHAN, 2004; PEIXOTO et al., 2017; WOOLDRIDGE, 2010). If we denote by T={1,0} the presence or not of the treatment and by t={1,0} the periods after and before the policy implementation, respectively, the DiD estimator is given by (Equation 5.1):

$$\Delta_{DiD} = \{E[Y_i|T_i = 1, t = 1] - E[Y_i|T_i = 1, t = 0\} - \{E[Y_i|T_i = 0, t = 1] - E[Y_i|T_i = 0, t = 0]\} \quad (5.1)$$

In this case, the causal effect estimation relies on the identification assumption that treated and control groups have the same time trend for the outcome variable in the untreated state (notice that this does not mean the values of the outcome are the same but that they exhibit parallel paths across time). That is, the time trajectory of the outcome variable for the control group necessarily represents what would happen to the treated group if there was no intervention by the policy under analysis – thus, concurrent changes affect treated and untreated units with the same intensity. Intuitively, if the trajectories are similar during the period before treatment, then it seems reasonable to assume that the evolution of the control group after treatment closely represents what would happen to the treated group in the non-treatment situation (ANGRIST; PISCHKE, 2008; BERTRAND; DUFLO; MULLAINATHAN, 2004; PEIXOTO et al., 2017). The identification assumption cannot be directly tested. However, its plausibility can be approximately assessed with a graph depicting the outcome trends for treated and untreated groups before and after treatment.

If the DID assumption is true, any deviations in the trajectory of the outcome variable between the groups after the policy implementation (treatment) are due to the policy intervention. In other words, considering that the control group represents a valid counterfactual of the treatment group, the difference between the variation observed for the treatment group and the variation observed for the control group captures the causal effect of the intervention on the treated ones (FERRARO, 2009; PEIXOTO et al., 2017) (Figure 5.1). Although the DiD method requires parallel trends of the outcome variable

in the pretreatment period, they do not need to start from the same point. Hence arises a first major advantage of the method, the ability to deal with pre-existing differences between groups (PEIXOTO et al., 2017).

Figure 5.1 - Conceptual framework of differences-in-differences model estimation.

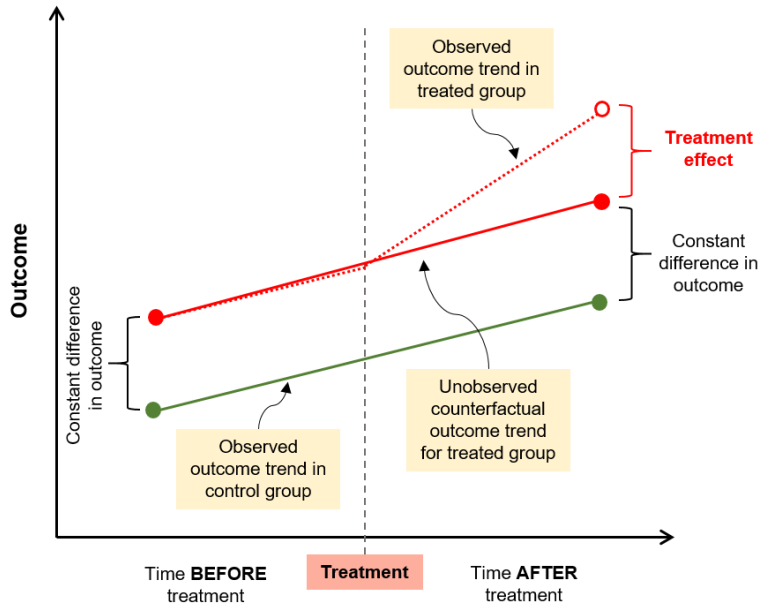

Source: Adpated from Angrist and Pischke (2008).

The DiD model can be written in the form of linear regressions to simplify its description. The commonest specification, for the case with two periods, before and after policy, is found below (Equation 5.2):

$$Y_{it} = \beta_0 + \beta_1 De_i + \beta_2 Dp_{it} + \beta_3 De_i * Dp_{it} + X'_{it}\alpha + \varepsilon_{it} \quad (5.2)$$

Where *i* indicates the observation unit and *t* the time. Y_{it} is the variable under analysis (outcome variable). *De* is a binary variable assigned one if the pixel is, or at some point will be, under treatment. *Dp* is another binary variable assigned one if the treatment is active in the current year. The isolated *De* and *Dp* terms capture the differences in the mean of the outcome variable between the treatment and control groups and between the period before and after treatment, respectively. The product coefficient between *De* and *Dp* (β_3) captures what specifically happened to the treatment group in the post-treatment period. It is the average treatment effect on the treated (ATT). Finally, ε_{it} represents the time-variant unobservables, being a random disturbance with zero mean.

The vector of controls X'_{it} contains observable characteristics that vary or not in time. Introducing these characteristics further increases the accuracy and precision of estimating the intervention causal effect. If they are not considered, part of the outcome variation would be mistakenly attributed to the treatment (PEIXOTO et al., 2017). In the case where more than two time periods are considered, Equation 5.2 should be rewritten as (Equation 5.3):

$$Y_{it} = \beta_0 + \beta_1 D_{it} + X'_{it} + \varepsilon_{it} \quad (5.3)$$

The term β_1 is the average treatment effect (PEIXOTO et al., 2017) as D_{it} takes value one if the treatment is active for the i-th individual in the *t*-th time. Another important addition to the DiD model is addressing a third source of bias from time-invariant unobservables that may be correlated with included covariates, hereafter referred to as "heterogeneity bias." That is, the disturbance term ε_{it} may be decomposed as $\varepsilon_{it} = \mu_i + u_{it}$ so that the econometric specification becomes (Equation 5.4):

$$Y_{it} = \beta_0 + \beta_1 D_{it} + X'_{it} + \mu_i + u_{it} \quad (5.4)$$

In this case, identification of the parameters may be achieved with a fixed-effects (FE) estimator, which transforms the model above by replacing variables by their deviations to their mean across time, thus eliminating a_i.

An important assumption in this specification is that the term ε_{it} cannot be correlated with the model variables. In other words, conditional on the adoption of fixed effect, μ_i, and the variables in X'_{it}, it is required that any time-varying unobserved factor that affects the outcome variable does not influence the decision to participate in the program (ANGRIST; PISCHKE, 2008; PEIXOTO et al., 2017).

Instead of the fixed-effects time-demeaning transformation, (5.4 could be estimated with the first differences of all variables included in the model, that is, with variables replaced by the difference between their value in the current period and one period before, which also eliminates μ_i (PEIXOTO et al., 2017). This way, the disturbance term of the model will be given by: $\Delta\varepsilon_{it} = \varepsilon_{it} - \varepsilon_{it-1}$. It is important to highlight that if this term presents a serial correlation, that is if the correlation of ε_{it} e ε_{it-1} is different from zero, underestimation of the standard error of the coefficient estimator of interest will probably

occur, leading to erroneous conclusions about the statistical significance of the treatment effect (BERTRAND; DUFLO; MULLAINATHAN, 2004). Some strategies can be adopted to minimize this problem, such as the bootstrapping technique applied to standard errors, which is used as a non-parametric way to address potential serial correlation and heteroskedasticity (BERTRAND; DUFLO; MULLAINATHAN, 2004; GALIANI; GERTLER; SCHARGRODSKY, 2005). In all estimations conducted in this chapter, clustered-standard errors, robust to serial correlation and heteroskedasticity, were relied on, together with bootstrapping.

5.2.1.3 Post-matching DiD regressions

Although matching estimators are widely used in the literature to estimate the treatment effect of specific policies, these estimators can also be used in combination with other econometric techniques such as DiD (IMBENS; WOOLDRIDGE, 2009; PEIXOTO et al., 2017). For example, treatment endogeneity (self-selection) is commonly addressed using matching. Subsequent application of DiD could address further endogeneity across cross-section units by looking at differences in variations (and assuming common trends). The main gain in combining these two estimators is to make identification assumptions valid in a wider range of possibilities, thus increasing the accuracy of the average treatment effect (ATE) estimation (IMBENS; WOOLDRIDGE, 2009; PEIXOTO et al., 2017).

Indeed, the selection-on-observables assumption of matching establishes that conditional on the vector of observable variables, for a reliable estimate of the causal effect, there cannot be any unobservable factor that simultaneously influences the decision to participate or not in the treatment and the potential outcomes (PEIXOTO et al., 2017). In other words, the assumption requires no selection into treatment based on unobservables (GALIANI; GERTLER; SCHARGRODSKY, 2005). However, when matching is paired with DiD, we do not need to be strict about this requirement, as unobservable time-invariant factors will be duly considered in the DiD estimate. Ferraro and Miranda (2017) applied matching to panel data in a two-step approach by ensuring comparability with sample selection and thus running the panel FE model. They showed that treatment effects estimated this way are closer to the ones in a Randomized controlled trial (RCT) sample. The latter estimator used in this study (FE), likewise DiD, assumes that trends are the

same for treated and untreated in the control state and also other four assumptions; (1) treated and untreated units respond the same way to common shocks, (2) treatment effect is additive and constant, (3) linear functional form, and (4) no dynamic lagged variables. The author claimed, then, that flexibilizing those assumptions is hardly possible. However, by applying matching before FE, results less susceptible to violation of at least one of the assumptions are obtained. If heterogeneity in treatment effect is due to observables, matching attenuates this, since assuming the same treatment effect for treated and non-treated is more plausible after conditioning on observables (FERRARO; MIRANDA, 2017).

In addition, the identification strategy here applied is to use matching in the first stage to pair treatments and control observations and build a valid counterfactual group. This mixed approach allows for conditioning on fixed effects and identifying the parameter of interest jointly with addressing self-selection unobservables (HECKMAN; ICHIMURA; TODD, 1998). As mentioned before, conventional matching methods assume that conditional on the covariates, the counterfactual outcome distribution of the treated units is the same as the observed outcome distribution of the units in the control group. The matched sample will not only ensure a valid counterfactual, but it will also improve the parallel trends of the outcome variable in the pre-treatment period between treatment and control groups. This way, matching may increase the parallelism of trends if it is based on factors related to concurrent changes (ABADIE; IMBENS, 2006; FERRARO; MIRANDA, 2017), ultimately being beneficial for the fulfillment of the assumptions required by DiD. Other examples using two-step identification strategies can be found in Andam et al. (2008), Arriagada et al. (2016), and Herrera et al. (2019).

5.2.2 Applications of causal inference econometrics: assessment of protected areas' effect

After conceptually introducing the methods we will adopt in this chapter, we present a brief bibliographic review of works that approach protected areas, using econometric techniques for data analysis. Matching and DiD estimators are widely used for policy evaluation. Specifically for the protected areas subject, Table 5.1 summarizes the main findings of studies measuring their effectiveness on different outcomes, mostly using econometrics.

The use of matching to balance covariates between treatment and control groups and, thus, deal with selection bias is extensively described in the literature (ANDAM et al., 2008; HERRERA; PFAFF; ROBALINO, 2019; NELSON; CHOMITZ, 2011; PFAFF et al., 2014, 2015a, 2015b; SHI et al., 2020; SZE et al., 2022; WENDLAND et al., 2015).

Table 5.1 - Summary of recent literature on the effect of protected areas on land cover changes. PAs = protected areas, PS = propensity score, CV = covariate matching, DiD = differences-in-differences, OLS = Ordinary least squares.

Reference	Analyzed time	Scale	Main methods	Main conclusion
(WEST et al., 2022)	2008-2017	Brazilian Amazon	Matching (PS, CV, and PSW) + Generalized synthetic control (GSC)	The management proxy (approved management plan) has a potential effect on reducing forest loss, but this effect is not significant for all PAs and years.
(SZE et al., 2022)	2010-2019	Pan-tropical	Nearest Neighbor Matching + regressions	Indigenous lands reduce deforestation and forest degradation more effectively than other PAs throughout the tropics.
(SHI et al., 2020)	1994-2015	Global	Matching (PS) + DiD	With the implementation of PAs, the global carbon sequestration capacity can be improved by 0.39%. This effect occurs if there is an upgrading of the PA category, the presence of a management plan, and an increase in local governments.
(AMIN et al., 2019)	2001-2009	Brazilian Amazon	Dynamic Spatial Durbin Model	The sustainable use PAs do not help to reduce deforestation. The spillover effects generated by integral PAs and indigenous lands lead to reduced deforestation in their vicinity.
(HERRERA; PFAFF; ROBALINO, 2019)	2000-2008	Brazilian Amazon	Matching (PS and CV) + regressions	Outside the deforestation arc, protected areas have little effect on deforestation, and the spillover is negligible. The effect inside and in the surrounding is only registered in federal PAs.
(ARRIAGADA; ECHEVERRIA; MOYA, 2016)	1986-2011	Chile	Matching	PAs are only able to reduce deforestation when compared to private areas.

(To be continued)

Table 5.1 – Continuation.

Reference	Analyzed time	Scale	Main methods	Main conclusion
(PFAFF et al., 2015b)	2000-2008	Brazilian Amazon	Matching (PS) + regressions	The siting of PAs varies across regions. PAs created in the deforestation arc are further from the pressure (non-forest), and the opposite is observed outside. After 2000, PA extent is less similar across PA types with little non-indigenous area created inside the arc. The effect of PAs on deforestation is always greater within the deforestation arc.
(PFAFF et al., 2015a)	2000-2008	Brazilian Amazon	Matching (PS) + regressions	Using matching, the measured effect of PAs on decreasing deforestation can be reduced by half. PAs closer to highways and cities have a greater impact on deforestation.
(WENDLAND et al., 2015)	1985-2010	Russia	Matching (PS) + regressions	PAs showed a little significant effect in reducing forest disturbance, with little difference between PAs near or far from cities and highways.
(PFAFF et al., 2014)	2000-2008	Brazilian state of Acre	Matching (PS and CV) + regressions	Sustainable use PAs are more commonly found in places with greater deforestation pressure and prevent more deforestation than integral protection PAs.
(NOLTE; AGRAWAL, 2013)	2000-2010	Amazon basin	Nearest Neighbor Matching	PAs with high management effectiveness indicators in 2005 did not perform better in reducing forest fires from 2000 to 2010.
(NOLTE et al., 2013)	2001-2010	Brazilian Amazon	Matching + regressions	The effectiveness of PAs in reducing deforestation is related to deforestation pressure at the site. Strictly PAs avoided more deforestation than sustainable use PAs. Indigenous lands were particularly effective in reducing deforestation in regions with greater pressure.
(JOPPA; PFAFF, 2011)	2000-2005	Global	Nearest Neighbor Matching	75% of the countries presented the effect of PAs on natural land cover conversion, which is weaker in areas farther away from roads, cities, and steeper slopes.
(NELSON; CHOMITZ, 2011)	2000-2008	Pan-tropical	Nearest Neighbor Matching	In Latin America, Strict and Multiple Use PAs substantially reduced fire occurrence, and indigenous areas reduced forest fire incidence by 16 percentage points.

(To be continued)

Table 5.1 – Conclusion.

Reference	Analyzed time	Scale	Main methods	Main conclusion
(SIMS, 2010)	2000	Thailand	OLS + Instrumental variables	PAs increased average consumption and reduced poverty rates but imposed low availability of land for agriculture. The gains are explained by the increase in tourism and are greater in areas with intermediate distances from large cities.
(SOARES-FILHO et al., 2010)	1997-2008	Brazilian Amazon	Inside vs. outside comparison of deforestation probability	PAs showed a significant inhibitory effect on deforestation and have the potential to avoid 8.0 ± 2.8 Pg of carbon emissions by 2050.
(ANDAM et al., 2008)	1960-1997	Costa Rica	Nearest Neighbor Matching	PAs reduce deforestation, and spillovers are negligible.
(NEPSTAD et al., 2006)	1997-2000	Brazilian Amazon	Inside vs. outside comparison	PAs with human residents reduce deforestation and fire. However, the difference in effectiveness against deforestation and fire of PAs without human residents and indigenous lands was insignificant.

Protected areas' relative performance against deforestation and fire in the Brazilian Amazon was evaluated by (NEPSTAD et al., 2006). The authors used a naïve comparison between buffers outside and inside protected areas and found that protected areas, including those that allow human residency, have reduced deforestation and fire. However, they point out that indigenous lands are generally created closer to areas under greater pressure from deforestation, and therefore their performance would be more relevant. Although the authors recognize the importance of protected areas placement and other factors that affect their performance, they do not consider these limitations in their assessment. They only attest that the approach used overestimates the inhibition of deforestation in cases where protected areas were established close to existing roads or the boundaries of existing colonization projects. A similar approach was applied by (SOARES-FILHO et al., 2010). However, the authors deepen their analysis by adopting a Bayesian method, which considers the differential effects of spatial determinants on the spatial prediction of deforestation. By doing this, they partially resolve the selection bias issues, ensuring that the probability map of deforestation, used to compare inside and outside protected areas buffers, is controlled for landscape characteristics. The authors found that the expansion of protected areas from 2004 to 2006 in the Brazilian Amazon

was responsible for 37% of the region's total reduction in deforestation without provoking leakage. Their results also confirm that not considering cofounders of the causal effect could potentially overestimate the role of protected areas.

Several other studies have delved into applying econometric methods to avoid this naive comparison and overestimating the effectiveness of protected areas. Andam et al. (2008) applied matching methods to evaluate the impact of deforestation in protected areas in Costa Rica from 1960 to 1997. Three facts that hamper the effectiveness measurement of protected areas are highlighted; (1) the impossibility of directly measuring the deforestation that would have occurred in the absence of legal protection (i.e., the counterfactual is not observed), (2) the bias that can be embedded, since protection is not randomly assigned, and (3) the displacement (spillovers) that can be induced by protection to neighboring forests. Considering these three aspects, the authors used matching methods and found that 10% of the protected forests would have been deforested in case of protection absence. However, they showed that conventional approaches would have substantially overestimated avoided deforestation by over 65%. Arriagada et al. (2016) also adopted a matching approach to measuring the effectiveness of the protected areas against deforestation in Chile from 1986 to 2011. The authors found that protected areas can only reduce deforestation compared to private areas.

Another study by Nelson and Chomitz (2011) used a matching approach to address this key analytic problem. It is highlighted that protected areas placement is likely to occur on marginal lands with low pressure for deforestation. Thus, the authors argued that a naïve comparison of deforestation rates between these low-pressure areas and unprotected lands, in general, would give an inflated estimate of the protection effectiveness. They analyzed the effectiveness of different protected area categories in reducing tropical forest fires considering the global tropical forest biome. They used forest fires as a high-resolution proxy for deforestation, disregarding the occurrence of fire uncoupled to deforestation. The authors found that strict and multi-use protected areas substantially reduced forest fires in Latin America, being the latter more effective.

Additionally, indigenous areas reduced fire incidence by 16 percentage points, 2.5 times as much as unmatched comparison with unprotected areas would suggest. Nolte and Agrawal (2013) also evaluated the effectiveness of protected areas on forest fires using

matching. However, they split their sample according to the level of protected area management effectiveness measured by qualitative indicators. They found that, in general, protected areas avoided forest fires compared to similar unprotected areas. Surprisingly, their results showed that better-managed areas avoided fewer fires compared to unprotected areas than protected areas with low levels of management effectiveness. This result shows that fire occurrence may relate less to land use regulation policies and more to socio-climatic conditions.

Several studies have highlighted the advantages of adopting methods combined with matching to assess protected area effectiveness, thus facilitating compliance with assumptions and improving the accuracy of the causal effect estimate (e.g., HERRERA; PFAFF; ROBALINO, 2019; NOLTE et al., 2013; PFAFF et al., 2014, 2015a, 2015b; SZE et al., 2022). Wendland et al. (2015) matched protected areas to control observations and compared coefficients in a post-matching approach, comparing fixed versus random-effects models. Their analysis considers the Russian protected area network from 1985 to 2010. No statistically significant effect of protected areas over deforestation was found, considering Strict and Multiple-Use protected areas. The authors highlight that random-effects estimates differed qualitatively and quantitatively from those of fixed effects. It serves as a cautionary note for evaluations where time-invariant unobservables are important. As Wendland et al. (2015), Tasker and Arima (2016) also applied matching combined with post-matching regressions to measure the relative impact of precipitation and anti-deforestation policies on fire frequency and extent in the Brazilian Amazon from 2001 to 2013. In this case, the authors wanted to evaluate the role of two environmental policies, one being protected areas and rainfall variation over fires. They used matching estimators to identify the counterfactual scenario of what would have happened with fire in the absence of policies. The post-matching regression, then, was used to estimate the effect of both policies and the rainfall variation on the outcome variable. Their results show that the increment on protected areas did not impact fires once you control for other covariates. Nevertheless, the authors highlight that the overall level of protected areas still impacts fires, even if additional areas were not as effective. The inhibitory effect may increase as the frontier advances into the forests and closer to newly established protected areas.

DiD is also widespread in the conservation area, mainly in public policy evaluations (e.g., ASSUNÇÃO; ROCHA, 2019; CISNEROS; ZHOU; BÖRNER, 2015), although its specific use to evaluate protected areas is still rare. For example, in 2008, the Brazilian government implemented a policy to prioritize anti-deforestation actions and sanctions on the most deforesting municipalities in the Amazon, which are commonly called blacklisted municipalities. Assunção and Rocha (2019) used a DiD approach to compare deforestation in blacklisted and non-blacklisted municipalities before and after the blacklisting policy. They found that blacklisting has significantly reduced deforestation, mainly due to monitoring and law enforcement intensification. Cisneros et al. (2015) adopted a similar approach to evaluate the same policy, and the authors also found that listed municipalities showed a greater reduction in deforestation.

The joint use of matching with specifically DiD is a promising strategy in evaluating environmental programs, and it was first described in Heckman et al. (1998). Ferraro and Miranda (2017) demonstrated how this combination of methods mitigates common concerns about specifying the correct model identification, the nature of treatment effect heterogeneity, and how time enters the model. They suggested a two-step approach by first ensuring comparability with sample selection with matching and then running the panel Fixed Effects (FE) estimator. They claim that matching the assumption of the same treatment effect for treated and untreated is more plausible after conditioning on observables. Also, if heterogeneity in treatment effect is due to observables, matching attenuates this homogenizing of the observation units. Another study was conducted by Shi et al. (2020), using propensity score matching and DiD methods to separate the time effect and policy effect of the construction of protected areas on carbon sequestration capacity. Their results revealed that the carbon sequestration capacity could be improved by 0.39% by constructing global protected areas. Nolte et al. (2017) also adopted a joint approach using matching and DiD to evaluate sub-national policies on curbing deforestation. They used post-matching DiD to deal with potential influence from unobservable time-invariant variables. Other recent studies pursuing similar approaches agree that combining designs is more likely to approximate a randomized controlled trial (e.g., ALIX-GARCIA; SIMS; YAÑEZ-PAGANS, 2015; JONES; LEWIS, 2015).

Indeed, combining matching to select a balanced subsample and then using it in an Ordinary Least Squares (OLS) estimator, such as DiD, is a reasonable approach to measure an envisaged causal effect (IMBENS; WOOLDRIDGE, 2009). It is already clear that, in the case of protected areas, there is no randomization of the policy implementation, so a selection bias needs to be addressed. Furthermore, the effect of these areas on fire, similarly to what happens with deforestation, is influenced not only by observable variables but also by unobservables, such as socioeconomic and institutional simultaneous changes. These issues need to be duly considered for an unbiased measure of the causal effect of protected areas on fire. Although selection bias has already been widely described and addressed in the literature, even if only considering the effect of protected areas on deforestation, the combination of econometrics designs to evaluate protected areas' effectiveness on fires and deforestation is still rare. The current scientific literature does not provide details on how this combination is done using the matching and DiD model. Notwithstanding, some studies adopt this identification strategy, endorsing its potential to accurately estimate the effect of protected areas on fire. This chapter aimed to fill this methodology gap by proposing a two-step approach, considering the matching and DiD model, to measure the effect of protected areas on fire occurrence in the Amazon Basin.

5.3 Materials and methods

5.3.1 Study area

The study area comprises the whole extension of the Amazon Basin (EVA; HUBER, 2005), excluding the subregions of ‘Planalto’ and ‘Andes.’ Even not including the whole region classified as Amazonia *sensu latissimo* by Eva and Huber (2005), for this study, we refer to the region considered the Amazon basin since only approximately 18% of the area was excluded. This area spans nine South American countries: Bolivia, Brazil, Colombia, Ecuador, French Guiana, Guyana, Peru, Suriname, and Venezuela, and it adds up to more than 6 million square kilometers (Table 4.1 and Figure 5.2). All nine countries host 95% of the remaining Amazonian old-growth forests (EVA; HUBER, 2005).

Figure 5.2 - Study area.

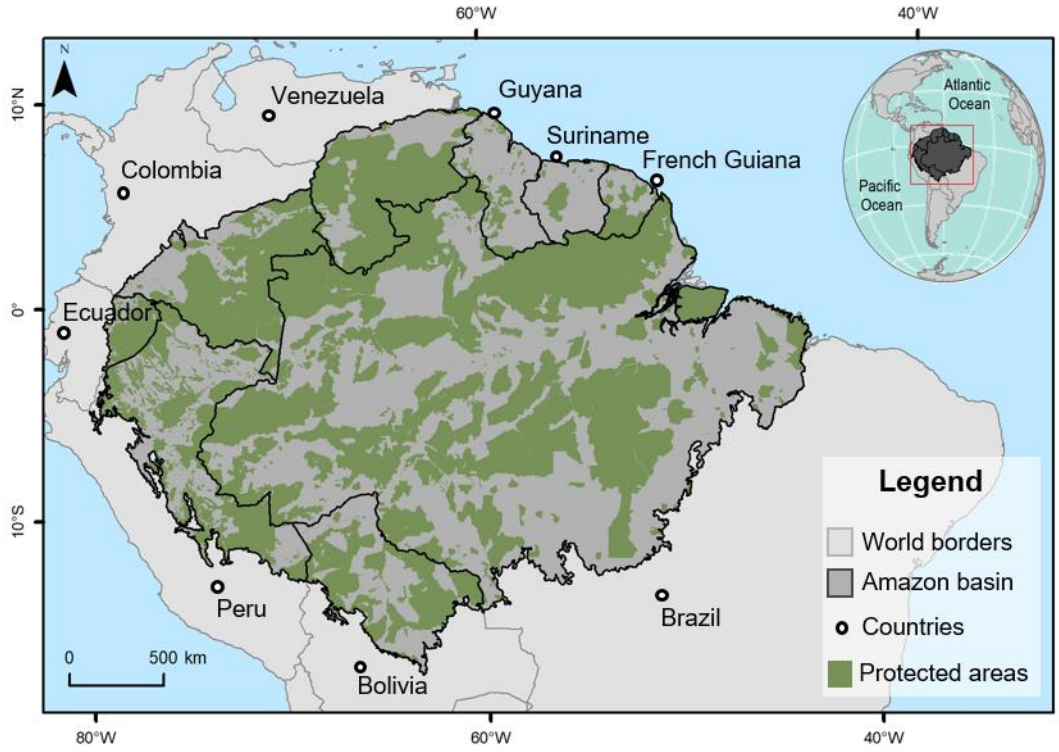

Data from Eva et al. (2005) (Amazon basin limit) and RAISG (protected areas).

Across the study area, it was registered 1,346,923 km² of burned area from 2003 to 2020[16], being the largest area recorded in 2010 (143,217 km²). Normalizing the area outside and inside protected areas to get the burned rate per square kilometre per year, we found that outside protected areas burned almost two-thirds more than inside. When we consider active fires, which is the fire hotspot occurrence[17], outside protected areas registered more than double registries per square kilometre per year (Figure 5.3). In this way, we already know a priori that fire occurrence inside protected areas is lower than outside. However, we do not know whether this difference is due to the presence of land use regulation through protection or other pre-existing factors or circumstances that may have influenced this scenario.

[16] Taking into account only the MCD64A1 burned area product.
[17] For more details, see Section 5.3.3.

Figure 5.3 - Burned area (km²) and active fires (count) rate outside and inside protected areas in the Amazon Basin.

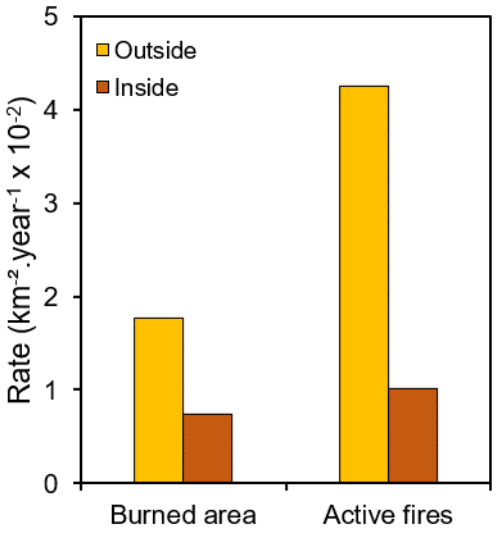

Breaking down the rate of burned area and active fires each year, we can see a similar pattern: the rate of fire occurrence per square kilometer per year is always lower within protected areas (Figure 5.4). However, the difference between inside and outside is not constant over time, which confirms that factors other than protection influence the occurrence of fire both inside and outside. Indeed, climatic variations can influence the occurrence of fire in the region once ignitions occur. It is possible to observe the peaks of fire occurrence in extremely dry years in the Amazon region, mainly in 2005, 2010, and 2015/2016 (ANDERSON et al., 2018; ARAGÃO et al., 2018; SILVA JUNIOR et al., 2019). Nevertheless, we can also observe the constant increase in the occurrence of fires from 2018 to 2020, both outside and inside protected areas, which may reflect political setbacks in the environmental agenda of the Amazonian countries, and, consequently, loss of governance in these areas (DE OLIVEIRA et al., 2020; MATAVELI; DE OLIVEIRA, 2022; SILVA JUNIOR et al., 2021a).

Figure 5.4 - Burned area (a) and active fires (b) rate outside and inside protected areas from 2003 to 2020 in the Amazon Basin. The dependent variable is displayed on the x-axis for visualization purposes.

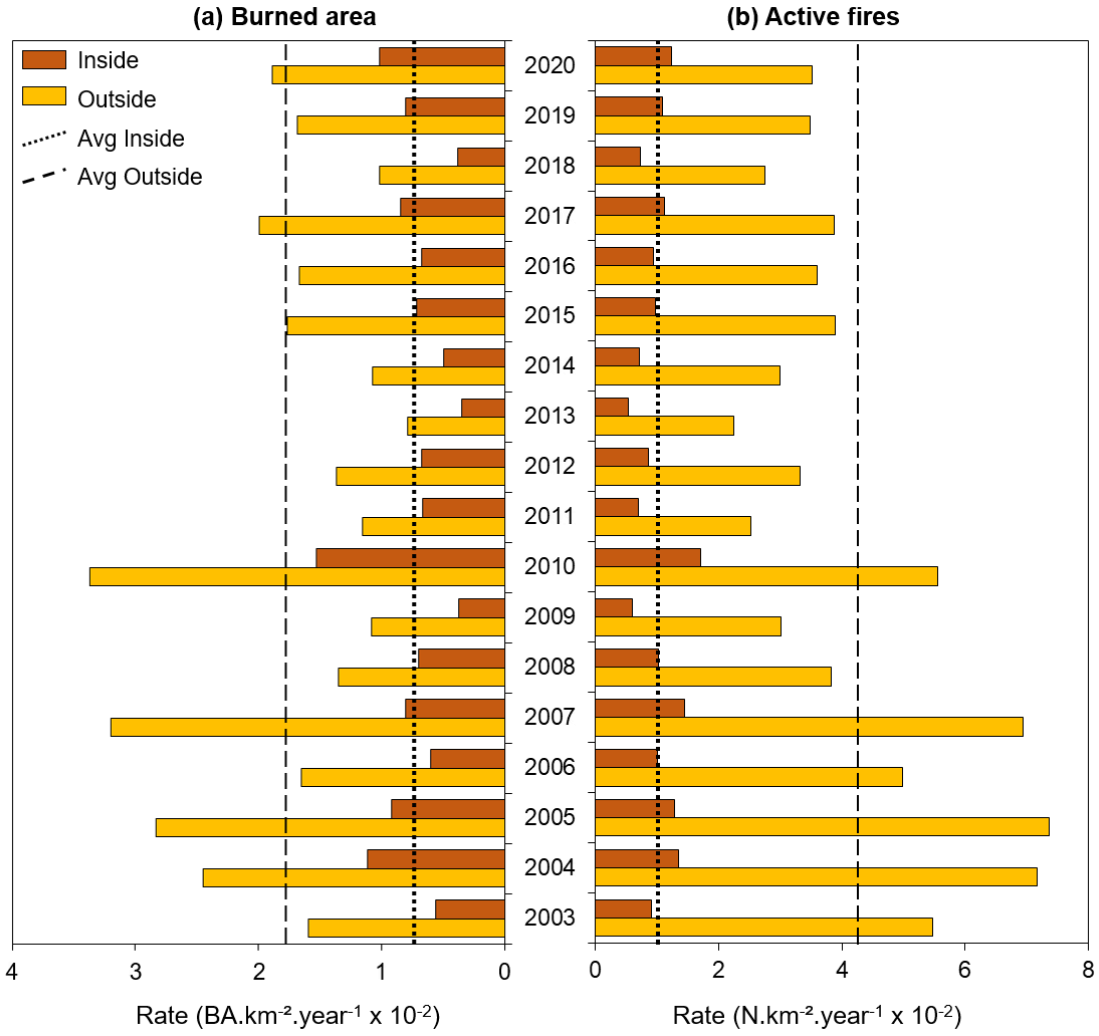

5.3.2 Data analysis

The objective is to estimate the average treatment effect (ATE) of protected areas on fire frequency and extent, that is, how many active fire detections or burned hectares would be avoided was a land pixel protected. To avoid a naïve comparison and isolate the protection effect from the effects caused by other factors that influence fires in the Amazon, we adopted a two-step approach using matching combined with DiD. First, we needed to find a counterfactual group that adequately depicted the non-protection situation. The fire level in the potential state in which the pixel is protected should be subtracted from the state in which the pixel is not protected, i.e., its counterfactual[18].

[18] For more details, see Section 5.2.1.

Nevertheless, in a given time step, only one of these states is factual, that is, observable. There is need thus to estimate the counterfactual fire levels. For this, we used matching on covariates which select the most similar control pixel in all relevant variables driving fire level as the counterfactual for each treated pixel. This step is necessary once it mitigates the fact that pixels are intentionally selected for being protected or not, based on their agricultural profitability, cost of enforcement, and ecological richness, among other factors that are non-observable by the analyst. Besides these drivers being correlated with drivers of fire level. By taking this first step, we are then addressing the selection bias.

However, pairing treated and control pixels to eliminate the bias from the intentional selection of pixels to be protected is a necessary albeit not sufficient condition for accurate estimation of the ATE. A second bias comes from other changes that occur simultaneously with the protection of pixels (e.g., other policies, microclimatic change, etc.), explaining part of fire level variation. Finally, a third bias arises when time-invariant unobserved variables affect fire level. We addressed these two additional biases with the post-matching DiD model combined with a fixed effects estimator. In the next sections, we describe in detail the methods used in our identification strategy.

5.3.2.1 First stage: matching

We used a matching approach to build a control group, given the challenge of selecting pixels outside protected areas that would work as a valid counterfactual to pixels within protected areas. This challenge is better explained in Section 5.2.1. Briefly, a valid control is an outside pixel that, compared to an inside pixel, presents similar values of variables that could influence whether a pixel is protected or not. Then, the most similar outside pixel is selected to match each inside pixel.

A critical assumption in matching approaches is that all significant confounding variables have been included (NELSON; CHOMITZ, 2011), which is impossible to verify directly. Therefore, theoretically, the wider the set of potentially influential variables considered, the lower the bias. In this study, we considered three classes of covariates: weather, land use, and land profitability (Table 5.2). The data specifications and sources are detailed in Section 5.3.3.

We used a one-to-one nearest-neighbor covariate matching with replacement, using a generalized version of the Mahalanobis distance metric (as suggested by ANDAM et al., 2008; ARRIAGADA; ECHEVERRIA; MOYA, 2016; FERRARO; HANAUER, 2014; FERRARO; MIRANDA, 2017; HERRERA; PFAFF; ROBALINO, 2019). The matching algorithm automatically selects comparable controls from the control pool of observations. Considering that we used a matching method with replacement, one control may be paired with the treated observations multiple times.

The dynamic nature of our treatment creates a challenge. Choosing a reference year for matching is not trivial due to the possibility of the comparable subset of untreated observations changing across time. The usual way of applying matching, which *a priori* is a time-static method, is to take the pretreatment period as a reference for the covariates (ARRIAGADA; ECHEVERRIA; MOYA, 2016; HERRERA; PFAFF; ROBALINO, 2019; WENDLAND et al., 2015). However, in the dataset analyzed here, there is no obvious pre-treatment period as protected areas have been gradually created. The solution followed, which was to rely on a single moment of the period of analysis for the sake of matching, was also adopted in previous studies. It assumes that matched control would remain good comparison observations for the treated throughout the analysis period. For this, the covariates matching is based on cannot change considerably across time, at least not enough to alter the set of unprotected comparable pixels. For instance, Herrera et al. (2019) assessed the protected area effect on deforestation in two periods, 2000-2004 and 2004-2008, in the Brazilian Amazon, finding a larger estimated avoided deforestation in the former period, revealing a time-decaying protection effect. In this case, matching was applied based on data from a single period, and the authors did not assess the effect of alternative reference years. This may indicate that relying on a single year for matching does not make much difference to results for the case of Amazon. Another example of static matching for analysis of dynamic protection was applied by Arriagada et al. (2016), who estimated the deforestation impact on Chilean protected areas from 1986 to 2011. As far as the paper is informative, all protected areas created in the analysis period were taken into a unique matching exercise implicitly deemed as satisfactorily stable across the whole period.

Recognizing that there is not a single moment when protected areas come into existence, the challenge of choosing a reference year becomes relevant. Some studies adopt repeated matching for different periods to overcome this issue, giving dynamism to the analysis. One example is Paiva et al. (2015), in which the effects of protected areas on deforestation in the Brazilian mid-western savanna were studied. Four cohorts were considered among the years 1986, 1996, 2002, and 2008 with matching repeated for each. Andam et al. (2008) also suggested a dynamic matching approach to assess the protected area effect on deforestation in Costa Rica. In order to ensure the validity of the set of comparable controls across the whole 1960 to 1997 period, the authors distinguished two cohorts, and matching was applied separately to each. The sources of bias addressed with such a repeated matching approach were the dynamism of protected statuses of plots. These studies showed that the reference year choice could considerably change the comparable control set, an important aspect of the causal effect identification strategy.

Choosing the reference year for applying matching in the case of a time-dynamic treatment is indeed a challenge. However, the literature still does not agree on a single strategy to fully address this issue. The common practice is adopting one strategy followed by robustness tests with other approaches. However, in this chapter, we will not delve into this aspect, adopting a single strategy considering the average year as the reference for matching. Therefore, the Mahalanobis distances were estimated using an average year, defined as the set of averages across time for all considered covariates at the cross-sectional level. Thus, we assume that the average year matched treatment-control observations remain good for all periods (2003-2020). We implemented matching using the "psmatch2" in Stata v16 (developed by users; LEUVEN; SIANESI, 2003).

We tested three matching specifications regarding the constraint on the maximum distance between the treated and the matched untreated. These specifications are three thresholds for the Mahalanobis distance between treated and potentially comparable untreated, namely: no caliper, which means no restrictions, a caliper size of one standard deviation, and a caliper size of half standard deviation (SD). The use of calipers consists of adding an upper bound to the treated vs. untreated differences on covariates, seeking to increase matching quality. The matching performance is directly proportional to how likely the comparable controls are to each treated observation; thus, the upper bound is a

tolerance threshold for the Malahanobis distance above which further deviation is not tolerated. Moreover, as Ferraro and Miranda (2017) clarify, calipers entail a trade-off of increasing matching quality (and, thus, potentially, parallelism) and, simultaneously, reducing generality by reducing the subsample composed of the comparable units, which may also reduce statistical power.

We used Mahalanobis (nearest neighbor) one-to-one (with replacement) matching, following the approach used in several studies (e.g., ARRIAGADA; ECHEVERRIA; MOYA, 2016; HERRERA; PFAFF; ROBALINO, 2019; NOLTE; AGRAWAL, 2013). All three studies used a caliper based on the SD of the covariates. First, one unit of standard deviation was used as the upper bound, that is, in the case that, for a pair of treated and untreated observations, if at least one of the covariates presented a difference between treated and untreated above one standard deviation of the covariate, the treated observation was ignored. The caliper with half standard deviation upper bound was also tested. The caliper approach is a refinement of no caliper matching, in which treated observations may also not be used whether they are not comparable to any control.

In detail, we evaluated the matching performance considering the trade-off between the cost and benefits of each specification. The cost was measured by the number of observations excluded in each specification, which consequently would impact the generality, that is, the scope of validity within the Amazon basin. The benefits are measured by improving covariate balance and common support, two aspects related to the matching quality. Imbens (2015) suggested that the balance was assessed based on Rubin's table (RUBIN, 2001), comparing the level before and after matching. Following Rosenbaum and Rubin (1985) and Rubin (2001), the variance ratio was used to measure homogeneity. It weights the coefficient vector by the variance-covariance matrix of the estimators. A variance ratio belonging to the intervals [0.5, 0.8) or (1.25, 2] is "of concern," according to Rubin (2001). Balance is "bad," i.e., there is no homogeneity if the variance ratio is below 0.5 or above 2.

Additionally, visual representations of matching quality were evaluated based on "balance" and "common support" graphs. The first compares the empirical distribution of treatment probabilities for the sample as a whole (situation "before matching") with that of the subsample containing treated (observations inside protected areas) and only

untreated-comparable observations ("after matching"). In the second situation, it is expected to have full or at least considerably greater homogeneity between curves. The common support graph, in its turn, allows checking if there is, for both groups separately, a non-zero frequency of observations in all sub-intervals of the treatment probability range. We expected that, after matching, the common support graph presents near-zero relative frequency at levels 0 and 100% treatment probability[19]. Also, frequencies for each range of treatment probability must be equal or as close as possible, configuring a (horizontally) "mirrored" image between treated and untreated frequencies.

5.3.2.2 Second stage: Differences-in-Differences model

In the second stage of the empirical strategy, the post-matching approach, we used a differences-in-differences (DiD) model to measure the average treatment effect (ATE) of protection on fire. We make the second stage more far-fetched by including DiD instead of simple regression. We consider that there could be concurrent changes (socioeconomic and institutional) in the context of fire occurrence in protected areas. The general model equation, adapted from Equation 5.4, is described below (Equation 5.5):

$$\boldsymbol{Fire_{it} = \beta_0 + \beta_1 D\_PA_{it} + X'_{it} + \mu_i + u_{it}} \quad (5.5)$$

Where *i* indicates the pixel and *t* year, i.e., pixels observed annually are our units of observation, and we know whether they are located in an active protected area or not. *Fire* measures burned area in a fraction of the area of the pixel, or active fire count per pixel for robustness tests. *D_PA* is a dummy that takes one if the pixel falls within an active protected area. With "active" meaning already created protected areas in the current year. β_1 is the difference-in-difference estimate for the average treatment effect (ATE). The vector *X'* contains the time-varying observable covariates, which are considered to attenuate estimation bias. μ_i is the individual fixed effects term. When we consider the

[19] The common support assumption behind matching requires that all treated observations have a comparable control unit. If the probability of a pixel being treated, that is, being within a protected area, is 100%, it will not have a comparable pair in the control group, since the probability of finding a treated pixel with zero probability of treatment is null. The opposite is also true, if the probability of a pixel being within a protected area is 0%, then this control unit will not have a comparable in the treatment group. This condition includes observational units outside the common support. So, the common support graph before matching is expected to have a higher frequency of 0% treatment probability in the untreated group and 100% in the treated group. After matching, the fraction of the covariates domain with common support is expected to increase, reflecting in a higher median frequencies of treatment probability conditioned on the vector of covariates *X* ($0 < P(Dp=1|X) < 1$) (PEIXOTO et al., 2017).

fixed effects estimator, all time-fixed variables are eliminated, including μ_i, while all parameters on time-varying variables are preserved. In this case, only parameters on time-varying independent variables can be estimated. Finally, ε_{it} represents the model error.

In vector *X*, we considered covariates that potentially impact burned area estimation, our dependent variable, and protected area placement, aiming to capture the variability that was not measured by matching. Thus, the covariate vector includes variables on the proportion of deforestation of primary and secondary forests, forests, farming, non-forest natural formations, non-vegetated area, flooded forests, mangroves, and savanna. Besides that, it also included total precipitation, mean temperature, maximum cumulative water deficit (MCWD), mean precipitation and temperature during the dry season, population, and forest edge length. All variables and their respective specifications are described in detail in Section 5.3.3.

With Amazonian protected areas created gradually and not all at once, the treatment started at different years across different pixels. This is addressed, following the common convention in DiD research (BONILLA-MEJÍA; HIGUERA-MENDIETA, 2019; CHAGAS; AZZONI; ALMEIDA, 2016; GALIANI; GERTLER; SCHARGRODSKY, 2005), with a treatment dummy taking value one if the pixel is treated in the current year, zero otherwise (*D_PA*). The coefficient of such variable, β_1 in Equation 5.5, is identified to the extent the error term is uncorrelated with the variable D_PA_{it}. We control for observables as explained above, whereas unobservables are controlled for by the prior matching approach and, additionally, by including fixed effects in this post-matching stage. By bringing in the timing dimension with DiD, we can control for year-fixed effects that pick up anything that affects the average level of fire in a given year, i.e., we identify β_1 from within year variation.

As Arriagada et al. (2016) make clear, the identification assumption underlying the DiD estimator is that the counterfactual expected fire trend of treated units in the untreated state is the same as the factual expected trend of control pixels. As the authors argue, this assumption can be made "more plausible" by adopting a pre-matching stage. However, such a procedure is the option for a different identification assumption, which is that the trend of comparable untreated pixels could be taken as the counterfactual for the untreated state trend of treated pixels, with "comparable" meaning a high likelihood of being

treated. The validity of this assumption is attested graphically by the treated and control time trends being approximately parallel in the matched sample (as judged by the synchronicity of peaks and valleys) and more parallel than in the full sample (see Figure 5.11).

We estimated the protection effect on fire with three different estimators to test for results' robustness and, consequently, sources of estimation bias. Reminding the two sources of bias (threats to identification) should be addressed to describe the estimators is useful. First, unobserved heterogeneity bias, whose source is the panel structure of the data, and the second, concurrent changes bias, due to the influence of changes on the dependent variable that are concurrent with the change whose causal effect is measured. The three adopted estimators were: the fixed-effects (FE) estimator for panel data, the differences-in-differences (DiD) estimator for panel data pooled under the assumption of zero correlation between the covariates and the unobserved heterogeneity term, and a complete DiD-FE estimator, which addressed both unobserved heterogeneity bias, also assuming that the trends were parallel in the untreated state for treated and untreated.

All the estimators were based on clustered standard errors to account for correlation between disturbance terms belonging to the same cross-sectional unit. Additionality to clustering the standard errors on the pixel level, we also clustered at the department level to account for potential correlation among pixels from the same department. At the department level, important fire management decisions are made, and provides a reasonable spatial distance from that correlation across units could happen (WENDLAND et al., 2015). We also repeated all estimations with the bootstrapping of standard errors using 200 replications. The bootstrapping is a non-parametric way to address potential serial correlation and heteroskedasticity (BERTRAND; DUFLO; MULLAINATHAN, 2004; GALIANI; GERTLER; SCHARGRODSKY, 2005).

We also visually evaluated the parallelism of trends of treated and control groups. One key characteristic of the intervention under study is the geographically variable timing of its introduction. That is, different pixels started being treated at different years. This makes it impossible to draw a classical DiD plot with lines for treated and untreated and a single divide for before and after treatment. Two types of plots were formulated to circumvent that. The first is a parallel trend graph along all years of the analysis period

(as in WENDLAND et al., 2015). This graph attempts to reveal whether: (i) the trends are indeed parallel, comparing pixels that are currently treated and that were never treated, (ii) matching improved parallelism along the whole period, and (iii) controls are systematically above treated in terms of burned area (or active fires). The plot included three lines, controls, currently treated, that is, the pixels that are treated in the current year, and not currently treated, that is, the pixels that are not treated in the current year but will eventually be. By looking at three time series, the temporal aspect was included in the analysis of parallelism, comparing the burned area incident in those protected areas that have not yet been implemented, both with the unprotected group and with the protected areas already in place. The second plot classifies pixel-year observations regarding the time since treatment, showing the average burned area (or active fires) for each value of such variable. With this, a break in the trend of the average burned area before and after treatment should become apparent (with a lower trend being expected after treatment). This plot, which contains the dynamical treatment visualization, is thus, a visual assessment of the significance of ATE.

Finally, we applied a sensitivity test (ROSENBAUM, 2002) to the influence of unobservables on the estimated effect of protected areas on fire detections (as in ARRIAGADA; ECHEVERRIA; MOYA, 2016; PAIVA; BRITES; MACHADO, 2015). The test's main assumption is that unobservable factors could drive the selection of pixels to belong or not to protected areas and influence their effect. In this case, a potentially estimated lower fire level within protected areas is, in fact, due to unobservables. This way, the test aims to answer how likely it is to have an unobservable strong enough to make the results unreliable as a measure of the protected area effect. To verify if this is the case, the test considers multiple degrees of the influence of unobservables (Γ). It computes, for each, upper (p^+) and lower (p^-) bounds for the (type-I error) probability of rejecting the hypothesis of a null effect of protected areas on fires when the hypothesis is true. The analyst should thus understand the maximum degree for which the probability is still not larger than 5% as the maximum degree of influence of unobservables for which results remain reliable (i.e., the maximum degree of unobservables' influence that results can resist; PAIVA; BRITES; MACHADO, 2015). If such a degree is referred to as the "degree of reference," an alternative explanation of the test's result would be as follows. If there is reason to believe that there are unobservables that could increase the likelihood

of not having fire inside a protected area in a magnitude at least equal to the degree of reference, then results are not reliable.

Nevertheless, Rosenbaum's test was reported by previous studies as an excessively severe judgment of the quality of a causal effect estimate (ARRIAGADA; ECHEVERRIA; MOYA, 2016; DIPRETE; GANGL, 2004). It is thus reasonable to understand the test's result mainly as an indication that unobservables, if the degree of reference is not seen as large, exert a non-negligible influence on results. We converted the two fire-dependent variables (burned area and active fires) to binary variables to apply the test. These variables took value one in the case the original variable was positive, given the share of pixels in which fire was detected in none of the years was 67% or 76%, respectively, for the point and areal fire measures. Thus, we considered the Mcnemar version of Rosenbaum's test with simplified binomial distribution formulas (ROSENBAUM, 2002).

5.3.3 Data

All data were pre-processed, clipped to the study area boundary, and incorporated into a regular grid with an approximately 5 by 5 km spatial resolution. The method of resampling each data is further explained in the following section. The econometric approaches were then applied using the regular grid pixel as the observational unit. In detail, the universe for statistical analysis comprises 87,728 pixels after matching (see Section 5.4.2), of which 72,288 are within protected areas. The time dimension is from 2003 to 2020, and the panel was strongly balanced, i.e., no missing values across pixels or time.

Protected areas data was obtained from the Amazon Network of Georeferenced Socio-Environmental Information (RAISG, from the Portuguese acronym, Table 5.2). It was downloaded in July 2021, including the updates till 2020[20]. It used data from National and Departmental Natural Protected Areas and Indigenous Territories, jointly called protected areas. Protected areas without a creation date were excluded from the dataset after consulting local experts with knowledge of the current situation, which confirmed the impossibility of specifying an exact date. This represented 12% of our PA dataset. Also, these cases were spatially concentrated, mainly belonging to Ecuador (137),

[20] Downloaded from https://www.amazoniasocioambiental.org/pt-br/mapas in November 2020.

Guyana (108), and Peru (108). Pixels that overlap between PA categories were also excluded, representing 4% of the total pixels.

The protected area information was incorporated into the regular 5 km grid, considering the centroid of each pixel. A binary variable was created to receive one of the pixel centroid falls within a protected area, which we call ever treated, and 0 otherwise. All information regarding the respective protected area, such as creation year, size, and category, was then incorporated into that specific pixel. Another binary variable was created to designate whether the pixel is within an active protected area in the current year or not. If the creation date is before the current year, this binary variable receives 1, and 0 otherwise. The same reasoning was used to classify all grid pixels in each country, department, and municipality in the Amazon basin. Administrative[21] limits at all levels were homogenized between countries to represent the same management sphere. Table D.1 provides the data source and level adopted by each country to represent the country, department, and municipality.

[21] Downloaded from https://data.humdata.org/ in December 2020.

Table 5.2 - Dataset description and specifications.

	Definition	Source	Original resolution	Measurement unit	Time span
		Dependent variables			
BA	Annual burned area proportion within the pixel.	MCD64A1	500m	% pixel	2003-2020
AF	Annual active fire count within the pixel.	MCD14ML - Aqua	Vectorial data	Count	2003-2020
		Weather factors			
precMean; precTotal; precDry	Average annual precipitation, total annual precipitation, and average annual precipitation during the dry season, respectively.	CHIRPS	0.05° (~ 5 km)	mm	2003-2020
MCWD	Average annual maximum cumulative water deficit	Silva Junior et al. (2021)	0.05° (~ 5 km)	mm	2003-2020
tempMean; tempDry	Average annual temperature and average annual temperature during the dry season, respectively.	MOD11A2	1km	°C	2003-2020
		Land use and land cover factors			
DFpri	Annual primary forest deforestation proportion within the pixel.	Silva-Junior et al. (2021)	30m	% pixel	2003-2020
DFsec	Annual secondary forest deforestation proportion within the pixel.	Silva-Junior et al. (2021)	30m	% pixel	2003-2020
secForest	Annual secondary forest proportion within the pixel.	Silva-Junior et al. (2021)	30m	% pixel	2003-2020
frag	Annual non-natural forest edge length.	Silva-Junior et al. (2021)	30m	km	2003-2020
forest	Annual forest proportion within the pixel.	MapBiomas PanAmazonia c3	30m	% pixel	2003-2020
farming	Annual farming proportion within the pixel.	MapBiomas PanAmazonia c3	30m	% pixel	2003-2020
nonForestNatural	Annual non-forest natural formations proportion within the pixel.	MapBiomas PanAmazonia c3	30m	% pixel	2003-2020
savanna	Annual savanna proportion within the pixel.	MapBiomas PanAmazonia c3	30m	% pixel	2003-2020
nonVegetated	Annual non-vegetated area proportion within the pixel.	MapBiomas PanAmazonia c3	30m	% pixel	2003-2020
mangrove	Annual mangrove proportion within the pixel.	MapBiomas PanAmazonia c3	30m	% pixel	2003-2020
floodedForest	Annual flooded forests proportion within the pixel.	MapBiomas PanAmazonia c3	30m	% pixel	2003-2020
		Land profitability factors			
distRoad; distPavRoad	Distance to the nearest road and paved road, respectively.	RAISG	Vectorial data	km	Time invariant
distRiver	Distance to the nearest navigable river.	HydroSheds	Vectorial data	km	Time invariant
pop	Annual population count.	WorldPop	1km	Count	2003-2020
distUrban	Distance to the nearest urban center.	University of Columbia - Urban Extents Grid v1	Vectorial data	km	Time invariant
distPopulated	Distance to the nearest most populated pixel within each municipality.	WorldPop	Vectorial data	km	Time invariant
slope	Mean slope within the pixel.	SRTM	90m	%	Time invariant
elevation	Mean elevation within the pixel.	SRTM	90m	km	Time invariant
soil	Binary variables indicating pixels with no or slight limitation to plant growth regarding toxicity, rooting conditions, oxygen availability to roots, nutrient retention capacity, nutrient availability, and workability.	HWSD v1.2	10km	Binary variables	Time invariant

We used two sources of fire data for our dependent variables; the Moderate Resolution Imaging Spectroradiometer (MODIS) burned area product MCD64A1 version 6 (GIGLIO, LOUIS et al., 2015) and the MODIS active fire product MCD14ML version 6 (GIGLIO, LOUIS, 2000), filtered for data acquired from Aqua platform with a level of confidence higher than 30. The burned area data were incorporated into the regular 5 km grid considering the proportion of the annual burned area within the largest pixel. The active fires were also grouped annually and incorporated into the grid, considering the count in each pixel (Figure D.1). After incorporating the first fire metric into the grid, we found that the percentage of pixels without fire at any period was large (Table 5.3). This fact can weaken the results of causal estimates, and due to this, a second fire metric was adopted to test the robustness of our estimates. Table 5.3 shows that non-zero pixels rate, i.e., pixels that recorded fire in at least one year, at pixel level are relatively high, which means that the occurrence of fire is a phenomenon with considerable recurrence in the study region.

Table 5.3 - Proportion of pixels with zero or non-zero detection of fire.

Fire measure/statistic	Zero pixel-years	Non-zero pixel-years	Non-zero rate at pixel-year level*	Pixels with zero in all years*	Pixels without zero in at least one year	Non-zero rate at pixel level
Burned area	2,982,765	340,359	10%	121,415	63,203	34%
Active fires	2,670,493	652,631	20%	105,290	79,328	43%

Note: * Zero pixel-years/total (Nxt)

We also used a set of covariates to control for observables cofounders of protected areas placement and fire occurrence. Finally, considering our temporal and spatial scale, we considered the largest number of variables that could potentially cause selection bias and would be feasible to measure. This includes three classes of variables; (1) Weather factors, (2) Land use and land cover (LULC) factors, and (3) Land profitability factors. Table 5.2 details the definition and specification of each dataset considered. Table D.2 presents the context of the choice of each variable included and literature references that use such variables in similar approaches.

The weather factors are expected to influence the environment's susceptibility to fire, and they include three variables. The first consists of precipitation measures obtained from Rainfall Estimates from Rain Gauge and Satellite Observations (CHIRPS; FUNK et al.,

2015). The second one includes the maximum cumulative water deficit (MCWD), which was calculated globally by Silva Junior et al. (2021b), using the methodology presented in Aragão et al. (2007). The MCWD is a measure of drought severity, corresponding to the maximum value of the monthly accumulated water deficit reached for each pixel within the year. In addition, the MCWD is a useful indicator of meteorologically induced water stress without considering local soil conditions and plant adaptations, which are poorly understood in Amazonia (ARAGÃO et al., 2007). And finally, temperature measures were obtained from the Land Surface Temperature and Emissivity (LST&E) product MOD11A2 version 6 (WAN, ZHENGMING; HOOK, SIMON; HULLEY, GLYNN, 2015b).

The average precipitation and temperature during the dry season are the onset and duration of spatially explicit dry season periods defined by Carvalho et al. (2021). The authors defined dry season length as the number of consecutive months with rainfall lower than 100 mm (average from 1981 to 2019). This threshold is used because of tropical forests' mean monthly evapotranspiration value (VON RANDOW et al., 2004). With the persistence of rainfall below it, evapotranspiration exceeds rainfall, which can be used as an indicator of water deficit in these ecosystems (ARAGÃO et al., 2007; MALHI et al., 2002). This way, dry season timing is delimited by grouping pixels that share the same month for the onset and end of the dry season, resulting in 74 homogeneous regions across the Amazon basin. The average of the variables was calculated differently considering the specific dry season timing in each of these regions.

The weather factors were annually grouped from 2003 to 2020 and incorporated into the regular grid using different metrics, as detailed in Table 5.2. The spatial distribution is illustrated in Figure D.2.

The LULC factors are expected to influence the occurrence of fire and protected area placement. Although not a rule, the creation of protected areas is more likely to happen in regions with more forest, and fire does not occur if there is no combustible material for such. These factors include information obtained from the Annual Land-Use and Land-Cover Mapping Project (MapBiomas PanAmazonia collection 3) or secondary data developed by Silva Junior et al. (2020b). MapBiomas classified 36 years of images from the Landsat satellite series (30-m spatial resolution) using a theoretical algorithm

implemented in the Google Earth Engine platform (GORELICK et al., 2017). Details about the processing of the dataset and class definition, can be found in MapBiomas (2021). This dataset provides annual information on forest extension, farming, non-forest natural formations, non-vegetated area, savanna, mangrove, and flooded forest. In addition to these classes, it was also considered secondary forest and deforestation of primary and secondary forest obtained from Silva Junior et al. (2020b).

From the forest formation class map from 1985 (the first year classified by MapBiomas), every pixel that transforms into any non-natural class in the following year is then classified as primary forest deforestation. Deforestation of primary forests only happens once, and it is impossible to return the pixel to a primary forest in any time. This pixel that is no longer a primary forest can become several classes, and if at some point it reverts to a forest, it is classified as a secondary forest. Secondary forests' deforestation occurs when secondary forests are converted to any non-natural class in the following year. This type of deforestation can happen several times since secondary forests are reversible. Lastly, we calculated a forest fragmentation measurement using forest edges length as a proxy. From binary annual forest and non-forest maps, we calculated the Euclidean distance from each forest pixel to the nearest non-non-forest pixel. Considering that the spatial data resolution is 30 m, the forest edge is composed of forest pixels that have a distance of 30 m to the non-forest class. The edge length is then the sum of the edge pixels multiplied by 30 for each larger pixel of the regular 5 km grid. As we are interested in non-natural forest edges, the non-forest class excluded natural non-forest classes such as water and savanna.

All LULC classes from 2003 to 2020 were incorporated into the regular 5 km grid, considering the annual proportion of each class within the largest pixel (Figure D.3). The forest edge length data was incorporated into the regular grid by the annual sum within each pixel. MapBiomas and its secondary data were processed entirely in Google Earth Engine (GEE).

Land profitability factors are also associated with both likelihoods of fire occurrence and protected area placement. Protected areas are commonly created on marginal lands where productive activity would not be advantageous (NEPSTAD et al., 2006). On the other hand, productivity and accessibility indicators increase the possibility of fire ignition

sources, which in the case of Amazonia is mostly anthropic. These factors include distances to roads, paved roads, rivers, urban centers, populated areas, population count, slope, elevation, and soil limitation to plant growth. We used road data downloaded from RAISG and calculated the euclidean distance from each pixel centroid of our regular 5 km grid to the nearest road and separately to the nearest paved road. River data was obtained from the HydroSHEDS v1 (LEHNER; VERDIN; JARVIS, 2008; LINKE et al., 2019) project website[22] and consisted of the river network across the Amazon basin.

As we are interested in using distance to rivers as a proxy for accessing consumer markets or product flow, we had to filter the overly detailed original data to get only the main waterways. To support our filter choice, we considered, for the Brazilian territory, the intersection of the hydrographic network of HydroSHEDS with a map of navigable rivers. In detail, we got the names of the navigable rivers from the Brazilian Waterway Network, downloaded from the Brazilian Open Data Portal[23]. The names were used to select the navigable rivers of the Brazilian hydrographic network[24]. Next, we considered filters using the mean and the 95% to 99% percentiles of the maximum flow accumulation of stream in the original data, and we calculated the intersection in each case with the navigable river network we created (Figure 5.5). The 98% percentile (397,146 cells) had a higher proportion of intersection (40%), with a smaller mapped length difference than navigable rivers. We, therefore, filtered for rivers with a maximum flow accumulation (number of cells) of streams higher than 397,147, considering that filtering the HydroSHEDS data with this threshold would be the closest we could get to a mapping of navigable rivers. After the filtering, we calculated the Euclidean distance from each pixel centroid of our regular 5 km grid to the nearest river.

[22] https://www.hydrosheds.org/
[23]https://dados.gov.br/dataset/malha-hidroviaria/
[24]Obtained from the National Spatial Data Infrastructure Portal (INDE) https://metadados.inde.gov.br/geonetwork/

Figure 5.5 - Mean and 95% to 99% percentiles of the maximum flow accumulation of stream (number of cells) from the HydroSHEDS hydrographic network data. The total mapped area of rivers in each case is compared with the area of Brazilian navigable rivers.

	Max flow accumulation of stream cut (N cells)	Total (km)	Total length of navigable rivers (km)	Difference (total - total navigable) (km)	Intersection with navigable rivers (km)	% Intersection
Mean	60,233	78,992	31,304	47,688	15,859	20%
95%	86,011	65,405	31,304	34,101	15,075	23%
96%	125,359	52,791	31,304	21,487	14,204	27%
97%	200,500	40,192	31,304	8,888	13,074	33%
98%	397,147	26,779	31,304	-4,525	10,684	40%
99%	1,176,884	13,066	31,304	-18,238	4,419	34%

The population count was obtained from the WorldPop data. The WorldPop project combines a range of geospatial datasets into a flexible regression tree framework to reallocate contemporary aggregated spatial population count data (LLOYD et al., 2019). The original resolution of the data is 1 km, so summing was used as an aggregation method to incorporate it annually into the regular 5 km grid.

We use two distance metrics for urban centers. The first considered the urban extents data developed by the Global Rural-Urban Mapping Project version 1, hosted by the University of Columbia (CENTER FOR INTERNATIONAL EARTH SCIENCE INFORMATION NETWORK (CIESIN) et al., 2011). Urban extents illustrate the shape and area of urbanized places, with 5,000 or more inhabitants and stableboy delineated by night-time lights. First, we calculated the Euclidean distance from each pixel centroid of our regular 5 km grid to the nearest urban area. The second metric considered the 5 km pixel of our grid with the highest population number in each municipality. This was done by averaging the 2003 to 2020 population count per pixel. With this average, each municipality's pixel with the highest population count was identified. Subsequently, we calculated the Euclidean distance from each pixel centroid of our regular 5 km grid to the nearest most populated pixel.

Elevations were obtained from the Shuttle Radar Topography Mission (SRTM) data. In the GEE platform, we used the SRTM Digital Elevation Data Version 4 provided by NASA/CGIAR. This SRTM digital elevation data version has been processed to fill data voids (JARVIS et al., 2008). We calculated the slope from the digital elevation data using

GEE's “terrain” tool. The spatial distribution of the land profitability variables is illustrated in Figure D.4.

Protected areas' establishment is likely to be influenced by soil characteristics, as they can demonstrate how favorable the soil is for cultivation. We used data from the Harmonized World Soil Database (HWSD) v1.2 (FISCHER et al., 2008) on the soil qualities for crop production. The data provides us with seven soil quality indicators for crop cultivation (nutrient availability, nutrient retention capacity, rooting conditions, oxygen availability to roots, excess salts, toxicities, and workability), which are classified according to the degree of limitation to plant growth[25]. For our work, we created 14 binary variables, indicating for each pixel of our regular 5 km grid if:

- the pixel is classified as soil or not for each soil quality indicator provided; and
- the pixel has no or slight limitation for each soil quality indicator provided.

Since some of these dummy variables are highly correlated (Figure 5.6), which can generate collinearity error, we used them to perform a Principal Component Analysis (PCA), and we used only the first component as a soil variable. To validate the use of the PCA index as a soil quality variable, the eigenvectors of the first component must have coefficients with the same sign for all variables considered (Table D.3). This criterion is necessary to ensure that the PCA index is interpreted as having an increasing value with the degree of suitability of the soil for plant growth (and this is because all the component variables assume a higher value, in this case, value 1, when there is greater suitability for this). We would not have a coherent soil suitability indicator if there were any negative signs, as some suitability measures would be negatively correlated with the index. Indeed, the correlation matrix presents all positive and significant (p-value < 0.05) correlation coefficients in relation to the PCA index (Figure 5.6). Therefore, the PCA index can be used in place of the soil variables.

[25] Details of estimation procedures for the individual soil qualities from soil characteristics in HWSD can be found at http://webarchive.iiasa.ac.at.

Figure 5.6 - Correlation matrix between soil dummy variables. All correlation coefficients were statistically significant, with a confidence level of 95%. The highest the correlation coefficient, the redish the colour.

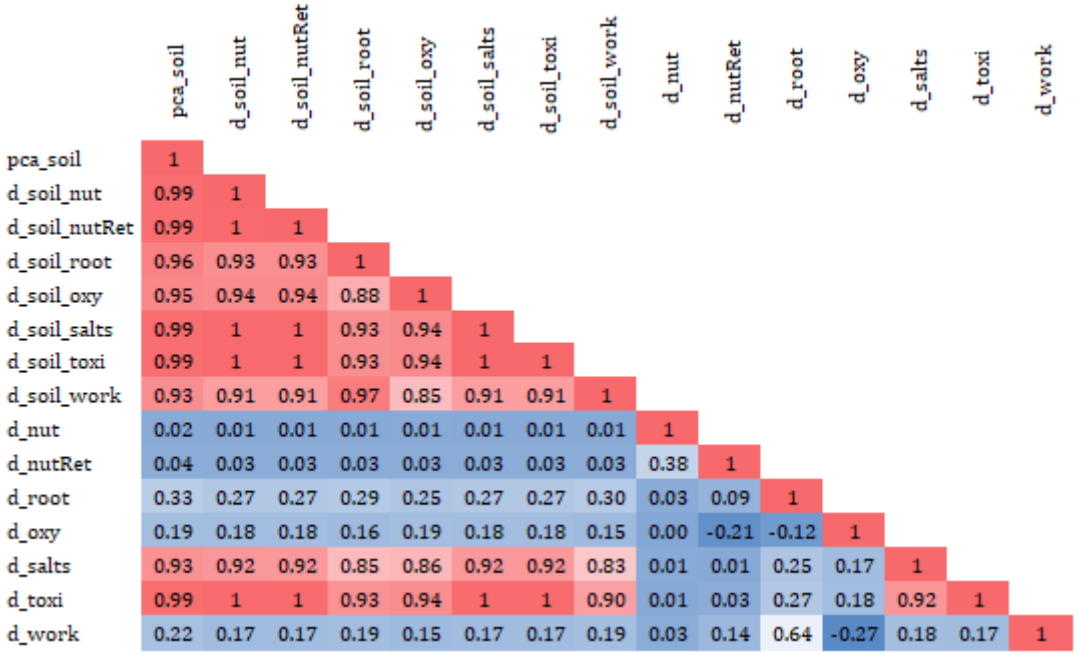

	pca_soil	d_soil_nut	d_soil_nutRet	d_soil_root	d_soil_oxy	d_soil_salts	d_soil_toxi	d_soil_work	d_nut	d_nutRet	d_root	d_oxy	d_salts	d_toxi	d_work
pca_soil	1														
d_soil_nut	0.99	1													
d_soil_nutRet	0.99	1	1												
d_soil_root	0.96	0.93	0.93	1											
d_soil_oxy	0.95	0.94	0.94	0.88	1										
d_soil_salts	0.99	1	1	0.93	0.94	1									
d_soil_toxi	0.99	1	1	0.93	0.94	1	1								
d_soil_work	0.93	0.91	0.91	0.97	0.85	0.91	0.91	1							
d_nut	0.02	0.01	0.01	0.01	0.01	0.01	0.01	0.01	1						
d_nutRet	0.04	0.03	0.03	0.03	0.03	0.03	0.03	0.03	0.38	1					
d_root	0.33	0.27	0.27	0.29	0.25	0.27	0.27	0.30	0.03	0.09	1				
d_oxy	0.19	0.18	0.18	0.16	0.19	0.18	0.18	0.15	0.00	-0.21	-0.12	1			
d_salts	0.93	0.92	0.92	0.85	0.86	0.92	0.92	0.83	0.01	0.01	0.25	0.17	1		
d_toxi	0.99	1	1	0.93	0.94	1	1	0.90	0.01	0.03	0.27	0.18	0.92	1	
d_work	0.22	0.17	0.17	0.19	0.15	0.17	0.17	0.19	0.03	0.14	0.64	-0.27	0.18	0.17	1

Note: pca_soil = first component resulted from the PCA; d_soil_i = dummy variable indicating if the pixel is classified as soil or, being i any of the soil quality indicators; d_i = dummy variable indicating if the pixel has no or slight limitation for I, being i any of the soil quality indicators. Soil quality indicators are nutrient availability, nutrient retention capacity, rooting conditions, oxygen availability to roots, excess salts, toxicities, and workability.

5.4 Results

5.4.1 Descriptive analysis

The statistical summary of variables for the average year before matching is found in Table 5.4. Treated and control pixels differed in the outcome variables, i.e., pixels within protected areas presented a 60% lower burned area proportion and a 78% lower count of active fires.

Treated pixels are generally farther away from urban centers, populated areas, and roads when we analyze the average year statistics (Figure 5.7). They are located in steeper and higher terrains, presenting a share of forest coverage on average 39% larger than control pixels. Control pixels, in turn, generally present 1.143% more farming area, 254% more secondary forest area, and 102% more forest edge length characterizing a less forested environment and with greater forest fragmentation. Except for the dry season period, treated pixels presented, on average, higher average annual and total annual precipitation, with a higher MCWD, showing that protected areas are less exposed to water stress than

areas outside. In addition, the average temperature inside protected areas was lower than outside. Although the average rainfall during the dry season inside these areas was less than outside, the average temperature was 16% lower. This general analysis is evidence that, even though protected areas are under increasing threat, they still hold most of the forests and play a role in curbing deforestation and forest degradation. Besides, they are buffers against the effects of climate change, holding essential climatic conditions to the survival of the ecosystems.

Table 5.4 - Summary statistics of variables (average year dataset before matching).

Variable		Obs.	Mean	Std. Dev.	Min.	Max.	CV (%)
Treatment dummy		**184,618**	**0.50**	**0.50**	**0**	**1**	**100%**
	Treated	92,638	1	0	1	1	0%
	Controls	91,980	0	0	0	0	0%
BA (%)*		**184,618**	**1.31%**	**4.24%**	**0%**	**71.26%**	**324%**
	Treated	92,638	0.75%	3.67%	0%	68.73%	486%
	Controls	91,980	1.87%	4.68%	0%	71.26%	251%
AF (N)		**184,618**	**0.88**	**2.92**	**0**	**209**	**333%**
	Treated	92,638	0.32	1.67	0	83	520%
	Controls	91,980	1.43	3.69	0	209	258%
distUrban (km)		**184,618**	**206.98**	**180.61**	**0.00**	**961.34**	**87%**
	Treated	92,638	228.75	172.47	0.00	948.43	75%
	Controls	91,980	185.05	185.89	0.00	961.34	100%
distPopulated (km)		**184,618**	**68.26**	**47.02**	**0.00**	**295.51**	**69%**
	Treated	92,638	84.85	49.95	0.00	295.51	59%
	Controls	91,980	51.54	36.99	0.00	211.25	72%
distRiver (km)		**184,618**	**127.06**	**116.02**	**0.03**	**671.95**	**91%**
	Treated	92,638	131.15	109.22	0.03	658.85	83%
	Controls	91,980	122.94	122.35	0.03	671.95	100%
distRoad (km)		**184,618**	**74.74**	**74.81**	**0.00**	**417.84**	**100%**
	Treated	92,638	88.01	68.29	0.00	414.89	78%
	Controls	91,980	61.37	78.61	0.00	417.84	128%
distPavRoad (km)		**184,618**	**111.47**	**91.02**	**0.00**	**428.18**	**82%**
	Treated	92,638	133.64	85.20	0.00	428.18	64%
	Controls	91,980	89.14	91.24	0.00	427.74	102%
elevation (m)		**184,618**	**188.93**	**133.66**	**0.00**	**2,202.47**	**71%**
	Treated	92,638	200.10	138.97	1.16	2,202.47	69%
	Controls	91,980	177.68	127.10	0.00	2,050.53	72%
slope (%)		**184,618**	**3.14**	**2.58**	**0.00**	**30.36**	**82%**
	Treated	92,638	3.43	2.81	0.00	30.36	82%
	Controls	91,980	2.85	2.29	0.00	29.42	80%
pca_soil		**184,618**	**-1.58E-08**	**2.94**	**-25.38**	**0.60**	**-1.8E+10%**
	Treated	92,638	0.12	2.26	-25.38	0.60	1811%
	Controls	91,980	-0.13	3.49	-25.38	0.60	-2784%
DFpri (%)*		**184,618**	**0.27%**	**0.62%**	**0%**	**5.41%**	**231%**
	Treated	92,638	0.09%	0.33%	0%	5.08%	383%
	Controls	91,980	0.45%	0.78%	0%	5.41%	171%
DFsec (%)*		**184,618**	**0.20%**	**0.48%**	**0%**	**8.10%**	**243%**
	Treated	92,638	0.06%	0.23%	0%	7.04%	398%
	Controls	91,980	0.34%	0.60%	0%	8.10%	180%

(To be continued)

Table 5.4 – Conclusion.

Variable		Obs.	Mean	Std. Dev.	Min.	Max.	CV (%)
forest (%)*		**184,618**	**74.41%**	**33.95%**	**0%**	**100%**	**46%**
	Treated	92,638	86.54%	26.53%	0%	100%	31%
	Controls	91,980	62.18%	36.15%	0%	100%	58%
secForest (%)*		**184,618**	**2.45%**	**4.92%**	**0%**	**58.81%**	**201%**
	Treated	92,638	1.08%	3.01%	0%	51.67%	279%
	Controls	91,980	3.82%	5.97%	0%	58.81%	156%
farming (%)*		**184,618**	**10.98%**	**22.48%**	**0%**	**99.96%**	**205%**
	Treated	92,638	1.64%	6.38%	0%	96.14%	389%
	Controls	91,980	20.39%	28.23%	0%	99.96%	138%
nonForestNatural (%)*		**184,618**	**4.61%**	**16.01%**	**0%**	**100%**	**347%**
	Treated	92,638	4.28%	15.59%	0%	100%	364%
	Controls	91,980	4.94%	16.41%	0%	100%	332%
nonVegetated (%)*		**184,618**	**0.11%**	**1.48%**	**0%**	**96.18%**	**1347%**
	Treated	92,638	0.05%	0.70%	0%	72.60%	1435%
	Controls	91,980	0.17%	1.97%	0%	96.18%	1152%
floodedForest (%)*		**184,618**	**3.99%**	**15.25%**	**0%**	**100%**	**382%**
	Treated	92,638	3.91%	15.12%	0%	100%	387%
	Controls	91,980	4.08%	15.37%	0%	100%	377%
mangrove (%)*		**184,618**	**0.05%**	**1.35%**	**0%**	**90.85%**	**2871%**
	Treated	92,638	0.07%	1.75%	0%	90.85%	2429%
	Controls	91,980	0.02%	0.75%	0%	55.59%	3459%
savanna (%)*		**184,618**	**0.71%**	**5.27%**	**0%**	**97.40%**	**745%**
	Treated	92,638	0.57%	4.69%	0%	97.40%	830%
	Controls	91,980	0.85%	5.79%	0%	96.46%	681%
precMean (mm)		**184,618**	**197.69**	**42.39**	**58.36**	**430.61**	**21%**
	Treated	92,638	205.36	45.04	75.74	430.61	22%
	Controls	91,980	189.97	38.00	58.36	411.11	20%
precTotal (mm)		**184,618**	**2,372.27**	**508.64**	**700.33**	**5,167.38**	**21%**
	Treated	92,638	2,464.27	540.51	908.91	5,167.38	22%
	Controls	91,980	2,279.61	456.00	700.33	4,933.28	20%
tempMean (°C)		**184,618**	**28.13**	**1.68**	**17.80**	**37.61**	**6%**
	Treated	92,638	27.57	1.21	17.80	37.61	4%
	Controls	91,980	28.69	1.89	19.29	36.86	7%
MCWD (mm)		**184,618**	**-205**	**408**	**-17,156**	**0**	**199%**
	Treated	92,638	-171	283	-6,759	0	165%
	Controls	91,980	-240	501	-17,156	0	209%
precDry (mm)		**184,618**	**44.86**	**30.10**	**0.00**	**156.82**	**67%**
	Treated	92,638	43.59	31.41	0.00	150.41	72%
	Controls	91,980	46.15	28.66	0.00	156.82	62%
tempDry (°C)		**184,618**	**22.54**	**11.84**	**0.00**	**39.45**	**52%**
	Treated	92,638	20.64	12.25	0.00	39.45	59%
	Controls	91,980	24.46	11.07	0.00	38.57	45%
pop (N x1000)		**184,618**	**0.12**	**2.36**	**0.00**	**372.04**	**1939%**
	Treated	92,638	0.03	0.52	0.00	86.05	1664%
	Controls	91,980	0.21	3.30	0.00	372.04	1551%
frag (km)		**184,618**	**17.64**	**23.90**	**0.00**	**305.94**	**135%**
	Treated	92,638	11.68	19.74	0.00	305.94	169%
	Controls	91,980	23.65	26.11	0.00	187.84	110%

Note: CV = Coefficient of variation (sd*100)/mean). (%)* = proportion within regular grid pixel. Statistics obtained by collapsed dataset, which refers to the average year, calculated for time-varying variables as the average value from 2003 to 2020.

Figure 5.7 - Mean ± Standard Deviation for each variable considered in our database, splitting into treated and control groups. The treated group consists of pixels within protected areas. The statistics refer to the whole dataset before matching. Red points are the median for each group. (*) signals for statistically significant ($p < 0.05$) comparisons between treated and control groups based on a Kruskal-Wallis test. If it appears, there are significant differences between the control and treatment groups.

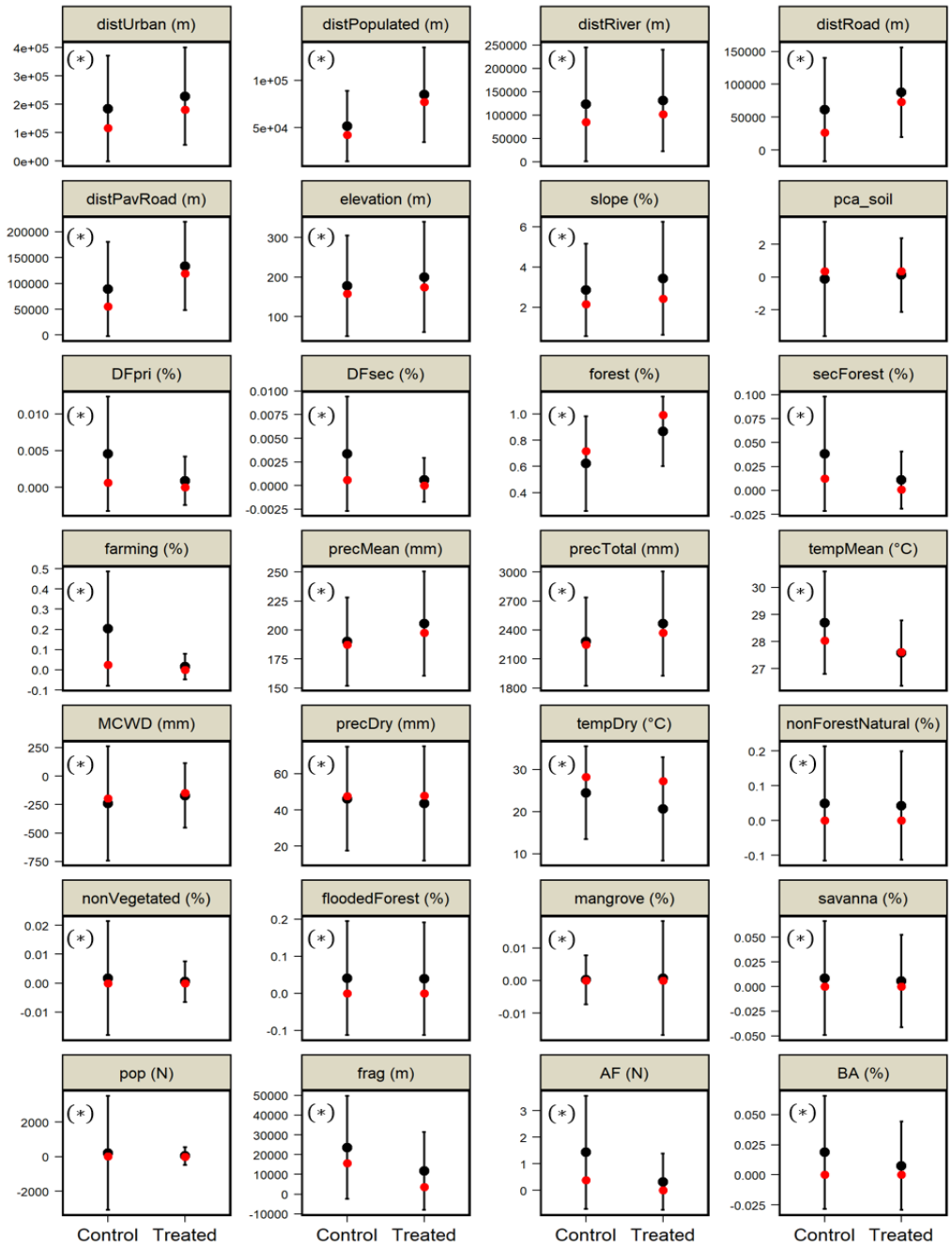

5.4.2 Matching

Comparing the matching performed considering no caliper, 1SD caliper, and 0.5SD caliper, one sees that the number of treated observations matched (on support) is reduced by 22% with 1SD caliper and 55% with 0.5SD caliper (Table 5.5 and Figure 5.8).

Table 5.5 - Sample size in each group considered for matching analysis.

	No caliper	1SD caliper	0.5SD caliper
Controls	91,980	91,980	91,980
Unmatched controls	75,025	76,540	80,695
Matched controls	16,955	15,440	11,285
Treated	92,638	92,638	92,638
Treated off support	0	20,350	51,139
Treated on support	92,638	72,288	41,499
Comparable sample	109,593	87,728	52,784

So the cost in terms of sample reduction is considerable. Control observations are also substantially reduced in factors of 83% and 88% with 1SD caliper and 0.5SD caliper, respectively, which reduces the pool of observations outside protected areas taken as a basis for comparison. The percentage of excluded controls due to caliper restrictions in relation to the total number of available controls in the three specifications that we considered is within the range of what has been observed and accepted in the literature (ARRIAGADA et al., 2016; ANDAM et al., 2008; NELSON&CHOMITZ, 2011). The same is true for reducing the total sample size (ARRIAGADA et al., 2016; ANDAM et al., 2008). Sample reduction is only one of the dimensions that should be accounted for in choosing caliper length, as it captures only the cost of information loss.

A complete evaluation requires looking at the benefits of a larger caliper, that is, the relative performance of the three methods in balance, common support, and parallel trends. Using the Rosenbaum and Rubin (1985) approach to check for covariates balance, matching without caliper presented 2% of variables in the “of concern” state and 0% in the “bad” state, that is, variables in which balance was not satisfactory (Table 5.6). The covariates not balanced were the proportion of farming and mangroves.

Figure 5.8 - Spatialization of the sample in each group considered for matching analysis. (a) Before matching. (b) After matching without caliper. (c) After matching with 1 SD caliper. (d) After matching with a 0.5 SD caliper.

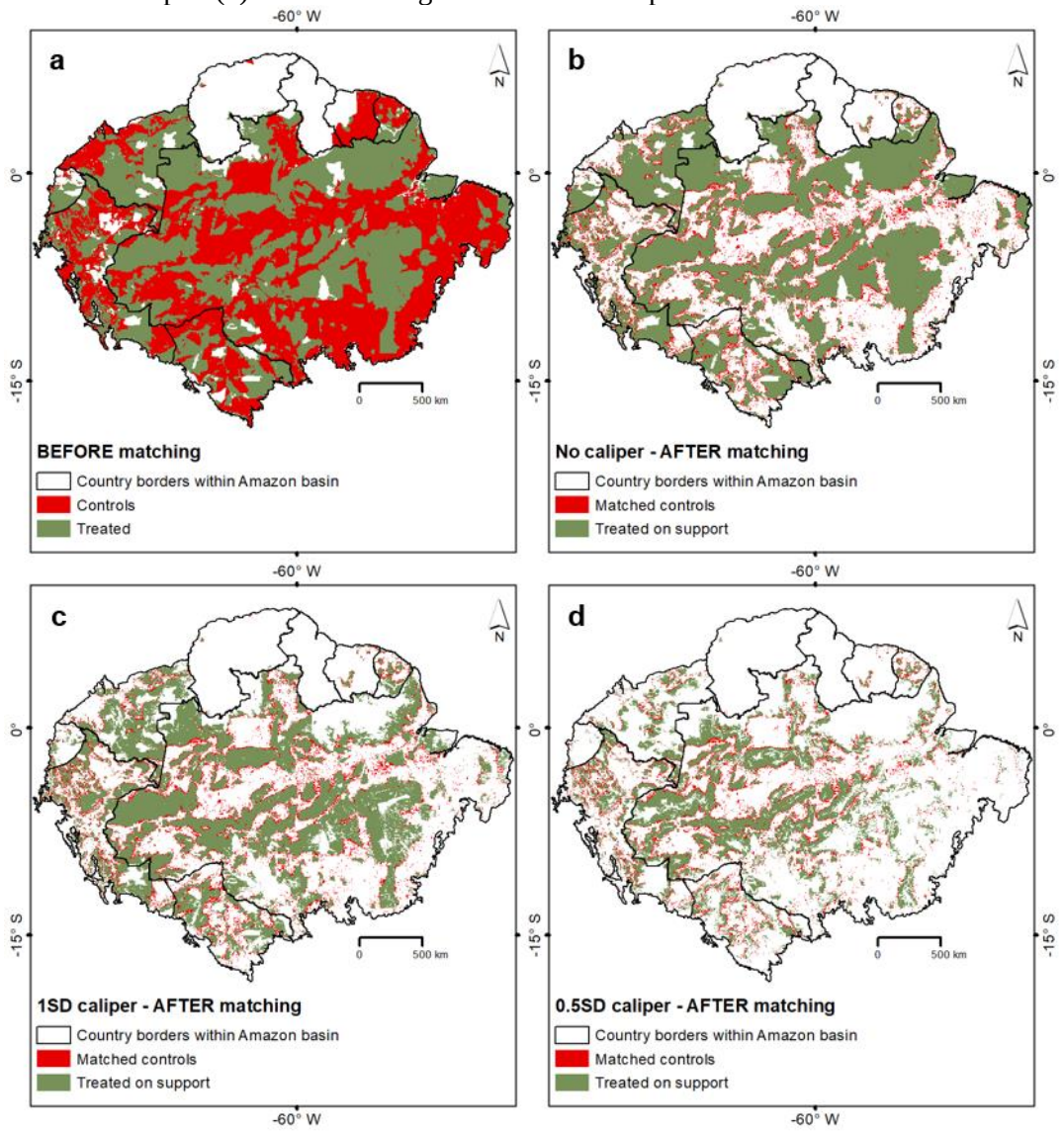

Table 5.6 - Checking the balance of the covariates using the Rosenbaum and Rubin (1985) specification for the three matching options considered (no caliper, 1SD caliper, and 0.5SD caliper).

Sample	*Unmatched*		*Matched*		Covariates not balanced after matching
	%concern	%bad	%concern	%bad	
No caliper	21	51	2	0	Farming and mangrove
1SD caliper	21	51	0	0	-
0.5SD caliper	21	51	0	1	Mangrove

of concern = variance ratio in [0.5, 0.8) or (1.25, 2]
bad = variance ratio <0.5 or >2

The balance graph, in which ideally, the two empirical distribution curves should overlap completely, showed clearly that the control distribution is displaced to the left relatively (Figure 5.9a, Figure 5.9b). This means that a low probability of treatment is more frequent among the untreated, as expected. Even without matching, the overlap between the two distributions is visually non-negligible, even though it increased substantially with matching.

Figure 5.9 - The kernel density of matching in the treatment group and the control group before matching (a) and after matching, considering the three matching options; no caliper (b), 1SD caliper (c), and 0.5SD caliper (d).

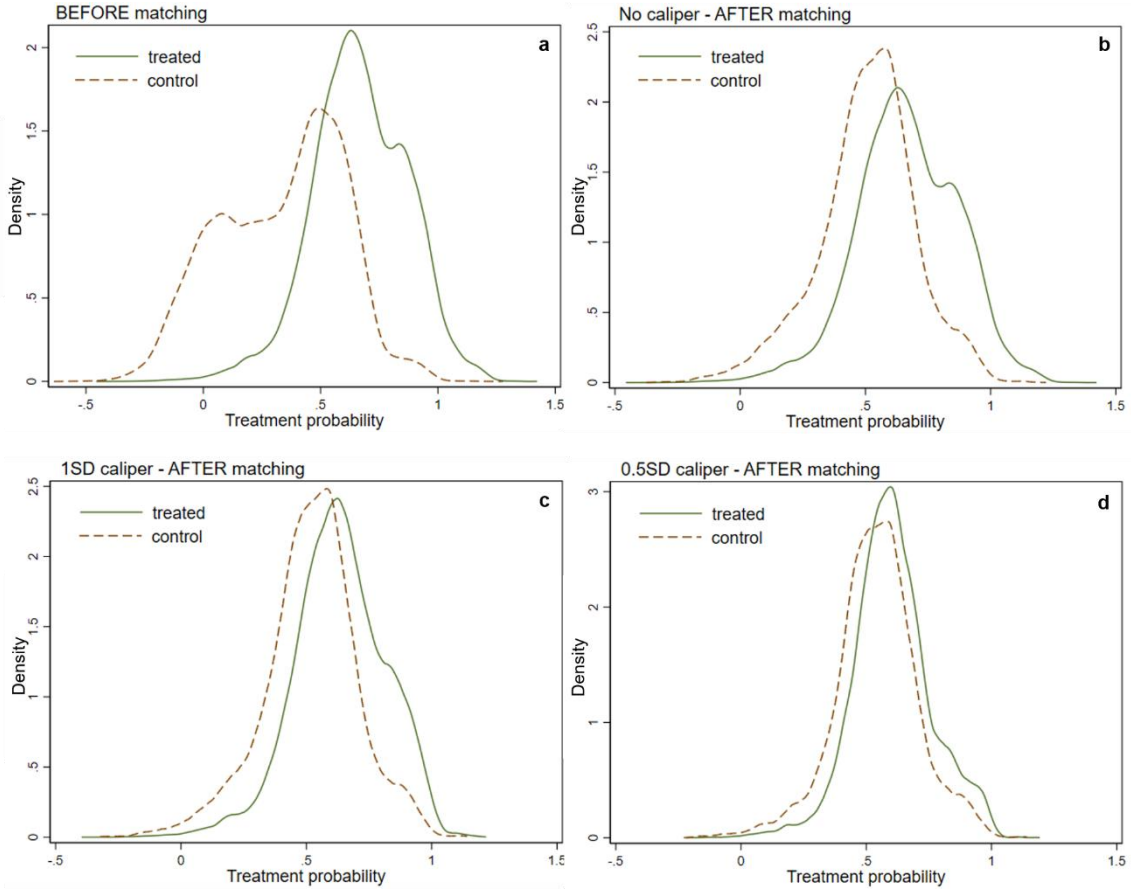

Figure 5.10 - Common support graph for treated and untreated groups, considering the three matching options; no caliper before (a) and after (b) matching, 1SD caliper before (c) and after (d) matching, and 0.5SD caliper before (e) and after (f) matching. According to the caliper, the treatment group was divided into on and off support.

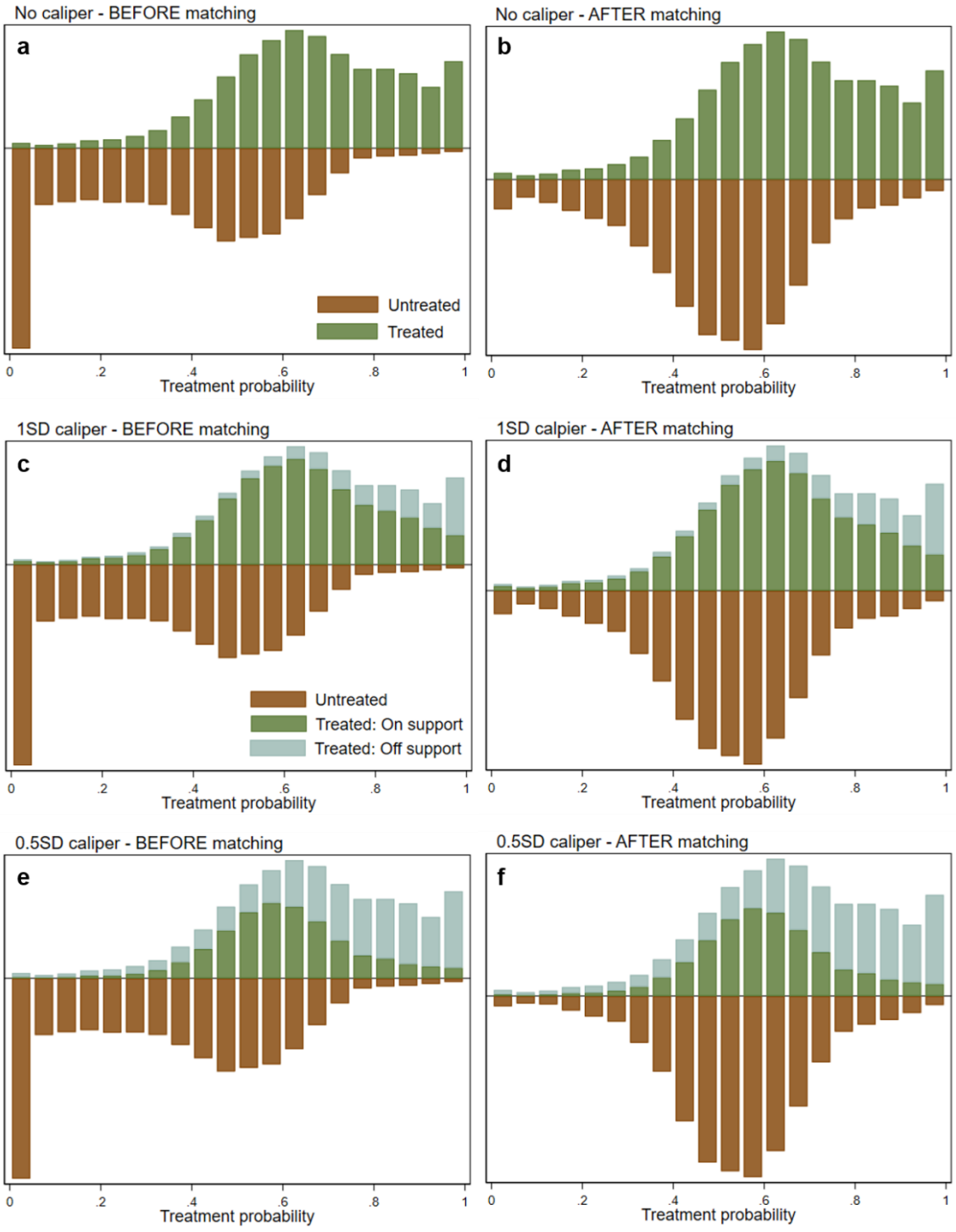

The second dimension of performance is the common support graph, which should ideally show the same distribution of treatment probabilities for treated and untreated. Before

matching, a low probability of treatment is highly recurrent among the untreated, and a high probability of treatment is more frequent among the treated than expected (Figure 5.10a, Figure 5.10b). The most visible effect of matching was to reduce the observations with near zero probability of treatment, in accordance with the common support assumption of matching that extreme probabilities of treatment should not happen. The similarity of the treatment probability distribution increased notoriously under matching with the probability mass being re-allocated to the center of the graph (Figure 5.10c-f).

The third and final dimension of performance is the evaluation of parallel time trends across treated and control groups and whether parallelism increased. Even before matching, the similarity of burned area trends across protected and control areas is striking and strongly suggests that parallel trends are a reasonable assumption for our data (Figre 5.11a). All the matching specifications made the two curves (treated and control) more similar in their trends. However, this effect was not large, probably because the trends were already highly parallel before matching (Figure 5.11b-d).

Figure 5.11 - Parallel trends of the average burned area from 2003 to 2020. Burned area trends inside protected areas (treated) and outside (control), before matching (a) and after matching, considering the three matching options; no caliper (b), 1SD caliper (c), and 0.5SD caliper (d).

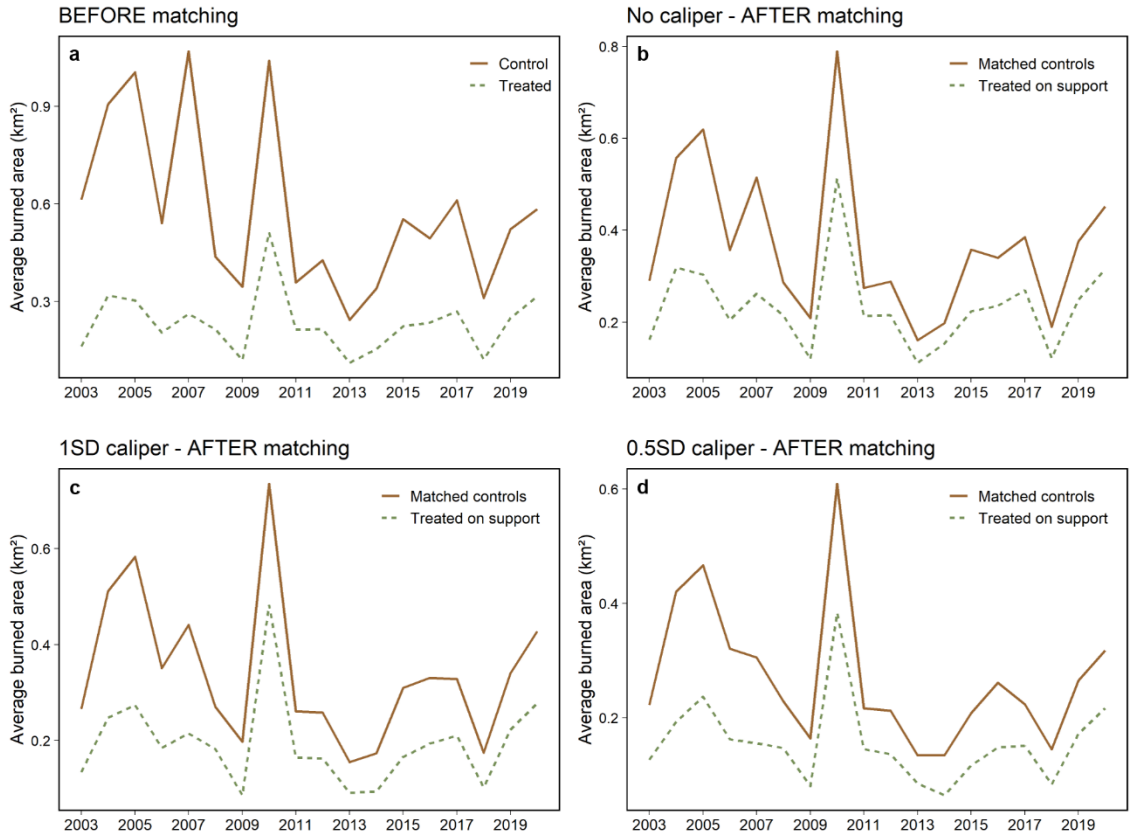

Regarding variables' balance, the gain from a 1SD caliper was reduced from 2% to zero the variables with "of concern" status (Table 5.6). Thus, the highest level of variable balance was achieved with a 1SD caliper. The overlapping was larger with the 1SD caliper, mainly near the peak probability, around 50% (Figure 5.9c). In the common support graph, it is clear that the caliper worked to reduce the frequency of high treatment probability, especially the frequency near 100% probability (Figure 5.10c and Figure 5.10d). The similarity of the distributions increased considerably with the transfer of probability mass in the treated distribution from the right to the left of the graph. This is, again, a way to ensure that the assumption of common support is verified, that is, that extreme treatment probabilities are not observed in the sample. Comparable controls (untreated) were also diminished, contributing to the increased similarity that Figure 5.9c reveals.

Evaluating the performance of matching with 0.5SD caliper, there was a loss of balance with 1% of variables switching to the "bad" state. There was no change in the "of concern" status, which remained null. There was a sensible gain in terms of overlapping in the balance graph, with the peak probability of the treated being increased. However, this gain that half caliper brought is smaller compared with the no caliper baseline (Figure 5.9d). The common support graph reveals that the exclusion of treated pixels (treated off support) embraced those at high probability levels and across medium probabilities. In a lower degree, even pixels with a low probability of treatment were excluded, which seems to show that the exclusion extended over the entire distribution of treatment probability, being excessive in terms of the excluded positions. Of course, this generated a gain in an increased similarity of the histograms, which became more concentrated at the center of the graph.

The best performance among the options considered was achieved by the 1SD caliper matching, considering the results of the matching approach presented in the previous paragraphs. It better-balanced gains and losses. Half caliper was a worse balance because of the 1% "bad" balance status of covariates and the excessive range of exclusion of treated (treated off support), revealed by the common support graph. All this loss is for a small gain in the balance graph and, of course, for a larger gain in the support graph but at the cost of a great reduction of the sample to less than half. Indeed, the main cost of half caliper is the 52% reduction in the sample, strongly affecting the generality of analysis results, which was considerably smaller at 1SD caliper, which imposed a 20% reduction. Therefore, all matches not equal to or within 1 SD of each covariate were dropped, and the sample obtained by matching with a 1 SD caliper was then used for post-matching analysis to measure the ATE.

An examination of the excluded sample strata after matching 1 SD caliper reveals that unmatched controls are 20% closer to the Brazilian deforestation arc than matched controls. In addition, treated pixels on support are 45% closer to the arc. Which further attests to the success of matching-based covariate balancing. We know that anthropic pressure is not limited to Brazil (and its deforestation arc). However, as we are dealing here with averages and the Brazilian area encompasses most of the study area, it greatly

influences the analyses. Table D.4 details the descriptive statistics of the different post-matching groups for all variables.

5.4.3 Differences-in-Differences (DiD)

Before matching, greater parallelism is observed between control and not currently treated rather than control and currently treated. The clear peak in 'not currently treated' is caused by a disastrous fire due to the extreme drought of 2010 in an area that was to be protected, particularly in the *Área Municipal de Conservación y Manejo Bajo Madidi*, in Bolivia, that was only designated in 2019. The burned area that occurred in this area in 2010 corresponded to 44% of the total burned area registered in not currently protected pixels in the same year. The increase of parallelism with matching is notorious and applies to the comparison of control both with not currently treated and currently treated. Further increase in parallelism with caliper matching is not visible (Figure 5.12). In all graphs, the current trend is below the never-treated trends and ever-treated but not currently treated, as expected. The picture is less clear when comparing the trends of the never treated and treated but not currently treated, as initially (from 2003 to 2009) the former is above, what is reverted thereby in nearly all remaining years, with treated but not currently treated lying above controls. In summary, protection seems to be effective only when active.

Matching increased parallelism, and trends are parallel over time, consistent with the DiD premise that the trend is the same comparing controlled and treated before treatment. In Figure 5.12b, the orange dashed line of ever-treated but not currently treated has decreasing reliability due to the sharp diminishment in the subsample on which it is based, as all ever protected become ultimately protected. Over time, the size difference between the two subsamples becomes different by orders of magnitude. For instance, in 2008, the order of magnitude of the currently protected subsample size before matching was 10^4 and close to 10^5 (84,397), whereas in the latter, it was 10^3. In 2016, the orders of magnitude were 10^4 vs. 10^2, which is why the graphs stopped by 2015.

Figure 5.12 - Parallel trends of the average burned area from 2003 to 2020, considering dynamic protection status. Burned area trends inside active protected areas (currently treated), inside inactive protected areas (not currently treated), and outside (control) before matching (a) and after 1SD caliper matching (b).

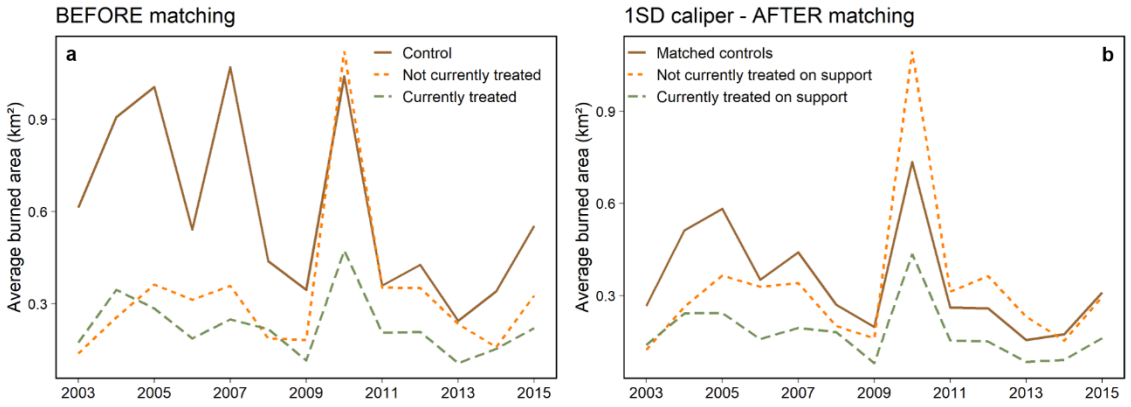

Figure 5.12 suggests that the naive treatment effect is larger; thus, without matching, the effect would be overestimated. The expected hierarchy of relative level of the three subgroups (three lines) is clearer with matching; that is, control is greater than not currently treated, which in turn is greater than currently treated. This hierarchy was broken in 2009, which is probably due to the average of the not currently treated becoming already unreliable due to the small sample size. As explained above, this could happen due to the one order of magnitude difference in subsample size comparing not currently treated to currently treated and matched controls since 2008, once the average captures very particular cases, being more subjected to outliers. Also, even if the 2003-2009 period suggests that protection is effective even before becoming active, such effect is smaller than active protection. Therefore, the estimation of the ATE by the coupled matching-DiD approach, which measures only the active protection effect, indeed captures the largest part of the protection area.

One hypothesis to explain these patterns is that protected areas were initially created at places where deforestation pressure was lower, as this was less incompatible with economic interests and thus more practically feasible. However, over the years, the expansion of the protected areas network and the advance of the deforestation arc occurred, making the subsample not currently treated to represent an area under greater pressure. Figure 5.13a clearly shows a steep decrease in distance from protected areas to the deforestation arc until 2008, and after that, the distance continues to decrease, but

more gradually. The gradual decrease in the distance between protected areas and areas under pressure from deforestation can also be seen in Figure 5.13b.

Figure 5.13 – Mean distance from pixels within protected areas in Brazil to the deforestation arc in the eastern Brazilian Amazon (a) and from pixels within protected areas in the Amazon basin to the nearest of the 20 most deforested municipalities in each country each year.

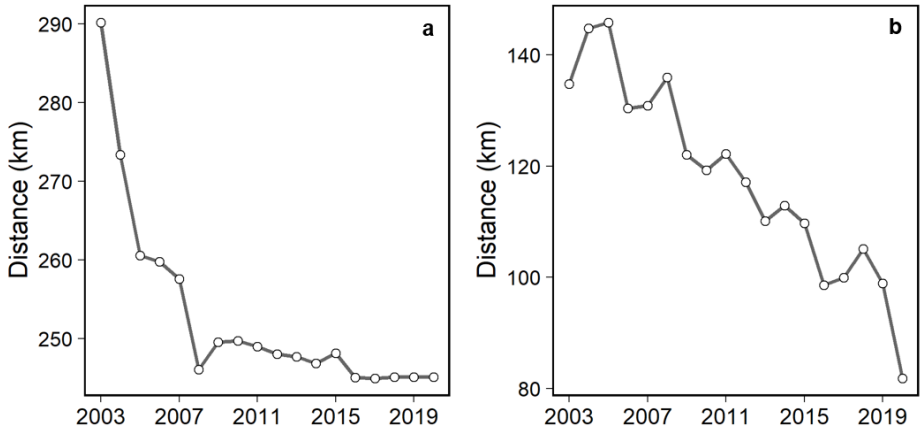

The same analysis was carried out using active fires instead of burned areas (Figure 5.14). The treatment effect is more evident in this case, comparing controls to ever-treated pixels. Unlike the burned area graph, the curves using active fires showed that between 2007 and 2009, the average fire occurrence in currently treated was higher than not currently treated, even after matching. This reinforces that protected areas also burn, and in this particular period, they registered an average of 0.31 active fires per year and 0.19 km² before matching (or 0.29 and 0.15 after matching, respectively). Besides that, in this period, there was a steep decrease in the distance from protected areas to deforestation pressure (Figure 5.13), which could have boosted fire within them.

Figure 5.14 - Parallel trends of average active fire count from 2003 to 2020, considering dynamic protection status. Active fire trends inside active protected areas (currently treated), inside inactive, protected areas (not currently treated), and outside (control) before matching (a) and after 1SD caliper matching (b).

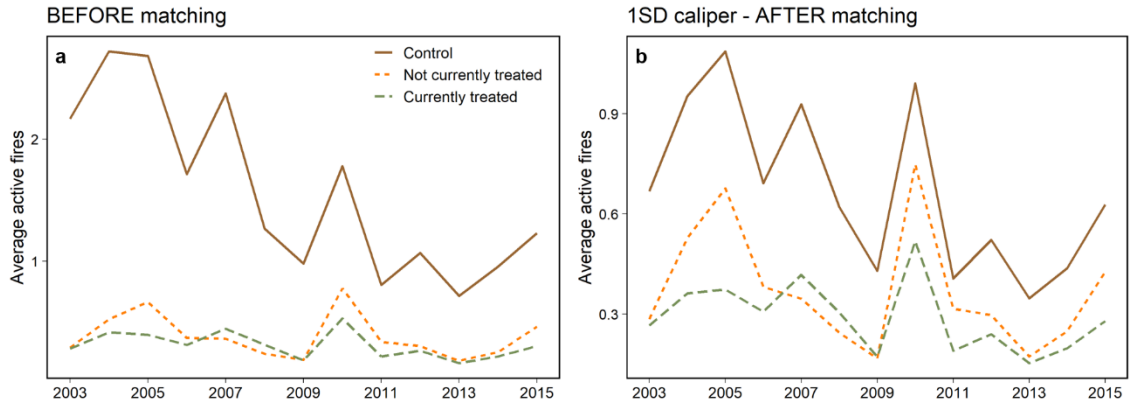

The differences-in-differences approach brings timing to the analysis, and its traditional trend break graph shows the dependent variable with a clear mark before and after treatment. Given the dynamic nature of our treatment variable, i.e., protection status, our trend break graph was built by plotting the average burned area per year since treatment, only for ever-treated pixels. First, considering the whole dataset, in which time since treatment ranges from 16 years before treatment to 60 years after, the trend break is clear with a visibly lower level during the active protection period. This is highlighted by the fact that the blue horizontal line at the lowest burned area level achieved before protection is close to or above most of the trend after protection (Figure 5.15a). That becomes even clearer, zooming in to the time of 16 years before and after treatment (Figure 5.15b), thus ensuring equal time spans before and after treatment. In this case, it was only omitted pixels that were protected before the beginning of the analysis period in 2003, thus keeping 56% of the protected pixels. Therefore, considering only ever-treated pixels, there is a clear fall in the burned area trend when protection is active, which gives a visual indication of a negative ATE.

Figure 5.15 - Average burned area per year since treatment for ever-treated pixels, covering 16 years before and 60 years after treatment (a) and 16 years before and after treatment (b).

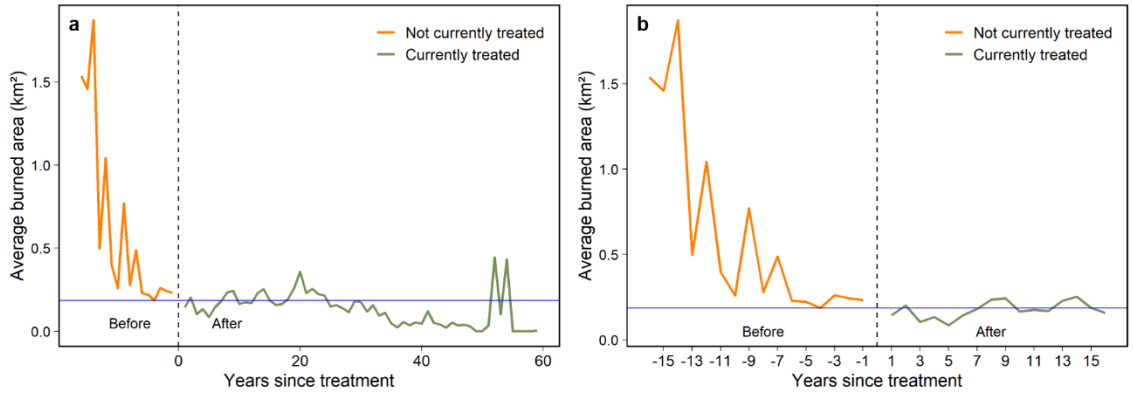

The same analysis was carried out using active fires instead of burned areas (Figure 5.16), which resulted in similar patterns. The small number of observations could explain the fire peak in the older currently treated protected areas. Observations in which the treatment occurred 48 to 59 years prior to the current analyzed year corresponded to only 0.19% of the treated group. This small sample makes the average more subjected to outliers.

Figure 5.16 - Average active fire count per year since treatment for ever-treated pixels, covering 16 years before and 60 years after treatment (a) and 16 years before and after treatment (b).

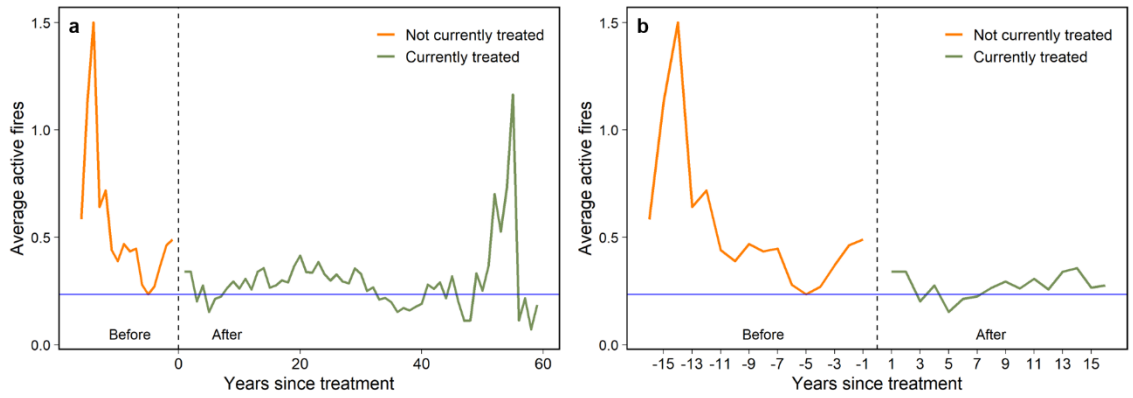

5.4.4 Average Treatment Effect (ATE) estimation

The second stage estimates reveal a statistically negative effect of the protected area in the burned area (Table 5.7) and active fires (Table 5.8), thus showing that protection could reduce fires. This was robust to estimator specification (FE, DiD, and DiD-FE) and

clustered disturbances since both clustering at the pixel level, department level. Bootstrapping were also applied to residuals (Table D.5, Table D.6). Indeed, the ATE estimate did not change across estimators, being for all of them -0.000728 ($p < 0.001$) and -0.0439 ($p < 0.001$) for the burned area and active fires, respectively. If the average pixel-year became protected, it would have an average area burned fraction 0.0007 points lower, which is 0.5% of the 0.13 burned area average among all pixels. Converting the fraction of pixel burned into pixel area would be a decrease of the burned area to about 0.02 km² (2 ha.pixel^{-1}.year^{-1}) – that is, for each land patch of 2,800 ha protected, 2 hectares are prevented from being burned per year. If the average pixel-year became protected, it would have a number of active fires 0.0439 lower, 5% of the 0.88 average. It is important to highlight that the ATE is bounded above by the fact that protected areas already have a low level of fire (so the reduction of a low level must be low). The complete tables with all covariate coefficients can be found in Table D.5 and Table D.6.

Table 5.7 - Differences-in-differences estimation of the protected area effect on the burned area.

Dependent variable: Burned area	FE	DiD	DiD-FE
Average treatment effect (ATE)	-0.000728*** (0.0002)	-0.000728*** (0.0002)	-0.000728*** (0.0002)
N	1579104	1579104	1579104
F	164.7	290.06	307.12
p	0	0	0
Overall R^2	0.0839		
N clusters	87728	87728	87728

Notes: +p<0.10,*p<0.05,**p<0.01,***p<0.001. The dependent variable is the burned area proportion within each pixel-year. Treatment is a dummy variable that equals one if a pixel is within an active protected area and zero otherwise. FE = fixed-effects estimator for panel data, DiD = differences-in-differences estimator for panel data pooled under the assumption of zero correlation between the covariates and the unobserved heterogeneity term, DiD-FE = estimator addressing both unobserved heterogeneity bias and assuming that the trends were parallel in the untreated state for treated and untreated. All specifications include year and Amazonian department dummies interacted with a deterministic time trend. Covariate controls include within pixel proportion of primary and secondary forest deforestation, forest, farming, non-forest natural formations, non-vegetated area, flooded forests, mangroves, and savanna. Besides that, controls also included total precipitation, mean temperature, maximum cumulative water deficit (MCWD), mean precipitation and temperature during the dry season, population, and forest edge length. Robust standard errors clustered at the pixel level in parentheses.

The department-clustered estimates of ATE (Table D.7) were significant only at the 10% level and for the count measure of fires (not for the burned area). This was expected due to the considerable reduction of the variability of residuals based on standard error calculations since the number of observational units was diminished 1790 fold. However, the significant reduction was amplified by a feature of the data, the excess of zeros in the dependent variable, that is, fire was not detected in most pixel-years. This was confirmed

with dependent binary variables (Table D.8), which took value one in the case of fire detection. Considering these binary dependent variables, the significance level of the estimates was still 1% for SE clustered at pixel level and 5% when clustered at the department level. Even with the significance level achieved with department clustering being lower than with pixel-clustering, it remained in accordance with the level at which the nullity of a parameter is commonly rejected ($p > 0.05$). Therefore, the negative causal effect of protected areas on fire stood out as the test of clustering standard errors at a much higher aggregation level than the cross-sectional observations.

Table 5.8 - Differences-in-differences estimation of the protected area effect on active fires.

Dependent variable: Active fire	FE	DiD	DiD-FE
Average treatment effect (ATE)	-0.0439***	-0.0439***	-0.0439***
	(0.0066)	(0.0067)	(0.0066)
N	1579104	1579104	1579104
F	281.2	449.69	476.15
p	0	0	0
Overall R^2	0.0782		
N clusters	87728	87728	87728

Notes: +p<0.10,*p<0.05,**p<0.01,***p<0.001. The dependent variable is the active fire count within each pixel-year. Treatment is a dummy variable that equals one if a pixel is within an active protected area and zero otherwise. FE = fixed-effects estimator for panel data, DiD = differences-in-differences estimator for panel data pooled under the assumption of zero correlation between the covariates and the unobserved heterogeneity term, DiD-FE = estimator addressing both unobserved heterogeneity bias and assuming that the trends were parallel in the untreated state for treated and untreated. All specifications include year and Amazonian department dummies interacted with a deterministic time trend. Covariate controls include within pixel proportion of primary and secondary forest deforestation, forest, farming, non-forest natural formations, non-vegetated area, flooded forests, mangroves, and savanna. Besides that, controls also included total precipitation, mean temperature, maximum cumulative water deficit (MCWD), mean precipitation and temperature during the dry season, population, and forest edge length. Robust standard errors clustered at the pixel level in parentheses.

The sensitivity test for unobservables (Table D.9 and Table D.10) showed that an unobservable capable of increasing the likelihood of not having fire inside a protected area by at least 1.35 fold, as a ratio of the likelihood outside, would be enough to turn the result non-reliable for over 58% of the fire measure vs. year combinations. This is similar to Arriagada et al. (2016) results for Chilean protected areas containing deforestation, where an influence of 1.35 degrees was already enough to raise the p-value above 5%. It is unclear which non-observable could influence the results achieved in this chapter, and with the Rosenbaum test being a "worst-case scenario" (ARRIAGADA; ECHEVERRIA; MOYA, 2016), its results remain useful. They, first of all, attest that, even after matching and DiD estimators were applied, some irreducible uncertainty on the magnitude of the

protected area effect on fire remained (in line with the test's interpretation by ARRIAGADA; ECHEVERRIA; MOYA, 2016). The test also suggests that the estimated effect is subjected to a non-negligible degree of uncertainty due to unobservables driving both selections of pixels to belong to protected areas and the effect of protected areas on fires. One example of relevant unobservables on this subject is region-specific environmental policies, which could influence both protected areas establishment and fire occurrence. In Brazil, one such policy is the PPCDAm. Thus, Rosenbaum's sensitivity test tells us that if PPCDAm increases the ratio between the probabilities of fire not occurring and occurring within protected areas by more than 35%, then, in fact, the results are invalid. As mentioned before, this uncertainty is irreducible since we do not have information about the local execution of the PPCDAm at the pixel scale.

5.5 Discussion

In this chapter, we evaluated the role of protected areas on fire occurrence in the Amazon basin from 2003 to 2020. Our analysis was motivated by the growing threat that Amazonian ecosystems have faced in recent years. The occurrence of fire has achieved record levels annually in the region, and carbon emissions from forest degradation already exceed those caused by deforestation (SILVA JUNIOR et al., 2021c). Fire is anthropically introduced in this tropical environment, mainly because of the agricultural frontier expansion and land grabbing. The increased fire occurrence in the Amazon, whether due to increased deforestation or climate change, poses a serious threat to the forest and its functionality.

On the other hand, protected areas appear to be the last patches of healthy ecosystems that are resilient to recent changes. It is estimated that protected areas in the Brazilian Amazon account for 54% of forest remnants and contain 56% of its carbon (SOARES-FILHO et al., 2010). Thus, protected areas are essential carbon reservoirs for maintaining the planet's climate balance. Our results confirmed that the creation of protected areas reduced fire occurrence and extent in the Amazon basin from 2003 to 2020. Our findings corroborate with prior studies that also attested to an inhibitory effect of protected areas on fires (NELSON; CHOMITZ, 2011; NEPSTAD et al., 2006; NOLTE; AGRAWAL, 2013). The reduction coefficient we found for active fires (-0.0439) is consistent with the one found by Nelson and Chomitz (2011) for Strict Protected Areas in Latin America for the 2000-

2008 period. In this study, the authors found an inhibitory effect of fire four times greater for indigenous lands, showing the importance of analyzing the protection categories separately. Tasker and Arima (2016) was the only study to include fire extent when evaluating the effectiveness of protected areas on fires. Similar to our results, they found reduction coefficients consistently low in magnitude (coefficients < 0.01) for the burned area, albeit their results were insignificant. The comparison of our results in absolute values with Tasker and Arima (2016) study is made impossible by differences in the strategies for identifying the causal effect of protected areas on fire.

Although Nepstad et al. (2006) also found a negative effect of protected areas on fire, in this study, the authors only measured the relative performance of these areas. The study disregards unobservable confounders and concurrent changes that could influence fire occurrence inside and outside protected areas, and, consequently, inflate the estimated effect. The authors emphasize that the study is an initial comparative assessment of protected area performance in the Brazilian Amazon by using fire occurrence along the protection perimeter as a proxy for the threat of imminent degradation. After the Nepstad et al. (2006) study, other studies pointed to econometric strategies as being robust in assessing the effect of protected areas, both on deforestation and fire (e.g., ANDAM et al., 2008; ARRIAGADA; ECHEVERRIA; MOYA, 2016; HERRERA; PFAFF; ROBALINO, 2019; JOPPA; PFAFF, 2011; NELSON; CHOMITZ, 2011; NOLTE et al., 2013; NOLTE; AGRAWAL, 2013; PFAFF et al., 2014, 2015a, 2015b; SZE et al., 2022; TASKER; ARIMA, 2016; WENDLAND et al., 2015). All these studies addressed the non-randomization of protected area creation (selection bias), most of the time using matching estimators. However, matching alone does not find comparisons that are identical to treated pixels (HERRERA; PFAFF; ROBALINO, 2019), which makes the adoption of post-matching regressions relevant. Herrera et al. (2019) claimed the importance of the post-matching step as a robustness check, in which the matched sample could be used to control for remaining differences in covariates.

Nevertheless, even after 15 years of methodological development on the topic, it is still unclear how to deal with both selection endogeneity and, at the same time, control for unobservable heterogeneity. Combining matching with DiD confers the advantage of controlling for a wide range of socioeconomic and environmental predictors, besides the

policy, and at the same time for unobservable time-invariant factors and heterogeneous time-varying characteristics. Indeed, this joint approach was already used in policy evaluation (ALIX-GARCIA; SIMS; YAÑEZ-PAGANS, 2015; FERRARO; MIRANDA, 2017; GALIANI; GERTLER; SCHARGRODSKY, 2005; PEIXOTO et al., 2017), but never to estimate the effect of protected areas on fires. We attested that matching combined with DiD is a suitable approach, resulting in an unbiased estimate of the average treatment effect of protected areas on fire occurrence. Unlike deforestation, fire is highly influenced by climatic conditions and existing ground cover (fuel for the fire). Therefore, controlling for time-varying characteristics is critical to obtain an unbiased estimate in this context. Our study advanced in describing the fire phenomenon for the Amazon basin, adding a greater number of variables and, thus, providing a more comprehensive and accurate analysis than in previous studies.

The fact that we have attested that protected areas have a significant negative effect on fire and that other studies have already shown a similar effect on deforestation becomes extremely relevant to the environmental policy agenda. We believe that protected areas can help to accomplish international goals, such as the Sustainable Development Goals (SDGs) from Agenda 2030. In addition, carbon sequestration capacity can be improved by 0.39% by constructing global protected areas (SHI et al., 2020). Besides being critical to the accomplishment of the National Determined Contributions (NDCs), this central role in reducing carbon emissions makes protected areas promising objects within the scope of Reduction of Emissions from Deforestation and Forest Degradation (REDD+) projects. Thus, this environmental strategy can make these global environmental goals compatible with support for local livelihoods, generating socio-environmental sustainability for traditional communities.

However, even though effective against deforestation and fires and historically serving as shields against human threats, protected areas are increasingly at risk. Taking the Amazon basin as a whole, there was a decrease of 11% in deforestation rate per year from 2017 to 2020, compared to the average rate from 2003 to 2016. In contrast, in the same period, there was an increase of 74% in deforestation within protected areas. The same pattern can be observed with fires. In the same period, while there was a 10% decrease in the burned area across the basin, within protected areas, the burned area per year increased

by 18%. These rates reflect the increase in agricultural areas (46%) and forest fragmentation (26%) recorded within protected areas (Figure 5.17).

Figure 5.17 - Percentage difference of deforestation of primary forest, burned area, farming, and forest fragmentation taking the mean annual rate from 2017 to 2020 compared to the mean annual rate from 2003 to 2016. The percentages were calculated both for the Amazon basis and per country. The numbers were also split into outside and inside protected areas.

Total	% deforestation	% burned area	% farming	% forest fragmentation
Bolivia	-42%	-18%	46%	25%
Brazil	-16%	-5%	12%	7%
Colombia	72%	-4%	21%	6%
Ecuador	1%	-69%	7%	5%
French Guiana	17%	-77%	24%	15%
Guyana	-11%	50%	-6%	10%
Peru	35%	-29%	21%	14%
Suriname	165%	-8%	16%	9%
Venezuela	39%	-5%	13%	13%
Amazon basin	-11%	-10%	14%	8%

Outside PAs	% deforestation	% burned area	% farming	% forest fragmentation
Bolivia	-55%	-33%	38%	11%
Brazil	-27%	-14%	10%	-1%
Colombia	53%	-8%	19%	-4%
Ecuador	-11%	-100%	4%	-2%
French Guiana	21%	-81%	16%	11%
Guyana	-24%	48%	-13%	7%
Peru	21%	-34%	18%	9%
Suriname	165%	-32%	15%	7%
Venezuela	-41%	-33%	0%	-46%
Amazon basin	-22%	-19%	12%	0%

Inside PAs	% deforestation	% burned area	% farming	% forest fragmentation
Bolivia	6%	7%	90%	48%
Brazil	73%	31%	42%	27%
Colombia	166%	36%	42%	16%
Ecuador	15%	-38%	12%	8%
French Guiana	12%	-74%	39%	21%
Guyana	29%	132%	8%	19%
Peru	89%	8%	44%	22%
Suriname	178%	-5%	22%	35%
Venezuela	201%	70%	200%	24%
Amazon basin	74%	18%	46%	26%

Note: The % refers to the mean annual rate between 2017 to 2020 compared to the mean annual rate between 2003 to 2017. PAs = Protected areas.

Individualizing the member countries of the Amazon basin, Bolivia and Brazil showed the same pattern as the basin as a whole: a decrease in the annual rate of deforestation and burned area between 2017 and 2020 compared to the 2003-2016 period, in contrast to an increase in both phenomena within protected areas. All countries registered deforestation increases within protected areas, and only Ecuador (38%) and French Guiana (74%)

decreased their burned area rates within these areas. Surprisingly, only Guyana registered an increase in burned areas outside protected areas (48%). Ecuador reached a 100% decrease in the burned area outside protected areas. Venezuela, which overall decreased burned area by 5%, showed a 33% decrease in the burned area outside protected areas, at the cost of a 70% increase within them. The same country registered an increase of farming land by 200% within protected areas. These numbers demonstrate that decision-makers from all countries in the Amazon basin must review public policies regarding protected areas and create new strategies that guarantee their integrity.

This time cut from 2017 to 2020 has a strong political connotation for Brazil. In 2016, the country's current president, Dilma Roussef, was impeached, marking the end of a 14-year period in which the Workers' Party was in power. It was at the beginning of this period, in 2004, that the Action Plan for the Prevention and Control of Deforestation in the Legal Amazon (PPCDAm) was launched, aiming to gradually and continuously reduce deforestation in the Legal Amazon, as well as to provide subsidies to a more sustainable regional development. During its first phase, which occurred from 2004 to 2008, the most remarkable action was the creation of more than 600 thousand square kilometers of protected areas, and 62% of the initial budget for this phase was allocated to land and territorial planning. Although there were many challenges on the environmental agenda to be overcome at the time, such as the effective management of these areas, from 2017 onwards, there were setbacks in the environmental legislature and in the political scenario that put even the existence of these protected areas at risk (MATAVELI; DE OLIVEIRA, 2022; RORATO et al., 2021; VILLÉN-PÉREZ et al., 2020). If, on the one hand, Brazil has proved the feasibility of maintaining forests over most of the Brazilian Amazon through enforcement of environmental legislation, on the other hand, it also proved that progress on the environmental agenda is fragile and highly susceptible to the political scenario.

In conclusion, the fire-inhibiting capacity of these areas is only one aspect of the effectiveness of protected areas. However, it already demonstrates that their management is, in a certain way, effective in preventing forest degradation, in line with conservation strategies. Protected areas occupy 59% of the Amazon basin area, and their maintenance

and effectiveness enhancement should be among the priorities of debates on environmental agendas.

5.6 Future considerations

In this study, we made methodological advances in policy evaluation. We showed that the coupled use of matching and DiD econometric estimators are robust and suitable for measuring the effect of protected areas on fires in the Amazon. However, there is still a lot of room for improvement, and future work should focus on:

(i) Analyzing the categories of protected areas separately in order to consider the particularities of each category and then obtain more accurate estimators for each context;

(ii) Test the robustness of the results for alternatives to the average year used in the matching. The choice of the reference year is a challenge, and it can influence results;

(iii) apply dynamic matching so that time-varying characteristics are considered when choosing the counterfactual group;

(iv) repeat the DiD estimates without applying the matching to choose the counterfactual group in order to measure the influence of this step on the final results;

(v) test the results' robustness for different protected area time cohorts to measure the influence of political phases on the results.

6 GENERAL DISCUSSION

This thesis shows the imminent and growing threat protected areas face in the Amazon basin. The three factors conditioning fire occurrence in this tropical environment (ALENCAR; RODRIGUES; CASTRO, 2020) is changing, turning the Amazon into an amplified fire-prone system. We show here that these favorable fire dynamics affect the natural ecosystems found within protected areas, even if these areas have an inhibitory effect on the fire. The pressure on the forest, whether by deforestation related to land grabbing, agriculture expansion (ARMENTERAS et al., 2019; DE OLIVEIRA et al., 2020; MATAVELI et al., 2021), or mining (MATAVELI; DE OLIVEIRA, 2022; RORATO et al., 2021; VILLÉN-PÉREZ et al., 2020) is fragmenting the landscape. Forest edges, in turn, accumulate conditions that allow fire to enter the forest. It has already been seen that about 95% of active fires and the most intense ones were found in the first km from the edges of forest areas (SILVA JUNIOR et al., 2018). We found that 28% of the maximum extent of areas that have already been affected by fire in the Amazon basin from 2003 to 2020 were within protected areas.

Studies also found that in areas with up to 0.1 people per km², population density increases fire frequency by 10 to 20% relative to its value at no population (KNORR et al., 2014). Specifically for Amazon, we found that this value could be up to 22 times higher. From 2003 to 2020, protected areas in the Amazon have an average of one habitant per km², a density more than seven times lower than what is found outside. Despite being higher than the global turning point of 0.1 habitants per km², it is still more than twice that of the Amazon. In addition, we still show that the population within protected areas has been growing over the years. This means that the population configuration within protected areas in the Amazon and their temporal dynamics point to an increase in threats to the forest.

Concomitantly with the pressure over the forest and the population densification, climate change is also influencing fire dynamics in the Amazon (ARAGÃO et al., 2018; SILVA JUNIOR et al., 2019). Low humidity generates ideal conditions for intentional fires to leak into forests as dry seasons get longer and drier. Silva Junior et al. (2019) confirmed that during the drought that occurred in 2015/2016, positive active fire anomalies resulted from increased burned forests. Previous studies have pointed to an annual increase rate in

the average temperature of 0.03°C in the Brazilian Amazon for 1973 – 2013 (ALMEIDA et al., 2017). Regionally, this increase can reach 2.5°C in the southeastern Brazilian Amazon, analyzing the period from 2010 to 2018 (GATTI et al., 2021). Here we also found an overall increase of 0.03°C during the dry season per year from 2003 to 2020. However, depicting the Amazon on protection status, the average temperature increase during the dry season reaches 0.04°C within protected areas and 0.05°C outside. Even at a slower rate, the climate is changing within protected areas, and this variation leads to greater vulnerability to fire.

Translating fire impacts into economic costs, Campanharo et al. (2019) estimated for Acre state in 2010 a total loss of US$ 243.36 $\pm$ 85.05 million, and from 2008 to 2012, US$ 307.46 + 85.41 million. This cost estimation included direct impact on land use and land cover, carbon stocks, CO_2 emissions, and indirect impact on human illness. However, forest fires' socio-economic and environmental impacts can be much broader. Indeed, a United Nations report claims that wildfires could impact as many as 8 Sustainable Development Goals (Table 6.1) from Agenda 2030 (UNITED NATIONS ENVIRONMENT PROGRAMME, 2022). Contextualizing, the 2030 Agenda for Sustainable Development, universally adopted in 2015, is a plan to create a better and more sustainable future for all in just 15 years through 17 Sustainable Development Goals (SDGs).

Coincidentally, the sixth report of the Intergovernmental Panel on Climate Change (IPCC) relates protected areas to eight SDGs. According to the report, protected areas bring fundamental social, economic, and environmental benefits for adapting to climate change. Of the SDGs impacted by fire, at least six are considered protected areas benefits. Once again, this reinforces the importance of these areas for mitigating the impacts caused by fire, leading the Amazon region towards truly sustainable development. Furthermore, the member nations of the Amazon region have not only committed to the Agenda 2030. Under the scope of COP26, countries have updated their Intended National Determined Contributions (iNDCs), establishing their own emissions reduction targets as a global effort to stop climate change (FCCC, 2021). Even if national targets are shallow and unrealistic and often not enough to keep the global climate at a safe level (FCCC, 2021), they are the only attempt to make the effort of national governments something concrete and official. National targets are an official commitment that authorities and civil society

can demand. In this context, protected areas are essential allies for achieving the goals established in all countries, and not prioritizing them signals a movement against what is expected of a nation committed to sustainable development.

Table 6.1 - Impacts of wildfire on Sustainable Development Goals (SDG).

SDG	Description	Fire impact
1	No poverty	Increased desertification and land degradation
		Impacts on agriculture: reduction in soil fertility, stability and water infiltration and retention characteristics
		Impacts on foraging: loss of food sources and conversion of vegetation
		Displacement and loss of livelihoods
		Women and girls tend to experience greater impacts from poverty, food insecurity, and displacement
2	Zero hunger	Increased desertification and land degradation
		Impacts on agriculture: reduction in soil fertility, stability and water infiltration and retention characteristics
		Impacts on foraging: loss of food sources and conversion of vegetation
		Displacement and loss of livelihoods
		Women and girls tend to experience greater impacts from poverty, food insecurity, and displacement
5	Gender equality	Increased desertification and land degradation
		Impacts on agriculture: reduction in soil fertility, stability and water infiltration and retention characteristics
		Impacts on foraging: loss of food sources and conversion of vegetation
		Displacement and loss of livelihoods
		Women and girls tend to experience greater impacts from poverty, food insecurity, and displacement
3	Good health and well-being	Loss of environmental values
		Pressure on health and other services
		Loss of historically and culturally important nature, artifacts, places, and buildings
		Loss of homes/livelihoods
		Impacts on mental health
		Food insecurity
		Decreased air quality
6	Clean water and sanitation	Post-fire runoff
		Increased nutrients, sediment, contaminants
		Loss of water and sanitation infrastructure
13	Climate action	Changes in albedo
		Release of greenhouse gases and particulate matter
14	Life below water	Post-fire runoff
		Increased nutrients, sediment, contaminants
15	Life on land	Loss of ecosystems and biodiversity

Source: United Nations Environment Programme (2022).

Controversially, several environmental setbacks have been recorded in the Amazon (FERRANTE; FEARNSIDE, 2021, 2022; FERREIRA et al., 2014; MATAVELI; DE OLIVEIRA, 2022; RORATO et al., 2021; VILLÉN-PÉREZ et al., 2020). Many of these

setbacks and anti-environmental actions primarily impact protected areas. Instead of advancing in creating these areas, ensuring governance and better management, recurrent attacks on their existence drive illegal activities and invasion (FERRANTE; FEARNSIDE, 2022; MATAVELI; DE OLIVEIRA, 2022). Among the several negative impacts this scenario is causing, as previously detailed, it has also caused increased violence in these areas, a result of tension between traditional and indigenous communities and squatters (PHILLIPS, 2022). In this way, it is evident that measures need to be adopted urgently so that protected areas recover their governance and gain management capacity in order to be able to deliver all the benefits they are intended for.

Nevertheless, future studies are still needed to assess the full range of impacts fire can have on natural ecosystems inside and outside protected areas. Thus, it will be possible to inform policy and decision-makers of the risk magnitude to which these ecosystems may be exposed. In addition, further studies are also needed to assess the effectiveness of different protected areas categories concerning fire-related impacts to support specific actions according to the fire use context. Finally, it is imperative that a better understanding be prioritized of the social benefits of protected areas and the suitability of adopting alternatives to fire use as a tool by communities residing in these areas.

7 CONCLUDING REMARKS

This thesis provided evidence of the protected areas' effect on fire occurrence in the Amazon basin from 2003 to 2020, emphasizing their effectiveness in preventing fires and their critical role in maintaining essential ecosystem functions for biodiversity preservation and human well-being. The results presented here can support public policies or private actions aimed at improving the management of these areas to maximize their inhibitory effect against fire, as well as promoting studies to create new areas.

From 2003 to 2020, the Amazon basin registered an annual average of 79,196 km², with the burned area peak in 2010. Of the total area that burned throughout this period, only 28% was registered within protected areas. Among what annually burns inside protected areas, 17% are registered within Indigenous lands, and only 3% within Indirect Use protected areas. Although Brazil is the country that registered the highest burned area rate per year (51,304 km²), Suriname (74%) and Bolivia (42%) are the ones that registered the greatest shares of what burns inside protected areas. On average, it burned 14,438 km² of old-growth forests annually, representing 18% of the total. Of that, 75% is registered outside protected areas annually, and 15% is within Indigenous lands. Bolivia is the country that burns the largest share of forest, considering the total forested area in each country.

Even though protected areas have recorded significantly smaller burned areas than their surroundings over the years, the proportion of inside burning in relation to the total burned per year has been increasing in recent years, signaling an increase in the threat to which these areas are exposed. This growing threat is also evidenced by the increase in deforestation within these areas, the forest fragmentation, the increase in population, and the local climate change, which is already perceived in several parts of the Amazon basin. These factors combined to transform a humid tropical environment, even if reasonably preserved as protected areas, into a fire-prone system. However, even with all these factors present, fire does not occur in this environment if there is no fire ignition. This thesis showed that, like the burned area, the proportion of fire ignitions that occur within protected areas in relation to the total detected annually is increasing over the years. Even so, 85% of all the area that burns inside protected areas started with ignitions outside these areas, which shows that they are victims of the forest degradation that occurs around them

and depend not only on their inside preservation but on the maintenance of their buffer zones.

The change in the way of quantifying the effect of protected areas on fire occurrence, obtained in Chapter 5, improved the estimates and contributed to the extensive literature that proposes unbiased methods to assess the causal effects of environmental programs. These estimates indicated a negative effect of protection on fire occurrence, translated into 2 ha of avoided burned area per year within protected areas.

REFERENCES

ABADIE, A.; IMBENS, G. W. Large sample properties of matching estimators for average treatment effects. **Econometrica**, v. 74, n. 1, p. 235–267, 2006.

ABADIE, A.; IMBENS, G. W. Bias-corrected matching estimators for average treatment effects. **Journal of Business & Economic Statistics**, v. 29, n. 1, p. 1–11, 2011.

ALENCAR, A. A. C. et al. Long-term Landsat-based monthly burned area dataset for the brazilian biomes using deep learning. **Remote Sensing**, v. 14, n. 11, p. 2510, 2022.

ALENCAR, A. A.; NEPSTAD, D.; MOUTINHO, P. Carbon emissions associated with forest fires in Brazil. In: MOUTINHO, P.; SCHWARTZMAN, S. (Ed.). **Tropical deforestation and climate change**. [S.l.]: IPAM, 2009. p. 132.

ALENCAR, A.; NEPSTAD, D.; DIAZ, M. C. V. Forest understory fire in the brazilian Amazon in ENSO and Non-ENSO years: area burned and committed carbon emissions. **Earth Interactions**, v. 10, n. 6, p. 1–17, 2006.

ALENCAR, A.; RODRIGUES, L.; CASTRO, I. **Amazônia em chamas: o que queima - e onde**. Brasília: IPAM Amazônia, 2020.

ALIX-GARCIA, J. M.; SIMS, K. R. E.; YAÑEZ-PAGANS, P. Only one tree from each seed? environmental effectiveness and poverty alleviation in Mexico's payments for ecosystem services program. **American Economic Journal: Economic Policy**, v. 7, n. 4, p. 1–40, 2015.

ALMEIDA, C. T. et al. Spatiotemporal rainfall and temperature trends throughout the brazilian Legal Amazon, 1973-2013. **International Journal of Climatology**, v. 37, n. 4, p. 2013–2026, 2017.

ALMEIDA, D. R. A. DE et al. Contrasting fire damage and fire susceptibility between seasonally flooded forest and upland forest in the Central Amazon using portable profiling LiDAR. **Remote Sensing of Environment**, v. 184, p. 153–160, 2016.

ALONSO-CANAS, I.; CHUVIECO, E. Global burned area mapping from ENVISAT-MERIS and MODIS active fire data. **Remote Sensing of Environment**, v. 163, p. 140–152, 2015.

AMIN, A. et al. Neighborhood effects in the Brazilian Amazônia: protected areas and deforestation. **Journal of Environmental Economics and Management**, v. 93, p. 272–288, 2019.

ANDAM, K. S. et al. Measuring the effectiveness of protected area networks in reducing deforestation. **Proceedings of the National Academy of Sciences**, v. 105, n. 42, p. 16089–16094, 2008.

ANDELA, N. et al. A human-driven decline in global burned area. **Science**, v. 356, n. 6345, p. 1356–1362, 2017.

ANDELA, N. et al. The global fire atlas of individual fire size, duration, speed and direction. **Earth System Science Data**, v. 11, n. 2, p. 529–552, 2019.

ANDERSON, L. O. et al. Detecção de cicatrizes de áreas queimadas baseada no modelo linear de mistura espectral e imagens índice de vegetação utilizando dados multitemporais do sensor MODIS/TERRA no estado do Mato Grosso, Amazônia brasileira. **Acta Amazonica**, v. 35, n. 4, p. 445–456, 2005.

ANDERSON, L. O. et al. Disentangling the contribution of multiple land covers to fire-mediated carbon emissions in Amazonia during the 2010 drought: drought, fire and C emission in Amazonia. **Global Biogeochemical Cycles**, v. 29, n. 10, p. 1739–1753, 2015.

ANDERSON, L. O. et al. Development of a point-based method for map validation and confidence interval estimation: a case study of burned areas in Amazonia. **Journal of Remote Sensing & GIS**, v. 06, n. 01, 2017.

ANDERSON, L. O. et al. Vulnerability of Amazonian forests to repeated droughts. **Philosophical Transactions of the Royal Society B: Biological Sciences**, v. 373, n. 1760, e 20170411, 2018.

ANDERSON, L. O. et al. Modelo conceitual de sistema de alerta e de gestão de riscos e desastres associados a incêndios florestais e desafios para políticas públicas no Brasil. **Territorium**, v. 26, n.1, p. 43–61, 2019.

ANDERSON, L. O. et al. An alert system for seasonal fire probability forecast for South American protected areas. **Climate Resilience and Sustainability**, 2021.

ANDREAE, M. O. et al. Smoking rain clouds over the Amazon. **Science, New Series**, v. 303, n. 5662, p. 1337–1342, 2004.

ANGRIST, J. D.; PISCHKE, J. S. **Mostly harmless econometrics: an empiricist's companion**. [S.l.]: Princeton University Press, 2008.

ARAGÃO, L. E. O. C. et al. Spatial patterns and fire response of recent Amazonian droughts. **Geophysical Research Letters**, v. 34, n. 7, L07701, 2007.

ARAGÃO, L. E. O. C. et al. Interactions between rainfall, deforestation and fires during recent years in the Brazilian Amazonia. **Philosophical Transactions of the Royal Society B: Biological Sciences**, v. 363, n. 1498, p. 1779–1785, 2008.

ARAGÃO, L. E. O. C. et al. 21st Century drought-related fires counteract the decline of Amazon deforestation carbon emissions. **Nature Communications**, v. 9, n. 1, p. 536, 2018.

ARAGÃO, L. E. O. C.; SHIMABUKURO, Y. E. The Incidence of fire in Amazonian forests with implications for REDD. **Science**, v. 328, n. 5983, p. 1275–1278, 2010.

ARMENTERAS, D. et al. Changing patterns of fire occurrence in proximity to forest edges, roads and rivers between NW Amazonian countries. **Biogeosciences**, v. 14, n. 11, p. 2755–2765, 2017.

ARMENTERAS, D. et al. Curb land grabbing to save the Amazon. **Nature Ecology & Evolution**, v. 3, n. 11, p. 1497–1497, 2019.

ARMENTERAS, D. et al. Fire-induced loss of the world's most biodiverse forests in Latin America. **Science Advances**, v. 7, n. 33, eabd3357, 2021.

ARMENTERAS, D.; SCHNEIDER, L.; DÁVALOS, L. M. Fires in protected areas reveal unforeseen costs of Colombian peace. **Nature Ecology & Evolution**, v. 3, n. 1, p. 20–23, 2019.

ARRIAGADA, R. A.; ECHEVERRIA, C. M.; MOYA, D. E. Creating protected areas on public lands: is there room for additional conservation? **Plos One**, v. 11, n. 2, e0148094, 2016.

ARTÉS, T. et al. A global wildfire dataset for the analysis of fire regimes and fire behaviour. **Scientific Data**, v. 6, n. 1, p. 296, 2019.

ASSUNÇÃO, J.; GANDOUR, C.; ROCHA, R. Deforestation slowdown in the Brazilian Amazon: prices or policies? **Environment and Development Economics**, v. 20, n. 6, p. 697–722, 2015.

ASSUNÇÃO, J.; ROCHA, R. Getting greener by going black: the effect of blacklisting municipalities on Amazon deforestation. **Environment and Development Economics**, v. 24, n. 2, p. 115–137, 2019.

BACCINI, A. et al. Estimated carbon dioxide emissions from tropical deforestation improved by carbon-density maps. **Nature Climate Change**, v. 2, n. 3, p. 182–185, 2012.

BALCH, J. K. et al. Size, species, and fire behavior predict tree and liana mortality from experimental burns in the Brazilian Amazon. **Forest Ecology and Management**, v. 261, n. 1, p. 68–77, 2011.

BALCH, J. K. et al. The susceptibility of southeastern Amazon forests to fire: insights from a large-scale burn experiment. **BioScience**, v. 65, n. 9, p. 893–905, 2015.

BALTAR, V. T.; SOUSA, C. A. DE; WESTPHAL, M. F. Mahalanobis' distance and propensity score to construct a controlled matched group in a Brazilian study of health promotion and social determinants. **Revista Brasileira de Epidemiologia**, v. 17, n. 3, p. 668–679, 2014.

BARBER, C. P. et al. Roads, deforestation, and the mitigating effect of protected areas in the Amazon. **Biological Conservation**, v. 177, p. 203–209, 2014.

BARBOSA, R. I.; FEARNSIDE, P. M. Incêndios na Amazônia brasileira: estimativa da emissão de gases do efeito estufa pela queima de diferentes ecossistemas de Roraima na

passagem do evento “El Nino” (1997/98). **Acta Amazonica**, v. 29, n. 4, p. 513–534, 1999.

BARLOW, J. et al. Large tree mortality and the decline of forest biomass following Amazonian wildfires. **Ecology Letters**, v. 6, n. 1, p. 6–8, 2002.

BARLOW, J. et al. Clarifying Amazonia’s burning crisis. **Global Change Biology**, v. 26, n. 2, p. 319–321, 2020.

BASTARRIKA, A. et al. BAMS: a tool for supervised burned area mapping using Landsat data. **Remote Sensing**, v. 6, n. 12, p. 12360–12380, 2014.

BEHLING, H. et al. Late Quaternary Araucaria forest, grassland (Campos), fire and climate dynamics, studied by high-resolution pollen, charcoal and multivariate analysis of the Cambará do Sul core in southern Brazil. **Palaeogeography, Palaeoclimatology, Palaeoecology**, v. 203, n. 3, p. 277–297, 2004.

BERENGUER, E. et al. A large-scale field assessment of carbon stocks in human-modified tropical forests. **Global Change Biology**, v. 20, n. 12, p. 3713–3726, 2014.

BERENGUER, E. et al. Tracking the impacts of El Niño drought and fire in human-modified Amazonian forests. **Proceedings of the National Academy of Sciences**, v. 118, n. 30, e2019377118, 2021.

BERTRAND, M.; DUFLO, E.; MULLAINATHAN, S. How much should we trust Differences-in-Differences estimates?. **The Quarterly Journal of Economics**, v. 119, n. 1, p. 249–275, 2004.

BIVAND, R.; RUNDEL, C. **rgeos: Interface to Geometry Engine - Open Source ('GEOS')**. 2018. Available from: https://rdrr.io/cran/rgeos/.

BONILLA-MEJÍA, L.; HIGUERA-MENDIETA, I. Protected areas under weak institutions: evidence from Colombia. **World Development**, v. 122, p. 585–596, 2019.

BOSCHETTI, L. et al. Global validation of the collection 6 MODIS burned area product. **Remote Sensing of Environment**, v. 235, e 111490, 2019.

BOSCHETTI, M.; STROPPIANA, D.; BRIVIO, P. A. Mapping burned areas in a mediterranean environment ssing soft integration of spectral indices from high-resolution satellite images. **Earth Interactions**, v. 14, n. 17, p. 1–20, 2010.

BRANCALION, P. H. S. et al. Fake legal logging in the Brazilian Amazon. **Science Advances**, v. 4, n. 8, eaat1192, 2018.

BRANDO, P. M. et al. Fire-induced tree mortality in a neotropical forest: the roles of bark traits, tree size, wood density and fire behavior. **Global Change Biology**, v. 18, n. 2, p. 630–641, 2012.

BRANDO, P. M. et al. Abrupt increases in Amazonian tree mortality due to drought–fire interactions. **Proceedings of the National Academy of Sciences**, v. 111, n. 17, p. 6347–6352, . 2014.

BRASIL. MINISTÉRIO DO MEIO AMBIENTE (MMA).**Plano de ação para prevenção e controle do desmatamento na Amazônia Legal**. Brasília: MMA, 2004.

BRASIL. PRESIDÊNCIA DA REPÚBLICA. **Constituição da República Federativa do Brasil.** 1988. Available from: http://www.planalto.gov.br/ccivil_03/constituicao/constituicao.htm. Access on: 11 Nov. 2017

BRASIL. PRESIDÊNCIA DA REPÚBLICA. **Decreto nº 2661, de 8 de julho de 1998:** regulamenta o parágrafo único do art. 27 da Lei nº 4.771, de 15 de setembro de 1965 (código florestal), mediante o estabelecimento de normas de precaução relativas ao emprego do fogo em práticas agropastoris e floretais. 1998. Available from: http://www.planalto.gov.br/ccivil_03/decreto/D2661.htm.

BRASIL. PRESIDÊNCIA DA REPÚBLICA. **Lei nº 12651, de 25 de maio de 2012:** dispõe sobre a proteção da vegetação nativa; altera as Leis nos 6.938, de 31 de agosto de 1981, 9.393, de 19 de dezembro de 1996, e 11.428, de 22 de dezembro de 2006; revoga as Leis nos 4.771, de 15 de setembro de 1965, 2012. Available from: http://www.planalto.gov.br/ccivil_03/_Ato2011-2014/2012/Lei/L12651.htm.

BRASIL. PRESIDÊNCIA DA REPÚBLICA. **Lei nº 13465, de 11 de julho de 2017:** dispõe sobre a regularização fundiária rural e urbana, sobre a liquidação de créditos concedidos aos assentados da reforma agrária e sobre a regularização fundiária no âmbito da Amazônia Legal., 2017. Available from: http://www.planalto.gov.br/ccivil_03/_ato2015-2018/2017/lei/l13465.htm.

BRASIL. PRESIDÊNCIA DA REPÚBLICA. **Decreto Nº 9.578, de 22 de novembro de 2018:** consolida atos normativos editados pelo Poder Executivo federal que dispõem sobre o Fundo Nacional sobre Mudança do Clima, de que trata a Lei nº 12.114, de 9 de dezembro de 2009, e a Política Nacional sobre Mudanças climáticas. 2018. Available from: http://www.planalto.gov.br/ccivil_03/_Ato2015-2018/2018/Decreto/D9578.htm#art25.

BRINCK, K. et al. High resolution analysis of tropical forest fragmentation and its impact on the global carbon cycle. **Nature Communications**, v. 8, n. 1, e14855, 2017.

BRITO, B. et al. Stimulus for land grabbing and deforestation in the Brazilian Amazon. **Environmental Research Letters**, v. 14, n. 6, e 064018, 2019.

BUSH, M. B. et al. Fire, climate change and biodiversity in Amazonia: a Late-Holocene perspective. **Philosophical Transactions of the Royal Society B: Biological Sciences**, v. 363, n. 1498, p. 1795–1802, 2008.

CAMPANHARO, W. et al. Translating fire impacts in southwestern Amazonia into economic costs. **Remote Sensing**, v. 11, n. 7, p. 764, 2019.

CAMPANHARO, W. A. et al. Hospitalization due to fire-induced pollution in the brazilian Legal Amazon from 2005 to 2018. **Remote Sensing**, v. 14, n. 1, p. 69, 2021.

CANO-CRESPO, A. et al. Forest edge burning in the Brazilian Amazon promoted by escaping fires from managed pastures: management fires burn tropical forests. **Journal of Geophysical Research: Biogeosciences**, v. 120, n. 10, p. 2095–2107, 2015.

CARDOZO, F. et al. Analysis and assessment of the spatial and temporal distribution of burned areas in the Amazon forest. **Remote Sensing**, v. 6, n. 9, p. 8002–8025, 2014.

CARMO, C. N. et al. Associação entre material particulado de queimadas e doenças respiratórias na região sul da Amazônia brasileira. **Revista Panamericana de Salud Pública**, v. 27, n. 1, p. 10–16, 2010.

CARVALHO, N. et al. The distribution and overlap of public and private lands in the Brazilian Amazon. Submitted.

CARVALHO, N. S. et al. Spatio-temporal variation in dry season determines the Amazonian fire calendar. **Environmental Research Letters**, v. 16, n. 12, e 125009, 2021.

CENTER FOR INTERNATIONAL EARTH SCIENCE INFORMATION NETWORK (CIESIN) et al. **Global rural-urban mapping project, version 1 (GRUMPv1): urban extents grid.** Columbia University, 2011. Available from: <https://sedac.ciesin.columbia.edu/data/collection/grump-v1>. Access on: 5 May 2022.

CENTER FOR INTERNATIONAL EARTH SCIENCE INFORMATION NETWORK-CIESIN-COLUMBIA UNIVERSITY. **Documentation for the gridded population of the world, version 4 (GPWv4), revision 11 data sets**. [S.l.]: Columbia University, 2018.

CHAGAS, A. L. S.; AZZONI, C. R.; ALMEIDA, A. N. A spatial difference-in-differences analysis of the impact of sugarcane production on respiratory diseases. **Regional Science and Urban Economics**, v. 59, p. 24–36, 2016.

CHAVE, J. et al. Improved allometric models to estimate the aboveground biomass of tropical trees. **Global Change Biology**, v. 20, n. 10, p. 3177–3190, 2014.

CHEN, Y. et al. A pan-tropical cascade of fire driven by El Niño/ Southern Oscillation. **Nature Climate Change**, v. 7, p. 8, 2017.

CHUVIECO, E. et al. Generation and analysis of a new global burned area product based on MODIS 250 m reflectance bands and thermal anomalies. **Earth System Science Data**, v. 10, n. 4, p. 2015–2031, 2018.

CHUVIECO, E. et al. Historical background and current developments for mapping burned area from satellite Earth observation. **Remote Sensing of Environment**, v. 225, p. 45–64, 2019.

CHUVIECO, E.; MARTÍN, M. P.; PALACIOS, A. Assessment of different spectral indices in the red-near-infrared spectral domain for burned land discrimination. **International Journal of Remote Sensing**, v. 23, n. 23, p. 5103–5110, 2002.

CISNEROS, E.; ZHOU, S. L.; BÖRNER, J. Naming and shaming for conservation: evidence from the brazilian Amazon. **Plos One**, v. 10, n. 9, e0136402, 2015.

COCHRANE, M. A. Fire science for rainforests. **Nature**, v. 421, n. 6926, p. 913–919, 2003.

COCHRANE, M. A.; SCHULZE, M. D. Fire as a recurrent event in tropical forests of the eastern amazon: effects on forest structure, biomass, and species composition1. **Biotropica**, v. 31, n. 1, p. 2–16, 1999.

COUTINHO, A. C. et al. **TerraClass**. São José dos Campos: INPE, 2013.

COX, P. M. et al. Increasing risk of Amazonian drought due to decreasing aerosol pollution. **Nature**, v. 453, n. 7192, p. 212–215, 2008.

DA PONTE, E. et al. Assessing the wildfire activity in protected areas of the Amazon basin. In: EGU GENERAL ASSEMBLY, 2021. **Abstracts….** [S.l.]: EGU, 2021. p. EGU21-7200.

DE AZEVEDO, T. R. et al. SEEG initiative estimates of Brazilian greenhouse gas emissions from 1970 to 2015. **Scientific Data**, v. 5, n. 1, e 180045, 2018.

DE OLIVEIRA, G. et al. Rapid recent deforestation incursion in a vulnerable indigenous land in the brazilian Amazon and fire-driven emissions of fine particulate aerosol pollutants. **Forests**, v. 11, n. 8, p. 829, 2020.

DINIZ, C. G. et al. DETER-B: The new Amazon near real-time deforestation detection system. **IEEE Journal of Selected Topics in Applied Earth Observations and Remote Sensing**, v. 8, n. 7, p. 3619–3628, 2015.

DIPRETE, T. A.; GANGL, M. Assessing bias in the estimation of causal effects: Rosenbaum bounds on matching estimators and instrumental variables estimation with imperfect instruments. **Sociological Methodology**, v. 34, n. 1, p. 271–310, 2004.

ELOY, L. et al. From fire suppression to fire management: advances and resistances to changes in fire policy in the savannas of Brazil and Venezuela. **The Geographical Journal**, v. 185, n. 1, p. 10–22, 2019.

EUFEMIA, L. et al. Fires in the Amazon region: quick policy review. **Development Policy Review**, e12620, 2022.

EVA, H. D.; HUBER, O. **A proposal for defining the geographical boundaries of Amazonia**. Luxembourg: Luxembourg: Office for Official Publications of the European Communities, 2005.

FANIN, T.; VAN DER WERF, G. R. Relationships between burned area, forest cover loss, and land cover change in the Brazilian Amazon based on satellite data. **Biogeosciences**, v. 12, n. 20, p. 6033–6043, 2015.

FERRANTE, L.; FEARNSIDE, P. M. Brazil's political upset threatens Amazonia. **Science**, v. 371, n. 6532, p. 898–898, 2021.

FERRANTE, L.; FEARNSIDE, P. M. Mining and Brazil's Indigenous peoples. **Science**, v. 375, n. 6578, p. 276–276, 2022.

FERRARO, P. J. Counterfactual thinking and impact evaluation in environmental policy. **New Directions for Evaluation**, v. 2009, n. 122, p. 75–84, 2009.

FERRARO, P. J.; HANAUER, M. M. Quantifying causal mechanisms to determine how protected areas affect poverty through changes in ecosystem services and infrastructure. **Proceedings of the National Academy of Sciences**, v. 111, n. 11, p. 4332–4337, 2014.

FERRARO, P. J.; MIRANDA, J. J. Panel data designs and estimators as substitutes for randomized controlled trials in the evaluation of public programs. **Journal of the Association of Environmental and Resource Economists**, v. 4, n. 1, p. 281–317, 2017.

FERREIRA, J. et al. Brazil's environmental leadership at risk. **Science**, v. 346, n. 6210, p. 706–707, 2014.

FINER, M. et al. Future of oil and gas development in the western Amazon. **Environmental Research Letters**, v. 10, n. 2, e 024003, 2015.

FISCHER, G. et al. **Global Agro-ecological Zones Assessment for Agriculture (GAEZ).** IIASA; FAO, 2008. Available from: <https://gaez.fao.org/>. Access on: 5 May 2022

FORNACCA, D.; REN, G.; XIAO, W. Performance of three MODIS fire products (MCD45A1, MCD64A1, MCD14ML), and ESA Fire_CCI in a mountainous area of northwest Yunnan, China, characterized by frequent small fires. **Remote Sensing**, v. 9, n. 11, p. 1131, 2017.

FRAMEWORK CONVENTION ON CLIMATE CHANGE (FCCC). **Nationally determined contributions under the Paris Agreement.** United Nations, 2021. Available from: <https://unfccc.int/documents/306848>. Access on: 23 June 2022

FRIEDLINGSTEIN, P. et al. Update on CO2 emissions. **Nature Geoscience**, v. 3, n. 12, p. 811–812, 2010.

FUNDACIÓN SOLÓN. **Las leyes incendiarias en Bolivia**. 2020. Available from: <https://fundacionsolon.org>.

FUNK, C. et al. The climate hazards infrared precipitation with stations—a new environmental record for monitoring extremes. **Scientific Data**, v. 2, n. 1, e 150066, 2015.

GALIANI, S.; GERTLER, P.; SCHARGRODSKY, E. Water for life: the impact of the privatization of water services on child mortality. **Journal of Political Economy**, v. 113, n. 1, p. 83–120, 2005.

GATTI, L. V. et al. Drought sensitivity of Amazonian carbon balance revealed by atmospheric measurements. **Nature**, v. 506, n. 7486, p. 76–80, 2014.

GATTI, L. V. et al. Amazonia as a carbon source linked to deforestation and climate change. **Nature**, v. 595, n. 7867, p. 388–393, 2021.

GELDMANN, J. et al. Effectiveness of terrestrial protected areas in reducing habitat loss and population declines. **Biological Conservation**, v. 161, p. 230–238, 2013.

GIGLIO, L. **MODIS thermal anomalies/fire products.** NASA, 2000. Available from: <https://earthdata.nasa.gov/earth-observation-data/near-real-time/firms/mcd14ml>. Access on: 5 May 2022.

GIGLIO, L. et al. **MCD64A1 MODIS/Terra+Aqua burned area monthly L3 global 500m SIN grid V006.** NASA, 2015. Available from: <https://lpdaac.usgs.gov/products/mcd64a1v006/>. Access on: 5 May 2022.

GIGLIO, L. et al. An enhanced contextual fire detection algorithm for MODIS. **Remote Sensing of Environment**, v. 87, n. 2–3, p. 273–282, 2003.

GIGLIO, L. et al. The collection 6 MODIS burned area mapping algorithm and product. **Remote Sensing of Environment**, v. 217, p. 72–85, 2018.

GIGLIO, L.; RANDERSON, J. T.; VAN DER WERF, G. R. Analysis of daily, monthly, and annual burned area using the fourth-generation global fire emissions database (GFED4): analysis of burned area. **Journal of Geophysical Research: Biogeosciences**, v. 118, n. 1, p. 317–328, 2013.

GIGLIO, L.; SCHROEDER, W.; JUSTICE, C. O. The collection 6 MODIS active fire detection algorithm and fire products. **Remote Sensing of Environment**, v. 178, p. 31–41, 2016.

GORELICK, N. et al. Google Earth engine: planetary-scale geospatial analysis for everyone. **Remote Sensing of Environment**, v. 202, p. 18–27, 2017.

HAALBOOM, B. J.; CAMPBELL, L. M. Scale, networks, and information strategies: exploring indigenous peoples' refusal of a protected area in Suriname. **Global Networks**, v. 12, n. 3, p. 375–394, 2012.

HANNAH, L. Protected areas and climate change. **Annals of the New York Academy of Sciences**, v. 1134, n. 1, p. 201–212, 2008.

HANTSON, S.; PUEYO, S.; CHUVIECO, E. Global fire size distribution is driven by human impact and climate: spatial trends in global fire size distribution. **Global Ecology and Biogeography**, v. 24, n. 1, p. 77–86, 2015.

HAUGAASEN, T.; BARLOW, J.; PERES, C. A. Surface wildfires in central Amazonia: short-term impact on forest structure and carbon loss. **Forest Ecology and Management**, v. 179, n. 1–3, p. 321–331,2003.

HAWBAKER, T. J. et al. Mapping burned areas using dense time-series of Landsat data. **Remote Sensing of Environment**, v. 198, p. 504–522, 2017.

HECKMAN, J. J.; ICHIMURA, H.; TODD, P. Matching as an econometric evaluation estimator. **Review of Economic Studies**, v. 65, n. 2, p. 261–294, 1998.

HERRERA, D.; PFAFF, A.; ROBALINO, J. Impacts of protected areas vary with the level of government: comparing avoided deforestation across agencies in the Brazilian Amazon. **Proceedings of the National Academy of Sciences**, v. 116, n. 30, p. 14916–14925, 2019.

HIJMANS, R. J. **raster: Geographic Data Analysis and Modeling**. 2017. Available from: https://cran.r-project.org/web/packages/raster/raster.pdf.

HUMBER, M. L. et al. Spatial and temporal intercomparison of four global burned area products. **International Journal of Digital Earth**, v. 12, n. 4, p. 460–484, 2019.

IMBENS, G. W. Matching methods in practice: three examples. **Journal of Human Resources**, v. 50, n. 2, p. 373–419, 2015.

IMBENS, G. W.; WOOLDRIDGE, J. M. Recent developments in the econometrics of program evaluation. **Journal of Economic Literature**, v. 47, n. 1, p. 5–86, 2009.

INSTITUTO BRASILEIRO DE GEOGRAFIA E ESTATÍSTICA (IBGE). **Base de informações do censo demográfico 2010: resultados do universo por setor censitário.** Rio de Janeiro: IBGE, 2011. Available from: <http://www.censo2010.ibge.gov.br/resultados>. Access on: 1 Mar. 2018.

INSTITUTO NACIONAL DE PESQUISAS ESPACIAIS (INPE). **Portal do monitoramento de queimadas e incêndios**. São José dos Campos: INPE, 2017. Available from: <http://www.inpe.br/queimadas>.

INSTITUTO NACIONAL DE PESQUISAS ESPACIAIS (INPE). **Projeto de Monitoramento do Desmatamento na Amazônia Brasileira por Satélite (PRODES)**. São José dos Campos: INPE, 2022. Available from: <http://www.obt.inpe.br/OBT/assuntos/programas/amazonia/prodes>.

INTERGOVERNMENTAL PANEL ON CLIMATE CHANGE (IPCC). **Fifth assessment report of the intergovernmental panel on climate change**. New York: Cambridge University Press, 2013.

JARVIS, A. et al. **Hole-filled SRTM for the globe version 4, available from the CGIAR-CSI SRTM 90m database.** CGIAR Consortium for Spatial Information, 2008. Available from: <http://srtm.csi.cgiar.org/>. Access on: 5 May 2022

JIMÉNEZ-MUÑOZ, J. C. et al. Record-breaking warming and extreme drought in the Amazon rainforest during the course of El Niño 2015–2016. **Scientific Reports**, v. 6, p. 33130, 2016.

JOLLY, W. M. et al. Climate-induced variations in global wildfire danger from 1979 to 2013. **Nature Communications**, v. 6, n. 1, p. 7537, 2015.

JONES, K. W.; LEWIS, D. J. Estimating the counterfactual impact of conservation programs on land cover outcomes: the role of matching and panel regression techniques. **Plos One**, v. 10, n. 10, e0141380, 2015.

JOPPA, L. N.; PFAFF, A. Global protected area impacts. **Proceedings of the Royal Society B: Biological Sciences**, v. 278, n. 1712, p. 1633–1638, 2011.

JUSTICE, C. O. et al. The MODIS fire products. **Remote Sensing of Environment**, v. 83, n. 1–2, p. 244–262, 2002.

KAUFFMAN, J. B.; CUMMINGS, D. L.; WARD, D. E. Relationships of fire, biomass and nutrient dynamics along a vegetation gradient in the brazilian Cerrado. **The Journal of Ecology**, v. 82, n. 3, p. 519, 1994.

KING, G.; NIELSEN, R. Why propensity scores should not be used for matching. **Political Analysis**, v. 27, n. 4, p. 435–454, 2019.

KNORR, W. et al. Impact of human population density on fire frequency at the global scale. **Biogeosciences**, v. 11, n. 4, p. 1085–1102, 2014.

LAURANCE, W. F. et al. An Amazonian rainforest and its fragments as a laboratory of global change. **Biological Reviews**, v. 93, n. 1, p. 223–247, 2018.

LAURANCE, W. F.; WILLIAMSON, G. B. Positive feedbacks among forest fragmentation, drought, and climate change in the Amazon. **Conservation Biology**, v. 15, n. 6, p. 1529–1535, 2001.

LEHNER, B.; VERDIN, K.; JARVIS, A. New global hydrography derived from spaceborne elevation data. **Eos, Transactions American Geophysical Union**, v. 89, n. 10, p. 93, 2008.

LEUVEN, E.; SIANESI, B. **PSMATCH2: Stata module to perform full Mahalanobis and propensity score matching, common support graphing, and covariate imbalance testing**. 2003. Available from: https://ideas.repec.org/c/boc/bocode/s432001.html.

LI, W. et al. Observed change of the standardized precipitation index, its potential cause and implications to future climate change in the Amazon region. **Philosophical**

Transactions of the Royal Society B: Biological Sciences, v. 363, n. 1498, p. 1767–1772, 2008.

LI, W.; FU, R.; DICKINSON, R. E. Rainfall and its seasonality over the Amazon in the 21st century as assessed by the coupled models for the IPCC AR4. **Journal of Geophysical Research**, v. 111, n. D2, D02111, 2006.

LIMA, A. et al. Land use and land cover changes determine the spatial relationship between fire and deforestation in the Brazilian Amazon. **Applied Geography**, v. 34, p. 239–246, 2012.

LIMA, C. H. R.; AGHAKOUCHAK, A.; RANDERSON, J. T. Unraveling the role of temperature and rainfall on active fires in the brazilian Amazon using a nonlinear poisson model. **Journal of Geophysical Research: Biogeosciences**, v. 123, n. 1, p. 117–128, 2018.

LINKE, S. et al. Global hydro-environmental sub-basin and river reach characteristics at high spatial resolution. **Scientific Data**, v. 6, n. 1, p. 283, 2019.

LIZUNDIA-LOIOLA, J. et al. A spatio-temporal active-fire clustering approach for global burned area mapping at 250 m from MODIS data. **Remote Sensing of Environment**, v. 236, e 111493, 2020.

LLOYD, C. T. et al. Global spatio-temporally harmonised datasets for producing high-resolution gridded population distribution datasets. **Big Earth Data**, v. 3, n. 2, p. 108–139, 2019.

LONG, T. et al. 30 m Resolution global annual burned area mapping based on Landsat images and Google Earth Engine. **Remote Sensing**, v. 11, n. 5, p. 489, 2019.

LONGO, M. et al. Aboveground biomass variability across intact and degraded forests in the Brazilian Amazon. **Global Biogeochemical Cycles**, v. 30, n. 11, p. 1639–1660, 2016.

MAILLARD, O. et al. Relationship of forest cover fragmentation and drought with the occurrence of forest fires in the department of Santa Cruz, Bolivia. **Forests**, v. 11, n. 9, p. 910, 2020.

MALHI, Y. et al. Energy and water dynamics of a central Amazonian rain forest. **Journal of Geophysical Research: Atmospheres**, v. 107, n. D20, p. LBA 45-1-LBA 45-17, 2002.

MALHI, Y. et al. Climate change, deforestation, and the fate of the Amazon. **Science**, v. 319, n. 5860, p. 169–172, 2008.

MALHI, Y. et al. Exploring the likelihood and mechanism of a climate-change-induced dieback of the Amazon rainforest. **Proceedings of the National Academy of Sciences**, v. 106, n. 49, p. 20610–20615, 2009.

MAPBIOMAS. **Documento Teórico Base de Algoritmos (ATBD)** RAISG - MapBiomas Amazonía - Colección 3. [S.l.]: Mapbiomas, 2021.

MARENGO, J. A. et al. The drought of Amazonia in 2005. **Journal of Climate**, v. 21, n. 3, p. 495–516, 2008.

MARENGO, J. A. et al. The drought of 2010 in the context of historical droughts in the Amazon region: drought Amazon 2010. **Geophysical Research Letters**, v. 38, n. 12, 2011.

MARENGO, J. A. et al. Changes in climate and land use over the Amazon region: current and future variability and trends. **Frontiers in Earth Science**, v. 6, 2018.

MATAVELI, G. A. V. et al. The emergence of a new deforestation hotspot in Amazonia. **Perspectives in Ecology and Conservation**, v. 19, n. 1, p. 33–36, 2021.

MATAVELI, G.; DE OLIVEIRA, G. Protect the Amazon's indigenous lands. **Science**, v. 375, n. 6578, p. 275–276, 2022.

MATTHEWS, H. D.; WYNES, S. Current global efforts are insufficient to limit warming to 1.5°C. **Science**, v. 376, n. 6600, p. 1404–1409, 2022.

MEDDENS, A. J. H. et al. Spatiotemporal patterns of unburned areas within fire perimeters in the northwestern United States from 1984 to 2014. **Ecosphere**, v. 9, n. 2, e02029, 2018.

MELCHIORRE, A.; BOSCHETTI, L. Global analysis of burned area persistence time with MODIS data. **Remote Sensing**, v. 10, n. 5, p. 750, 2018.

MELILLO, J. M. et al. Protected areas' role in climate-change mitigation. **Ambio**, v. 45, n. 2, p. 133–145, 2016.

MESSINA, J. P.; COCHRANE, M. A. The forests are bleeding: how land use change is creating a new fire regime in the Ecuadorian Amazon. **Journal of Latin American Geography**, v. 6, n. 1, p. 85–100, 2007.

MISTRY, J. et al. New perspectives in fire management in South American savannas: the importance of intercultural governance. **Ambio**, v. 48, n. 2, p. 172–179, 2019.

MITHAL, V. et al. Mapping burned areas in tropical forests using a novel machine learning framework. **Remote Sensing**, v. 10, n. 2, p. 69, 2018.

MORELLO, T.; ANJOLIM, J. Gender wage discrimination in Brazil from 1996 to 2015: a matching analysis. **EconomiA**, v. 22, n. 2, p. 114–128, 2021.

MORITZ, M. A. et al. Learning to coexist with wildfire. **Nature**, v. 515, n. 7525, p. 58–66, 2014.

MORTON, D. C. et al. Cropland expansion changes deforestation dynamics in the southern Brazilian Amazon. **Proceedings of the National Academy of Sciences**, v. 103, n. 39, p. 14637–14641, 2006.

MORTON, D. C. et al. Agricultural intensification increases deforestation fire activity in Amazonia. **Global Change Biology**, v. 14, n. 10, p. 2262–2275, 2008.

MORTON, D. C. et al. Mapping canopy damage from understory fires in Amazon forests using annual time series of Landsat and MODIS data. **Remote Sensing of Environment**, v. 115, n. 7, p. 1706–1720, 2011.

MOUILLOT, F. et al. Ten years of global burned area products from spaceborne remote sensing—a review: analysis of user needs and recommendations for future developments. **International Journal of Applied Earth Observation and Geoinformation**, v. 26, p. 64–79, 2014.

MOURAO, P. R.; MARTINHO, V. D. Forest fire legislation: reactive or proactive? **Ecological Indicators**, v. 104, p. 137–144, 2019.

NAEHER, L. P. et al. Woodsmoke health effects: a review. **Inhalation Toxicology**, v. 19, n. 1, p. 67–106, 2007.

NAGELKERKE, N. J. D. A note on a general definition of the coefficient of determination. **Biometrika**, v. 78, n. 3, p. 691–692, 1991.

NAIDOO, R. et al. Evaluating the impacts of protected areas on human well-being across the developing world. **Science Advances**, v. 5, n. 4, eaav3006, 2019.

NELSON, A.; CHOMITZ, K. M. Effectiveness of strict vs. multiple use protected areas in reducing tropical forest fires: a global analysis using matching methods. **Plos One**, v. 6, n. 8, e22722, 2011.

NEPSTAD, D. et al. Inhibition of Amazon deforestation and fire by parks and indigenous lands: inhibition of Amazon deforestation and fire. **Conservation Biology**, v. 20, n. 1, p. 65–73, 2006.

NEPSTAD, D. et al. The end of deforestation in the Brazilian Amazon. **Science**, v. 326, n. 5958, p. 1350–1351, 2009.

NEPSTAD, D. C. et al. Large-scale impoverishment of Amazonian forests by logging and fire. **Nature**, v. 398, n. 6727, p. 505–508, 1999.

NOBRE, C. A. et al. Land-use and climate change risks in the Amazon and the need of a novel sustainable development paradigm. **Proceedings of the National Academy of Sciences**, v. 113, n. 39, p. 10759–10768, 2016.

NOGUEIRA, E. M. et al. Brazil's Amazonian protected areas as a bulwark against regional climate change. **Regional Environmental Change**, v. 18, n. 2, p. 573–579, 2018.

NOLTE, C. et al. Governance regime and location influence avoided deforestation success of protected areas in the Brazilian Amazon. **Proceedings of the National Academy of Sciences**, v. 110, n. 13, p. 4956–4961, 2013.

NOLTE, C. et al. Decentralized land use zoning reduces large-scale deforestation in a major agricultural frontier. **Ecological Economics**, v. 136, p. 30–40, 2017.

NOLTE, C.; AGRAWAL, A. Linking management effectiveness indicators to observed effects of protected areas on fire occurrence in the Amazon rainforest: management effectiveness and fire. **Conservation Biology**, v. 27, n. 1, p. 155–165, 2013.

OLIVEIRA, M. T. DE et al. Regeneration of riparian forests of the Brazilian Pantanal under flood and fire influence. **Forest Ecology and Management**, v. 331, p. 256–263, 2014.

OTÓN, G.; PETTINARI, M. L. **ESA CCI ECV fire disturbance: D3.3.4 product user guide - LTDR, version 1.0**. [S.l.: s.n.], 2019.

OVERBECK, G. E. et al. The South Brazilian grasslands – a South American tallgrass prairie? parallels and implications of fire dependency. **Perspectives in Ecology and Conservation**, v. 16, n. 1, p. 24–30, 2018.

PACHECO, C. E.; AGUADO, M. I.; MOLLICONE, D. Identification and characterization of deforestation hot spots in Venezuela using MODIS satellite images. **Acta Amazonica**, v. 44, n. 2, p. 185–196, 2014.

PADILLA, M. et al. Assessing the temporal stability of the accuracy of a time series of burned area products. **Remote Sensing**, v. 6, n. 3, p. 2050–2068, 2014.

PADILLA, M. et al. Comparing the accuracies of remote sensing global burned area products using stratified random sampling and estimation. **Remote Sensing of Environment**, v. 160, p. 114–121, 2015.

PAIVA, P. F. P. R. et al. Deforestation in protect areas in the Amazon: a threat to biodiversity. **Biodiversity and Conservation**, v. 29, n. 1, p. 19–38, 2020.

PAIVA, R. J. O.; BRITES, R. S.; MACHADO, R. B. The role of protected areas in the avoidance of anthropogenic conversion in a high pressure region: a matching method analysis in the core region of the brazilian Cerrado. **Plos One**, v. 10, n. 7, e0132582, 2015.

PARISIEN, M.-A.; MORITZ, M. A. Environmental controls on the distribution of wildfire at multiple spatial scales. **Ecological Monographs**, v. 79, n. 1, p. 127–154, 2009.

PAUSAS, J. G.; KEELEY, J. E. A burning story: the role of fire in the history of life. **BioScience**, v. 59, n. 7, p. 593–601, 2009.

PEDROSO JÚNIOR, N. N.; MURRIETA, R. S. S.; ADAMS, C. A agricultura de corte e queima: um sistema em transformação. **Boletim do Museu Paraense Emílio Goeldi – Ciências Humanas,** v. 3, n. 2, p. 22, 2008.

PEDROSO-JUNIOR, N. N.; ADAMS, C.; MURRIETA, R. S. S. Slash-and-burn agriculture: a system in transformation. In: LOPES, P.; BEGOSSI, A. (Ed.). **Current trends in human ecology**. Cambridge: Cambridge Scholars Publishing, 2009. p. 12–34.

PEIXOTO, B. et al. **Avaliação econômica de projetos sociais**. 3.ed. ed. São Paulo: Fundação Itaú Social, 2017.

PENHA, T. V. et al. Burned area detection in the Brazilian Amazon using spectral indices and GEOBIA. **Revista Brasileira de Cartografia**, v. 72, n. 2, p. 253–269, 2020.

PEREIRA, J. M. C. et al. Spectral characterisation and discrimination of burnt areas. In: CHUVIECO, E. (Ed.). **Remote sensing of large wildfires**. Berlin: Springer, 1999. p. 123–138.

PEREIRA, J. M. C. et al. A simulation analysis of the detectability of understory burns in miombo woodlands. **Remote Sensing of Environment**, v. 93, n. 3, p. 296–310, 2004.

PERZ, S. G.; ARAMBURÚ, C.; BREMNER, J. Population, land use and deforestation in the pan Amazon basin: a comparison of Brazil, Bolivia, Colombia, Ecuador, Perú and Venezuela. **Environment, Development and Sustainability**, v. 7, n. 1, p. 23–49, 2005.

PESSÔA, A. C. M. et al. Intercomparison of burned area products and its implication for carbon emission estimations in the Amazon. **Remote Sensing**, v. 12, n. 23, p. 3864, 2020.

PETRAS, J. The geopolitics of plan Colombia. **Monthly Review**, v. 53, n. 1, p. 30, 2001.

PETTINARI, M. L.; CHUVIECO, E. **ESA CCI ECV fire disturbance: D3.3.3 product user guide - MODIS, version 1.0**. [S.l.: s.n.], 2018.

PFAFF, A. et al. Governance, location and avoided deforestation from protected areas: greater restrictions can have lower impact, due to differences in location. **World Development**, v. 55, p. 7–20, 2014.

PFAFF, A. et al. Protected areas' impacts on Brazilian Amazon deforestation: examining conservation – development Interactions to Inform Planning. **PLOS ONE**, v. 10, n. 7, p. e0129460, 2015a.

PFAFF, A. et al. Protected area types, strategies and impacts in Brazil's Amazon: public protected area strategies do not yield a consistent ranking of protected area types by impact. **Philosophical Transactions of the Royal Society B: Biological Sciences**, v. 370, n. 1681, e 20140273, 2015b.

PHILLIPS, T. **How the final journey of Dom Phillips and Bruno Pereira ended in tragedy**. Available from: <https://www.theguardian.com/world/2022/jun/17/dom-phillips-bruno-pereira-final-journey>. Access on: 20 June 2022.

PIVELLO, V. R. The use of fire in the Cerrado and Amazonian rainforests of Brazil: past and present. **Fire Ecology**, v. 7, n. 1, p. 24–39, 2011.

PLENIOU, M.; KOUTSIAS, N. Sensitivity of spectral reflectance values to different burn and vegetation ratios: A multi-scale approach applied in a fire affected area. **ISPRS Journal of Photogrammetry and Remote Sensing**, v. 79, p. 199–210, 2013a.

PLENIOU, M.; KOUTSIAS, N. **Relationships between vegetation indices and different burn and vegetation ratios: a multi-scale approach applied in a fire affected area**. In: HADJIMITSIS, D. G. et al. (Ed.). **Proceedings of SPIE.** 2013b. Available from: <http://proceedings.spiedigitallibrary.org/proceeding.aspx?doi=10.1117/12.2028349>. Access on: 11 Sept. 2014.

R CORE TEAM. **R: a language and environment for statistical computing.** Vienna, Austria: R Foundation for Statistical Computing, 2020. Available fromn: https://www.r-project.org.

RANDERSON, J. T. et al. Global burned area and biomass burning emissions from small fires: BURNED AREA FROM SMALL FIRES. **Journal of Geophysical Research: Biogeosciences**, v. 117, n. G4, 2012.

RIBEIRO NETO, G. G. et al. Attributing the 2015/2016 Amazon basin drought to anthropogenic influence. **Climate Resilience and Sustainability**, v. 1, n. 1, e25, 2022.

RICKETTS, T. H. et al. Indigenous lands, protected areas, and slowing climate change. **PLoS Biology**, v. 8, n. 3, e1000331, 2010.

RIKS BV. **MCK reader: methods of the map comparison kit**. Maastricht: Research Institute for Knowledge Systems (RIKS BV), 2011. Available from: <http://www.riks.nl/mck>.

RIKS BV. **Map comparison Kit 3: user manual**. Maastricht: Researsh Institute for Knowledge Systems (RIKS BV), 2013. Available from: <http://www.riks.nl/mck>.

RODRIGUES, J. A. et al. How well do global burned area products represent fire patterns in the Brazilian Savannas biome? an accuracy assessment of the MCD64 collections. **International Journal of Applied Earth Observation and Geoinformation**, v. 78, p. 318–331, 2019.

RODRÍGUEZ, I. et al. **A Study of the use of fire and by Amerindian communities the South Rupununi, Guyana, with recommendations for sustainable land management**. [S.l.]: Forest Peoples Project, 2011.

RORATO, A. C. et al. Environmental threats over Amazonian indigenous lands. **Land**, v. 10, n. 3, p. 267, 2021.

ROSAN, T. M. **Estimativa de emissões de CO2 por desmatamento e degradação florestal utilizada como subsidio para definição de municípios prioritários para monitoramento e controle**. 2017. Dissertação (Mestrado em Sensoriamento Remoto) - Instituto Nacional de Pesquisas Espaciais - INPE, São José dos Campos, 2017.

ROSENBAUM, P. R. Sensitivity to hidden bias. In: ROSENBAUM, P. R. (Ed.). **Observational studies**. New York, NY: Springer, 2002. p. 105–170.

ROSENBAUM, P. R.; RUBIN, D. B. The bias due to incomplete matching. **Biometrics**, v. 41, n. 1, p. 103–116, 1985.

ROY, D. P.; BOSCHETTI, L. Southern Africa validation of the MODIS, L3JRC, and GlobCarbon burned-area products. **IEEE Transactions on Geoscience and Remote Sensing**, v. 47, n. 4, p. 1032–1044, 2009.

RUBIN, D. B. Using propensity scores to help design observational studies: application to the tobacco litigation. **Health Services and Outcomes Research Methodology**, v. 2, n. 3, p. 169–188, 2001.

RUDEL, T. K. et al. Changing drivers of deforestation and new opportunities for conservation. **Conservation Biology**, v. 23, n. 6, p. 1396–1405, 2009.

RUIZ, J. et al. Burned area mapping in the North American Boreal Forest using Terra-MODIS LTDR (2001–2011): a comparison with the MCD45A1, MCD64A1 and BA GEOLAND-2 products. **Remote Sensing**, v. 6, n. 1, p. 815–840, 2014.

RYAN, K. C. et al. **Wildland fire in ecosystems: effects of fire on cultural resources and archaeology**. Ft. Collins, CO: U.S. Department of Agriculture, 2012. Available from: <https://www.fs.usda.gov/treesearch/pubs/40417>. Access on: 25 Apr. 2022.

SALVIO, G. M. M.; GOMES, C. R. Protected area systems in South American countries. **Floresta e Ambiente**, v. 25, n. 4, 2018.

SANTOS, D.; SALOMÃO, R.; VERÍSSIMO, A. **Fatos da Amazônia 2021.** Imazon, 2021. Available from: <https://amazonia2030.org.br/fatos-da-amazonia-2021/>. Acesso em: 20 May 2022

SCHROEDER, W. et al. The New VIIRS 375 m active fire detection data product: algorithm description and initial assessment. **Remote Sensing of Environment**, v. 143, p. 85–96, 2014.

SHI, H. et al. Global protected areas boost the carbon sequestration capacity: evidences from econometric causal analysis. **Science of The Total Environment**, v. 715, p. 137001, 2020.

SHI, Y.; MATSUNAGA, T.; YAMAGUCHI, Y. High-resolution mapping of biomass burning emissions in three tropical regions. **Environmental Science & Technology**, v. 49, n. 18, p. 10806–10814, 2015.

SHIMABUKURO, Y. E. et al. Fraction images derived from Terra Modis data for mapping burnt areas in Brazilian Amazonia. **International Journal of Remote Sensing**, v. 30, n. 6, p. 1537–1546, 2009.

SHIMABUKURO, Y. E. et al. Assessment of forest degradation in Brazilian Amazon due to selective logging and fires using time series of fraction images derived from Landsat ETM+ images. **Remote Sensing Letters**, v. 5, n. 9, p. 773–782, 2014.

SHIMABUKURO, Y. E. et al. Estimating burned area in Mato Grosso, Brazil, using an object-based classification method on a systematic sample of medium resolution satellite images. **IEEE Journal of Selected Topics in Applied Earth Observations and Remote Sensing**, v. 8, n. 9, p. 4502–4508, 2015.

SILVA, C. V. J. et al. Drought-induced Amazonian wildfires instigate a decadal-scale disruption of forest carbon dynamics. **Philosophical Transactions of the Royal Society B: Biological Sciences**, v. 373, n. 1760, e 20180043, 2018a.

SILVA, S. S. DA et al. Dynamics of forest fires in the southwestern Amazon. **Forest Ecology and Management**, v. 424, p. 312–322, 2018b.

SILVA, J. M. N. et al. Assessing the feasibility of a global model for multi-temporal burned area mapping using spot-vegetation data. **International Journal of Remote Sensing**, v. 25, n. 22, p. 4889–4913, 2004.

SILVA JUNIOR, C. et al. Deforestation-induced fragmentation increases forest fire occurrence in central Brazilian Amazonia. **Forests**, v. 9, n. 6, p. 305, 2018.

SILVA JUNIOR, C. H. L. et al. Fire responses to the 2010 and 2015/2016 Amazonian droughts. **Frontiers in Earth Science**, v. 7, p. 97, 2019.

SILVA JUNIOR, C. H. L. et al. Persistent collapse of biomass in Amazonian forest edges following deforestation leads to unaccounted carbon losses. **Science Advances**, v. 6, n. 40, eaaz8360, 2020a.

SILVA JUNIOR, C. H. L. et al. Benchmark maps of 33 years of secondary forest age for Brazil. **Scientific Data**, v. 7, n. 1, p. 269, 2020b.

SILVA JUNIOR, C. H. L. et al. The Brazilian Amazon deforestation rate in 2020 is the greatest of the decade. **Nature Ecology & Evolution**, v. 5, n. 2, p. 144–145, 2021a.

SILVA JUNIOR, C. H. L. et al. **Global CHIRPS MCWD (Maximum Cumulative Water Deficit) dataset.** Zenodo, 2021b. Available from: <https://zenodo.org/record/4903340>. Acesso em: 5 May 2022

SILVA JUNIOR, C. H. L. et al. Amazonian forest degradation must be incorporated into the COP26 agenda. **Nature Geoscience**, v. 14, n. 9, p. 634–635, 2021c.

SILVA JUNIOR, C. A. DA et al. Fires drive long-term environmental degradation in the Amazon Basin. **Remote Sensing**, v. 14, n. 2, p. 338, 2022.

SILVA, S. et al. Queimadas urbanas em Rio Branco, Acre: mapeamento e comunicação de impactos à sociedade. In: SIMPÓSIO BRASILEIRO DE SENSORIAMENTO REMOTO, 19., 2019. **Anais...** São José dos Campos: INPE, 2019.

SILVA, S. S. et al. **Relatório executivo:qQueimadas 2019 - Acre**. Cruzeiro do Sul: Acre Queimadas, 2020.

SILVEIRA, M. V. F. et al. Drivers of fire anomalies in the Brazilian Amazon: lessons learned from the 2019 fire crisis. **Land**, v. 9, n. 12, p. 516, 2020.

SIMS, K. R. E. Conservation and development: evidence from Thai protected areas. **Journal of Environmental Economics and Management**, v. 60, n. 2, p. 94–114, 2010.

SMIRNOV, N. V. Estimate of deviation between empirical distribution functions in two independent samples. **Bulletin of Mathematics University Moscou**, v. 2, n. 2, p. 3–14, 1939.

SOARES-FILHO, B. et al. Role of Brazilian Amazon protected areas in climate change mitigation. **Proceedings of the National Academy of Sciences**, v. 107, n. 24, p. 10821–10826, 2010.

SORRENSEN, C. Potential hazards of land policy: conservation, rural development and fire use in the Brazilian Amazon. **Land Use Policy**, v. 26, n. 3, p. 782–791, 2009.

SZE, J. S. et al. Reduced deforestation and degradation in indigenous lands pan-tropically. **Nature Sustainability**, v. 5, n. 2, p. 123–130, 2022.

TASKER, K. A.; ARIMA, E. Y. Fire regimes in Amazonia: the relative roles of policy and precipitation. **Anthropocene**, v. 14, p. 46–57, 2016.

TSELA, P. et al. Validation of the two standard MODIS satellite burned-area products and an empirically-derived merged product in South Africa. **Remote Sensing**, v. 6, n. 2, p. 1275–1293, 2014.

UNITED NATIONS ENVIRONMENT PROGRAMME. **Spreading like wildfire - the rising threat of extraordinary landscape fires**. Nairobi: A UNEP Rapid Response Assessment, 2022. Available from: <https://www.unep.org/resources/report/spreading-wildfire-rising-threat-extraordinary-landscape-fires>. Access on: 20 June 2022.

URIARTE, M. et al. Depopulation of rural landscapes exacerbates fire activity in the western Amazon. **Proceedings of the National Academy of Sciences**, v. 109, n. 52, p. 21546–21550, 2012.

VALE, M. M. et al. The COVID-19 pandemic as an opportunity to weaken environmental protection in Brazil. **Biological Conservation**, v. 255, e 108994, 2021.

VILLÉN-PÉREZ, S. et al. Brazilian Amazon gold: indigenous land rights under risk. **Elementa: Science of the Anthropocene**, v. 8, p. 31, 2020.

VISSER, H.; DE NIJS, T. The map comparison kit. **Environmental Modelling & Software**, v. 21, n. 3, p. 346–358, 2006.

VON RANDOW, C. et al. Comparative measurements and seasonal variations in energy and carbon exchange over forest and pasture in South West Amazonia. **Theoretical and Applied Climatology**, v. 78, n. 1, p. 5–26, 2004.

WAN, Z.; HOOK, S.; HULLEY, G. **MOD11B3 MODIS/Terra land surface temperature/emissivity monthly L3 global 6km SIN grid V006.** NASA, 2015a. Available from: <https://lpdaac.usgs.gov/products/mod11b3v006/>. Access on: 3 June 2022

WAN, Z.; HOOK, S.; HULLEY, G. **MOD11A2 MODIS/Terra land surface temperature/emissivity 8-Day L3 global 1km SIN grid V006.** NASA, 2015b. Available from: <https://lpdaac.usgs.gov/products/mod11a2v006/>. Access on: 5 May 2022

WENDLAND, K. J. et al. Protected area effectiveness in european Russia: a postmatching panel data analysis. **Land Economics**, v. 91, n. 1, p. 149–168, 2015.

WEST, T. A. P. et al. Potential conservation gains from improved protected area management in the Brazilian Amazon. **Biological Conservation**, v. 269, e 109526, 2022.

WOOLDRIDGE, J. M. **Econometric analysis of cross section and panel data**. 2.ed. Cambridge, MA, USA: MIT Press, 2010.

YWATA, A. X. C.; ALBUQUERQUE, P. H. M. Métodos e modelos em econometria espacial: uma revisão. **Revista Brasileira de Biometria**, v. 29, n. 2, p. 273–306, 2011.

ZAPATA-RÍOS, X. et al. Spatiotemporal patterns of burned areas, fire drivers, and fire probability across the equatorial Andes. **Journal of Mountain Science**, v. 18, n. 4, p. 952–972, 2021.

ZARIN, D. J. et al. Legacy of fire slows carbon accumulation in Amazonian forest regrowth. **Frontiers in Ecology and the Environment**, v. 3, n. 7, p. 365–369, 2005.

APPENDIX A - SUPPLEMENTARY MATERIAL FROM CHAPTER 2

Table A.1 - Protected area national categories description according to country-specific regulatory instruments and their related category proposed by this study, as well as the IUCN category. IU = Indirect use protected areas. DU = Direct use protected areas. IL = Indigenous lands.

National categories	Description	Description source	Regulatory instrument	Category	IUCN category
Bolivia					
National Park	The purpose of the National or Departmental Park category is the strict and permanent protection of representative samples of ecosystems or biogeographic provinces and the resources of flora, fauna, as well as geomorphological, scenic, or landscape that contain and have a surface that guarantees continuity of the ecological and evolutionary processes of their ecosystems. In these areas, the extractive or consumptive use of its renewable or non-renewable resources and infrastructure works is prohibited, except for scientific research, ecotourism, environmental education, and subsistence activities of native peoples, duly qualified and authorized. These categories provide the population with opportunities for tourism and recreation in nature, scientific research, monitoring of ecological processes, interpretation, environmental education, and ecological awareness according to their zoning, management plans, and regulatory standards.	https://www.lexivox.org/norms/BO-RE-DS24781.html	General Regulation of Protected Areas, July 31, 1997	IU	II
Wildlife Reserve	The National or Departmental Wildlife Reserve category is intended to protect, manage, and sustainably be used under official surveillance. In this category, intensive and extensive uses are foreseen, both of a non-extractive or consumptive nature and an extractive nature according to its zoning. The latter, subject to strict control and monitoring, referred exclusively to the management and use of wildlife.	https://www.lexivox.org/norms/BO-RE-DS24781.html	General Regulation of Protected Areas, July 31, 1997	DU	IV
Wildlife Refuge	It aims for the protection and special management of areas to ensure the existence of endangered species.	https://pt.slideshare.net/ANCBSCregionalSantaC/08-juan-renjifo-ll-areas-protegidas-de-santa-cruz/30	Ministry resolution No 340/88	DU	IV
Wildlife Sanctuary	The purpose of the National or Departmental Sanctuary category is the strict and permanent protection of sites that host endemic, threatened, or endangered species of wild flora and fauna, a natural community, or a unique ecosystem.	https://www.lexivox.org/norms/BO-RE-DS24781.html	General Regulation of Protected Areas, July 31, 1997	DU	IV
Scientific Ecological and Archaeological Reserve	Archaeological importance and cultural heritage.	http://www.museonoelkempff.org/cgb/areas-protegidas/areas-protegidas-departamentales/areas-protegidas-departamentales-beni/	Administrative resolution n 139-96 (12/16/96) of the Prefecture and General Command of Beni	DU	V
Biosphere Reserve	It aims to protect the flora, fauna, water resources, and the region's general biodiversity. It generally covers a defined geographic area that incorporates a high-profile natural feature in close contact with human society. It largely focuses on improving the livelihoods of indigenous and traditional communities.		D.S. Nº 19191, 1982	DU	VI
Integrated Management Natural Area	The National or Departmental Integrated Management Natural Area category is to make the conservation of biological diversity compatible with the sustainable development of the local population. It constitutes a mosaic of units that include representative samples of ecoregions, biogeographic provinces, natural communities or species of flora and fauna of singular importance, zones of traditional systems of land use, zones for multiple uses of natural resources, and core zones of strict protection.	https://www.lexivox.org/norms/BO-RE-DS24781.html	General Regulation of Protected Areas, July 31, 1997	DU	VI
Natural Monument	The category of National or Departmental Natural Monument has as its fundamental objective the preservation of outstanding natural features of particular singularity, due to their spectacular, scenic, or scenic character, of geological, physiographic formations or paleontological deposits. In addition, this category of management includes the conservation of the biological diversity the area contains.	https://www.lexivox.org/norms/BO-RE-DS24781.html	General Regulation of Protected Areas, July 31, 1997	DU	VI

(To be continued)

Table A.1 - Continuation.

National categories	Description	Description source	Regulatory instrument	Category	IUCN category
Strictly Management Area Model	It has the bjective of making compatible the sustainable development of the local population and the conservation of biological diversity through the implementation of practical actions and processes that contribute to the integral management of the forest, through the active participation of the local population that promotes the management and use of natural resources and existing biodiversity.	https://issuu.com/conservacionamazonica/docs/brochure_ami-santa_rosa_2018	Municipal Law Nº 07/2017	DU	VI
Municipal Reserve	The objective of its creation is to conserve and contribute to protecting the environment and natural resources to maintain the ecological balance of the forest on a regional and local scale. It allows the connectivity (biological corridors) of the Ecological Reserve areas of the forest concessions and the areas of ecological easements on rivers, lagoons, and existing mountains, enhancing the capacity to conserve biodiversity.	https://www.biobol.org/index.php/areas-protegidas/ap-santa-cruz	Municipal resolutions	DU	VI
Municipal conservation and management area	Sub-national areas that work like National or Departmental Integrated Management Natural Area aim to make the conservation of biological diversity compatible with the sustainable development of the local population. It constitutes a mosaic of units that include representative samples of ecoregions, biogeographic provinces, natural communities or species of flora and fauna of singular importance, zones of traditional systems of land use, zones for multiple uses of natural resources, and core zones of strict protection.	https://www.conservation.org/bolivia/areas-protegidas/area-municipal-de-conservacion-y-manejo-del-bajo-madidi	Municipal resolutions	DU	VI
Municipal Protected Area	Geographical areas with values of biological diversity and associated cultural resources, located within the municipal and territorial jurisdiction and declared in perpetuity as such, in accordance with the municipal development objectives that will be managed in a comprehensive manner in order to conserve and restore diversity values biological and associated cultural resources that exist in its interior and in its buffer zones to provide environmental goods and services to society.	https://www.portalces.org/sites/default/files/ap_municipales.pdf	Ley de Municipalidades – autonomía	DU	VI
Regional Park	It works as buffer zones to protect important reserves from forest degradation, serving as complementary areas to protect landscapes and biodiversity. It can include private properties with an agricultural and livestock tradition, which imposes the progressive advance of low-scale deforestation, causing the area's deterioration in the medium term. And it also is created as a response to the request of local communities as a means of defense against pressures on fauna.	http://www.museonoelkempff.org/cgb/areas-protegidas/areas-protegidas-departamentales/areas-protegidas-departamentales-beni/	Municipal resolutions	DU	VI
Indigenous Territory	Given the pre-colonial existence of the peasant native indigenous nations and peoples and their ancestral dominion over their territories, their self-determination is guaranteed within the framework of the unity of the State, which consists of their right to autonomy, self-government, their culture, the recognition of its institutions and the consolidation of its territorial entities, in accordance with this Constitution and the law. The rights of indigenous and native peoples and communities over their community lands of origin are guaranteed, taking into account their economic, social, and cultural implications and the use and sustainable exploitation of renewable natural resources, in accordance with the provisions of article 171 ° of the Political Constitution of the State.	https://www.lexivox.org/norms/BO-CPE-20090207.html / https://www.lexivox.org/norms/BO-L-1715.html	Political State Constitution 2009	IL	VI
Brasil					
Biological Reserve	Preservation of the biota and other natural attributes, without direct human interference or environmental modifications, except for the measures to recover its altered ecosystems and the management actions necessary to recover and preserve the natural balance, biological diversity, and ecological processes.	http://www.planalto.gov.br/ccivil_03/leis/l9985.htm	Lei 9.985, de 18 de julho de 2000	IU	I-A
Ecological Station	Preservation of nature and development of scientific research.	http://www.planalto.gov.br/ccivil_03/leis/l9985.htm	Lei 9.985, de 18 de Julho de 2000	IU	I-A
National or State Park	Preservation of natural ecosystems of great ecological importance and scenic beauty, making possible the accomplishment of scientific research and the development of activities of education and environmental interpretation, recreation in contact with nature, and ecological tourism.	http://www.planalto.gov.br/ccivil_03/leis/l9985.htm	Lei 9.985, de 18 de julho de 2000	IU	II
Natural Monument	Preservation of rare, unique, or great scenic beauty natural sites.	http://www.planalto.gov.br/ccivil_03/leis/l9985.htm	Lei 9.985, de 18 de Julho de 2000	IU	III

(To be continued)

Table A.1 - Continuation.

National categories	Description	Description source	Regulatory instrument	Category	IUCN category
Wildlife Refuge	Protect natural environments where conditions for the existence or reproduction of species or communities of the local flora and/or resident or migratory fauna are assured.	http://www.planalto.gov.br/ccivil_03/leis/l9985.htm	Lei 9.985, de 18 de julho de 2000	IU	III
Fauna Reserve	It aims to protect the biological diversity of animal populations of native, terrestrial, or aquatic species, resident or migratory, suitable for technical-scientific studies on the sustainable economic management of faunal resources. The Pau D'Oleo Fauna Reserve is in public ownership and domain, and private land titles are not allowed in its interior.	https://documentacao.socioambiental.org/ato_normativo/UC/3121_20180327_122109.pdf	Decree nº. 22.683, of March 20th, 2018	DU	IV
Area of Relevant Ecological Interest	Maintain natural ecosystems of regional or local importance and regulate the permissible use of these areas to make them compatible with nature conservation objectives.	http://www.planalto.gov.br/ccivil_03/leis/l9985.htm	Lei 9.985, de 18 de Julho de 2000	DU	IV
Environmental Protected Area	Protect biological diversity, discipline the occupation process and ensure the sustainability of natural resources use.	http://www.planalto.gov.br/ccivil_03/leis/l9985.htm	Lei 9.985, de 18 de julho de 2000	DU	V
Extractive Reserve	Protect the livelihoods and culture of traditional extractivist populations and ensure the sustainable use of the unit's natural resources.	http://www.planalto.gov.br/ccivil_03/leis/l9985.htm	Lei 9.985, de 18 de julho de 2000	DU	VI
National or State Forest	Sustainable use of forest resources and scientific research, emphasizing methods for sustainable exploitation of native forests.	http://www.planalto.gov.br/ccivil_03/leis/l9985.htm	Lei 9.985, de 18 de Julho de 2000	DU	VI
Sustainable Development Reserve	Preserve nature, ensuring the conditions and means necessary for the reproduction and improvement of the ways and the quality of life, as well as natural resources exploited by traditional populations, enhancing, conserving, and improving knowledge and techniques of environmental management developed by these populations.	http://www.planalto.gov.br/ccivil_03/leis/l9985.htm	Lei 9.985, de 18 de julho de 2000	DU	VI
Indigenous Territory	Indigenous Land (TI) is a portion of the national territory, which after a regular administrative demarcation process, in accordance with the established legal precepts, passes, after ratification by Presidential Decree for the property of the Union, inhabited by one or more indigenous communities, used by these in their productive, cultural, well-being and physical reproduction activities. Therefore, it is a property of the Union, and as such, it is inalienable and unavailable, and the rights over it are imprescriptible.	http://www.funai.gov.br/index.php/2014-02-07-13-24-32	CF/88, Lei 6001/73 – Estatuto do Índio, Decreto n.º 1775/96	IL	VI
Colombia					
Nature Reserve	Area in which primitive conditions of flora, fauna, and geological formations exist and is destined for the conservation, investigation, and study of its natural resources.	https://www.minambiente.gov.co/images/GestionIntegraldelRecursoHidrico/pdf/normativa/Decreto_2811_de_1974.pdf	Decreto 2811 del 18 de Diciembre de 1974	IU	I-A
National Natural Park	Area of extension that allows its ecological self-regulation and whose ecosystems, in general, have not been substantially altered by human exploitation or occupation, and where plant and animal species, geomorphological complexes, and historical or cultural manifestations have scientific, educational value, aesthetic and recreational national and for its perpetuation is subjected to an adequate management regime.	https://www.minambiente.gov.co/images/GestionIntegraldelRecursoHidrico/pdf/normativa/Decreto_2811_de_1974.pdf	Decreto 2811 del 18 de Diciembre de 1974	IU	II
National Protective Forest Reserves	Geographical space in which forest ecosystems maintain their function. However, their structure and composition have been modified, and the associated natural values are made available to the human population to be used for their preservation, sustainable use, restoration, knowledge, and enjoyment. This public or private property area is reserved for the establishment or maintenance and sustainable use of forests and other natural vegetation cover.	https://www.suin-juriscol.gov.co/viewDocument.asp?id=1872443	Decreto 2372 de 2010	DU	V

(To be continued)

Table A.1 - Continuation.

National categories	Description	Description source	Regulatory instrument	Category	IUCN category
Indigenous Territory	The Indigenous Territories were conceived as spaces of local government that should not be forced to reproduce the organizational structure of the municipalities (City Hall, City Council, among others), and therefore have the challenge of innovating in the definition of efficient and culturally appropriate administrative structures to each people, or to each group of peoples that propose to govern together in the same territorial unit. Presidential Decree No. 632 of 2018, when providing for the functioning of Indigenous Territories, allows the guarantee of collective ownership of Indigenous Lands and the exercise of political rights of self-government.	http://www.suin-juriscol.gov.co/viewDocument.asp?ruta=Decretos/30034960	Decreto 632 de 2018	IL	VI
Ecuador					
Ecological Reserve	They are natural areas of variable extensions with little human intervention. These are areas with outstanding natural resources or sites of species of great national significance. The main objective is to save genetic matter, ecological diversity, scenic beauties, special phenomena, and environmental regulation for scientific investigation of natural elements and phenomena and environmental education. When no conflicts exist with research and education, recreation and tourism activities are allowed in limited areas.	http://areasprotegidas.ambiente.gob.ec/es/info-snap	Art.405 de la Constitución de la República del Ecuador del 2008/ Art. 5 y 67 de la ley Forestal y de Conservación y Vida Silvestre del 10 de Septiembre del 2004	IU	I-A
Biological Reserve	Large conservation area (more than 10,000 ha) whose main conservation objectives are complete ecosystems and their species, little altered and minimal human presence, at least in the distribution area of the main conservation object. In this type of reserve, the priority activities will be biological, ecological, and environmental research, with environmental education also being possible as a secondary activity. The restriction on using its natural resources will be very high (very restricted) to guarantee the development of ecological processes.	http://areasprotegidas.ambiente.gob.ec/es/info-snap	Art.405 de la Constitución de la República del Ecuador del 2008/ Art. 5 y 67 de la ley Forestal y de Conservación y Vida Silvestre del 10 de Septiembre del 2004	IU	I-B
National Park	Large conservation area (more than 10,000 ha) whose main conservation objectives are landscapes, complete ecosystems, and species. Their environments should be kept little altered, with a minimum human presence. The priority activities will be related to research and environmental monitoring, with the development of nature tourism being feasible to support the conservation of natural resources. The usage restriction level is high (restricted).	http://areasprotegidas.ambiente.gob.ec/es/info-snap	Art.405 de la Constitución de la República del Ecuador del 2008/ Art. 5 y 67 de la ley Forestal y de Conservación y Vida Silvestre del 10 de Septiembre del 2004	IU	II

(To be continued)

Table A.1 - Continuation.

National categories	Description	Description source	Regulatory instrument	Category	IUCN category
Fauna Production Reserve	Medium-sized areas (between 5,000 and 10,000 ha) whose priority conservation objectives are ecosystems and species susceptible to management, which should be little altered, but have a medium level of human presence (they depend on local biological resources). The priority actions are related to sustainable wildlife management, environmental education, ecosystem restoration, and nature-oriented tourism. The level of use restriction will be low (slightly restricted).	http://areasprotegidas.ambiente.gob.ec/es/info-snap	Art.405 de la Constitución de la República del Ecuador del 2008/ Art. 5 y 67 de la ley Forestal y de Conservación y Vida Silvestre del 10 de Septiembre del 2004	DU	IV
Indigenous Territory	The indigenous territories are foreseen in the 1998 Political Constitution, Art. 84, whereby it is established that the State will recognize and guarantee the following collective rights to the indigenous peoples: to conserve the imprescriptible property of the community lands, which will be inalienable, unattachable and indivisible, Except for the power of the State to declare its public utility. These lands will be exempt from paying the property tax, maintain ancestral possession of community lands, and obtain their free adjudication in accordance with the law.	http://www.ecuanex.net.ec/constitucion/titulo03c.html	Art.84 de la Constitución Política del Ecuador del 1998	IL	VI
French Guiana					
Forest Biological Reserve	Integral biological reserves (RBI) are protected areas mainly in a forest environment, logging is prohibited, and the forest is returned to natural evolution. The objectives are knowledge of the natural functioning of ecosystems and the development of biodiversity associated with old trees and dead wood (rare insects, fungi, etc.). The RBI are veritable "laboratories of nature.	https://www.onf.fr/onf/recherche/+/27a::reserves-biologiques-des-espaces-naturels-remarquables-en-foret-publique.html	Forest Code	IU	I-B
Land Acquired By Conservatoire Du Littoral (National Seaside And Lakeside Conservancy)	The Coastline and Lakeshore Protection Agency have the authority to purchase coastal land to protect it. Acquired assets become part of its legal domain. The Agency does not manage the land itself. It entrusts management, through contractual agreements, to NGOs or local authorities. These agreements include provisions related to the protection of such areas. CENs may enter into agreements with public or private entities to manage statutory or non-statutory natural areas, such as nature reserves or private land, respectively. They have been established to protect and manage natural areas, whether such areas belong to them or not.	https://www.iucn.org/downloads/france_en.pdf	Environment code - Article L321-1 and the following	DU	IV
Nature Reserve	Nature reserves may be created if conservation of the flora and fauna, soils, water, mineral and fossil deposits, and the overall natural environment is of particular importance or if protection is required from human activities likely to degrade them. Nature reserves are complementary to other protected area categories. They differ from national parks by the specificity of their objectives and because they generally cover a smaller area. Nature reserves may be established on public or private property.	https://www.iucn.org/downloads/france_en.pdf	Environment code - Article L332-1 to 332.27	IU	I-A
National Park - Buffer Zone/Area Of Adhesion	According to the Environmental Code, a national park may be created in terrestrial or marine areas when the preservation of the natural environment, especially flora and fauna, soil and subsoil, air and water, landscape, and, as appropriate, the cultural heritage, is of special interest, and when it is important to protect them by preventing degradation and damage likely to have an impact on their diversity, composition, appearance, and evolution. Buffer zones are peripheral areas, given their geographical continuity and ecological links with core areas. They contribute to protecting the national park core area while pursuing sustainable development objectives in an exemplary way. While industrial and mining activities are forbidden in the core area of a park, they are not prohibited in buffer zones.	https://www.iucn.org/downloads/france_en.pdf	Environment code - Articles L331-1 à L331-28	DU	VI
National Park	National park core areas aim for the protection and scientific reference of national and international importance, which enables the monitoring of ecological succession, particularly as part of biological diversity and climate change monitoring. It also enables visitors to discover nature, recharge their batteries and relax. The park core area would benefit from the strictest protection, allowing little room for exceptions (except for greater protection in the strictest reserve established within the core area).	https://www.iucn.org/downloads/france_en.pdf	Article 3, Order of 23 February 2007 / Environment code Articles L331-1 à L331-28	IU	II

(To be continued)

Table A.1 - Continuation.

National categories	Description	Description source	Regulatory instrument	Category	IUCN category
Regional Nature Reserve	It has the objective of protect of the site to maintain its integrity, participating in scientific research to improve knowledge in tropical ecology, and realizing public accessibility to raise awareness for the conservation of natural heritage.	https://www.reserve-tresor.fr/en/the-reserve/history/	Prefectural Decree No 598 ID / 4B of 20/05/1997	IU	II
Area of Relevant Ecological Interest	This is not a measure of regulatory protection but an inventory. It corresponds to the census of outstanding natural land areas. The designation of this area is based primarily on the presence of species or groups of species with strong heritage interest. The presence of at least one population of critical species defines it.	https://en.wikipedia.org/wiki/Zone_naturelle_d%27int%C3%A9r%C3%AAt_%C3%A9cologique,_faunistique_et_floristique		DU	VI
Natural Monument	Areas with picturesque and scientific nature, which preservation is of general interest.	https://side.developpement-durable.gouv.fr/Default/doc/SYRACUSE/227623/arrete-d-inscription-des-sites-du-bassin-versant-et-des-chutes-de-la-crique-voltaire-commune-de-sain?_lg=fr-FR		IU	III
Regional Nature Park	The objective is the valorization of the local patrimonial area through sustainable development.	https://www.parcs-naturels-regionaux.fr/en	Environment code (articles L333-1 to L333-4)	DU	VI
Indigenous Territory	Areas of Collective Land Use Rights, concessions, and transfers give only a simple right to use the land.	https://www.iwgia.org/en/french-guiana.html		IL	VI
	Guyana				
Other conservation sites	Conservation International (CI) leased conservation concession to prevent logging and to ensure the preservation of natural biodiversity and wildlife within the forest ecosystem. The conservation concession follows the same legal model as a standard timber sales agreement, except that the land is held as a reserve rather than harvested for timber.	https://www.cbd.int/financial/pes/guyana-pesconcession.pdf	Private initiative	IU	II
Managed Resource Use Area	Managed Resource Protected Area must be an area that contains predominantly natural systems. It is managed to provide a sustainable flow of natural products and services to meet local needs while still protecting natural ecosystems and maintaining ecosystem services. The Management authority may permit the following activities in a Managed Resource Protected Area: (a) scientific research; (b) environmental monitoring; (c) recreation; (d) low-level eco-logically sustainable activities.	https://doe.gov.gy/published/document/5ae8f345b4d000153ca57a98	Act n° 14 of 2011. Protected Areas Act 2011. / Amerindian Act, 2006	DU	VI
Indigenous Territory	The Amerindian Act 2006 provides for the transfer of land rights from the State to a designated Village Council, and the Village Council is responsible for allocating land to residents. The Council is not allowed to dispose of any interest, right, or title to Village lands but may grant leases of up to 10% of its lands for a period of up to fifty years for agriculture, tourism, or other sustainable use, provided a majority of the residents are in agreement. If the land is to be leased to an outsider, 75% of the residents must agree, and the Council must obtain the advice of the Minister of Amerindian Affairs.	https://parliament.gov.gy/documents/acts/4680-act_no_6_of_2006.pdf	Amerindian Act 2006	IL	VI

(To be continued)

Table A.1 - Continuation.

National categories	Description	Description source	Regulatory instrument	Category	IUCN category
Peru					
National Park	Areas that constitute representative samples of the natural diversity of the country and its large ecological units. Within them, the ecological integrity of one or more ecosystems, the associations of wild flora and fauna, the successional and evolutionary processes, and other associated landscape and cultural characteristics are protected with an intangible nature.	https://sinia.minam.gob.pe/normas/ley-areas-naturales-protegidas	Law nº 26834 - Ley de Áreas Naturales Protegidas	IU	II
National Sanctuary	Areas where a species' habitat or a community of flora and fauna is intangible, as well as natural formations of scientific and landscape interest.	https://sinia.minam.gob.pe/normas/ley-areas-naturales-protegidas	Law nº 26834 - Ley de Áreas Naturales Protegidas	IU	III
Protected Forest	Areas are established to guarantee the protection of the upper or collecting basins, the river banks, and other watercourses and, in general, to protect fragile lands against erosion. In addition, they allow the use of resources and the development of those activities that do not endanger the vegetation cover.	https://sinia.minam.gob.pe/normas/ley-areas-naturales-protegidas	Law nº 26834 - Ley de Áreas Naturales Protegidas	DU	V
Communal Reserve	Areas destined for conserving wild flora and fauna for the benefit of neighboring rural populations. The use and commercialization of resources will be done under management plans, approved and supervised by the authority, and conducted by the beneficiaries themselves. They can be established on soils of greater capacity for agriculture, livestock, forestry, or protection use and humidity.	https://sinia.minam.gob.pe/normas/ley-areas-naturales-protegidas	Law nº 26834 - Ley de Áreas Naturales Protegidas	DU	VI
National Reserve	Areas destined for the conservation of biological diversity and the sustainable use of resources of wild flora and fauna, aquatic or terrestrial. They allow the commercial use of natural resources under management plans, approved, supervised, and controlled by the competent national authority.	https://sinia.minam.gob.pe/normas/ley-areas-naturales-protegidas	Law nº 26834 - Ley de Áreas Naturales Protegidas	DU	VI
Reserved Zone	Reserved Zones are those areas that, meeting the conditions to be considered Protected Natural Areas, require the completion of complementary studies to determine, among others, the extension and category that correspond to them as such, as well as the viability of their management. In this sense, it should be noted that, unlike the definitive Protected Natural Areas, the Reserved Zones are not established in perpetuity and could eventually be deactivated if, in the categorization process, it is determined that they do not qualify for any category.	https://sinia.minam.gob.pe/normas/ley-areas-naturales-protegidas	Law nº 26834 - Ley de Áreas Naturales Protegidas	DU	VI
Indigenous Territory	Indigenous people hold title to substantial portions of Peru, primarily in the form of communal reserves. The Law of Prior Consultation of Indigenous or Original Peoples requires these to be consulted before legislation or other actions could affect their rights. In 2013, Peru delegated responsibility for titling indigenous communities to regional governments, but progress is slow because the process is complicated, and regional governments lack resources and capacity.	https://thetenurefacility.org/timeline/peru/		IL	VI
Suriname					
Nature Reserve	To protect and preserve the natural resources present in Suriname, the President may designate land and waters belonging to the Land Domain as a nature reserve by decree. In order to be designated as a nature reserve, an area must meet the following requirements: that it deserves government protection by alternating nature and landscape beauty and/or the presence of scientifically or culturally important flora, fauna, and geological objects. It is prohibited in a nature reserve: to deliberately or through negligence cause damage to the soil conditions, the natural beauty, the fauna, the flora or to carry out actions that would detract from the value of the reserve as such; to camp, make a fire, cut wood or burn charcoal, unless with written permission from the Head of 's Lands Bosbeheer and with due observance of the conditions set therein; to hunt, to fish and to have with him a dog, a firearm or any hunting or trapping device without a permit from the Head of the Lands Bosbeheer. The Head of 's Lands Bosbeheer can grant written permission to certain persons to run a business in an unenclosed part of a nature reserve in accordance with a plan approved by him or to cooperate in the exercise of a business, with the express reservation that these persons or companies do not cause any damage or harm to the reserve as such. The Head of 's Lands Bosbeheer may grant written permission to certain persons to collect forest and forest by-products, graze livestock or engage in fishing in certain parts of nature reserves designated by him, under conditions set by him.	Nature Conservation Act 1954 (https://www.ecolex.org/details/legislation/nature-conservation-act-1954-lex-faoc032835/)	Nature Conservation Act 1954	IU	I-A

(To be continued)

Table A.1 - Conclusion.

National categories	Description	Description source	Regulatory instrument	Category	IUCN category
Multiple Use Management Area	Protected area with sustainable use of natural resources.	https://whsrn.org/multiple-use-management-areas-create-crucial-habitat-for-shorebirds-in-suriname/	Nature Conservation Act 1954	DU	VI
Forest Reserve	Forest reserves are not protected areas, but in practice, no extractive concessions are given in these areas. It is possible to convert the status of a forest reserve or part thereof into a protected area, for example, for educational or research purposes.	https://www.cbd.int/pa/doc/ts64-case-studies/suriname-en.pdf		DU	VI
Venezuela					
National Park	Regions are established for the protection and conservation of natural scenic beauties and flora and fauna of national importance, which the public can better enjoy when placed under official surveillance. Directly related to the conservation of the natural heritage and maintenance of the ecological balance. Includes recreational, scientific, and educational use.	Peña & Vieira 2014 (https://www.scribd.com/document/343106250/Las-ABRAE-Versus-Las-Areas-Protegidas-en-Venezuela)	Convention for the Protection of Flora, Fauna and the Natural Scenic Beauties of the Countries of America, 1941, Art 1	IU	II
Natural Monument	Regions, objects, or living species of animals or plants of aesthetic interest, are given absolute protection to conserve a specific object or species of flora or fauna by declaring a region, an object, or species isolated. They are inviolable except for proper scientific research. They provide absolute and perpetual protection to geographical features and sites of exceptional beauty or rarity.	Peña & Vieira 2014 (https://www.scribd.com/document/343106250/Las-ABRAE-Versus-Las-Areas-Protegidas-en-Venezuela)	Convention for the Protection of Flora, Fauna and the Natural Scenic Beauties of the Countries of America, 1941, Art 1 / Decree No. 276 of 1989	IU	III
Indigenous Territory	Lands that indigenous people ancestral and traditionally occupy are necessary to develop and guarantee their ways of life. With the participation of indigenous peoples, it is the National Executive's responsibility to demarcate and guarantee the right to collective property of their lands, which will be inalienable, imprescriptible, unattachable, and non-transferable in accordance with the provisions of this Constitution and the law.	https://venezuela.justia.com/federales/constitucion-de-la-republica-bolivariana-de-venezuela/titulo-iii/capitulo-viii/	Constitution, 1999, art. 119	IL	VI

APPENDIX B - SUPPLEMENTARY MATERIAL FROM CHAPTER 3

Table B.1 - Overview of fire occurrence available products.

Name	Developer	Scale	Type of information	Time span	Sensors/ inputs	Methods	Spatial resolution	Format	Temporal composition	Limitation	Data access	Reference
MCD14ML	NASA	Global	Active fire	2000 – present	MODIS	The algorithm uses brightness temperatures and reflectance information to eliminate obvious non-fire pixels, and the remain is considered in subsequent contextual analysis.	1000 m	Vector - points	Monthly – possible to know the burn date within the month	Severe temporal and spatial biases may arise in any MODIS fire time series analysis employing time intervals shorter than eight days. Cloud obscuration, a lack of coverage, or misclassification in the land/sea mask may be responsible for known fires that do not appear in the dataset. However, this will be impossible to determine with only the information provided in the fire location files.	Open access	(GIGLIO et al., 2003)
VNP14IMGTDL_NRT	NASA	Global	Active fire	2012 - present	VIIRS	Multispectral contextual algorithm to identify sub-pixel fire activity and other thermal anomalies. It includes information on confidence level, FRP, and day or nighttime fire.	375 m	Vector - points	Sub-daily	Although its improved spatial resolution provides greater response over small fires and improved mapping of large fires perimeters, Frequent data saturation prevents sub-pixel fire characterization.	Open access	(SCHROEDER et al., 2014)

(To be continued)

Table B.1- Continuation.

Name	Developer	Scale	Type of information	Time span	Sensors/inputs	Methods	Spatial resolution	Format	Temporal composition	Limitation	Data access	Reference
Fire cci v.5.0	ESA	Global	Burned area	2001 - 2016	MODIS (MOD09GQ – surface reflectance + MOD09GA – quality flags + MCD14ML – active fires)	A hybrid approach was adopted, combining information on active fires and temporal changes in reflectance. First, burned pixels are detected, and then a contextual procedure is run to improve the delineation of the burned patch.	250 m	Raster (3 layers) - detection date 0: not burned 1 to 366: day of the first detection -1: not observed in the month -2: not burnable - confidence level (1-100) - land cover (extracted from Land Cover CCI maps)	Monthly – possible to know the Julian day of the first detection within the month and consequently to identify pixels that burn more than once during a calendar year	The date of the burned pixel may correspond from one to several days after the actual burning date, depending on image availability and cloud cover. All validation results showed worse performance than MCD64 products from NASA.	Open access	(CHUVIECO et al., 2018)
Fire cci v.5.1	ESA	Global	Burned area	2001 - 2019	MODIS (MOD09GQ – surface reflectance + MOD09GA – quality flags + MCD14ML – active fires)	A hybrid approach was adopted, combining information on active fires and temporal changes in reflectance. First, burned pixels are detected, and then a contextual procedure is run to improve the delineation of the burned patch.	250 m	Raster (3 layers) - detection date 0: not burned 1 to 366: day of the first detection -1: not observed in the month -2: not burnable - confidence level (1-100) - land cover (extracted from Land Cover CCI maps)	Monthly – possible to know the Julian day of the first detection within the month and consequently to identify pixels that burn more than once during a calendar year	The date of the burned pixel may correspond from one to several days after the actual burning date, depending on image availability and cloud cover. Fire cci v.5.1 was found less sensitive (11% lower estimations) than MCD64A1 c6 in tropical and temperate fires in Southern Hemisphere South America. The validation metrics showed an important underestimation of total burned area, with higher omission and commission errors, which could be attributed to the coarse spatial resolution of the input images, which implies missing small-size fires (< 100 ha).	Open access	(LIZUNDIA-LOIOLA et al., 2020)

(To be continued)

Table B.1 - Continuation.

Name	Developer	Scale	Type of information	Time span	Sensors/inputs	Methods	Spatial resolution	Format	Temporal composition	Limitation	Data access	Reference
FireCCILT10	ESA	Global	Burned area	1982 – 2017 (exception of 1994)	AVHRR	The algorithm uses LTDR and CCI Land Cover products, reflectance, and spectral indices as input to a multiannual monthly model generated within Random Forest. MCD64A1 dataset is used as a training sample.	0.25°	Raster (it is not binary; it includes how much of each pixel was burned using MCD64A1 as a comparison)	Monthly	Although it has the biggest time available, its method-modeled variables and their uncertainty are not accounted for to build the final product. The validation performed does not consider the entire time.	Open access	(OTÓN; PETTINARI, 2019)
MCD64A1 c6	NASA	Global	Burned area	2000 - present	MODIS	It uses MODIS surface reflectance data coupled with 1 km MODIS active fire observations. The algorithm uses a burn-sensitive vegetation index (VI) to create dynamic thresholds to produce the composite data.	500 m	Raster (5 layers) - Burn Date - Burn Date Uncertainty - Quality Assurance - First Day - Last Day	Monthly – possible to know the date of burn (ordinal day of the calendar year on which the burn occurred)	Burned areas in cropland should generally be treated as low confidence due to the inherent difficulty in mapping agricultural burning reliably. Unable to adequately map the occurrence of small fires, what can cause underestimation of overall burned area. It does not individualize the burnt scars.	Open access	(GIGLIO et al., 2018)
GWIS	JRC	Global	Burned area	2003 - 2016	MODIS	It corresponds to the post-processing of the MCD64A1 product. To identify individual fire events on a global scale, the methodology consists of grouping the burnt pixels in individual burnt scars using a region growth approach.	500 m	Vector - polygons	Multi-annually – It is provided a vector dataset with the entire time, but it is possible to know the initial and final burn day of each burnt scar	Although it has the advantage of individualizing the burned areas, since it uses MCD64A1, it also incorporates all limitations inherent of its methodology.	Data available upon request	(ARTÉS et al., 2019)

(To be continued)

Table B.1 - Continuation.

Name	Developer	Scale	Type of information	Time span	Sensors/inputs	Methods	Spatial resolution	Format	Temporal composition	Limitation	Data access	Reference
GFED4	UM	Global	Burned area Monthly emissions Fractional contributions of different fire types	1997 - present	MODIS	Its algorithm combine MODIS burned area maps with active fire data from TRMM VIRS and the ATSR family of sensors. It is derived exclusively from MCD64A1 c5.1 aggregated to 0.25° spatial resolution.	0.25°	Raster – it is provided a mean burn-date uncertainty dataset for the daily product	Monthly Daily (from Aug-2000)	It does not include small fires (<100ha) - product GFED4s include them. It underestimates the extent of cropland burning. Cloud cover degrades the detection of active fires and fire scars; thus, the burned area in persistently cloudy regions may be systematically underestimated. Since it uses MCD64A1, it also incorporates all limitations inherent in its methodology.	Open access	(GIGLIO; RANDERSON; VAN DER WERF, 2013)
GABAM	IRSDE / CAS	Global	Burned area	2015	Landsat 8 OLI	The automated algorithm implemented on GEE. It uses reflectance and spectral indices information as input for a Random Forest model. A final step consists of burned area shaping through a region-growing approach.	30 m	Raster (binary)	Annually	Landsat coarse temporal resolution might cause omission errors in tropical zones due to the quick recovery of the vegetation surface. The lowest overall accuracy was found on Broadleaved Evergreen Forests, which can trap the use of the such methodology in tropical regions. It is not provided uncertainty for each pixel.	Open access	(LONG et al., 2019)
Landsat Burned Area	NASA	National - US	Burned area	1984 - present	Landsat TM Landsat ETM+ Landsat OLI	An algorithm based on the Landsat Burned Area Essential Climate Variable algorithm. It is a supervised approach that uses gradient-boosted regression models implemented in Python.	30 m	Raster (binary)	Annually - binary annual burn classification	Occasionally some burned area is incorrectly classified as being water.	Open access	(HAWBAKER et al., 2017)

(To be continued**)**

Table B.1 - Continuation.

Name	Developer	Scale	Type of information	Time span	Sensors/inputs	Methods	Spatial resolution	Format	Temporal composition	Limitation	Data access	Reference
TREES	TREES - INPE	Regional – Brazilian Amazon	Burned area	2006 - 2016	MODIS	It uses a hybrid classification. An LSM is performed. Then, the shade fraction image is segmented and unsupervised, and classified. Subsequently, a manual edition is performed to improve the final map's accuracy.	250 m	Vector	Annually – each file contains information from June to October. It is possible to know the burn month but not the burn day.	It is not operational, and its time series continuity is not secure. Besides, it is regional, so its use is restricted to the Brazilian Amazon.	Data available upon request	(ANDERSON et al., 2005, 2015; SHIMABUKURO et al., 2009)
DETER B	INPE	Regional – Brazilian Amazon	Burned area	2016 - present	WFI AWiFS	The forest cover change pattern is identified by visual interpretation based on five main elements (color, tonality, texture, shape, and context). It uses the LSM technique and its multispectral image in color composition to the visual interpretation.	64 m	Vector	Annually – it follows the same year pattern that PRODES project (from July to August). It is possible to know the date of the image used to map the burnt scar.	The distinction between burnt scar and degradation classes is not clear. Considering only the burnt scar class, the total burned area is underestimated. There is not a long time series to be analyzed. Besides, it is regional, so its use is restricted to the Brazilian Amazon.	Open access	(DINIZ et al., 2015)

(To be continued)

Table B.1 - Continuation.

Name	Developer	Scale	Type of information	Time span	Sensors/inputs	Methods	Spatial resolution	Format	Temporal composition	Limitation	Data access	Reference
Acre Queimadas	UFAC	Regional – Acre	Burned area	1984 - 2016	Landsat TM Landsat OLI	It uses the CLASlite 3.0 software to perform an SLM model. The fraction is generated a burn-scar index (BSI) image. Subsequently, the BSI is sliced, defining thresholds by trial and error to identify forest-fire scars. There is no standard or fixed threshold for this identification, which changes from scene to scene according to fire intensity, vegetation contrast, and image noise.	30 m	Vector	Annually – it was considered images from September to December	The algorithm can miss some fires because they are not strong enough to reach the canopy, affecting only the forest's understory. Fires can also be missed if they occur after the date of the mapping image or in small forest fragments. Besides, targets like shading by thin clouds and smoke or vegetation under extreme water stress can be confused with the burnt scar in the classification process. It only considers fires in forested areas. For this, it uses a deforestation mask. Besides, it is regional, so its use is restricted to the Acre state.	Data available upon request	(SILVA et al., 2018b)

(To be continued)

Table B.1 - Conclusion.

Name	Developer	Scale	Type of information	Time span	Sensors/inputs	Methods	Spatial resolution	Format	Temporal composition	Limitation	Data access	Reference
Global Fire Atlas	NASA	Global	Burned area Ignition point	2003 - 2016	MODIS	It uses MCD64A1 c6 to track the dynamics of individual fires to determine the timing and location of ignitions and fire size, duration, daily expansion, fire line length, speed, and direction of spread. The approach uses two filters to account for uncertainties on the day of the burn in order to map the location and timing of fire ignitions and the extent and duration of individual fires. Subsequently, each individual fire's growth dynamics are tracked to estimate the daily expansion, fire line length, speed, and direction of spread.	500 m	Vector – polygon, and point	Annually – It is possible to know the start and end dates for each burnt scar or ignition point. It also provides a daily gridded raster of fire line, speed, the direction of spread, and the day of the burn.	The algorithm assumes that fires progress continuously through time and space. If cloud coverage or smoke is persistent, fire continuity can break, increasing the risk of artificially splitting single fires into multiple parts. Burn date uncertainty may also lead to multiple "extinction points," outliers in the estimated burn day along the edges of a fire. The coarse resolution can cause an underestimation of the overall burned area. Since it uses MCD64A1, it also incorporates all limitations inherent of its methodology.	Open access	(ANDELA et al., 2019)

APPENDIX C - SUPPLEMENTARY MATERIAL FROM CHAPTER 4

Table C.1 - Annual burned area per land use and land cover class, as well as their respective percentages in parenthesis. The last row brings burned area rate and standard deviation in parenthesis. for = forest; sec = secondary forest; nat = other natural formations; dfs = deforestation of secondary forest; dfp = deforestation of old growth forest; far = farming; oth = other.

	for (km^2)	sec (km^2)	nat (km^2)	dfs (km^2)	dfp (km^2)	far (km^2)	oth (km^2)	total (km^2)
2003	12,168 (16%)	948 (1%)	34,330 (46%)	577 (1%)	7,004 (9%)	18,739 (25%)	206 (0%)	73,973
2004	18,960 (18%)	1,340 (1%)	48,312 (46%)	604 (1%)	7,504 (7%)	27,475 (26%)	261 (0%)	104,455
2005	21,417 (16%)	1,689 (1%)	57,845 (44%)	512 (0%)	6,447 (5%)	42,204 (32%)	226 (0%)	130,340
2006	11,664 (15%)	969 (1%)	36,786 (48%)	298 (0%)	3,387 (4%)	22,751 (30%)	117 (0%)	75,973
2007	30,479 (22%)	3,067 (2%)	43,944 (32%)	597 (0%)	3,457 (3%)	54,175 (40%)	281 (0%)	135,999
2008	9,760 (14%)	986 (1%)	32,158 (47%)	289 (0%)	1,727 (3%)	22,880 (34%)	152 (0%)	67,954
2009	4,654 (13%)	736 (2%)	18,128 (50%)	170 (0%)	585 (2%)	11,637 (32%)	114 (0%)	36,024
2010	34,431 (21%)	2,837 (2%)	77,194 (47%)	533 (0%)	1,558 (1%)	46,465 (28%)	275 (0%)	163,293
2011	8,487 (16%)	1,109 (2%)	32,218 (61%)	285 (1%)	592 (1%)	10,446 (20%)	97 (0%)	53,234
2012	12,088 (18%)	1,502 (2%)	32,873 (48%)	379 (1%)	1,155 (2%)	19,870 (29%)	141 (0%)	68,008
2013	3,940 (11%)	609 (2%)	20,932 (60%)	192 (1%)	516 (1%)	8,740 (25%)	66 (0%)	34,996
2014	8,253 (17%)	1,319 (3%)	21,084 (43%)	414 (1%)	1,094 (2%)	16,734 (34%)	142 (0%)	49,039
2015	12,523 (19%)	2,017 (3%)	26,651 (40%)	542 (1%)	1,664 (2%)	23,232 (35%)	139 (0%)	66,768
2016	12,753 (17%)	1,631 (2%)	39,326 (54%)	467 (1%)	1,443 (2%)	17,277 (24%)	165 (0%)	73,062
2017	19,221 (21%)	2,974 (3%)	35,139 (38%)	557 (1%)	1,788 (2%)	32,490 (35%)	163 (0%)	92,332
2018	5,884 (16%)	749 (2%)	19,036 (50%)	205 (1%)	1,186 (3%)	10,630 (28%)	134 (0%)	37,823
2019	15,796 (21%)	1,785 (2%)	32,253 (42%)	465 (1%)	2,377 (3%)	23,979 (31%)	161 (0%)	76,815
2020	17,403 (20%)	2,508 (3%)	35,245 (41%)	740 (1%)	3,045 (4%)	26,271 (31%)	223 (0%)	85,436
Mean	14,438	1,599	35,747	435	2,585	24,222	170	79,196
(sd)	(8,258)	(792)	(14,553)	(165)	(2,214)	(12,671)	(62)	(35,450)

Table C.2 - Annual burned area per land use and land cover class, normalized by total land cover class area. The last row brings burned area rate and standard deviation in parenthesis. for = forest; sec = secondary forest; nat = other natural formations; dfs = deforestation of secondary forest; dfp = deforestation of old growth forest; far = farming; oth = other.

	for	sec	nat	dfs	dfp	far	oth
2003	0.3%	0.8%	5.8%	5.7%	22.2%	3.8%	1.2%
2004	0.4%	1.2%	8.2%	5.2%	24.6%	5.3%	1.5%
2005	0.5%	1.4%	9.9%	5.4%	25.2%	7.8%	1.2%
2006	0.3%	0.8%	6.3%	2.8%	16.5%	4.0%	0.6%
2007	0.7%	2.4%	7.5%	6.3%	21.5%	9.3%	1.5%
2008	0.2%	0.8%	5.5%	2.9%	11.2%	3.8%	0.8%
2009	0.1%	0.5%	3.1%	1.8%	5.4%	1.9%	0.6%
2010	0.8%	2.1%	13.2%	5.4%	15.7%	7.6%	1.6%
2011	0.2%	0.8%	5.5%	3.1%	5.4%	1.7%	0.6%
2012	0.3%	1.0%	5.7%	3.8%	12.0%	3.2%	0.8%
2013	0.1%	0.4%	3.6%	1.7%	5.0%	1.4%	0.4%
2014	0.2%	0.8%	3.7%	3.4%	10.5%	2.6%	0.8%
2015	0.3%	1.3%	4.7%	4.2%	14.6%	3.6%	0.7%
2016	0.3%	1.0%	6.9%	3.3%	10.0%	2.6%	0.9%
2017	0.4%	1.8%	6.2%	5.3%	14.7%	4.8%	0.9%
2018	0.1%	0.4%	3.4%	1.9%	9.1%	1.6%	0.7%
2019	0.4%	1.0%	5.8%	3.1%	18.7%	3.5%	0.8%
2020	0.4%	1.4%	6.5%	3.2%	15.2%	3.8%	1.0%
Mean	0.3%	1.1%	6.2%	3.7%	16.3%	3.9%	0.9%

Table C.3 - Annual burned area per land use and land cover class inside and outside each of the protected area categories.

	2003	2004	2005	2006	2007	2008	2009	2010	2011	2012	2013	2014	2015	2016	2017	2018	2019	2020
Forest	**12,168**	**18,960**	**21,417**	**11,664**	**30,479**	**9,760**	**4,654**	**34,431**	**8,487**	**12,088**	**3,940**	**8,253**	**12,523**	**12,753**	**19,221**	**5,884**	**15,796**	**17,403**
Indirect use	257	373	416	268	518	244	136	857	347	341	120	251	303	494	400	224	350	889
Direct use	278	358	481	1,132	1,108	1,224	357	3,334	772	784	225	623	1,211	815	1,634	526	1,788	2,719
Indigenous land	625	1,888	1,123	839	3,346	912	379	4,882	2,272	2,656	804	1,370	2,594	3,637	3,506	965	3,130	3,531
Outside	11,007	16,342	19,396	9,425	25,507	7,381	3,782	25,359	5,096	8,306	2,792	6,009	8,415	7,807	13,681	4,169	10,527	10,263
Secondary forest	**948**	**1,340**	**1,689**	**969**	**3,067**	**986**	**736**	**2,837**	**1,109**	**1,502**	**609**	**1,319**	**2,017**	**1,631**	**2,974**	**749**	**1,785**	**2,508**
Indirect use	19	23	25	19	42	16	21	74	41	46	8	40	38	35	83	20	48	82
Direct use	13	34	34	53	60	60	52	102	34	79	21	61	136	72	180	49	131	179
Indigenous land	35	87	59	43	181	62	36	198	93	167	88	173	290	307	314	93	201	331
Outside	882	1,196	1,571	854	2,785	848	626	2,463	942	1,211	492	1,045	1,554	1,217	2,397	588	1,405	1,916
Other natural formations	**34,330**	**48,312**	**57,845**	**36,786**	**43,944**	**32,158**	**18,128**	**77,194**	**32,218**	**32,873**	**20,932**	**21,084**	**26,651**	**39,326**	**35,139**	**19,036**	**32,253**	**35,245**
Indirect use	1,252	2,168	1,827	827	2,141	1,477	762	3,921	2,595	2,277	1,003	1,773	1,760	2,656	1,559	1,102	1,453	2,259
Direct use	1,244	2,741	3,980	2,581	2,401	4,129	1,384	9,449	4,086	3,352	1,757	1,622	2,810	3,873	3,478	1,761	4,984	5,711
Indigenous land	8,583	11,801	14,078	9,890	11,067	9,386	5,928	19,613	9,537	10,020	7,165	7,510	8,417	10,386	12,788	5,958	10,108	10,865
Outside	23,251	31,601	37,959	23,488	28,335	17,166	10,053	44,211	16,000	17,224	11,008	10,178	13,665	22,412	17,315	10,215	15,708	16,410
Deforestation of secondary forest	**577**	**604**	**512**	**298**	**597**	**289**	**170**	**533**	**285**	**379**	**192**	**414**	**542**	**467**	**557**	**205**	**465**	**740**
Indirect use	4	5	5	4	6	3	4	10	3	4	1	4	9	4	12	3	9	14
Direct use	3	6	8	10	13	16	9	24	7	15	4	13	39	25	44	13	35	68
Indigenous land	6	23	15	5	18	15	5	22	13	12	6	24	30	26	40	17	44	88
Outside	564	570	483	278	559	256	151	477	263	348	181	373	463	412	461	172	377	570
Deforestation of primary forest	**7,004**	**7,504**	**6,447**	**3,387**	**3,457**	**1,727**	**585**	**1,558**	**592**	**1,155**	**516**	**1,094**	**1,664**	**1,443**	**1,788**	**1,186**	**2,377**	**3,045**
Indirect use	53	24	69	33	20	11	5	15	3	8	6	8	21	10	25	17	29	61
Direct use	65	81	156	335	391	210	67	155	59	135	47	115	248	191	321	167	451	686
Indigenous land	50	91	44	29	62	41	12	46	42	32	12	19	32	56	52	32	89	116
Outside	6,836	7,308	6,179	2,990	2,984	1,464	501	1,342	488	980	451	952	1,362	1,186	1,389	969	1,808	2,182
Farming	**18,739**	**27,475**	**42,204**	**22,751**	**54,175**	**22,880**	**11,637**	**46,465**	**10,446**	**19,870**	**8,740**	**16,734**	**23,232**	**17,277**	**32,490**	**10,630**	**23,979**	**26,271**
Indirect use	117	172	382	244	365	197	143	444	165	223	51	258	256	180	424	176	345	448
Direct use	132	246	558	1,386	1,496	1,806	593	2,562	460	1,282	243	914	1,743	967	2,825	1,048	2,624	2,878
Indigenous land	352	640	633	527	1,260	732	309	1,413	570	998	878	1,193	1,422	1,587	1,578	833	1,562	1,487
Outside	18,139	26,417	40,632	20,594	51,053	20,145	10,592	42,047	9,251	17,367	7,567	14,369	19,811	14,544	27,663	8,573	19,448	21,459
Other	**206**	**261**	**226**	**117**	**281**	**152**	**114**	**275**	**97**	**141**	**66**	**142**	**139**	**165**	**163**	**134**	**161**	**223**
Indirect use	2	6	11	1	10	1	2	5	4	7	0	2	3	4	3	5	8	4
Direct use	6	10	5	10	29	10	7	21	5	5	4	7	9	10	9	7	15	21
Indigenous land	35	64	44	23	68	26	27	71	21	44	22	54	27	44	42	25	47	56
Outside	162	181	167	83	174	115	78	177	67	85	39	79	100	108	109	98	91	142

APPENDIX D - SUPPLEMENTARY MATERIAL FROM CHAPTER 5

Table D.1 - Data source for each country's administrative boundaries.

Country	Source	Update year	Country	Department	Municipality
Bolivia	GeoBolivia: la Infraestructura de Datos Espaciales del Estado Plurinacional de Bolivia	Aug 2020	Level 0 = Country	Level 1 = Department	Level 3 = Municipality
Brazil	Instituto Brasileiro de Geografia e Estatística (IBGE)	Sep 2020	Level 0 = Country	Level 1 = State	Level 2 = Municipality
Colombia	Departamento Administrativo Nacional de Estadística (DANE)	Feb 2020	Level 0 = Country	Level 1 = Department	Level 2 = Municipality
Ecuador	Instituto Nacional de Estadística y Censos (INEC)	Sep 2020	Level 0 = Country	Level 1 = Province	Level 3 = Parish
French Guiana	Institut national de l'information géographique et forestière (IGN)	Feb 2020	Level 0 = Department	Level 1 = Arrondissement	Level 2 = Commune
Guyana	DEVInfo LAC project	Jul 2021	Level 0 = Country	Level 1 = Region	Level 2 = Boundary
Peru	Instituto Geográfico Nacional (IGN)	Jul 2020	Level 0 = Country	Level 1 = Region or autonomous province	Level 3 = District
Suriname	www.gadm.org	Oct 2019	Level 0 = Country	Level 1 = District	Level 2 = Resort
Venezuela	Instituto Nacional de Estadística	Feb 2021	Level 0 = Country	Level 1 = State, capital district, federal dependency	Level 3 = Parish

Source: Humdata (2021).

Table D.2 - Variable context to be included as covariate and references using similar variables. Although they are the same variables, in theory, their use in the different studies referenced follows specific contexts of each study, and their metrics may not be the same as those we used.

Variable	Context	Reference using the similar variable
	Weather factors	
Precipitation	Changes in precipitation during the critical dry-season months can sharply increase the likelihood of ground fires and larger, more destructive wildfires (LAURANCE; WILLIAMSON, 2001). Drier fuel, due to decreased precipitation, is more prone to burn. On the other hand, areas of extremely high rainfall are unlikely to be converted to agriculture, raising the chance to home a PA (NELSON; CHOMITZ, 2011).	(AMIN et al., 2019; ARRIAGADA; ECHEVERRIA; MOYA, 2016; HERRERA; PFAFF; ROBALINO, 2019; NELSON; CHOMITZ, 2011; NOLTE et al., 2017; NOLTE; AGRAWAL, 2013; PFAFF et al., 2014, 2015a, 2015b; SHI et al., 2020; SIMS, 2010; TASKER; ARIMA, 2016)
Maximum Cumulative Water Deficit (MCWD)	The frequency and intensity of droughts can positively influence the susceptibility to fires, once it could affect tree mortality, changing the canopy openness, the relative humidity, and the temperature (COCHRANE, 2003). Furthermore, more severe dry seasons affect the amount of vegetation transpiring water. Reduced transpiration lowers local atmospheric humidity levels and increases the probability of fires (LAURANCE; WILLIAMSON, 2001).	
Temperature	Temperature plays a strong role in fire occurrence in the Amazon. High temperatures during the dry season contribute to the rapid drying of decomposing material, making it more flammable. The influence of increased temperatures on the likelihood of fire occurrence can be larger than the effects of reduced rainfall (LIMA; AGHAKOUCHAK; RANDERSON, 2018).	(SHI et al., 2020; SIMS, 2010)
	Land use factors	
Deforestation of primary forest	Fire is commonly used in the deforestation process in the Amazon, being a cheap tool to burn the deforested material and, consequently, clear the area for agricultural use (MORTON et al., 2008). Furthermore, deforestation still creates forest edges, which are more vulnerable to fire, creating a positive feedback between deforestation and fire (SILVA JUNIOR et al., 2018).	(NOLTE et al., 2017)
Deforestation of secondary forest	Deforestation of secondary forests is also linked to the slash-and-burn process (COCHRANE, 2003; PAUSAS; KEELEY, 2009). Fire is often used as a tool to clear the land and maintain existing farmland and pasture. The slash-and-burn agriculture practice consists of cutting, drying, and burning the natural vegetation in a patch cultivated for years and then left to regrow (PIVELLO, 2011).	(TASKER; ARIMA, 2016)

(To be continued)

Table D.2 – Continuation.

Variable	Context	Reference using the similar variable
Secondary forest	Depending on the stage they are in, secondary forests may be more prone to fire, as they may have more open canopies, causing low relative humidity and high temperature inside. The fire recurrence in these forests alters their ability to accumulate carbon, making them highly susceptible to recurrent burning (ZARIN et al., 2005).	
Forest fragmentation	More fragmented landscapes with a greater proportion of edges tend to be more vulnerable to fire than landscapes with continuous and intact forests. This occurs due to changes in the original structural configuration of the forest, which changes the mass and energy balance (SILVA JUNIOR et al., 2018). In addition, fragmented forests tend to be drier due to lower humidity retention, higher temperature, and greater exposure to dry air masses and winds (Cochrane, 2008 synergisms). This condition, in addition to increased vulnerability to fire by itself, also causes higher tree mortality (LAURANCE et al., 2018), resulting in a large amount of fuel load available and, consequently, increasing the susceptibility to forest fires (BERENGUER et al., 2014).	(AMIN et al., 2019; ANDAM et al., 2008; HERRERA; PFAFF; ROBALINO, 2019; NOLTE et al., 2013; NOLTE; AGRAWAL, 2013; PFAFF et al., 2014, 2015a, 2015b; WENDLAND et al., 2015)
Forest	Primary tropical forests have dense canopies that allow the formation of humid microclimates with mild temperatures. The dense canopy retains much of the solar radiation that falls on the forests and is a barrier to winds. These characteristics confer contrary conditions to fire occurrence inside the forest.	(NOLTE et al., 2013, 2017; SZE et al., 2022)
Farming	Fires are often used as a tool to clear the land and maintain existing farmland and pasture, which makes their occurrence strongly associated with human activity (COCHRANE, 2003; PAUSAS; KEELEY, 2009). This way, fires in the Amazon are partially correlated with farming activities.	(ARRIAGADA; ECHEVERRIA; MOYA, 2016)
Non-forest natural formations	Natural non-forest formations include rocky outcrops, grasslands, and other formations. In general, these formations have lower biomass available for burning. However, like savannas, they are environments exposed to the occurrence of natural fire.	
Savanna	Savannas are environments adapted to sporadic fire, and their species composition and ecosystem functions are intertwined with natural fire occurrence. Unlike humid forests, natural fire ignitions by lightning is more frequent. The presence of a larger area of savanna may, therefore, impose a greater vulnerability to fire, even if it does not cause as many environmental impacts as when it occurs in humid forests.	(PFAFF et al., 2015a, 2015b; TASKER; ARIMA, 2016)

(To be continued)

Table D.2 – Continuation.

Variable	Context	Reference using the similar variable
Non-vegetated area	Areas without vegetation are generally urban or consolidated and, therefore, do not have as much flammable fuel to burn. Therefore, using fire as a soil management tool does not apply to this environment. An exception is the use of fire to burn garbage, common in urban areas in the Amazon (SILVA et al., 2019).	
Mangrove	Mangroves, like floodplain forests, are subject to climate change and, consequently, to longer and more intense periods of drought. As a result, they become more flammable and vulnerable to fire.	
Flooded forests	Seasonally flooded forests can suffer greater fire damage than upland forests, and canopy structure contributes to their greater susceptibility to fires (ALMEIDA et al., 2016).	
	Land profitability factors	
Distance to roads	Roads represent a channel for natural resources to flow from forests to markets; therefore, their proximityem is directly related to forest vulnerability to degradation processes, including fires. The closer to highways, the forests are more likely to be exploited. Then, this distance can be used as a proxy for market access.	(ANDAM et al., 2008; ARRIAGADA; ECHEVERRIA; MOYA, 2016; HERRERA; PFAFF; ROBALINO, 2019; JOPPA; PFAFF, 2011; NELSON; CHOMITZ, 2011; PFAFF et al., 2014, 2015a, 2015b; SIMS, 2010; SOARES-FILHO et al., 2010; SZE et al., 2022; WENDLAND et al., 2015)
Distance to rivers	Following the same road reasoning, rivers also represent a channel for natural resources to flow from forests to markets in the Amazon. Therefore, their proximity is directly related to forest vulnerability to degradation processes, including fires. The closer to rivers, the forests are more likely to be exploited. Then, this distance can be used as a proxy for market access.	ANDAM et al., 2008; ARRIAGADA; ECHEVERRIA; MOYA, 2016; NOLTE et al., 2017; PFAFF et al., 2015a; SIMS, 2010; SOARES-FILHO et al., 2010)
Population	In the Amazon, a humid tropical forest, fire ignition source is predominantly anthropogenic, and, consequently, there is a relationship between population density and fire occurrence. Population distribution is highly associated with fire persistence (Chuvieco, 2008). Furthermore, it is positively correlated with the spatial pattern of burned area (Andela, 2017), as humans have introduced fires for deforestation and agricultural management (Page, 2002; van der Werf, 2017; Kauano 2017).	AMIN et al., 2019; ANDAM et al., 2008; SZE et al., 2022)

(To be continued)

Table D.2 – Conclusion.

Variable	Context	Reference using the similar variable
Distance to urban centers and populated hotspots	Urban centers are trade markets for forests' natural resources. The closer to these centers, the greater the forest's vulnerability to degradation, including fires, due to the access ease to markets.	(ANDAM et al., 2008; ARRIAGADA; ECHEVERRIA; MOYA, 2016; JOPPA; PFAFF, 2011; NELSON; CHOMITZ, 2011; PFAFF et al., 2014, 2015a, 2015b; SIMS, 2010; WENDLAND et al., 2015)
Slope	Low slope terrains are preferable for performing agricultural activities as it facilitates production mechanization. Thus, lower slopes indicate an increase in land profitability and, consequently, a lower likelihood of establishing a protected area. As well as having a direct relation to suitability, slope and elevation are proxies for physical soil properties (NELSON; CHOMITZ, 2011).	(ARRIAGADA; ECHEVERRIA; MOYA, 2016; HERRERA; PFAFF; ROBALINO, 2019; JOPPA; PFAFF, 2011; NELSON; CHOMITZ, 2011; NOLTE et al., 2013; NOLTE; AGRAWAL, 2013; PFAFF et al., 2014, 2015a, 2015b; SIMS, 2010; SOARES-FILHO et al., 2010; SZE et al., 2022; WENDLAND et al., 2015)
Elevation	Following the same logic as slope, higher elevation decreases land profitability, as it hinders the production mechanization process. Consequently, the lower the elevation, the lower the likelihood of establishing a protected area. As well as having a direct relation to suitability, slope and elevation are proxies for physical soil properties, and elevation is a proxy for temperature (NELSON; CHOMITZ, 2011).	(ARRIAGADA; ECHEVERRIA; MOYA, 2016; JOPPA; PFAFF, 2011; NELSON; CHOMITZ, 2011; NOLTE et al., 2013; NOLTE; AGRAWAL, 2013; SIMS, 2010; SOARES-FILHO et al., 2010; SZE et al., 2022; WENDLAND et al., 2015)
Soil quality	The Amazon soil is not nutrient-rich; therefore, soil quality is an important factor for agricultural activity. Consequently, protected areas tend to be placed on land less suitable for agriculture and on soil with lower soil quality characteristics.	(ARRIAGADA; ECHEVERRIA; MOYA, 2016; NOLTE et al., 2017; PFAFF et al., 2014, 2015a, 2015b)

Figure D.1 - Fire occurrence spatial distribution, represented by the pixel proportion (a) or active fire number (b) in each 5 x 5 km pixel. Values are based on the mean from 2003 to 2020.

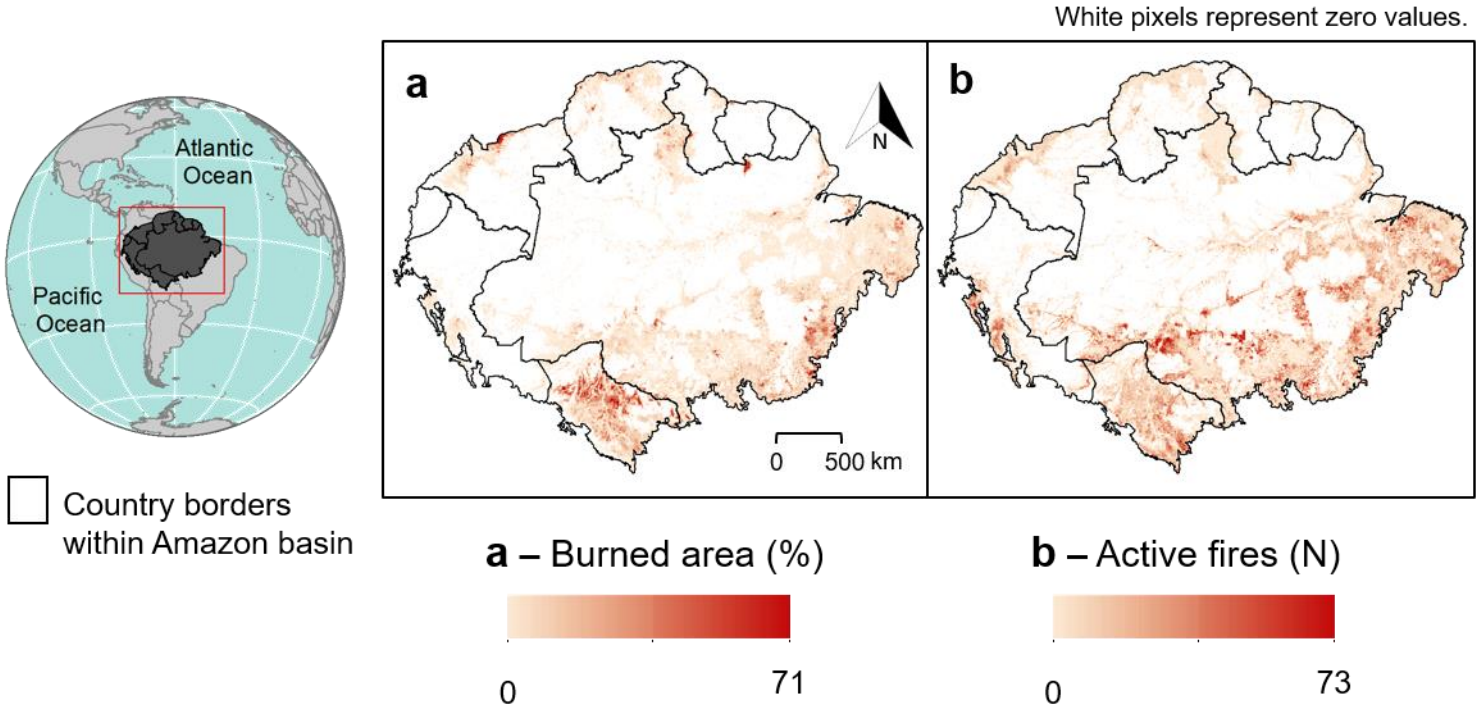

Figure D.2 - Weather variables spatial distribution, represented by the mean value in each 5 x 5 km pixel from 2003 to 2020.

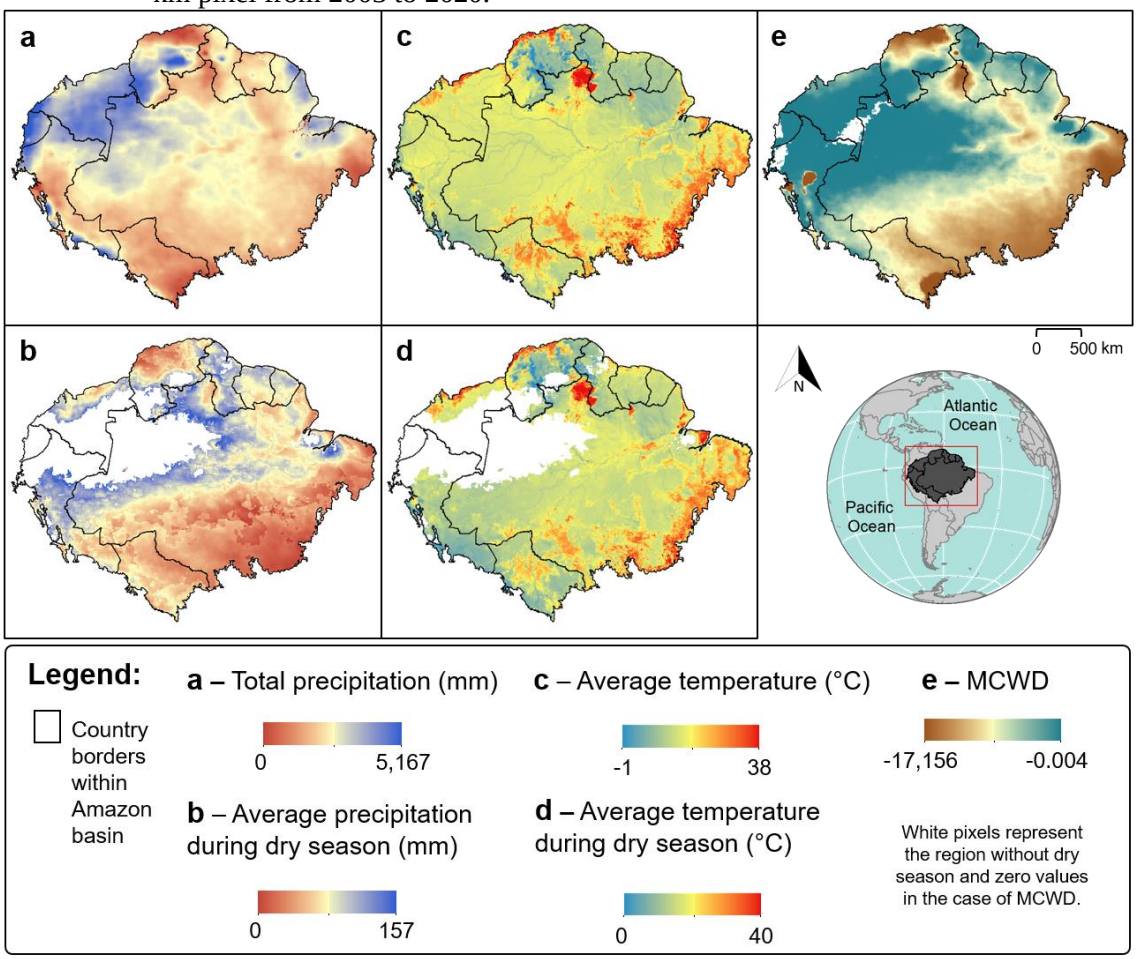

Figure D.3 - Land use and land cover classes spatial distribution, represented by the pixel proportion (except forest edge length) in each 5 x 5 km pixel. Values are based on the mean from 2003 to 2020.

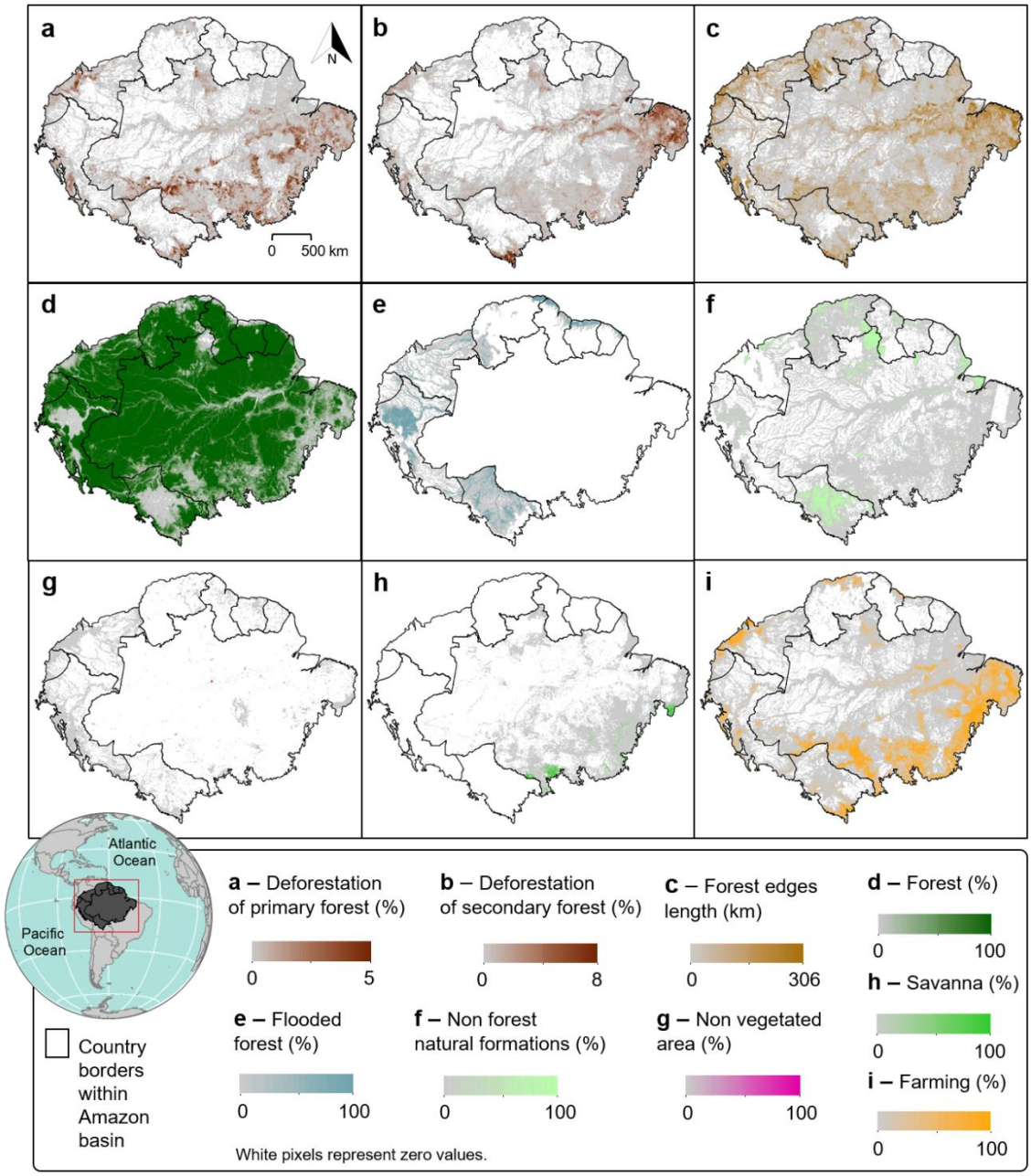

Figure D.4 - Land profitability variables spatial distribution. The mean value represents population count in each 5 x 5 km pixel from 2003 to 2020.

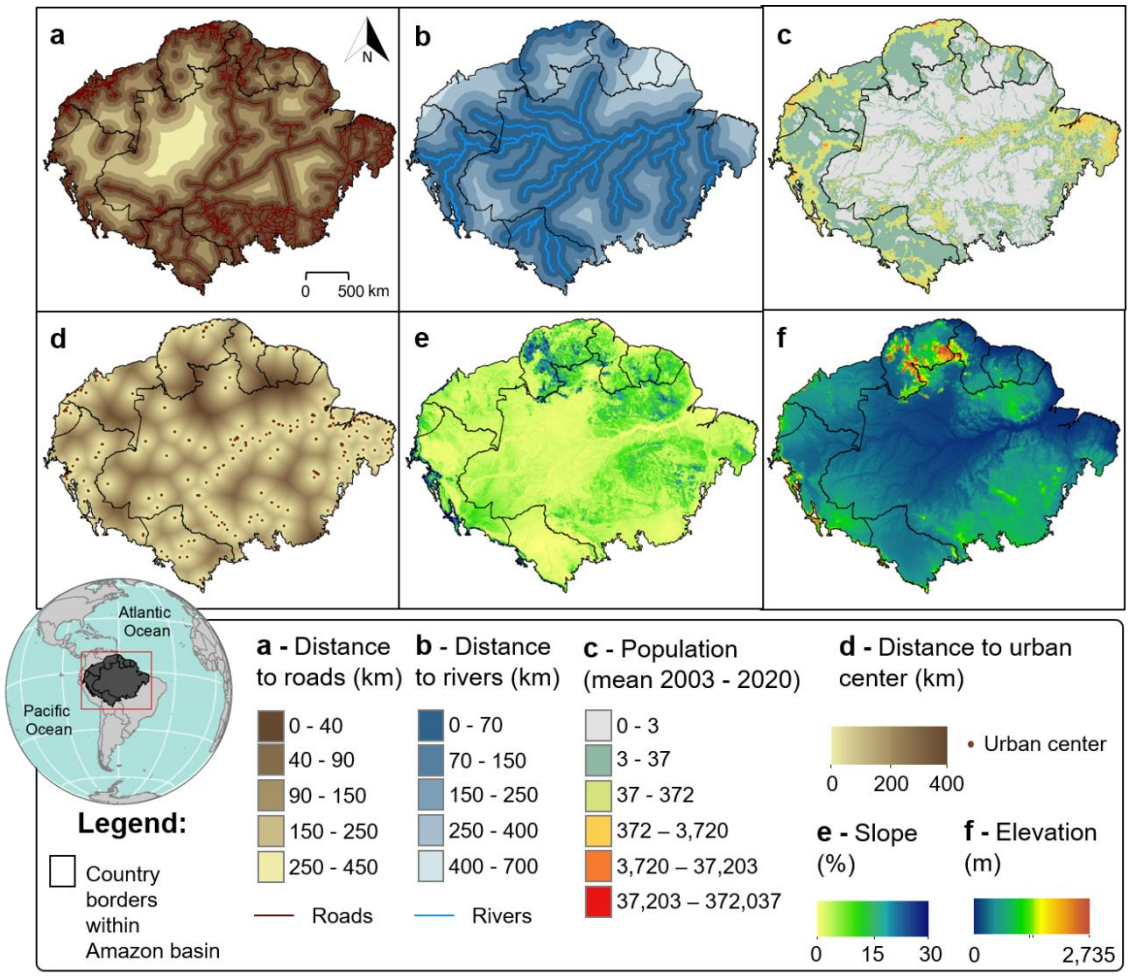

Table D.3 - Eigenvectors of Principal Component Analysis considering soil quality to plant growth variables.

Variable	Comp1	Comp2	Comp3	Comp4	Comp5	Comp6	Comp7	Comp8	Comp9	Comp10	Comp11	Comp12	Comp13	Unexplained
d_soil_nut	0.34	-0.03	0.02	-0.04	-0.01	0.02	-0.12	-0.09	-0.25	0.05	0.02	-0.62	0.65	0.00
d_soil_nutRet	0.34	-0.03	0.02	-0.04	-0.01	0.01	-0.12	-0.09	-0.24	0.05	0.13	-0.46	-0.75	0.00
d_soil_root	0.32	-0.01	0.00	-0.04	-0.01	-0.08	0.53	0.07	0.05	-0.78	-0.03	-0.02	0.00	0.00
d_soil_oxy	0.32	-0.04	0.03	-0.03	0.01	0.02	-0.22	-0.52	0.76	-0.01	-0.01	0.00	0.00	0.00
d_soil_salts	0.34	-0.03	0.02	-0.04	-0.01	0.01	-0.12	-0.10	-0.24	0.01	0.35	0.41	0.07	0.00
d_soil_toxi	0.34	-0.03	0.02	-0.04	-0.01	0.01	-0.12	-0.10	-0.24	0.01	0.35	0.41	0.07	0.00
d_soil_work	0.32	0.00	0.00	-0.03	-0.01	-0.11	0.68	0.12	0.15	0.62	0.01	0.02	0.00	0.00
d_nut	0.01	0.23	0.68	0.37	-0.60	0.00	0.01	-0.02	0.00	0.00	0.00	0.00	0.00	0.00
d_nutRet	0.01	0.38	0.58	-0.18	0.69	-0.01	-0.01	0.04	0.00	0.00	0.00	0.00	0.00	0.00
d_root	0.11	0.51	-0.32	0.39	0.07	-0.66	-0.15	0.04	0.01	-0.01	0.00	0.00	0.00	0.00
d_oxy	0.06	-0.44	0.06	0.79	0.39	0.15	0.04	0.01	-0.02	0.00	0.00	0.00	0.00	0.00
d_salts	0.32	-0.03	0.00	-0.03	-0.04	0.13	-0.33	0.81	0.33	-0.01	0.03	0.00	0.00	0.00
d_toxi	0.34	-0.03	0.02	-0.04	-0.01	0.02	-0.13	-0.06	-0.24	0.06	-0.86	0.26	-0.04	0.00
d_work	0.08	0.59	-0.31	0.20	0.00	0.71	0.11	-0.06	-0.02	0.00	0.00	0.00	0.00	0.00

Note: d_soil_i = dummy variable indicating if the pixel is classified as soil or, being i, any of the soil quality indicators; d_i = dummy variable indicating if the pixel has no or slight limitation for I, being i any of the soil quality indicators. Soil quality indicators are nutrient availability, nutrient retention capacity, rooting conditions, oxygen availability to roots, excess salts, toxicities, and workability.

Table D.4 - Summary statistics of the sample after matching 1SD caliper.

	Treated on support		*Treated off support*		*Matched controls*		*Unmatched controls*	
Variable	Mean	Std. Dev.	Mean	Std. Dev.	Mean	Std. Dev.	Mean	Std. Dev.
Treatment dummy	1	0	1	0	0	0	0	0
Burned area (% within a pixel)	0.63%	3.22%	1.21%	4.92%	1.10%	3.81%	2.02%	4.82%
Active fires (N)	0.30	1.64	0.38	1.78	0.65	2.25	1.59	3.90
distUrban (km)	214.26	165.45	280.21	186.48	212.56	184.38	179.51	185.70
distPopulated (km)	80.53	42.21	100.20	68.75	63.16	37.32	49.20	36.48
distRiver (km)	112.58	98.21	197.12	120.26	103.94	106.04	126.78	125.03
distRoad (km)	90.65	71.38	78.64	54.94	77.79	78.64	58.05	78.19
distPavRoad (km)	127.34	79.16	156.02	100.73	108.38	83.78	85.25	92.19
elevation (m)	177.54	107.91	280.24	195.75	165.01	117.86	180.23	128.73
slope (%)	2.99	2.24	4.97	3.89	2.77	2.31	2.87	2.29
pca_soil	0.19	2.08	-0.11	2.77	-0.04	3.18	-0.14	3.56
DFpri (% within a pixel)	0.08%	0.33%	0.10%	0.35%	0.19%	0.49%	0.51%	0.81%
DFsec (% within a pixel)	0.05%	0.18%	0.10%	0.35%	0.11%	0.31%	0.38%	0.64%
forest (% within a pixel)	87.82%	25.59%	82.02%	29.18%	76.61%	32.48%	59.27%	36.16%
secForest (% within a pixel)	0.85%	2.37%	1.88%	4.50%	1.71%	3.70%	4.25%	6.24%
farming (% within a pixel)	1.47%	6.11%	2.24%	7.21%	4.41%	11.19%	23.61%	29.50%
nonForestNatural (% within pixel)	3.25%	13.56%	7.96%	20.89%	5.72%	17.63%	4.79%	16.15%
nonVegetated (% within a pixel)	0.02%	0.17%	0.16%	1.46%	0.03%	0.26%	0.20%	2.16%
floodedForest (% within a pixel)	4.30%	16.15%	2.54%	10.57%	7.21%	20.21%	3.45%	14.12%
mangrove (% within a pixel)	0.00%	0.07%	0.33%	3.72%	0.00%	0.15%	0.03%	0.82%
savanna (% within a pixel)	0.47%	4.67%	0.90%	4.77%	0.72%	5.89%	0.88%	5.77%
precMean (mm)	205.41	42.26	205.17	53.77	198.36	39.47	188.27	37.47
precTotal (mm)	2,464.91	507.13	2,461.99	645.28	2,380.34	473.63	2,259.29	449.64
tempMean (°C)	27.64	1.02	27.31	1.68	27.86	1.28	28.86	1.95
MCWD	-154.88	223.61	-228.27	426.40	-169.26	256.51	-253.86	535.67
precDry (mm)	43.33	31.77	44.51	30.08	45.55	31.44	46.27	28.07
tempDry (°C)	20.42	12.33	21.40	11.95	21.40	12.14	25.08	10.74
pop (N)	18.00	101.09	79.03	1,097.19	37.51	184.61	247.92	3,613.37
frag (km)	9.96	16.72	17.76	27.09	15.91	22.13	25.21	26.57

Note: Statistics obtained by collapsed dataset refers to the average year, calculated for time-varying variables as the average value from 2003 to 2020.

Table D.5 - Differences-in-differences estimation of the protected area effect on the burned area - complete table.

Dependent variable: Burned area proportion within the pixel
Treatment: Pixel within an active protected area

	FE	DiD	DiD-FE	FE bootstrapped SEs	DiD bootstrapped SEs	DiD-FE bootstrapped SEs
Average treatment effect (ATE)	-0.000728***	-0.000728***	-0.000728***	-0.000728***	-0.000728***	-0.000728***
	(0.0002)	(0.0002)	(0.0002)	(0.0002)	(0.0002)	(0.0002)
DFpri	0.742***	0.742***	0.742***	0.742***	0.742***	0.742***
	(0.0247)	(0.0254)	(0.0247)	(0.0257)	(0.0251)	(0.0216)
DFsec	-0.0436	-0.0436	-0.0436	-0.0436	-0.0436	-0.0436
	(0.0504)	(0.0519)	(0.0504)	(0.0538)	(0.0461)	(0.0476)
forest	-0.0355***	-0.0355***	-0.0355***	-0.0355***	-0.0355***	-0.0355***
	(0.0102)	(0.0105)	(0.0102)	(0.0102)	(0.0099)	(0.0105)
farming	-0.0765***	-0.0765***	-0.0765***	-0.0765***	-0.0765***	-0.0765***
	(0.0114)	(0.0118)	(0.0114)	(0.0117)	(0.0104)	(0.0112)
NonForestNaturalArea	0.0601***	0.0601***	0.0601***	0.0601***	0.0601***	0.0601***
	(0.0139)	(0.0143)	(0.0139)	(0.0142)	(0.0132)	(0.0140)
nonVegetatedARea	-0.298***	-0.298***	-0.298***	-0.298***	-0.298***	-0.298***
	(0.0428)	(0.0440)	(0.0428)	(0.0412)	(0.0439)	(0.0433)
floodedForest	0.0300**	0.0300**	0.0300**	0.0300**	0.0300**	0.0300**
	(0.0111)	(0.0115)	(0.0111)	(0.0116)	(0.0106)	(0.0110)
mangrove	0.0963	0.0963	0.0963	0.0963	0.0963	0.0963
	(0.0661)	(0.0680)	(0.0661)	(0.0940)	(0.0930)	(0.0887)
savanna	0.210+	0.210+	0.210+	0.210+	0.210+	0.210+
	(0.1100)	(0.1130)	(0.1100)	(0.1090)	(0.1100)	(0.1080)
precTotal	-0.000000768***	-0.000000768***	-0.000000768***	-0.000000768***	-0.000000768***	-0.000000768***
	(0.0000)	(0.0000)	(0.0000)	(0.0000)	(0.0000)	(0.0000)
tempMedia	0.0230***	0.0230***	0.0230***	0.0230***	0.0230***	0.0230***
	(0.0005)	(0.0005)	(0.0005)	(0.0004)	(0.0004)	(0.0004)

(To be continued)

Table D.5 – Conclusion.

	FE	DiD	DiD-FE	FE bootstrapped SEs	DiD bootstrapped SEs	DiD-FE bootstrapped SEs
MCWD	-0.00000557***	-0.00000557***	-0.00000557***	-0.00000557***	-0.00000557***	-0.00000557***
	(0.0000)	(0.0000)	(0.0000)	(0.0000)	(0.0000)	(0.0000)
precSeca	0.0000338***	0.0000338***	0.0000338***	0.0000338***	0.0000338***	0.0000338***
	(0.0000)	(0.0000)	(0.0000)	(0.0000)	(0.0000)	(0.0000)
tempSeca	0.00446***	0.00446***	0.00446***	0.00446***	0.00446***	0.00446***
	(0.0002)	(0.0002)	(0.0002)	(0.0002)	(0.0002)	(0.0002)
ppp	0.000000774	0.000000774	0.000000774	0.000000774	0.000000774	0.000000774
	(0.0000)	(0.0000)	(0.0000)	(0.0000)	(0.0000)	(0.0000)
edges	0.000000132***	0.000000132***	0.000000132***	0.000000132***	0.000000132***	0.000000132***
	(0.0000)	(0.0000)	(0.0000)	(0.0000)	(0.0000)	(0.0000)
_cons	-0.692***	-0.692***	-0.692***	-0.692***	-0.692***	-0.692***
	(0.0164)	(0.0169)	(0.0164)	(0.0160)	(0.0161)	(0.0163)
N	1579104	1579104	1579104	1579104	1579104	1579104
chi^2				6517.3	14.77	13.85
F	164.7	290.06	307.12			
p	0	0	0	0	0.000122	0.000197
Overall R^2	0.0839			0.0839		
N clusters	87728	87728	87728	87728	87728	87728

Notes: +p<0.10,*p<0.05,**p<0.01,***p<0.001. The dependent variable is the burned area proportion within each pixel-year. Treatment is a dummy variable that equals one if a pixel is within an active protected area and zero otherwise. FE = fixed-effects estimator for panel data, DiD = differences-in-differences estimator for panel data pooled under the assumption of zero correlation between the covariates and the unobserved heterogeneity term, DiD-FE = estimator addressing both unobserved heterogeneity bias and assuming that the trends were parallel in the untreated state for treated and untreated. All specifications include year and Amazonian department dummies interacted with a deterministic time trend. Covariate controls include within pixel proportion of primary and secondary forest deforestation, forest, farming, non-forest natural formations, non-vegetated area, flooded forests, mangroves, and savanna. Besides that, controls also included total precipitation, mean temperature, maximum cumulative water deficit (MCWD), mean precipitation and temperature during the dry season, population, and forest edge length. Robust standard errors clustered at pixel level or bootstrapped using 200 replications in parentheses.

Table D.6 - Differences-in-differences estimation of the protected area effect on active fires - complete table.

Dependent variable: Active fire count within the pixel
Treatment: Pixel within an active protected area

	FE	DiD	DiD-FE	FE bootstrapped SEs	DiD bootstrapped SEs	DiD-FE bootstrapped SEs
Average treatment effect (ATE)	-0.0439***	-0.0439***	-0.0439***	-0.0439***	-0.0439***	-0.0439***
	(0.0066)	(0.0067)	(0.0066)	(0.0067)	(0.0067)	(0.0065)
DFpri	83.94***	83.94***	83.94***	83.94***	83.94***	83.94***
	(1.9070)	(1.9630)	(1.9070)	(1.9130)	(1.8710)	(1.8720)
DFsec	-15.95***	-15.95***	-15.95***	-15.95***	-15.95***	-15.95***
	(2.2440)	(2.3100)	(2.2440)	(2.0340)	(2.2210)	(2.2540)
forest	7.607***	7.607***	7.607***	7.607***	7.607***	7.607***
	(0.5120)	(0.5260)	(0.5120)	(0.5110)	(0.4960)	(0.5000)
farming	4.204***	4.204***	4.204***	4.204***	4.204***	4.204***
	(0.5450)	(0.5610)	(0.5450)	(0.5310)	(0.4570)	(0.5690)
NonForestNaturalArea	8.555***	8.555***	8.555***	8.555***	8.555***	8.555***
	(0.5920)	(0.6090)	(0.5920)	(0.5630)	(0.5360)	(0.6010)
nonVegetatedARea	-4.664+	-4.664	-4.664+	-4.664	-4.664+	-4.664+
	(2.8050)	(2.8870)	(2.8050)	(2.9420)	(2.7140)	(2.7990)
floodedForest	10.02***	10.02***	10.02***	10.02***	10.02***	10.02***
	(0.5620)	(0.5780)	(0.5620)	(0.5630)	(0.5260)	(0.5510)
mangrove	2.697	2.697	2.697	2.697	2.697	2.697
	(9.1590)	(9.4250)	(9.1590)	(14.1600)	(13.9000)	(15.0500)
savanna	17.53***	17.53***	17.53***	17.53***	17.53***	17.53***
	(1.9580)	(2.0150)	(1.9580)	(2.1150)	(1.9990)	(1.9750)
precTotal	-0.0000218***	-0.0000218***	-0.0000218***	-0.0000218***	-0.0000218***	-0.0000218***
	(0.0000)	(0.0000)	(0.0000)	(0.0000)	(0.0000)	(0.0000)
tempMedia	0.427***	0.427***	0.427***	0.427***	0.427***	0.427***
	(0.0084)	(0.0086)	(0.0084)	(0.0081)	(0.0082)	(0.0081)

(To be continued)

Table D.6 – Conclusion.

	FE	DiD	DiD-FE	FE bootstrapped SEs	DiD bootstrapped SEs	DiD-FE bootstrapped SEs
MCWD	-0.000228***	-0.000228***	-0.000228***	-0.000228***	-0.000228***	-0.000228***
	(0.0000)	(0.0000)	(0.0000)	(0.0000)	(0.0000)	(0.0000)
precSeca	-0.0000468	-0.0000468	-0.0000468	-0.0000468	-0.0000468	-0.0000468
	(0.0001)	(0.0001)	(0.0001)	(0.0001)	(0.0001)	(0.0001)
tempSeca	0.111***	0.111***	0.111***	0.111***	0.111***	0.111***
	(0.0049)	(0.0051)	(0.0049)	(0.0049)	(0.0047)	(0.0052)
ppp	-0.0000123	-0.0000123	-0.0000123	-0.0000123	-0.0000123	-0.0000123
	(0.0000)	(0.0000)	(0.0000)	(0.0000)	(0.0000)	(0.0000)
edges	0.0000147***	0.0000147***	0.0000147***	0.0000147***	0.0000147***	0.0000147***
	(0.0000)	(0.0000)	(0.0000)	(0.0000)	(0.0000)	(0.0000)
_cons	-21.38***	-21.38***	-21.38***	-21.38***	-21.38***	-21.38***
	(0.5620)	(0.5780)	(0.5620)	(0.5470)	(0.5610)	(0.5270)
N	1579104	1579104	1579104	1579104	1579104	1579104
chi^2				12086.7	42.82	45.11
F	281.2	449.69	476.15			
p	0	0	0	0	6.01E-11	1.87E-11
Overall R^2	0.0782			0.0782		
N clusters	87728	87728	87728	87728	87728	87728

Notes: +p<0.10,*p<0.05,**p<0.01,***p<0.001. The dependent variable is the active fire count within each pixel-year. Treatment is a dummy variable that equals one if a pixel is within an active protected area and zero otherwise. FE = fixed-effects estimator for panel data, DiD = differences-in-differences estimator for panel data pooled under the assumption of zero correlation between the covariates and the unobserved heterogeneity term, DiD-FE = estimator addressing both unobserved heterogeneity bias and assuming that the trends were parallel in the untreated state for treated and untreated. All specifications include year and Amazonian department dummies interacted with a deterministic time trend. Covariate controls include within pixel proportion of primary and secondary forest deforestation, forest, farming, non-forest natural formations, non-vegetated area, flooded forests, mangroves, and savanna. Besides that, controls also included total precipitation, mean temperature, maximum cumulative water deficit (MCWD), mean precipitation and temperature during the dry season, population, and forest edge length. Robust standard errors clustered at pixel level or bootstrapped using 200 replications in parentheses.

Table D.7 - Differences-in-differences estimation of the protected area effect on the burned area and active fires considering the standard errors clustered at the department level.

	Dependent variable: Burned area		*Dependent variable: Active fires*	
	FE	DiD-FE	FE	DiD-FE
Average treatment effect (ATE)	-0.000728	-0.000728	-0.0439+	-0.0439+
	(0.0006)	(0.0006)	(0.0253)	(0.0253)
DFpri	0.742***	0.742***	83.94***	83.94***
	(0.0968)	(0.0968)	(9.5540)	(9.5540)
DFsec	-0.0436	-0.0436	-15.95+	-15.95+
	(0.1730)	(0.1730)	(8.3300)	(8.3300)
forest	-0.0355	-0.0355	7.607**	7.607**
	(0.0327)	(0.0327)	(2.5040)	(2.5040)
farming	-0.0765	-0.0765	4.204	4.204
	(0.0837)	(0.0837)	(2.6240)	(2.6240)
NonForestNaturalArea	0.0601	0.0601	8.555**	8.555**
	(0.0510)	(0.0510)	(2.7010)	(2.7010)
nonVegetatedARea	-0.298**	-0.298**	-4.664	-4.664
	(0.0995)	(0.0995)	(3.8990)	(3.8990)
floodedForest	0.03	0.03	10.02***	10.02***
	(0.0249)	(0.0249)	(2.7870)	(2.7870)
mangrove	0.0963	0.0963	2.697	2.697
	(0.1210)	(0.1210)	(4.7470)	(4.7470)
savanna	0.210+	0.210+	17.53***	17.53***
	(0.1150)	(0.1150)	(3.0050)	(3.0050)
precTotal	-0.000000768	-0.000000768	-0.0000218	-0.0000218
	(0.0000)	(0.0000)	(0.0000)	(0.0000)
tempMedia	0.0230*	0.0230*	0.427**	0.427**
	(0.0103)	(0.0103)	(0.1580)	(0.1580)
MCWD	-0.00000557	-0.00000557	-0.000228	-0.000228
	(0.0000)	(0.0000)	(0.0002)	(0.0002)
precSeca	0.0000338	0.0000338	-0.0000468	-0.0000468
	(0.0000)	(0.0000)	(0.0005)	(0.0005)
tempSeca	0.00446+	0.00446+	0.111+	0.111+
	(0.0026)	(0.0026)	(0.0589)	(0.0589)
ppp	0.000000774	0.000000774	-0.0000123	-0.0000123
	(0.0000)	(0.0000)	(0.0001)	(0.0001)
edges	0.000000132+	0.000000132+	0.0000147**	0.0000147**
	(0.0000)	(0.0000)	(0.0000)	(0.0000)
_cons	-0.692*	-0.692*	-21.38***	-21.38***
	(0.3070)	(0.3070)	(5.4980)	(5.4980)
N	1579104	1579104	1579104	1579104
F	149.32	16707.2	630.17	8797
p	0	1.43E-87	0	6.92E-81
Overall R^2		0.0839		0.0782
N clusters	49	49	49	49

Notes: +p<0.10,*p<0.05,**p<0.01,***p<0.001. The dependent variable is the burned area proportion or the active fire count within each pixel per year. Treatment is a dummy variable that equals one if a pixel is within an active protected area and zero otherwise. FE = fixed-effects estimator for panel data, DiD-FE = estimator addressing both unobserved heterogeneity bias and assuming that the trends were parallel in the untreated state for treated and untreated. All specifications include year and Amazonian departments dummies interacted with a deterministic time trend. Covariate controls include within pixel proportion of primary and secondary forest deforestation, forest, farming, non-forest natural formations, non-vegetated area, flooded forests, mangroves, and savanna. Besides that, controls also included total precipitation, mean temperature, maximum cumulative water deficit (MCWD), mean precipitation and temperature during the dry season, population, and forest edge length. Robust standard errors clustered at the Amazonian department level are in parentheses.

Table D.8 - Differences-in-differences estimation of the protected area effect on burned area active fires, considering them as binary variables and standard errors clustered at the department level.

	Dependent variable: Burned area		*Dependent variable: Active fires*		*Dependent variable: Burned area*		*Dependent variable: Active fires*	
	FE	DiD-FE	FE	DiD-FE	FE	DiD-FE	FE	DiD-FE
Level of SE clusterization	Pixel	Pixel	Pixel	Pixel	Department	Department	Department	Department
Average treatment effect (ATE)	-0.00371***	-0.00371***	-0.00562***	-0.00562***	-0.00371*	-0.00371*	-0.00562*	-0.00562*
	(0.0007)	(0.0007)	(0.0009)	(0.0009)	(0.0016)	(0.0016)	(0.0023)	(0.0023)
DFpri	4.241***	4.241***	4.260***	4.260***	4.241***	4.241***	4.260***	4.260***
	(0.1020)	(0.1020)	(0.1130)	(0.1130)	(0.4750)	(0.4750)	(0.5440)	(0.5440)
DFsec	-0.192	-0.192	0.463*	0.463*	-0.192	-0.192	0.463	0.463
	(0.1780)	(0.1780)	(0.2040)	(0.2040)	(0.3720)	(0.3720)	(0.4330)	(0.4330)
forest	0.493***	0.493***	1.308***	1.308***	0.493*	0.493*	1.308***	1.308***
	(0.0449)	(0.0449)	(0.0600)	(0.0600)	(0.1990)	(0.1990)	(0.3370)	(0.3370)
farming	0.376***	0.376***	1.135***	1.135***	0.376	0.376	1.135**	1.135**
	(0.0466)	(0.0466)	(0.0622)	(0.0622)	(0.2370)	(0.2370)	(0.3340)	(0.3340)
NonForestNaturalArea	0.858***	0.858***	1.537***	1.537***	0.858**	0.858**	1.537***	1.537***
	(0.0564)	(0.0564)	(0.0751)	(0.0751)	(0.2700)	(0.2700)	(0.4070)	(0.4070)
nonVegetatedARea	-0.216	-0.216	2.301***	2.301***	-0.216	-0.216	2.301***	2.301***
	(0.2000)	(0.2000)	(0.3210)	(0.3210)	(0.4530)	(0.4530)	(0.3790)	(0.3790)
floodedForest	0.752***	0.752***	1.573***	1.573***	0.752**	0.752**	1.573***	1.573***
	(0.0503)	(0.0503)	(0.0670)	(0.0670)	(0.2200)	(0.2200)	(0.3730)	(0.3730)
mangrove	0.395	0.395	-0.288	-0.288	0.395	0.395	-0.288	-0.288
	(1.1050)	(1.1050)	(1.7460)	(1.7460)	(0.7080)	(0.7080)	(1.6670)	(1.6670)
savanna	0.966***	0.966***	2.217***	2.217***	0.966**	0.966**	2.217***	2.217***
	(0.1650)	(0.1650)	(0.1890)	(0.1890)	(0.2780)	(0.2780)	(0.4500)	(0.4500)
precTotal	-0.00000323***	-0.00000323***	-0.00000478***	-0.00000478***	-0.00000323	-0.00000323	-0.00000478	-0.00000478
	(0.0000)	(0.0000)	(0.0000)	(0.0000)	(0.0000)	(0.0000)	(0.0000)	(0.0000)
tempMedia	0.0478***	0.0478***	0.0430***	0.0430***	0.0478**	0.0478**	0.0430**	0.0430**
	(0.0008)	(0.0008)	(0.0008)	(0.0008)	(0.0167)	(0.0167)	(0.0134)	(0.0134)
MCWD	-0.0000308***	-0.0000308***	-0.0000329***	-0.0000329***	-0.0000308	-0.0000308	-0.0000329	-0.0000329
	(0.0000)	(0.0000)	(0.0000)	(0.0000)	(0.0000)	(0.0000)	(0.0000)	(0.0000)

(To be continued)

Table D.8 – Conclusion.

	Dependent variable: Burned area		*Dependent variable: Active fires*		*Dependent variable: Burned area*		*Dependent variable: Active fires*	
	FE	DiD-FE	FE	DiD-FE	FE	DiD-FE	FE	DiD-FE
Level of SE clusterization	Pixel	Pixel	Pixel	Pixel	Department	Department	Department	Department
precSeca	-0.0000666***	-0.0000666***	-0.000113***	-0.000113***	-0.0000666	-0.0000666	-0.000113	-0.000113
	(0.0000)	(0.0000)	(0.0000)	(0.0000)	(0.0001)	(0.0001)	(0.0001)	(0.0001)
tempSeca	0.0114***	0.0114***	0.00864***	0.00864***	0.0114*	0.0114*	0.00864*	0.00864*
	(0.0005)	(0.0005)	(0.0006)	(0.0006)	(0.0050)	(0.0050)	(0.0038)	(0.0038)
ppp	-0.000000628	-0.000000628	-0.00000618	-0.00000618	-0.000000628	-0.000000628	-0.00000618	-0.00000618
	(0.0000)	(0.0000)	(0.0000)	(0.0000)	(0.0000)	(0.0000)	(0.0000)	(0.0000)
edges	0.00000116***	0.00000116***	0.00000177***	0.00000177***	0.00000116***	0.00000116***	0.00000177***	0.00000177***
	(0.0000)	(0.0000)	(0.0000)	(0.0000)	(0.0000)	(0.0000)	(0.0000)	(0.0000)
_cons	-2.008***	-2.008***	-2.561***	-2.561***	-2.008***	-2.008***	-2.561***	-2.561***
	(0.0493)	(0.0493)	(0.0629)	(0.0629)	(0.5380)	(0.5380)	(0.4840)	(0.4840)
N	1579104	1579104	1579104	1579104	1579104	1579104	1579104	1579104
F	326.1	540.62	325.6	484.61	4825.2	183.31	18316.1	128.47
p	0	0	0	0	1.25E-74	0	1.58E-88	0
Overall R^2	0.142		0.0627		0.142		0.0627	
N clusters	87728	87728	87728	87728	49	49	49	49

Notes: +p<0.10,*p<0.05,**p<0.01,***p<0.001. The dependent variable is binary built from the burned area data or the active fire data for each pixel per year. Treatment is a dummy variable that equals one if a pixel is within an active protected area and zero otherwise. FE = fixed-effects estimator for panel data, DiD-FE = estimator addressing both unobserved heterogeneity bias and assuming that the trends were parallel in the untreated state for treated and untreated. All specifications include year and Amazonian departments dummies interacted with a deterministic time trend. Covariate controls include within pixel proportion of primary and secondary forest deforestation, forest, farming, non-forest natural formations, non-vegetated area, flooded forests, mangroves, and savanna. Besides that, controls also included total precipitation, mean temperature, maximum cumulative water déficit (MCWD), mean precipitation and temperature during the dry season, population, and forest edge length. Robust standard errors clustered at pixel or Amazonian department level in parentheses.

Table D.9 - Upper bound for the significance level (p+) of Rosenbaum's test of sensitivity to unobservables (binomial distribution test) for alternative degrees of influence of unobservables (1 to 1.45).

Variable	**Year**	Γ (Degree of influence of unobservables)									
		1	**1.05**	**1.1**	**1.15**	**1.2**	**1.25**	**1.3**	**1.35**	**1.4**	**1.45**
d_activeFire	2003	<0.0001	<0.0001	<0.0001	<0.0001	<0.0001	<0.0001	0.00074	0.04876	0.42299	0.88769
d_burnedArea	2003	<0.0001	<0.0001	<0.0001	<0.0001	<0.0001	0.00143	0.03243	0.2249	0.61528	0.90374
d_activeFire	2004	<0.0001	<0.0001	<0.0001	<0.0001	<0.0001	<0.0001	<0.0001	<0.0001	<0.0001	0.00025
d_burnedArea	2004	<0.0001	<0.0001	<0.0001	<0.0001	<0.0001	<0.0001	<0.0001	<0.0001	<0.0001	<0.0001
d_activeFire	2005	<0.0001	<0.0001	<0.0001	<0.0001	<0.0001	<0.0001	<0.0001	<0.0001	<0.0001	<0.0001
d_burnedArea	2005	<0.0001	<0.0001	<0.0001	<0.0001	<0.0001	<0.0001	<0.0001	<0.0001	<0.0001	<0.0001
d_activeFire	2006	<0.0001	<0.0001	<0.0001	<0.0001	0.00107	0.0755	0.5528	0.94947	0.999	1
d_burnedArea	2006	<0.0001	<0.0001	<0.0001	<0.0001	<0.0001	<0.0001	0.00291	0.05302	0.30195	0.7047
d_activeFire	2007	<0.0001	<0.0001	<0.0001	<0.0001	<0.0001	<0.0001	<0.0001	<0.0001	0.00071	0.04235
d_burnedArea	2007	<0.0001	<0.0001	<0.0001	<0.0001	<0.0001	0.00012	0.00761	0.11042	0.47317	0.85242
d_activeFire	2008	<0.0001	<0.0001	<0.0001	<0.0001	0.00013	0.01948	0.29422	0.82185	0.9901	0.99989
d_burnedArea	2008	<0.0001	0.00065	0.02873	0.25972	0.71112	0.9561	0.99753	0.99995	1	1
d_activeFire	2009	<0.0001	<0.0001	<0.0001	<0.0001	<0.0001	<0.0001	<0.0001	0.00169	0.06189	0.42088
d_burnedArea	2009	<0.0001	<0.0001	<0.0001	<0.0001	0.0036	0.05036	0.26184	0.62798	0.89507	0.98411
d_activeFire	2010	<0.0001	<0.0001	<0.0001	<0.0001	<0.0001	0.00603	0.19159	0.75853	0.98663	0.99988
d_burnedArea	2010	0.0003	0.02659	0.30692	0.80502	0.98479	0.99968	1	1	1	1
d_activeFire	2011	<0.0001	<0.0001	<0.0001	0.00248	0.11624	0.63828	0.96703	0.99945	1	1
d_burnedArea	2011	<0.0001	<0.0001	0.00637	0.0968	0.4361	0.82391	0.976	0.99857	0.99996	1
d_activeFire	2012	<0.0001	<0.0001	<0.0001	<0.0001	<0.0001	<0.0001	0.00152	0.07078	0.48681	0.9116
d_burnedArea	2012	<0.0001	<0.0001	<0.0001	0.00604	0.09191	0.42153	0.81249	0.97317	0.99832	0.99995
d_activeFire	2013	<0.0001	<0.0001	<0.0001	<0.0001	0.00016	0.02	0.28469	0.80439	0.98711	0.99981
d_burnedArea	2013	0.97925	0.99919	0.99999	1	1	1	1	1	1	1
d_activeFire	2014	<0.0001	<0.0001	<0.0001	<0.0001	<0.0001	<0.0001	0.00852	0.18283	0.69854	0.97078
d_burnedArea	2014	<0.0001	<0.0001	0.00085	0.02677	0.21904	0.62966	0.9181	0.99207	0.99965	0.99999
d_activeFire	2015	<0.0001	<0.0001	<0.0001	<0.0001	<0.0001	<0.0001	<0.0001	<0.0001	0.00188	0.07174
d_burnedArea	2015	<0.0001	<0.0001	<0.0001	<0.0001	<0.0001	<0.0001	0.00202	0.04261	0.27042	0.67614
d_activeFire	2016	<0.0001	<0.0001	<0.0001	<0.0001	<0.0001	<0.0001	<0.0001	0.00033	0.03097	0.34884
d_burnedArea	2016	0.84355	0.99256	0.99993	1	1	1	1	1	1	1
d_activeFire	2017	<0.0001	<0.0001	<0.0001	<0.0001	<0.0001	<0.0001	<0.0001	<0.0001	0.00106	0.05575
d_burnedArea	2017	<0.0001	<0.0001	<0.0001	0.0001	0.00799	0.12285	0.51478	0.88254	0.98913	0.99961
d_activeFire	2018	<0.0001	<0.0001	<0.0001	<0.0001	<0.0001	<0.0001	<0.0001	<0.0001	<0.0001	0.00065
d_burnedArea	2018	0.00098	0.04307	0.34389	0.80318	0.97998	0.99932	0.99999	1	1	1
d_activeFire	2019	<0.0001	<0.0001	<0.0001	<0.0001	<0.0001	<0.0001	<0.0001	<0.0001	<0.0001	<0.0001
d_burnedArea	2019	<0.0001	<0.0001	<0.0001	<0.0001	<0.0001	<0.0001	<0.0001	0.00012	0.00579	0.07744
d_activeFire	2020	<0.0001	<0.0001	<0.0001	<0.0001	<0.0001	<0.0001	<0.0001	<0.0001	<0.0001	<0.0001
d_burnedArea	2020	<0.0001	<0.0001	<0.0001	<0.0001	<0.0001	0.00486	0.11582	0.55522	0.92263	0.99609
Count < 0.05		**94%**	**94%**	**89%**	**83%**	**75%**	**67%**	**56%**	**42%**	**33%**	**22%**

Note: Γ is the degree to which unobservables increase the odds ratio of not having fire comparing treated (insides protected areas) and untreated (outside) pixels. So for Γ = 1, unobservables have no influence.

Table D.10 - Upper bound for the significance level (p+) of Rosenbaum's test of sensitivity to unobservables (binomial distribution test) for alternative degrees of influence of unobservables (1.5 to 2).

VariableA4A45:M79	Year	Γ (Degree of influence of unobservables)										
		1.5	**1.55**	**1.6**	**1.65**	**1.7**	**1.75**	**1.8**	**1.85**	**1.9**	**1.95**	**2**
d_activeFire	2003	0.99495	0.99995	1	1	1	1	1	1	1	1	1
d_burnedArea	2003	0.98861	0.99935	0.99998	1	1	1	1	1	1	1	1
d_activeFire	2004	0.01837	0.22895	0.7117	0.96531	0.99879	0.99999	1	1	1	1	1
d_burnedArea	2004	<0.0001	0.00011	0.00342	0.04062	0.20805	0.535	0.83179	0.96474	0.99574	0.9997	0.99999
d_activeFire	2005	<0.0001	0.00524	0.11214	0.53363	0.91022	0.99477	0.99991	1	1	1	1
d_burnedArea	2005	<0.0001	<0.0001	0.0005	0.01047	0.08708	0.33043	0.67483	0.90634	0.98456	0.99853	0.99992
d_activeFire	2006	1	1	1	1	1	1	1	1	1	1	1
d_burnedArea	2006	0.94024	0.99446	0.99976	0.99999	1	1	1	1	1	1	1
d_activeFire	2007	0.37885	0.85487	0.99128	0.99987	1	1	1	1	1	1	1
d_burnedArea	2007	0.98304	0.99921	0.99998	1	1	1	1	1	1	1	1
d_activeFire	2008	1	1	1	1	1	1	1	1	1	1	1
d_burnedArea	2008	1	1	1	1	1	1	1	1	1	1	1
d_activeFire	2009	0.8625	0.9903	0.9998	1	1	1	1	1	1	1	1
d_burnedArea	2009	0.99869	0.99994	1	1	1	1	1	1	1	1	1
d_activeFire	2010	1	1	1	1	1	1	1	1	1	1	1
d_burnedArea	2010	1	1	1	1	1	1	1	1	1	1	1
d_activeFire	2011	1	1	1	1	1	1	1	1	1	1	1
d_burnedArea	2011	1	1	1	1	1	1	1	1	1	1	1
d_activeFire	2012	0.99637	0.99996	1	1	1	1	1	1	1	1	1
d_burnedArea	2012	1	1	1	1	1	1	1	1	1	1	1
d_activeFire	2013	1	1	1	1	1	1	1	1	1	1	1
d_burnedArea	2013	1	1	1	1	1	1	1	1	1	1	1
d_activeFire	2014	0.99935	1	1	1	1	1	1	1	1	1	1
d_burnedArea	2014	1	1	1	1	1	1	1	1	1	1	1
d_activeFire	2015	0.46805	0.89513	0.99451	0.99992	1	1	1	1	1	1	1
d_burnedArea	2015	0.9315	0.99345	0.99971	0.99999	1	1	1	1	1	1	1
d_activeFire	2016	0.85007	0.99207	0.99991	1	1	1	1	1	1	1	1
d_burnedArea	2016	1	1	1	1	1	1	1	1	1	1	1
d_activeFire	2017	0.43519	0.88786	0.99456	0.99994	1	1	1	1	1	1	1
d_burnedArea	2017	0.99999	1	1	1	1	1	1	1	1	1	1
d_activeFire	2018	0.03373	0.31162	0.78832	0.97981	0.99944	1	1	1	1	1	1
d_burnedArea	2018	1	1	1	1	1	1	1	1	1	1	1
d_activeFire	2019	<0.0001	<0.0001	0.00146	0.04974	0.3591	0.81197	0.98183	0.99945	0.99999	1	1
d_burnedArea	2019	0.35947	0.74716	0.95116	0.99553	0.9998	1	1	1	1	1	1
d_activeFire	2020	<0.0001	<0.0001	0.00901	0.16513	0.64542	0.95325	0.99837	0.99998	1	1	1
d_burnedArea	2020	0.99994	1	1	1	1	1	1	1	1	1	1
Count < 0.05		**19%**	**14%**	**11%**	**8%**	**0%**	**0%**	**0%**	**0%**	**0%**	**0%**	**0%**

Note: Γ is the degree to which unobservables increase the odds ratio of not having fire comparing treated (insides protected areas) and untreated (outside) pixels. So for Γ = 1, unobservables have no influence.